

**AIX-MARSEILLE UNIVERSITE  
FACULTE DE MÉDECINE DE MARSEILLE**

**Ecole Doctorale des Sciences de la Vie et de la Santé**

**THÈSE**

*Présentée et publiquement soutenue devant*

**LA FACULTÉ DE MÉDECINE DE MARSEILLE**

Le 21 Juillet 2016

Par **Francesca Bonini**

Née le 04 Juin 1980 à Rome

**Le rôle du cortex frontal médian dans la supervision de l'action chez l'homme:  
études électrophysiologiques**

Pour obtenir le grade de DOCTORAT d'AIX-MARSEILLE UNIVERSITÉ  
SPÉCIALITÉ : *Neurosciences*

**Membres du Jury de la Thèse :**

Pr. François-Xavier ALARIO	Président	LPC, CNRS, Marseille, France
Dr. Céline AMIEZ	Examineur	U1208, INSERM, Lyon, France
Pr Pierre BURBAUD	Rapporteur	IMN, UMR 5293, CNRS, Bordeaux, France
Pr. Patrick CHAUVEL	Directeur	INS, INSERM UMR 1106, Marseille, France
Pr Franck VIDAL	Co-Directeur	LNC, UMR 7291, CNRS, Marseille, France
Pr. Wery van den WILDENBERG	Rapporteur	Department of Psychology, Amsterdam, Pays-Bas



*Cette thèse est le résultat du travail, de l'aide et du soutien de plusieurs personnes, que je souhaite remercier sincèrement :*

*Mes deux rapporteurs de thèse, Pierre Burbaud et Wery van den Wildenberg, qui ont généreusement accepté de prêter leurs connaissances et leurs compétences à la lecture critique et bienveillante de mon manuscrit.*

*Mes deux directeurs de thèse : Patrick Chauvel, qui m'a ouvert les portes de son service et celles du monde de la recherche et Franck Vidal, à qui je souhaite exprimer toute ma gratitude et toute mon estime pour ce qu'il m'a apporté scientifiquement et humainement pendant ces années.*

*Boris Burle aura été tout simplement indispensable, en plus d'être un ami (avec sa petite famille franco-italienne, accueillante et chaleureuse).*

*Andrea Brovelli, pour son aide précieuse et parce que false discovery rate, multi-taper method et autres similaires joyeusetés sont quand même plus digestes quand expliquées dans sa langue maternelle.*

*Les autres membres de l'INS, en particulier et dans le désordre, Catherine Liégeois-Chauvel, Daniele Schon, Jean-Michel Badier, Patrick Marquis, Samuel ... Un remerciement spécial va à Sophie Chen pour son aide fondamentale ainsi que pour sa gentillesse et ses gâteaux (fondamentaux aussi).*

*Les neurochirurgiens Romain Carron, Jean Régis et Didier Scavarda, qui avec leur travail ont permis de réaliser les expériences intracérébrales et qui m'ont guidé dans le labyrinthe des fissures, gyri, sillons et variables anatomiques.*

*Les anglophones natifs, Jennifer Coull, Marmaduke Woodman, Russell Hewett, Brenda Stevens et Aileen McGonigal, qui ont passé quelques unes des leurs soirées à corriger l'anglais du manuscrit.*

*Toute l'équipe du Service de Neurophysiologie Clinique, personnel médical, infirmières et secrétaires, qui supportent affectueusement mes défaillances et mes sautes d'humeur et qui savent toujours me faire oublier la fatigue et les difficultés.*

*Je remercie tout particulièrement Fabrice Bartolomei, qui m'a très patiemment et généreusement soulagé de mon activité d'assistante du service pour me permettre de terminer cette thèse, et Agnès Trébuchon, pour son aide morale et concrète ainsi que pour son sourire et son enthousiasme contagieux.*

*En fin ma famille. Italiens et français, amis et parents, de sang et acquis, humains et félins, proches et lointains, vieux et bébés, morts et vivants...*

*A ma famille, toute.*



# **The role of medial frontal cortex in action monitoring in humans:**

## **Electrophysiological studies of outcome modulated activities**

### **Abstract**

The capacity to evaluate the outcome of our actions is fundamental for adapting and optimizing behaviour. Indeed in flexible goal-directed behaviour, performance is continuously adjusted in order to avoid negative consequences and improve subsequent actions. This capability depends on an action monitoring system in charge of assessing ongoing actions, detecting errors, and evaluating outcomes.

Sensitivity to errors is considered to be the main manifestation of action monitoring, and electrical brain activity evoked by negative outcomes is thought to originate within the medial part of the frontal cortex. Likewise, functional neuroimaging studies suggest that this region has a decisive role in action monitoring. Nonetheless, the underlying neuronal network is incompletely characterised in humans.

In the two first studies, we investigated the anatomical substrates of action monitoring in humans using intracerebral local field potential (LFP) recordings of cerebral cortex from epileptic patients. Response evoked LFPs sensitive to outcome were recorded from the Supplementary Motor Area proper (SMA), with the largest LFPs occurring after errors and the smallest after correct responses. LFPs evoked exclusively by errors were recorded later and more rostrally in the medial prefrontal cortex. We then assessed gamma-frequency activity (60-180 Hz) - whose increase is considered a marker of neural recruitment during cognitive processing - induced by behaviourally relevant responses. Gamma power was modulated as a function of action outcome in a vast frontal and extra-frontal network.

In a third study we investigated the electro-magnetic activity evoked by internally versus externally delivered feedback using simultaneous recording of electroencephalography (EEG) and magnetoencephalography (MEG). While error related activity was detected by EEG (but not by MEG), feedback-related activity was detected by MEG, indicating that the sources of these two forms of outcome-modulated brain activity are different.

Our results show that the SMA is much more involved in action monitoring than previously thought. SMA rapidly and continuously assesses ongoing actions and likely engages more rostral prefrontal structures in the case of error. Processing of action errors and of negative externally delivered feedback therefore appears to be supported by distinct cortical networks.



## Résumé

La capacité à évaluer les résultats nos actions est fondamentale pour adapter et optimiser notre comportement. En effet dans les comportements dirigés vers un but, l'être humain est capable d'ajuster et modifier ses actions pour éviter les conséquences négatives et améliorer son niveau de performance au fil du temps. Cette habilité dépend de l'existence d'un système superviseur chargé d'évaluer l'action en cours, de détecter les erreurs, de déclencher souvent des corrections, et d'évaluer les conséquences de l'action.

La sensibilité aux erreurs est considérée comme l'une des principales manifestations de l'action du système superviseur et on considère que certaines activités électriques cérébrales évoquées par les erreurs sont générées par la partie médiane du cortex frontal. Ainsi, des études de neuroimagerie fonctionnelle suggèrent que cette région joue un rôle décisif dans la supervision de l'action. Néanmoins le réseau neuronal sous-jacent n'a pas été complètement caractérisé chez l'homme.

Dans les deux premières études nous avons étudié les bases anatomiques de la supervision de l'action chez l'homme au moyen des potentiels de champs locaux (LFP pour « *local field potentials* ») enregistrés dans le cortex cérébral de patients épileptiques.

Nous avons enregistré dans l'Aire Motrice Supplémentaire proprement dite (AMSp) des LFP évoqués par les réponses et modulés par la performance; les LFP plus amples survenaient après une erreur et les moins amples après une réponse correcte. Des LFP évoqués exclusivement par les erreurs ont été enregistrés plus tardivement et plus rostralement dans le cortex préfrontal médian.

Dans la deuxième étude, nous avons analysé les activités de hautes-fréquences de la bande gamma (60-180 Hz) induites par les réponses des sujets. Nous avons observé que ces activités gamma, dont l'augmentation est considérée un marqueur du recrutement neuronal, sont, elles aussi, modulées par la performance des sujets, mais dans un vaste réseau frontal et extra-frontal.

Dans une troisième étude, nous avons comparé les activités électromagnétiques évoquées par un feedback interne, à celles évoquées par un feedback externe, en utilisant des enregistrements simultanés électroencéphalographiques (EEG) et magnétoencéphalographiques (MEG). Une activité évoquée par les erreurs était visible sur les enregistrements EEG (mais pas sur les enregistrements MEG), alors qu'une activité évoquée par le feedback externe était bien visible sur les enregistrements MEG, indiquant que les générateurs de ces deux formes d'activité cérébrale, modulées par la performance, sont différents.

Nos résultats montrent une implication de l'AMSp dans la supervision de l'action chez l'homme, bien plus importante que ce que l'on soupçonnait auparavant. Cette structure évalue précocement, et de façon continue, l'action en cours et elle engage vraisemblablement des structures préfrontales plus rostrales en cas d'erreur seulement. Le traitement de l'erreur d'action, selon qu'il se fonde sur des informations internes ou externes est certainement sous-tendu par des réseaux corticaux différents.



# Table of Contents

<b>I.</b>	<b>INTRODUCTION</b> .....	<b>9</b>
1	COGNITIVE CONTROL: BEHAVIOURAL AND EMG EVIDENCE .....	11
1.1	RT tasks and time pressure paradigm .....	11
1.2	Behavioural evidence .....	12
1.3	Electromyography (EMG data): indirect evidence for on-line executive control and indirect evidence of action monitoring .....	16
2	MAGNETO AND ELECTROPHYSIOLOGY OF THE BRAIN .....	18
2.1	Origin of M/EEG signal .....	18
2.2	The role of generator's position and volume conduction on M/EEG signal .....	26
2.3	Possible solutions .....	29
2.4	High frequency neuronal oscillation.....	31
3	COGNITIVE CONTROL: EEG EVIDENCE.....	32
3.1	Error Negativity (Ne or ERN) .....	32
3.2	Error Positivity (Pe).....	35
3.3	Feedback related Negativity (FRN).....	37
4	STRUCTURES INVOLVED IN ACTION MONITORING AND UNDERLYING THE NE. ....	38
4.1	Anatomy, connectivity and functional organization of premotor and prefrontal cortex.....	38
4.2	The role of medial frontal cortex in action monitoring .....	46
5	ASSESSMENT OF CURRENT LITERATURE AND OPEN QUESTIONS .....	51
<b>II.</b>	<b>EXPERIMENTAL WORK</b> .....	<b>53</b>
6	COMMON METHODS TO EXPERIMENTAL PARTS 1 & 2 .....	53
6.1	Subjects and recording procedure.....	53
6.2	Simon Task .....	53
6.3	EMG recordings and trials classification.....	54
6.4	Behavioural Data.....	55



7	STUDY 1: ACTION MONITORING AND MEDIAL FRONTAL CORTEX: LEADING ROLE OF SUPPLEMENTARY MOTOR AREA .....	57
7.1	Introduction .....	57
7.2	Subjects & methods .....	58
7.3	Results .....	60
7.4	Discussion.....	73
8	STUDY 2: HIGH-GAMMA ACTIVITY INDUCED BY MOTOR RESPONSES IN PERFORMANCE MONITORING: RECORDINGS FROM HUMAN CEREBRAL CORTEX .....	79
8.1	Introduction .....	79
8.2	Materials & Methods .....	81
8.3	Results .....	84
8.4	Discussion.....	99
9	STUDY 3: DOES ERROR NEGATIVITY AND FEEDBACK-RELATED NEGATIVITY HAVE THE SAME CORTICAL GENERATOR? EVIDENCE FROM SIMULTANEOUS EEG/MEG RECORDINGS OF ERROR RELATED ACTIVITIES .....	104
9.1	Introduction .....	104
9.2	Materials and Methods .....	106
9.3	Results .....	111
9.4	Discussion.....	118
<b>III.</b>	<b>GENERAL DISCUSSION .....</b>	<b>123</b>
10	The SMA as a key node in action monitoring in humans.....	123
11	Ne/Ne-like: a unique generator for a unique mechanism .....	124
12	Prefrontal cortex and SMA in action monitoring .....	127
13	Outcome evaluation: from internally generated to externally delivered feedback .....	129
14	Pathologies and altered action monitoring .....	131
<b>IV.</b>	<b>CONCLUSIONS.....</b>	<b>134</b>
<b>V.</b>	<b>REFERENCES .....</b>	<b>137</b>



# I. INTRODUCTION

In their daily clinical practice doctors and surgeons perform therapeutic and diagnostic acts with the aim to identify diseases, treat pathology, remove tumours and repair lesions, briefly to cure patients. Nevertheless, unfortunately and despite their caution and vigilance, sometimes they can fail.

Imagine a neurosurgeon implanting depth electrodes in the brain of an anaesthetized patient. He has carefully planned the trajectory of electrodes and he is now introducing the probe through patient's skull. He feels (as he has repeated this gesture many times) the moment when the electrode traverse meninges and cerebral cortex, but at a certain point, the probe imperceptibly deviates. He realizes it, slightly retreats it and then he moves it forward with a slightly different trajectory. Implantation is concluded, patient is awakened. A brain computer tomography (CT) is performed: electrodes are well positioned and brain is undamaged.

Or, fortunately rarely, not: the surgeon did not perceive that something went wrong, one electrode has touched a small vessel, CT scan shows a cerebral hematoma...

Let's now imagine something less dramatic: a tennis player while serving. He strikes the ball strongly and speedily as we would make an ace, but the lineman signals: the ball has landed out. Fortunately, he has a second serve which is more likely to succeed, as he's decided to be more accurate and less fast. Even during a successful first serve, the player may have tossed the ball too high requiring a prompt adjustment of serving action.

These examples illustrate how human life (and of course also life of nearly all non human species) is characterized by a daily succession of planning, action, errors, corrections, reward or punishment, re-planning, re-performing and so on..., that is, by an eternal quest of

appropriate behaviour. To achieve such often unachievable appropriate behaviour humans are equipped with a “control system” which supervises and evaluates on-going activities, in order to rectify and modify them on-line. Once the action has been accomplished, this control system allows evaluation of the action’s outcome and adjusts subsequent behaviour in order to optimize performance and avoid subsequent errors. This ability to supervise and evaluate, which thus allows inhibition and correction of sensori-motor action, is called action monitoring and implicates detection and processing of errors and negative outcomes (or feedbacks).

Understanding how performance is evaluated, errors detected and actions corrected, and which conditions facilitate errors, in other words how action monitoring is implemented in the brain, represents a major issue for investigation. Indeed human error (beyond a tennis serve double fault) may represent a veritable risk, as in medical procedure, transport, nuclear industries ect

A classical approach for investigating action monitoring is based on analyzing errors, since errors reveal how the action monitoring system works better than successful behaviour does. To this end, in experimental situations, subjects are subject to temporal pressure, a procedure which facilitates errors. In this way, thank to the so-called reaction time tasks (RT tasks), behavioural analysis of performance and errors has led to the discovery of the supervisory system in humans. More recently, electrophysiological and metabolic neuroimaging studies have provided new insights on the control system, nowadays commonly accepted and called with the broader term of “executive control”. All these collected behavioural, electrophysiological and metabolic data, have allowed to formulate hypothesis about the anatomical and physiological substrates of action monitoring, as well as to speculate about its possible functioning (that is, different “models”).

In this introduction we will firstly review executive control and action monitoring in relation with behavioural and electromyography data obtained from RT paradigms. Secondly we will provide the basis of brain electrophysiology, to subsequently discuss the electroencephalographic (EEG) signatures of the monitoring system. Finally we will review anatomo-physiology of cerebral structures underlying action monitoring, as well as their relative role as supplied by metabolic, EEG and animal data.

# 1 COGNITIVE CONTROL: BEHAVIOURAL AND EMG EVIDENCE

## 1.1 RT tasks and time pressure paradigm

In RT tasks, each time a stimulus is presented, subjects have to respond as fast as they can, trying to avoid errors. RT is the time occurring from stimulus presentation to mechanical response. From a functional standpoint it represents, as the subject is under temporal pressure, the minimal time needed for sensori-motor information processing, which results in the motor response.

In “simple” RT tasks a unique stimulus is presented and a unique response is possible. As an example subjects have to execute a button press as soon as they perceive the stimulus, which can be visual (i.e. an image), auditory (i.e. a tone) or somatosensory.

On the other hand, “choice” RT tasks are characterized by different possible responses as a function of different stimuli. A stimulus-response association is previously learned, that is, subjects are instructed about which response they have to execute in relation to a certain stimulus. Figure I.1 illustrates a double choice RT task in which subjects have to identify the colour of a target stimulus and produce a mechanical right or left response as a function of the specified association between colour and response side.

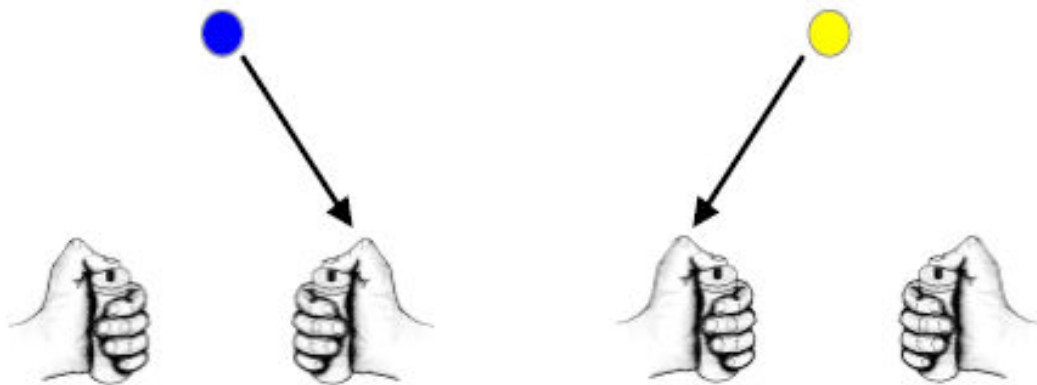


**Figure I.1 :** *An example of a two-choice choice RT task.*

*Subjects have to perform a right thumb button press in response to a blue target, and a left thumb button press in response to a yellow target.*

When subjects are subject to time pressure they tend to make more errors. Indeed time pressure facilitates errors, which are specifically action errors rather than detection errors, that

is to say, subjects fail to select and execute the response to be given rather than fail to correctly detect the stimulus (Rabbitt, 1996). This is due to the fact that, under temporal pressure, subjects make more errors the more rapidly they respond. In particular, if they are asked to respond as fast as they can, they might rush and even gamble, taking the risk of failing. On the other hand, if subjects are asked to be as accurate as they can, they will take their time to choose the correct response to the detriment of rapidity. This relationship between accuracy and RT observed from one experimental condition to another following manipulation of speed-accuracy instructions (“be more accurate” or “go faster”), are called speed-accuracy tradeoffs.

Other types of task allow cognitive control to be studied, namely Go/NoGo tasks (H Rosvold, A Mirsky, I Sarason, E.D Bransome Jr., 1956) and Stop tasks (Logan & Cowan, 1984; Ollmann, 1973). These require subjects to perform speeded motor responses on Go trials - when a target stimulus is presented - and to inhibit such responses on incidental NoGo trials - when a non-target stimulus is presented – or Stop trials which are characterised by a stop signal following the target stimulus. These tasks allow the investigation of response inhibition processes and show that, 1) the less frequently the No-Go trials are presented, the lower is the probability of successful response suppression, 2) the later stop signals are presented the lower the probability of successful response suppression (Dagenbach & Carr, 1994; Logan & Cowan, 1984; van den Wildenberg, van Boxtel, & van der Molen, 2003; van den Wildenberg, van der Molen, & Logan, 2002).

We will now see how analysis of RT, behavioural adjustment and EMG recordings during commission of errors reveals some of the mechanisms of action monitoring and error processing.

## **1.2 Behavioural evidence**

### **1.2.1 *Speed-accuracy changes***

In RT tasks, when subjects execute an erroneous response, they usually slow down in the next trial, that is, subsequent RT is longer (see figure 1.2). This phenomenon is called “post-error slowing” and suggests that a system in charge of controlling action execution exists, which operates from one trial to another (Rabbitt, 1996). Furthermore, the likelihood of error commission is lower in the  $n$  trial if the previous  $n-1$  trial was incorrect, that is a

reduction of error rate (ER) is noticed following errors (Laming, 1979). These post-error behavioural adaptation effects are considered to reflect cognitive control processes. In particular, post-error slowing is taken as a consequence of increased response caution (Botvinick, Braver, Barch, Carter, & Cohen, 2001; Brewer & Smith, 1989; Dutilh & Vandekerckhove, 2012), that is, after an error people can adaptively change their response thresholds, taking their time before initiating an action, thus becoming more cautious. Alternatively, post-error slowing can be considered as the consequence of attentional distraction due to error itself. In other words, the error would be an infrequent, surprising event that perturbs subjects and distracts them during the processing of the subsequent stimulus (Notebaert et al., 2009). Note that these two accounts may not be mutually exclusive.

Finally, on correct trials preceding errors, shorter RT has been observed (Gehering & Fencsik, 2001). Such pre-error speeding is equally deemed to reflect adaptation of response thresholds in subjects who become less cautious after several correct responses.

Pre-error speeding, post-error slowing and post-error ER reduction, are called speed-accuracy changes and indicate that subjects adapt their strategy during the task depending on their recent past performance. In other words, the monitoring system is able to detect and inform the quality of the emitted response and this ability allows for adjustments in strategy.

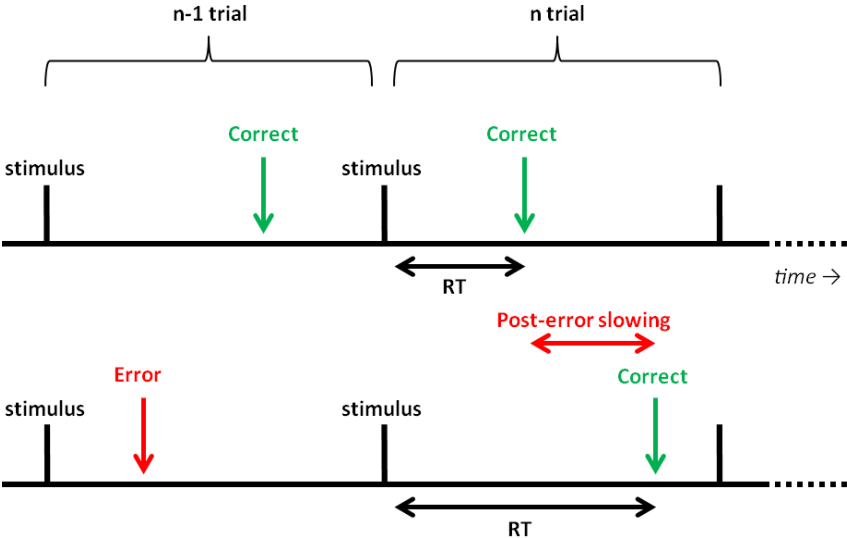


**Figure I.2 : Post-error slowing.**  
*Figure illustrates two series of trials: in the top panel the correct n trial is preceded by a correct response on the n-1 trial, while in the bottom panel it is preceded by an error. As shown in the figure the n trial RT depends on performance on the n-1 trial: in case of an error on the n-1 trial we observe a longer RT on the n trial, that is, a post-error slowing*

### 1.2.2 Congruency effects and sequential effects

In RT tasks, in order to investigate executive control, stimulus-response congruency can be manipulated. In particular, the spatial relationship between the stimulus and the response to be given affects performance and RT. A classical task manipulating spatial congruency is the Simon task (Craft & Simon, 1970). In this task subjects have to identify the colour of a target stimulus and respond with a left- or right-hand keypress according to the colour. The stimulus is presented on the right or on the left of a fixation point but stimulus location is irrelevant to the task (Figure I.3). On congruent trials the stimulus is presented on the side of the response to be given, that is, the stimulus is ipsilateral to the response. On incongruent trials the stimulus is presented on the opposite (contralateral) side of the requested response.

Behavioural data from the Simon task are informative about cognitive control. First, choice RTs are shorter in congruent compared to incongruent trials. This difference between two RTs is called the “congruency effect” (or “Simon effect”), whose size varies along the task, as a function of previous and/or subsequent trial.

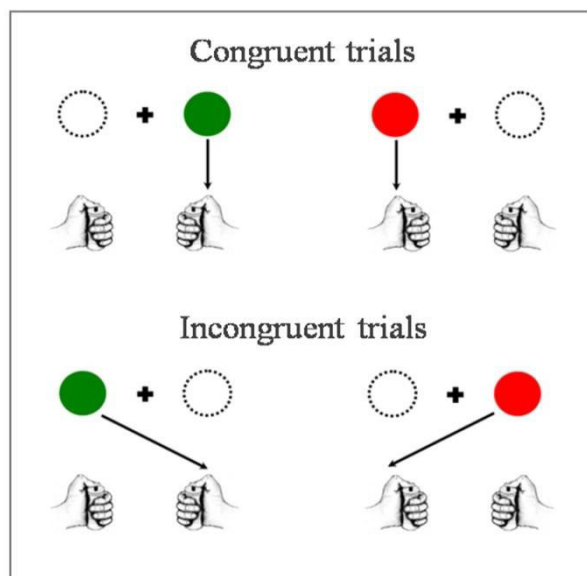


**Figure I.3 :** *Simon task.*

*In this between-hand choice RT task subjects have to respond with a right keypress for green stimuli and with a left keypress for red stimuli. At the same time they have to ignore a non-relevant attribute of the stimulus, that is, its position. In congruent trials stimulus position is on the same side of the requested response, on incongruent trials the stimulus is presented on the opposite side of the requested response.*

Indeed a sequential modulation of the Simon effect is observed: the congruity effect decreases when the preceding trial was incongruent, to such a point that the congruency effect can disappear or even reverse. i.e: this suggests a process of re-focalizing attention to the relevant dimension of the stimulus.

Secondly, similarly to RTs, error rate is higher on incongruent than on congruent trials and this phenomenon presents the same sequential effect (lower congruency effect on trials following an incongruent trial). Distributional analysis of RTs shows that the congruency effect decreases as RT increases, that is, the later the response is given the less stimulus location affects the RT (De Jong, Liang, & Lauber, 1994). Moreover for longer RTs, accuracy is similar for congruent and incongruent trials, while for shorter RTs only an increase in error rate is observed. These results suggest an early automatic capture by stimulus position, which is irrelevant for the task at hand and ought to be inhibited. Cognitive control allows active inhibition of the response automatically activated by the location of the stimulus. For shorter RTs, the mechanism for suppressing such an “automatic” response does not have enough time to develop: this give rise to an increase in error rate in incongruent trials, as well as to an increase of the congruency effect.

To summarise, executive control monitors and evaluates performance. Thanks to this evaluation function it can consequently adjust sensori-motor information processing in at least two ways: 1) with strategic adjustment, as revealed by speed-accuracy changes; 2) by re-focalizing selective attention to the relevant dimension of the stimulus.

Executive (or cognitive) control is thus composed of at least two concurrent functions: performance evaluation (usually called action monitoring) and organization of sensori-motor processing, the latter performed via strategic modification and selective attention.

In other words, namely in Simon’s words, “monitoring responses is an executive function that is a part of a system that guides behaviour and allows for corrections and adjustments that might be required when our actual responses do not match the responses we intended or when we predict outcomes and these outcome predictions fail” (Simons, Birbaumer, Coles, Graham, & Arne, 2010).

The action monitoring process of cognitive control is therefore a key function as it will act as a guide that triggers (or not) remediation and/or adaptation processes when required and only when required.

### **1.3 Electromyography (EMG data): indirect evidence for on-line executive control and indirect evidence of action monitoring**

Behavioural data, namely post-error slowing, pre-error speeding and sequential effects have shown that executive control operates trial by trial. Surface EMG recordings during the performance of between-hand choice RT tasks, have revealed on-line within-trial executive control.

Surface EMG, thanks to skin electrodes placed over the muscles, records electrical activity related to recruitment of muscle units, which starts before mechanical correct and incorrect responses and which sometimes does not result in a mechanical response at all.

It has been noticed that the EMG burst is reduced for erroneous responses. Indeed, when pianists play the wrong piano key, erroneous notes are imperceptibly quieter than correct ones. However, Allain et al (Allain, Carbonnell, Falkenstein, Burle, & Vidal, 2004) have shown that the initial slope of the EMG burst is the same for both erroneous and correct responses. The EMG slope reflects synchrony in activation of muscle fibres, thus, EMG bursts with different initial slopes indicate different motor commands (Hasbroucq, Akamatsu, Mouret, & Seal, 1995). The same EMG slope for errors and correct responses suggests that the initial command is the same and suggests that the subsequent reduced EMG burst for errors represents a (failed) attempt to inhibit the erroneous action.

Furthermore, EMG recordings have revealed that on some correct trials of between-hand choice reaction times tasks, although the correct response is emitted, an incorrect small muscular activation is detectable for the incorrect response (Hasbroucq, Possama, Bonnet, & Vidal, 1999; Smid, Mulder, & Mulder, 1990). These small EMG bursts do not reflect intercurrent muscular activity, since the RT in these trials is longer than in correct trials and a congruency effect cannot be found (Hasbroucq et al., 1999). Moreover Allain et al (Sonia Allain et al., 2004) found a small post-trial slowing following this type of correct trial, as well as a small pre-trial speeding. Thus trials characterized by these subliminal incorrect EMG activations, too small to result in a mechanical response, are considered as erroneous motor commands, detected and suppressed on time, and, for this reason, are commonly called “partial errors”(Figure I.4)

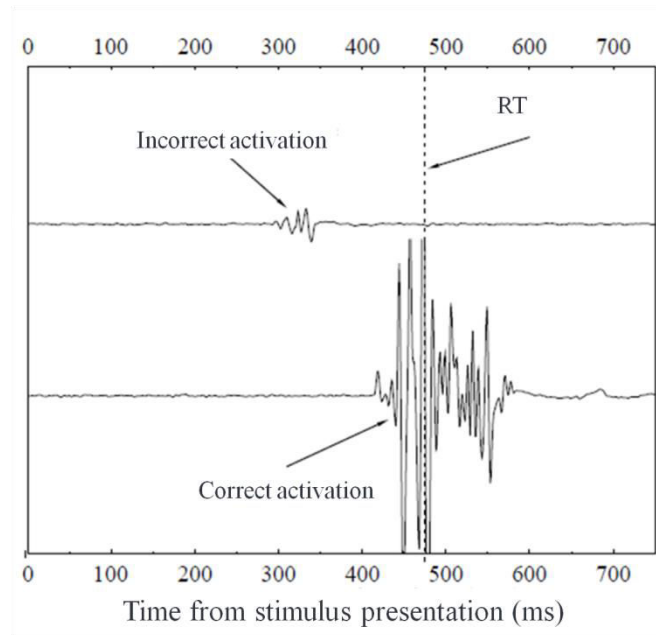


**Figure I.4 :** *Electromyographic activity during a partial error trial.*

*Time 0 corresponds to stimulus presentation; RT corresponds to the mechanical correct response. EMG activity of the muscle involved in the incorrect activation is a small EMG burst (top trace) preceding the correct activation, which results in a mechanical response corresponding to a larger EMG burst (bottom trace).*

Moreover, in Simon tasks, incorrect EMG activation on partial error trials are earlier for incongruent than for congruent conditions (as it is the case for full-blown errors). That is to say, incorrect EMG activation during partial errors is sensitive to stimulus position and shows a congruency (or Simon) effect (Hasbroucq et al., 1999). Nonetheless, as the « correction time », that is the time between the incorrect and correct EMG onsets, is longer for incongruent trials, there is no congruency effect on RTs for partial error trials (Rochet, Spieser, Casini, Hasbroucq, & Burle, 2014).

If we admit that partial errors are considered as subliminal errors which are aborted before reaching the response threshold and corrected, it must be admitted that the executive control system is able to detect these partial errors on line, before stopping and correcting them. Thus EMG data indirectly reveal that cognitive control allows partial errors to be detected *via* the action monitoring system, which is revealed to be a key element of this function.

Besides behavioural and EMG data, electroencephalographic (EEG) evidence for the existence of an action monitoring system have been reported since the 1990s. Before

addressing this topic, it is necessary to introduce the principles of brain electrophysiology, which is also important for the interpretation of present experimental data.

## **2 MAGNETO AND ELECTROPHYSIOLOGY OF THE BRAIN**

Electrical activity of the brain is measured by electroencephalography (EEG). The EEG was used for the first time in the 1920s by Hans Berger, who recorded human brain activity from the scalp. The EEG is the graphic representation of the time course of the difference in voltage between two different cerebral locations plotted over time. It results from the sum of electrical activity of synchronously activated neurons and, to a less degree, of glial electrical activity.

In fact neurons, thanks to their intrinsic electrical properties, are able to generate an electric potential  $V_e$  (a scalar measured in Volts), together with an electric field resulting from the difference in  $V_e$  between two locations. Electrical field (a vector whose amplitude is measured in Volts per distance) and magnetic field generate EEG and MEG signals. The difference in electrical potential between two locations and the subsequent (electro)-magnetic fields can be recorded with different techniques and different distances from the underlying neuronal population: from the scalp with EEG (the EEG in its broadest sense), from the cortical surface with electro-corticography (ECoG), and very near the source with intracerebral electrodes (iEEG), which record local field potentials (LFPs) that comprise extracellular field voltage deflection. The associated minute magnetic field is recorded with magnetoencephalography (MEG) by means of special sensors placed around the scalp, not in direct contact.

### **2.1 Origin of M/EEG signal**

#### **2.1.1 Cellular sources**

Electrical currents underlying M/EEG are transmembrane currents generated by ionic transfer through the cellular membrane during neuronal activation. All ionic transmembrane currents contribute to transmembrane potential variations but the relation between transmembrane variations and EEG variations is not direct. The more direct link is actually

between transmembrane currents and EEG. Let us consider, as an example, the case of the opening of a sodium channel. Its electrochemical gradient pushes  $\text{Na}^+$  ions from the extracellular towards the intracellular compartment and this ionic movement constitutes an inward current. This so-called "primary" inward current is matched by an equivalent outward current (because the resistance of the membrane is not infinite), distributed along the cell membrane, which attenuates with distance. The so called "imposed" inward and outward currents generate an intracellular diffusion current, as well as an electrical field in the surrounding extracellular milieu (Pernier, 2007). Since the extracellular milieu is conductive, the electrical field generated by the imposed currents also produces extracellular currents. These so-called "secondary" currents are passively conducted in the extracellular milieu. They circulate throughout the volume of the head in such a way that the current lines close up, thereby respecting the charge conservation principle. If these currents reach the scalp and are strong enough, they generate measurable potential variations that can be recorded with EEG. The same effects would occur in opposite direction with potassium channel opening. Because of the principle of superposition, all the different extracellular fields sum up to generate the EEG signal.

Therefore, the characteristics of a recorded potential waveform (i.e. its amplitude and frequency) depend on the proportional contribution of multiple sources. This in turns depends on some spatial and temporal properties. The first are mostly represented by the orientation of different sources at the neuronal population level, as well as the distance of the recording electrode from the source, as the  $V_e$  amplitude scales with the inverse of the distance  $r$ . Additionally, the temporal coordination of different current sources, that is their synchrony, is required for a detectable signal. In other words, both spatial and temporal summation is necessary to generate an EEG signal, but the importance of these summation effects decreases with the proximity of the recording electrode.

Detectable electrical brain activity thus depends mostly on neuronal activation, which in turn depends mainly on two main phenomena: the action potential (AP) and the post-synaptic potential (PSP).

Although EEG and MEG signals are ultimately due to the same initial primary currents, MEG signals are directly generated from intracellular diffusion currents while EEG signals are directly generated from extracellular electric field (as already indicated). Indeed, if we consider a dendrite (or an axon) as a straight conducting line, then, this circulation of

current along the straight line will induce a circular magnetic field around this line whose direction is given by the rule of Maxwell's corkscrew. As for electrical fields, magnetic fields obey the principle of superposition.

The APs are fast membrane depolarizations, lasting 1 to 3 milliseconds, generated at the level of the axon initial segment or, less frequently, at the dendrite or soma (an exception is represented by calcium spikes, lasting up to 100 ms). An AP consists of a rapid change in membrane potential with the transmembrane potential switching from negative to positive. The voltage of the AP is relatively ample, measuring about 100 mV. The AP actively propagates along the axon, and without loss of amplitude. Nonetheless, despite their high amplitude, the APs are too fast to summate temporally, even if the neuronal population has been activated in a quasi synchronic manner.

Moreover, a quadrupole configuration is created along the axonal axis (Pernier, 2007); therefore the resulting potential created by the spike decreases proportionally to the cube of its distance to the source. For all these reasons, APs do not contribute significantly to the EEG. Nonetheless, if a sufficient number of neurons is activated, the summed APs may be detected and measured by LFP, all the more when the recording electrode is near to the source. Moreover, if the EEG signal is filtered in a very high frequency band, a significant contribution of AP activity to the remaining EEG signal cannot be excluded.

EEG activity is mainly contributed by PSPs. These slower post-synaptic potentials are smaller than APs, measuring about 10 mV, but are slower, lasting 10 to 20 milliseconds. For this reason when a group of neurons in a brain structure is synchronously activated by an afferent input, PSPs can efficiently sum together and thus they can be captured by the EEG.

PSPs are generated in the post-synaptic dendrite or in the cellular soma or in the pre-synaptic axon, and can be excitatory (excitatory PSP or EPSP) and inhibitory (inhibitory PSP or IPSP). Its excitatory or inhibitory nature depends on the neurotransmitter with its respective receptor and, above all on the related ionic channel. Once the excitatory neurotransmitter has bound to the receptor and the ionic channel is open, intra and extracellular ions move throughout the cell membrane following their respective electrochemical gradient. Ionic flows that depolarise neuronal membrane are excitatory, while ionic flows that hyperpolarise it are inhibitory. For instance, in the case of the EPSP, sodium channels open and Na<sup>+</sup> ions flow into the cellular milieu following their electrochemical gradient and thus depolarizing the membrane. This generates a positive electric current

directed from the outside to the inside of the dendrite. On the other hand, an example of generation of IPSP is represented by potassium currents: potassium channels are opened and  $K^+$  ions, following their gradient, move in the opposite direction, that is, from inside the neuron to outside. This outward flow of  $K^+$  ions creates a positive outward current. Consequently, in the case of the EPSP, the inward positive current due to the opening of sodium channels generates an active sink in the extracellular space at the level of the synapse. At the same time, the incoming positive current flows along the dendrite's longitudinal axis in the extracellular medium, as indicated above. This outward flow generates distributed sources on dendrite/soma membranes at some distance to the synapse. In the case of the IPSP, an active source is formed at the level of the synapse while a distributed sink is created along the membrane.

Hence such a sink-source configuration, created by the EPSP in the extracellular medium near the dendrite membrane at the synapse, would constitute a current dipole if the sink and the source were localized at a definite point. In the example of a  $Na^+$ -generated inward current, this is true for the sink but not for the source, which is distributed along the membrane. Nevertheless, if the position of the synapse is clearly asymmetrical (i.e. localized to the distal or proximal part of the dendrite), the source-sink configuration can be approximated by a current dipole in which the sink represents the negative pole and the barycentre of the positive source can be approximated to the positive pole. The same dipole, but with opposite polarity, is associated to membrane polarity changes due to the IPSP.

We have seen how post-synaptic potentials, both excitatory and inhibitory, contribute to EEG signals. Nonetheless there are some inhibitory synapses which do not generate significant IPSP and thus cannot be detected by EEG. These are  $Cl^-$  channels which are opened following GABA-A neurotransmitter-receptor binding. As the  $Cl^-$  electrochemical gradient is most often close to the resting membrane potential, the opening of  $Cl^-$  channels does not generate significant net  $Cl^-$  currents, even if it is able to inhibit the membrane depolarization by neutralization of massive sodium flow inward. Such an inhibitory activity, called a "shunting effect"- cannot be detected by the EEG.

Furthermore, certain voltage channels, endow some neurons with electrical resonance properties (Llinas, 1988). These neurons respond more effectively if the afferent volleys are close to a given frequency range that represents their electrical resonance frequency. Moreover, for sufficiently high depolarization levels, the activation of these neurons induces

self-sustained membrane potential oscillations. Their contribution to EEG has not been completely determined yet. However, it is likely that they contribute to LFP in favourable recording conditions.

These oscillations range from gamma frequency band (30-90 Hz) in some cortical interneurons, to theta-delta frequency band (1-7 Hz).

Electrical synapses or gap-junctions, establishing a direct ionic passage from a neuron's intracellular medium to another, are barely detected by the EEG as no significant extracellular current is produced. However, as they improve neuronal synchrony, electrical synapses may contribute to amplifying signals captured at a distance.

Finally, slow frequency (<1Hz) transmembrane ionic currents also exist in glial cells. Since glial cells are at least as numerous as neurons in the human brain, their contribution to slow EEG or LFP shifts could be significant. Regarding LFPs, it seems that glial cells do contribute to variations below 1Hz (Amzica & Steriade, 2000). Regarding EEG, since the geometry of glial assemblies is not perfectly defined yet, it is difficult to decide whether or not they directly contribute to slow EEG shifts. Finally, Glial cells act on the size and the composition of the extracellular milieu. As a consequence, they modify the conductance of this milieu and, as such, they indirectly modify the propagation of extracellular currents, generated by neuronal activities, to recording electrodes (Birbaumer, Elbert, Canavan, & Rockstroh, 1990; Buzsaki, Anastassiou, & Koch, 2012).

### **2.1.2 Spatial summation of cellular sources: neuronal geometry**

The EEG is sensitive to neuronal activity only if a sufficiently large population of neurons is synchronously activated. In other words, in order to obtain an EEG signal, recording electrodes need to capture the variation of potentials created by a sufficiently large number of current dipoles generated by the PSPs of many neurons summed together.

An ideal current dipole is defined as the association of a sink and a source of opposite polarity but with small separation (relative to the observation point, see Figure I.5). The electrical potential of a dipole falls off as  $1/r$ . The electrical potential created by a current dipole is  $V(P) = (1/4\pi\sigma) \cdot [(M \cdot \cos \theta)/r^2]$ ; where  $\sigma$  is the medium's conductance,  $M$  the module of the dipole's moment,  $r$  the distance from the recording point to the middle of the

segment connecting the sink and the barycenter of the source, and  $\theta$  the angle formed by the dipole and the segment connecting its midpoint to the recording point P. Since  $\cos \pi/2 = 0$ , the electric potential recorded right above a tangential dipole is zero (Figure I.5).

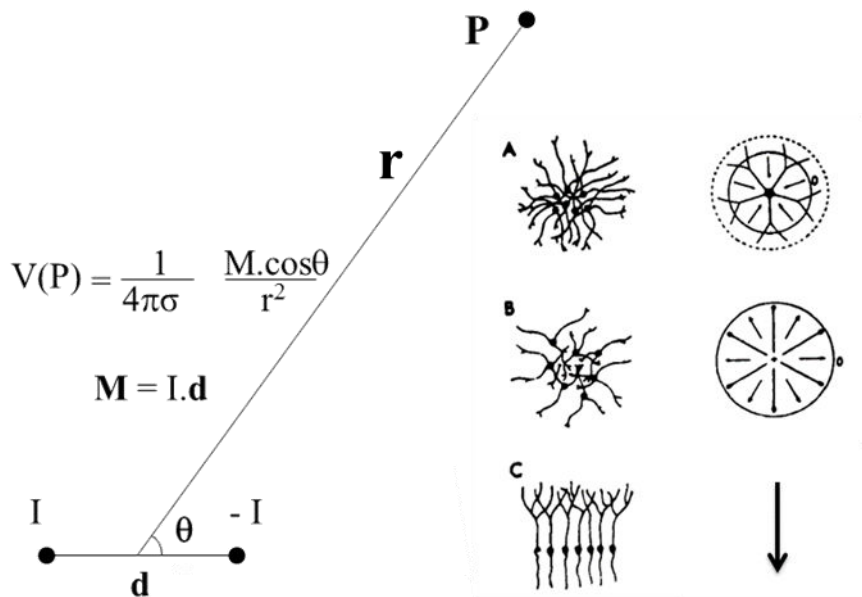


**Figure I.5 :** *Dipole and neuronal disposition*

**On the left:** electric potential created by a current dipole. **On the right:** the equivalent dipole created by neurons whose dendrites have a radial disposition (closed field geometry) with respect to the soma (A) is zero at distance, as well as for neurons randomly oriented (B); the equivalent dipole created by neurons parallel disposition (open field geometry) is showed in (C)

If a neuron's dipole is represented with a vector, the simultaneous activity of a number of neurons corresponds to the vector sum of all elementary dipoles. The resulting "equivalent" dipole depends on the neurons' spatial configuration (Figure I.5). If dendrites have a radial disposition with respect to cellular soma or if neurons are randomly oriented, the electrical field resulting from the simultaneous activation of all neurons, that is, the resulting equivalent dipole, is zero at a distance. These neurons generate so called "closed fields". This is the case of several subcortical structures, such as midbrain nuclei whose neurons do not have a laminar parallel disposition or even of some "rolled" cortical structures such as the hippocampal formation. On the other hand, if soma-dendrite's axes are all oriented in parallel, synchronous elementary activations of such a neuronal population can summate. This "open field" configuration results in currents that are conducted up to the recording electrode. Pyramidal

neurons of the cortex, for example, form open fields: they are arranged in palisades with the apical dendrites aligned perpendicularly to the cortical surface so that their summed elementary dipoles generate an equivalent dipole whose activity can be detected by electrodes placed at relatively large distances (Figure I.6).

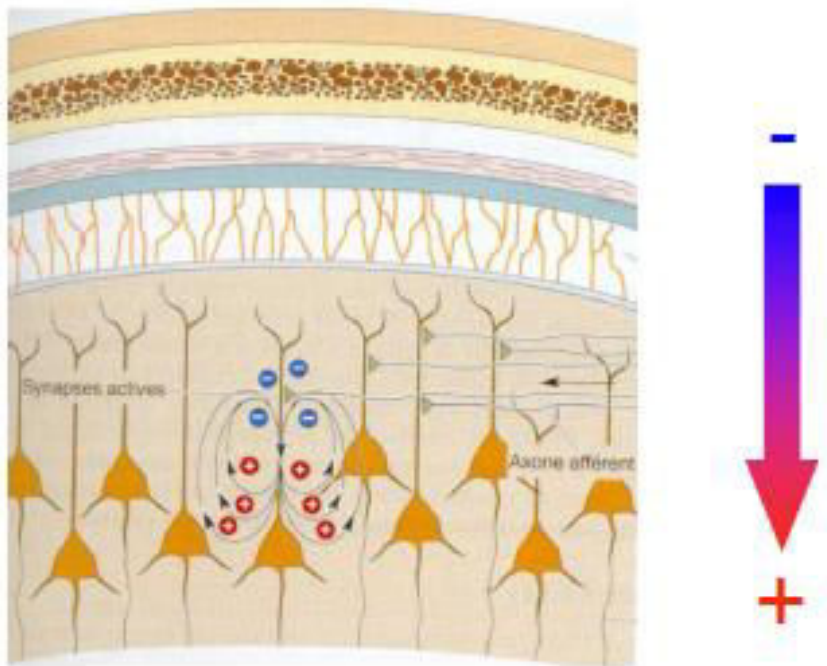


**Figure I.6 :** *Equivalent dipole*

*A dipole is created along the apical dendrite's axis of this pyramidal neuron receiving stimulation from surrounding neuron. The excitatory synapses at this point on dendrite generates an electric dipole whose negative pole is directed toward the scalp.*

To sum up, it is possible to record electrical activity of the brain and any transmembrane current, irrespective of its origin, contributes to an extracellular voltage deflection. Nonetheless:

1) The EEG represents mostly cortical activity, but certain subcortical structures because of their favourable cytoarchitectonic organization, can generate activity recorded with EEG (Lorente De No, 1947).

2) Within cortical activity, the EEG is able to detect almost exclusively pyramidal neurons' activity, or other neurons with palissadic organization, as they are disposed in an open field configuration which allows spatial summation. Activity from most interneurons is not visible;

3) Within pyramidal activity, the greatest contribution to the EEG signal comes from dendritic activity, that is, the PSPs. Actually these potentials are slower and long-lasting, which allows temporal summation;

4) Within dendritic activity, some synaptic activity with inhibitory effects cannot be detected (i.e. the  $\text{Cl}^-$  channels opening because of the absence of significant net transmembrane currents at the channel's opening). Likewise membrane voltage oscillations and gap-junctions' current are likely not "seen" by the EEG.

### **2.1.3 Synapse position and polarity**

Let's consider a pyramidal neuron located on a gyrus. Axons from contralateral cortex via corpus callosum create an excitatory synapse on the apical dendrites of superficial layers of the cortex (layers II-III). Subsequent EPSPs will generate a current elementary dipole whose negative pole will be superficial, as well as the negative pole of the equivalent dipole corresponding to the population to which it belongs, which will be oriented toward the scalp. Therefore, a negative deflection will be recorded by the EEG. On the other hand, if the cortico-cortical synapse is inhibitory, elementary and equivalent dipole orientations will be reversed, with a superficial positive pole, and a scalp electrode recording a positive deflection in voltage.

Now let's take a thalamo-cortical excitatory synapse. The axon originating in the thalamus raises the deeper layers (layer IV-V) and the synapse is near to the cellular soma. In this case the negative pole will be deep and the positive pole will be superficial, directed toward the scalp. Hence the scalp electrode will record a positive voltage deflection. Conversely, a thalamo-cortical inhibitory synapse will generate a negative voltage deflection at the EEG (Figure I.7).

Consequently, without any prior information, EEG does not allow the excitatory or inhibitory nature of the neuronal activity underlying the recorded potential deflection to be known. Nevertheless, it is clear that if two different conditions generate activity of different polarities, they represent two different physiological phenomena.

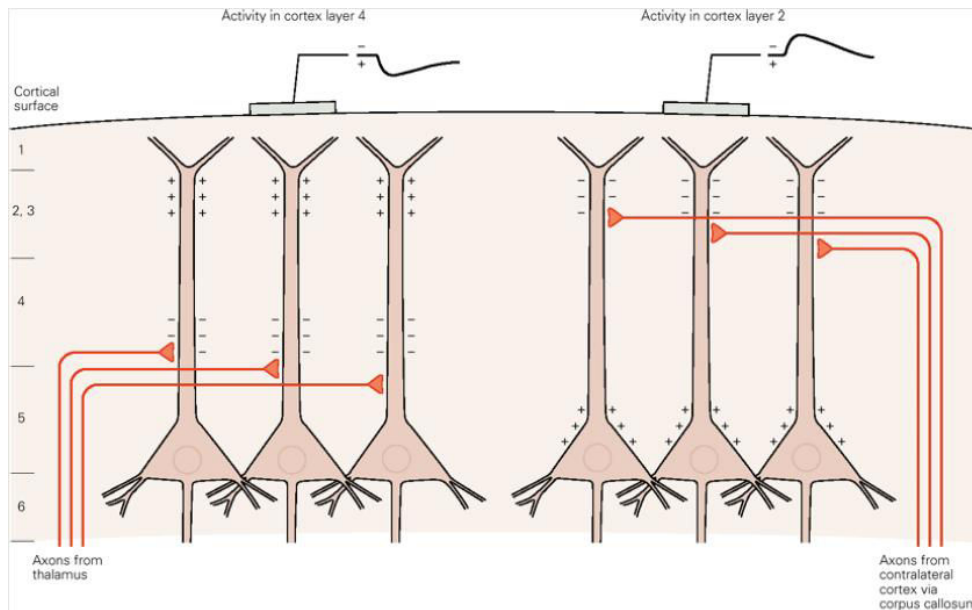


**Figure I.7 :** *Excitatory and inhibitory synapses*

**On the left:** excitatory thalamic input to basal dendrites in layers IV results in EPSP and an extracellular sink. A passive source is generated at the apical dendrites and current flows toward cell body, generating a positive potential at the surface. **On the right:** excitatory input to layer I generates an EPSP in apical dendrites and an active sink. A passive source is generated at the soma resulting in current flowing toward layer I, generating a negative potential at the surface

## 2.2 The role of generator's position and volume conduction on M/EEG signal

### 2.2.1 Cortex architecture and generator position

The amplitude and waveform of EEG and MEG potentials depend on magnitude, distance and orientation of the current generator. The electric potential of a dipole scales with the inverse of the square of distance  $r$  ( $1/r^2$ ) between the source and the recording site. Consequently, the larger the distance between the electrode and the current source, the less intense is the measured potential.

In addition, electrical potential  $V$  depends on the orientation of the dipole with respect to the recording site. To that effect, the highly folded nature of the human cortex substantially affects, in different and somehow opposite ways, the EEG and MEG signals recorded on the scalp. In fact, neurons located on a gyrus have apical dendrites perpendicular to the overlying scalp, and thus their equivalent dipole aligns with the scalp electrodes (these are called radial

dipoles). Instead, neurons located in the wall of a sulcus have dendrites located parallel to a tangent to the scalp at the recording site (these are called tangential dipoles) (Figure I.8).

Recorded potential  $V$  is directly proportional to the cosine of the angle between the dipole and the segment joining the recording site to the middle of dipole. As  $\cos 0 = 1$  and  $\cos \pi = -1$ , the recorded potential  $V$  at an electrode placed right above the generator is maximal (or minimal) if the dipole is radial. This is the case of neurons occupying the top of a gyrus, whose associated dipoles are radial (perpendicular to the scalp). On the other hand, as  $\cos \pi/2 = 0$ , recorded potential  $V$  at an electrode place right above the generator is zero if the dipole is tangential, as in the case of neurons located in the wall of a sulcus. Thus, for such a tangential dipole, maximal and minimal potentials are recorded by scalp electrodes located not directly above the dipole but at a certain distance, with resulting lower amplitude compared to a radial dipole of the same module.

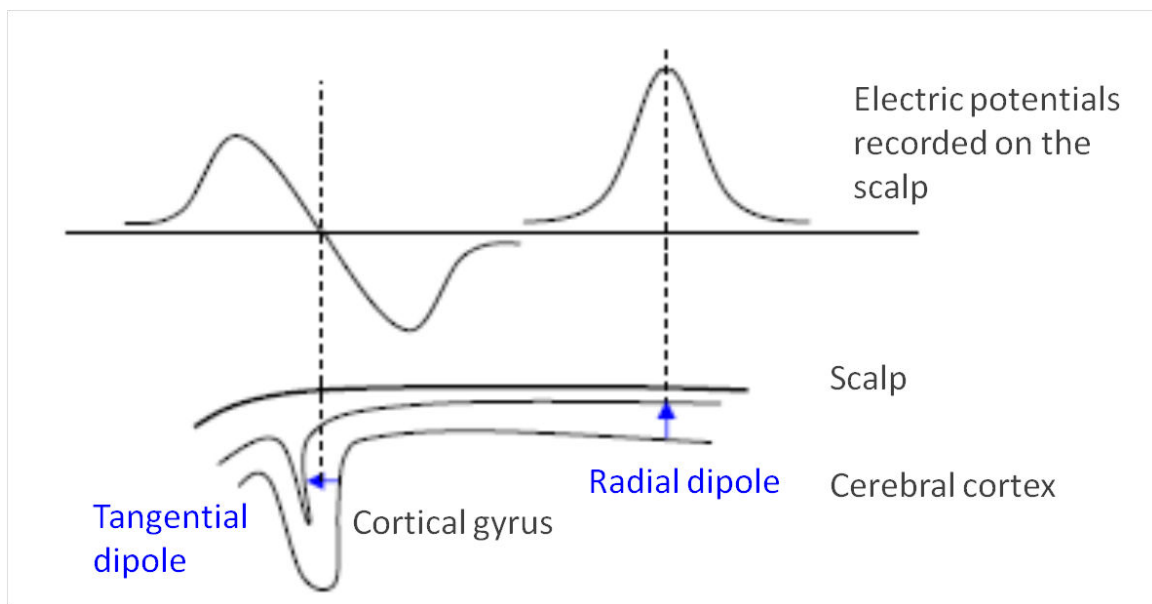


**Figure I.8 :** *Radial and tangential dipole measurement on the scalp.*

*Cortex is folded and orientation of the dipole layer can change. The dipole sheet lies along the gyrus and in to the adjacent sulci. Radial dipole (on the right) produces deflections in roughly one direction, while tangential dipole produces both directions of deflection.*

The orientation of neurons with respect to the skull is even more important for MEG signals. Magnetic fields are generated by intracellular diffusion currents generated by primary currents. These diffusion currents generate magnetic fields circulating around the direction of the current. These fields are able to generate induced current in conductive media such as the

brain. For radial currents, the induced currents generate themselves “secondary” magnetic fields which tend to cancel the “primary” ones. This results in almost unrecordable extracephalic fields. For tangential currents, cancellation is incomplete because of their much more asymmetric effects in the head volume, as compared to that of radial dipoles.

Therefore the MEG is able to detect mostly magnetic fields perpendicular to the scalp generated by tangential neuronal currents, that is, the ones located in the sulci. Contrarily, the magnetic field generated by neurons in cortical gyri, are oriented perpendicular to the skull and are not well detected by the MEG.

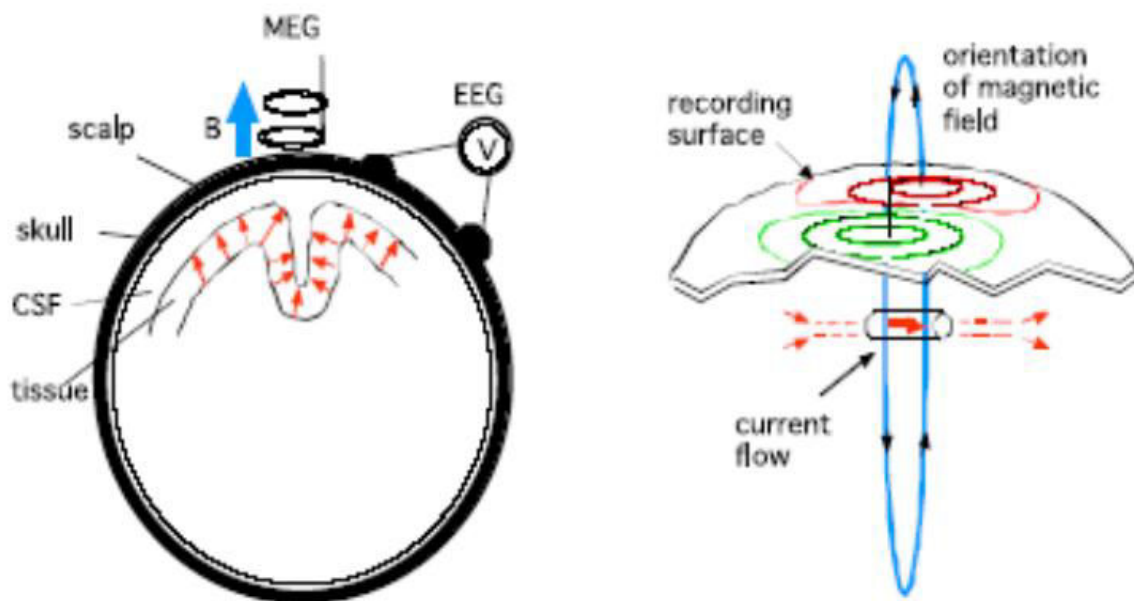


**Figure I.9 :** *Magnetic field of the brain.*

*A tangential current created by neurons located in the sulci generates a magnetic field perpendicular to the scalp which can be detected by the MEG.*

### 2.2.2 Volume conduction

To reach the recording sites on the scalp, electric currents have to cross a non-homogeneous biological medium composed of other cells, white matter, cerebrospinal fluid (CSF), meninges, skull bones and scalp. The phenomenon of current circulation through a volume is called volume conduction. The extent of this phenomenon depends on features of the conductive medium, namely the degree of isotropy and homogeneity of extracellular milieu. Skull bones have a high electrical resistance, therefore electric currents progress with difficulty through it; consequently electrical currents spread parallel to the skull surface,

where resistance is smaller, and thus creates a diffusion effect. Thus, electric potentials are “smeared” on the surface EEG and, as a consequence, two distinct but temporally and/or spatially close cortical generators appear as a unique diffuse scalp potential. This “blurring” effect is known as the volume conduction problem. Bone is transparent to magnetism and magnetic fields are not affected by the resistance of the skull (although MEG signals are not completely unaffected, because of the cancelling effects of induced intracerebral currents). Thus accurate reconstruction of the neuronal activity that produced the external magnetic fields requires simpler models than for EEG, that is to say, the volume conduction problem is easier to solve in MEG than in EEG.

## **2.3 Possible solutions**

### **2.3.1 Source estimation**

One, and probably the main, challenge of EEG and MEG recording is to solve the difficulty of identifying the neuronal generators of the recorded signal, based on the distribution of electrical potentials and magnetic fields obtained on the scalp. This problem is called the EEG/MEG “inverse problem” and it is an ill-posed problem because for all admissible output voltages, the solution is non-unique and unstable (the solution is highly sensitive to small changes in the noisy data) (Lopes da Silva, 2010). In other words, there is an infinite number of possible source configurations which could lead to a superficial pattern of scalp electric potentials and scalp magnetic fields. Hence, it is necessary to constrain the sources, that is, to make *a priori* assumptions about the nature and configuration of the sources (i.e. number of sources, sparsity, anatomical and neurophysiological constraints, etc) in order to reduce the range of possibilities. In other words, as there is no correct answer to the inverse problem, we can only find which one seems to be the best from an anatomophysiological standpoint among the alternatives we have considered. The accuracy and validity of the estimates depend to some extent on the biological correctness of the assumptions and priors adopted in the chosen model. There are different source models (not detailed here), that is, different mathematical models used to approximate the current density, which all require assumptions about brain physiology to make the problem soluble.

### 2.3.2 *Blind signal separation*

One might be interested in separating the different activity generated by different sources, starting from a scalp electromagnetic field, and thus also localizing sources themselves. To this end, blind source separation algorithms recover individual sources from a mixture of sources.

Principal component analysis (PCA) (Gorsuch, 1983) and independent component analysis (ICA) (Onton, Westerfield, Townsend, & Makeig, 2006) are statistical methods based on statistical interdependency of recorded signals. ICA is based on the assumption that scalp activity is a linear combination of a limited set of elementary brain signals, with temporal independence, i.e. the independent components. ICA allows each component from the mixture of components to be extracted, and thus to estimate the independent time courses and scalp topography of each different MEEG component. This method has been successfully used to study EEG components of error and correct response evoked potentials (S Hoffmann & Falkenstein, 2010; Roger, Bénar, Vidal, Hasbroucq, & Burle, 2010). PCA, is based on the same assumptions as ICA but it aims to reduce the numbers of variables in the dataset, by binning highly correlated variables together. Otherwise, spatial filtering can be used in order to improve spatial resolution of EEG signals. Surface Laplacian estimation (SL) (Hjorth, 1975) represents the spatial variation of an electric field and acts like a high-pass filter by removing the blurring effect of current diffusion through the skull. It is obtained by the computation of spatial second derivatives of recorded potential  $V$  (depending on  $x$  and  $y$  directions of the scalp tangential plan).

$$\Delta V(x,y) = \partial^2 V(x,y)/\partial x^2 + \partial^2 V(x,y)/\partial y^2$$

$\Delta V$ : Laplacien of the electric potential

$x$  and  $y$  : Cartesian coordinates of the plane tangential to the surface of the scalp

$V$ : function of these two variables, that describes the spatial distribution of the potential

SL is proportional in a location to the gradient of the radial component of the scalp current density (SCD) (Pernier, Perrin, & Bertrand, 1988), also called “current source density” (CSD). In other words, SL is maximal just at a current source (that is, where the current exits radially from the scalp) and minimal just at a current sink (that is, where the current enters through the scalp). Therefore, SL informs as to where the current exits or enters the scalp, so that it supplies a maximum just over the generator of a radial dipole and rapidly falls off with

distance. Concerning tangential dipoles, SL tightens the distance between positive and negative maxima, as compared to potential recordings, “deblurring” the scalp representation of underlying generators (Pernier et al., 1988). In this way electrical activity resulting from different generators is better separated, that is spatial resolution is markedly improved. Furthermore, SL also allows for a clear improvement in temporal resolution, since the two dimensions – spatial and temporal - are interdependent. Indeed, two different event-related potentials, owing to volume conduction, tend to spatially overlap on the scalp and as a consequence of this spatial fusion, their time courses can also overlap and mix, making them distorted (Burle et al., 2015). Therefore, improving the spatial separation by reducing volume conduction, allows a marked improvement of temporal separation of signals (Burle et al., 2015).

As we will see in the next chapter, SL has been used to uncover a small EEG component associated with action monitoring, which would otherwise be overlain by a larger EEG deflection (F Vidal, Hasbroucq, Grapperon, & Bonnet, 2000).

## **2.4 High frequency neuronal oscillation**

Cortical neurons in the mammalian forebrain are known to form neuronal networks which oscillate, that is, generate repetitive and rhythmic activity. These oscillating networks reflect coherent neuronal population behavior at different spatial scales. At the level of individual neurons, we can observe either oscillations in membrane potentials or rhythmic occurrence of action potentials, which produces oscillatory activation of post-synaptic neurons. At the level of neuronal ensembles, synchronized activity of a large number of neurons can give rise to macroscopic oscillation observed with EEG (Berger, 1929). Oscillations can be characterized by their amplitude, phase, and frequency, ranging from approximately 0.05 Hz to 500 Hz. These signals have been labeled as a function of their frequency from human scalp EEG with Greek letters: delta (0.5-4 Hz), theta (5-7 Hz), alpha (8-12 Hz), beta (12-30 Hz) and gamma (30-100 Hz). This classification was supported by multivariate statistical analysis of EEG spectral values (Lopes da Silva & Schomer, 2012; Lopes da Silva, 2011).

As these oscillations are phylogenetically conserved (Llinás, 2014), they are doubtlessly functionally relevant, and have aroused the interest of neuroscientists. In

particular, since the rise of broad-band digital EEG and MEG and the finding of 30-600 Hz oscillations in animal cortical and subcortical structures (Bressler & Freeman, 1980), gamma and high-gamma (from 60 Hz) oscillations (HGO) have attracted particular attention in recent decades. Indeed gamma oscillations have shown to be able to bind together, through a process of phase synchronization, the firing of neurons at a local level. In addition to local synchronization, this oscillatory activity enables connection of neuronal activity of spatially separated cortical areas (Roelfsema, Engel, König, & Singer, 1997). Thus, HGO are now acknowledged as a general and versatile mechanism of the neuronal processing of information, mediated by entrainment of neuronal networks. This way, relevant information could be transferred between distinct brain systems. EEG, MEG and i-EEG have enabled observation of the behavior of this high frequency activity during a variety of sensori-motor and cognitive tasks (C. S. Herrmann, Frund, & Lenz, 2010). Therefore, HGO and synchronization are widely considered to be involved in many cerebral functions such as perception, awareness, action and cognition (Engel, Fries, & Singer, 2001; Fries, Reynolds, Rorie, & Desimone, 2001).

### **3 COGNITIVE CONTROL: EEG EVIDENCE**

A small number of scalp-recorded event-related potential (ERP) components have been described, which are time-related to different aspects or steps of the evaluative process. Hence they are involved in, and directly or indirectly reflect, (a part of) the action monitoring process.

#### **3.1 Error Negativity (Ne or ERN)**

The Ne is a sharp, surface-negative ERP peaking just after error commission in RT tasks. It was first described in the early 1990s (Falkenstein, Hohnsbein, Hoormann, & Blanke, 1991) and is also called Error-related Negativity (W.J. Gehring, Goss, Coles, Meyer, & Donchin, 1993). Ne has a fronto-central maximum, starts about 30 ms after the incorrect EMG activity and culminates at about 50-70 ms after the mechanical response and 100 to 130 ms after EMG onset (Figure I.10).

Given its scalp topography, this electrophysiological component is thought to be generated in the medial aspect of the frontal lobe. Source localization studies (Dehaene, Posner, & Tucker, 1994; M. J. Herrmann, Ro, Ehlis, Heidrich, & Fallgatter, 2004; Van Veen & Carter, 2002), according to fMRI data (Debener et al., 2005; M Ullsperger & von Cramon, 2004) identify the Rostral Cingulate Zone (RCZ) and particularly the anterior cingulate cortex (ACC) as the generator of the Ne (refer to chapter 4 for more details). Alternatively the Supplementary Motor Area (SMA) has been suggested as a possible source of the Ne (Dehaene et al., 1994; Garavan, Ross, Murphy, Roche, & Stein, 2002; M. J. Herrmann et al., 2004; Roger et al., 2010).

The Ne is related to action errors, that is, to the execution of an action that should have been suppressed (also called errors of action in Stop tasks and Go/NoGo tasks; (Scheffers, Coles, Bernstein, Gehring, & Donchin, 1996) or to the execution of the incorrect choice of action (also called errors of choice in choice RT task). More generally, errors associated with decisions concerning actions generate a Ne. Ne has been described for incorrect responses given with the hand, finger, foot and eyes (Falkenstein, Hoormann, Christ, & Hohnsbein, 2000; C. Holroyd, Dien, & Coles, 1998; Nieuwenhuis, Ridderinkhof, Blom, Band, & Kok, 2001). Similarly the presence of the Ne does not depend on stimulus modality (visual or auditory, (Falkenstein et al., 1991). This suggests that the action monitoring system that the Ne represents is generic and modality non-specific.

Since the Ne was initially observed exclusively after incorrect responses, it has been considered specific to errors and interpreted as a signal of error detection ((Falkenstein et al., 1991; W.J. Gehring et al., 1993; C. Holroyd et al., 1998). Nonetheless Ne does not reflect error awareness, since error detection can be automatic and the Ne occurs even when an error is committed unconsciously (Hajcak, Donald, & Simons, 2003; Nieuwenhuis et al., 2001). Alternatively Ne is thought to represent the conflict between competitive responses (Yeung, Botvinick, & Cohen, 2004) or, in the context of reinforcement-learning theories, a signal of reward-prediction error (C. B. Holroyd & Coles, 2002).

Ne has been described in a totally de-afferented patient (Allain et al., 2004) who had no lemniscal sensitivity, namely proprioception. This demonstrates that the Ne can be generated by an internal signal, without the need for proprioceptive reafference.

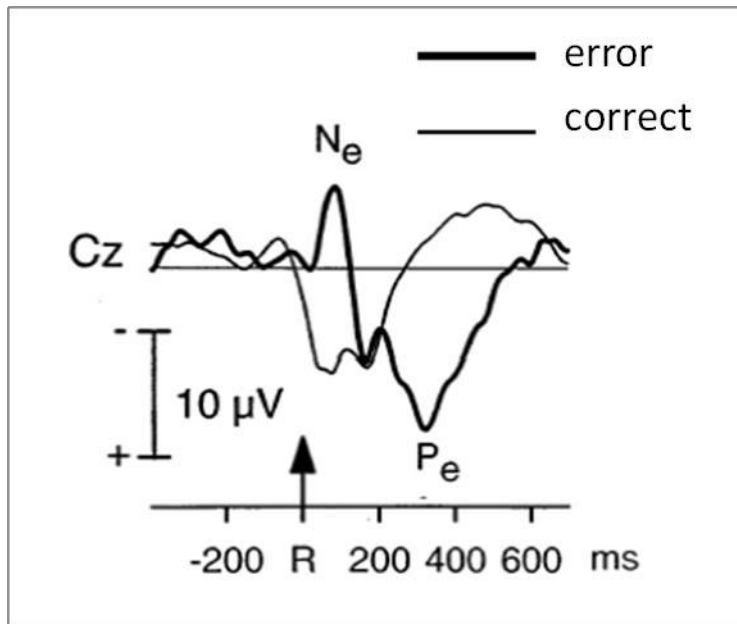


**Figure I.10 : The Error Negativity**

*Averaged response-locked ERP waveforms for both error and correct trials during a choice RT task (adapted from Falkenstein et al, 1991).*

### ***Ne on partial errors***

Finally, the Ne has also been observed during partial errors, that is, on correct trials preceded by an incorrect EMG activation on the wrong side (Scheffers et al., 1996; F Vidal et al., 2000). Ne of partial errors follows incorrect EMG activation, but it starts earlier (Masaki & Segalowitz, 2004) and it most often has a smaller amplitude compared to Ne of overt errors (F Vidal et al., 2000).

The presence of the Ne on incorrect EMG bursts supports the idea that 1) partial errors have a functional meaning in terms of on-line action control, and 2) the Ne represents a manifestation of error-related processing but it is not directly associated with error correction (Scheffers et al., 1996). This last hypothesis has been tested by Hajcak and Simon (Hajcak & Simons, 2008). These authors correlated Ne amplitude to the accuracy of the following trial in order to investigate whether the Ne could predict subsequent performance: whatever the sequence (correct-error-error or correct-error-correct) Ne amplitude on the second erroneous trial was the same. This result seems to confirm the idea that the Ne indicates the need for increasing cognitive control but it is not directly related with consequent behavioural adjustment.

### **Ne on correct trials: the Ne-like**

Finally a negative ERP, analogous to the Ne, has been described for correct responses. Called Correct-response Negativity by Ford (Ford, 1999), Ne-like by Vidal (F Vidal et al., 2000) and Correct Negativity (Nc) by Falkenstein (Falkenstein, 2004), it is a medialfrontal negativity, occurring just after response execution, topographically and morphologically similar to the Ne, but smaller than the Ne in normal individuals (Figure I.11). Actually Nc was first reported by Ford in schizophrenic patients, in whom it had the same amplitude as the Ne. Nonetheless, given its small amplitude in normal subjects (even smaller than the Ne during partial errors) early studies did not note the presence of this small negativity and its existence on correct trials was initially disputed (Michael G H Coles, Scheffers, & Holroyd, 2001; F Vidal, Burle, Bonnet, Grapperon, & Hasbroucq, 2003). Vidal et al were able to observe the Ne-like in normal subjects thanks to the computational power of Laplacian transformation, which acts as a high pass spatial filter and increases EEG spatial resolution (see chapter 2). In fact this technique revealed the Ne-like which is otherwise overlain by a more posterior and ample positive component (Burle et al., 2015; F Vidal et al., 2003, 2000).

Although the existence of the Ne-like is now widely accepted, its functional meaning is still debated. A primary question is: are the Ne and the Ne-like distinct components reflecting distinct processes within the cognitive control system? Or rather, are they equivalent manifestations of the same action monitoring process? The importance of this question lies in the fact that this last hypothesis would challenge almost all actual models accounting for the Ne.

## **3.2 Error Positivity (Pe)**

On error trials, immediately after the Ne, a broad positive component with centro-parietal topography can be observed (Falkenstein et al., 1991). It is usually called “Error Positivity” (Pe) and it culminates at about 300 msec after EMG onset (Figure I.10). As the Pe differs from the Ne in terms of scalp distributions and timing, it seems to reflect different aspect of error-related processing with respect to the Ne. Significantly the Pe is specific to overt errors, as it is absent on correct responses and on partial errors (F Vidal et al., 2000). Interestingly the Pe was found to be present exclusively in conscious errors or to be more pronounced for perceived than for unperceived errors (Nieuwenhuis et al., 2001). Moreover

when Pe amplitude is reduced, post-error slowing is also reduced or even absent (Murphy, Masaki, & Segalowitz, 2006). For these reasons the Pe is generally thought to be the electrophysiological correlate of error awareness. However some authors hypothesize that the Pe reflects the affective processing of errors or rather a P300-like component associated with the motivational significance of the error (Overbeek, Nieuwenhuis, & Ridderinkhof, 2005). Few studies have attempted to localise the generator of the Pe. Brazdil et al (Brázdil, Roman, Daniel, & Rektor, 2005), thanks to intracerebral ERP, propose multiple common cortical structures at the origin of the Pe and Ne, namely anterior cingulate cortex, mesial temporal structures and prefrontal regions. Other ERP scalp studies suggest a different generator for this positive late component, located in the posterior part of the ACC (M. J. Herrmann et al., 2004; Van Veen & Carter, 2002).

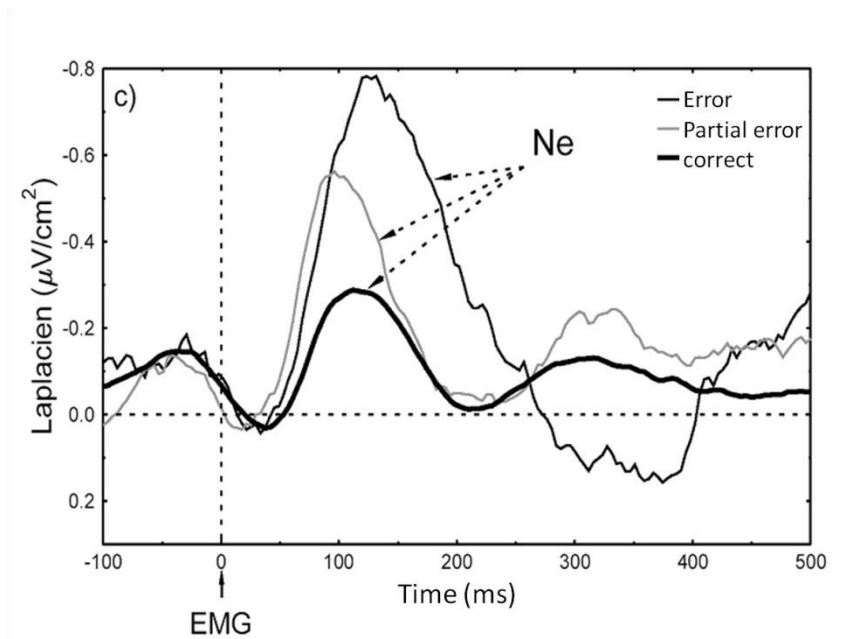


**Figure I.11 : The Ne and the Ne-like**

*Grand-averaged EMG-locked ERP waveforms for error, partial error and correct trials during a choice RT task. Amplitude of the Ne varies as a function of response types. Partial error evoke a negative ERP whose amplitude is smaller compared to errors, and correct responses evoke an even smaller, but well visible, negative deflection (adapted from Vidal et al, 2000).*

### 3.3 Feedback related Negativity (FRN)

In tasks delivering a feedback about response accuracy, a cerebral activity elicited by feedback presentation can be observed, clearly greater for negative than for positive feedback, called feedback-related negativity (FRN). This is a negative ERP with fronto-central polarity which has been associated to the Ne (Figure I.12). FRN is evoked by negative feedback whatever its modality (visual, auditory or somatosensory) (W.H.R. Miltner, Braun, & Michael, 1997). However contrary to the Ne, FRN peaks later, at about 250-330 msec after feedback delivery, and its amplitude is smaller. It was first described for a time-estimation task, which required subjects to respond with a button press after a 1-s interval and provided external feedback about response accuracy. Since then, the same FRN has been observed in reinforcement-learning situations, in which subjects have to learn a rule based on external feedback delivered on each trial that provides information about response accuracy (Ruchow, Grothe, Spitzer, & Kiefer, 2002). Source localization analysis and fMRI studies point to the ACC as the generator of the FRN, as for the Ne (Dehaene et al., 1994; M. J. Herrmann et al., 2004; C. B. Holroyd & Coles, 2002; Nieuwenhuis, Holroyd, Mol, & Coles, 2004; Ruchow et al., 2002; Van Veen & Carter, 2002). This has led authors to conclude that the mechanism of error processing reflected by the FRN for time estimation or reinforcement-learning tasks is the same as the one reflected by the Ne for RT tasks (W.H.R. Miltner et al., 1997). Therefore Ne and FRN are two ERPs that are considered to reflect a comparable physiological process of error evaluation, the Ne as a consequence of internal feedback, the FRN as a consequence of external feedback.

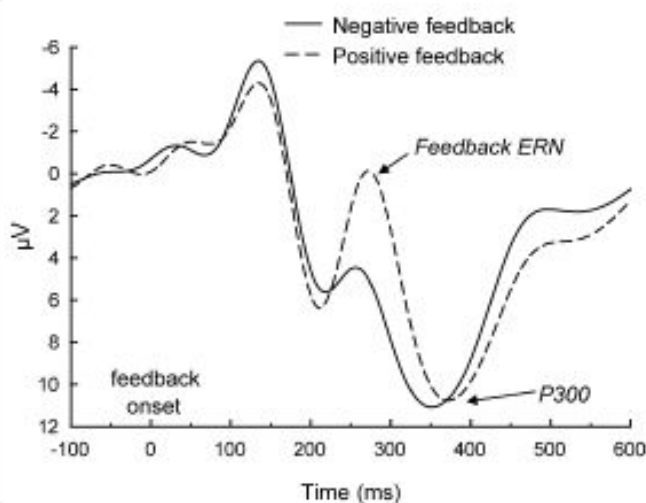


**Figure I.12 :** *The feedback-related negativity.*

*Averaged stimulus-related brain potential associated with negative and positive feedback (from Nieuwenhuis et al, 2004).*

## **4 STRUCTURES INVOLVED IN ACTION MONITORING AND UNDERLYING THE NE**

Evidence from functional neuroimaging studies, source localization studies and direct cerebral recordings in non-human primate converge in attributing various regions within the prefrontal (and medial premotor) cortex as participating in different aspects of cognitive control.

We will first review anatomy and connectivity of medial prefrontal and premotor areas of the frontal lobe, and secondly describe the presumed functions of the different regions in action monitoring

### **4.1 Anatomy, connectivity and functional organization of premotor and prefrontal cortex**

Prefrontal cortex can be roughly divided, anatomically and cytoarchitectonically, into three main divisions: lateral PFC (LPFC), medial prefrontal cortex (MFC) and orbitofrontal cortex (OFC). Premotor cortex also extends on both medial and lateral aspects of the frontal lobe.

Caudally on the medial wall we find the premotor cortex, which is constituted by agranular cortex and comprises the medial part of Brodmann areas (BA) 6 and 8 (note that BA8 is sometimes considered a border area between premotor and prefrontal cortex). BA6 is not a cytoarchitectonically and functionally homogeneous area, but is rather composed by different areas with different afferent and efferent connections underlying different functions in motor control (M Matelli & Luppino, 2001).

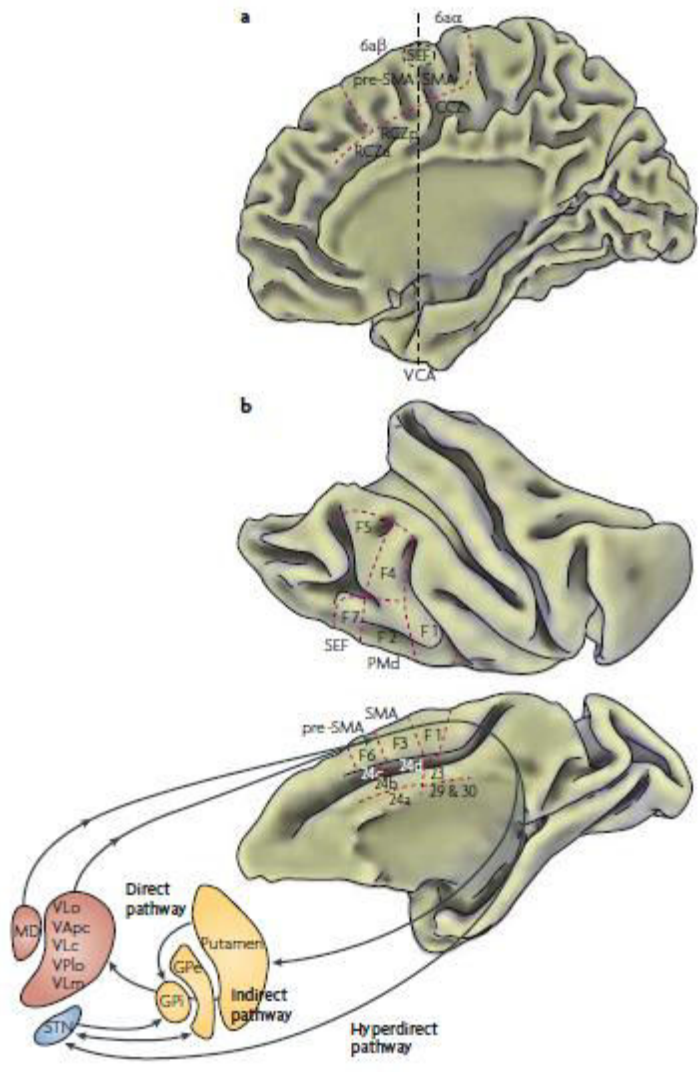


**Figure I.13 : Premotor areas**  
*Anatomy of the Supplementary Motor Areas in human and monkey and their connections with basal ganglia in monkey (from Nachev et al, 2008)*

***The Supplementary motor Area***

On the mesial aspect of Brodmann area 6 lies the supplementary motor area (SMA), which is located immediately anterior to BA4 (Penfield & Welch, 1951). Within this region a recent fractionation into two functionally distinct sub-areas has been proposed: the more caudal supplementary motor area (SMA or SMA proper) in BA 6aα (C. Vogt & Vogt, 1919) or field F3 (M Matelli & Luppino, 1991; Massimo Matelli, Luppino, & Rizzolatti, 1985), and the pre-supplementary motor area (pre-SMA) in the BA 6aβ or field F6 (M Matelli & Luppino, 1991; Massimo Matelli et al., 1985), virtually separated by the vertical line passing

through the anterior commissure (VCA line). The supplementary eye field lies at the border between SMA and pre-SMA, close to the paracentral sulcus. This subdivision is based on different cytoarchitectonic and connectivity patterns (M Matelli & Luppino, 1991, 2001) (Figure I.13). The SMA is somatotopically organized and has direct connections to primary motor cortex and spinal cord, suggesting a direct implication in motor output. Nonetheless SMA has more indirect projections to the spinal chord via the intermediate zone (lamina VI and lamina VII) than direct cortico-motoneuronal connections on lamina IX compared to primary motor cortex projections, suggesting rather that SMA contribute to preparation and selection of movements, which are known to involve spinal interneurons, via a modulation of the excitability of intrinsic spinal circuitry (Maier et al., 2002).

In contrast to SMA, pre-SMA is more strongly connected with prefrontal regions, as well as the Supplementary Eye Field (SEF), but both areas are connected with the insula, the superior temporal sulcus and the parietal lobe. Nonetheless, rostral SMA shows a more similar connectivity pattern with caudal pre-SMA rather than with caudal SMA, indicating an overlap in connectivity profiles within different subregions, rather than a clear segregation (Nachev, Kennard, & Husain, 2008).

Both SMA and pre-SMA are connected with basal ganglia: the internal segment of the globus pallidus (GPi) projects through the thalamus to both the SMA and the pre-SMA, which in turn sends efferents to the striatum. The striatum, connected directly and indirectly to the GPi, thus closes this cortico-subcortical loop (Akkal, Dum, & Strick, 2007). Even if both SMA and pre-SMA receive cerebellar input, as a whole they are dominated by basal ganglia input (Akkal et al., 2007).

Finally the SMAs have a hyperdirect connection to the subthalamic nucleus (STn) “an important route through which ongoing activity in cortical-basal ganglia circuits can be rapidly ‘broke’ by the SMC (Nachev et al., 2008).

The SMA and the pre-SMA represent particularly interesting regions for cognitive control. Indeed functional neuroimaging has provided evidence that these areas are involved in multiple aspects of motor behavior, such as movement execution, movement inhibition, motor learning and motor planning. Movement execution activates both SMA and pre-SMA but with a caudal to rostral shift of activation with increasing task complexity (Sergent, Zuck, Terriah, & B, 1992; Sergent, 1993). For example in pianists, pre-SMA is activated during the

cognitive/motor demands of playing unfamiliar pieces rather than while playing scales as for the SMA (Sergent et al., 1992; Sergent, 1993).

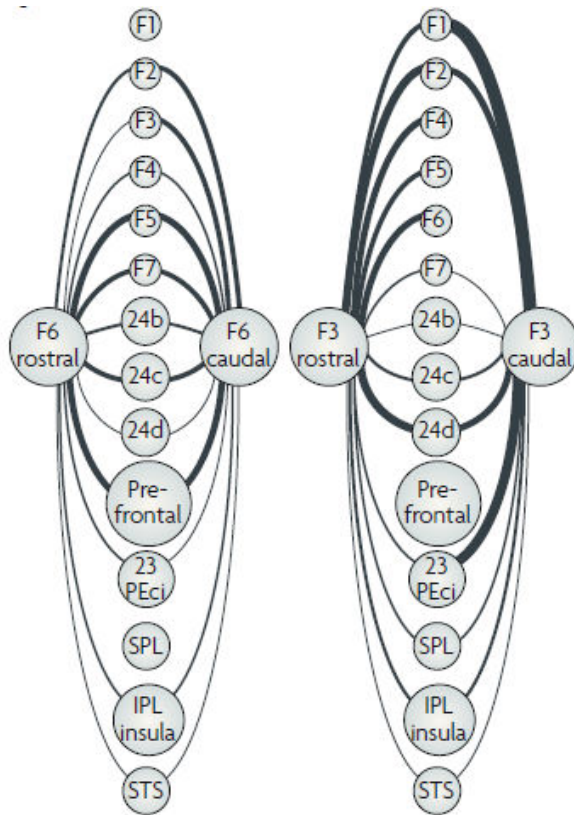


**Figure I.14 : Connectivity of the Supplementary Motor Areas**

*Synthesis of connectivity in monkey's SMAs (from Nachev et al, 2008). PEci: posterior part of the cingulate sulcus; SPL: superior parietal lobule; IPL: inferior parietal lobule; STS: superior temporal sulcus.*

Consistently, motor training produces a progressive decrease in pre-SMA activation (Friston, Frith, Passingham, Liddle, & Frackowiak, 1992) and performance improvement is associated with increasing of activation in the SMA (Grafton et al., 1992). These findings suggest that the SMA and pre-SMA are involved in motor learning and development of automaticity. Still these areas, and particularly the pre-SMA, also have a key role in voluntary action, as its activity seems to be greater for self-initiated movements than for externally triggered ones (Cunnington, Windischberger, Deecke, & Moser, 2002). The SMA (and the SEF) is also involved in movement inhibition, that is, suppressing motor programs that may be subconsciously primed for example by viewing graspable objects (Sumner et al., 2007). Finally, another function attributed to the SMA is time processing (Macar, Coull, & Vidal, 2006).

### *The Anterior Cingulate Gyrus*

On the medial wall of the cerebral hemispheres lies an annular circonvolution which includes the cingulate gyrus, the cingulate sulcus and the paracingulate gyrus, which all together constitute the cingulate cortex. Cingulate cortex can be divided along a rostro-caudal axis into a posterior granular region in the parietal lobe, the posterior cingulate cortex (PCC), and an anterior agranular region in the frontal lobe (except a “dysgarnular” organization in area 32) (Brodmann, 1909; B A Vogt, Rosene, & Pandya, 1979). This rostral part is called anterior cingulate cortex (ACC) and comprises BA 33, 24, 25 and 32.

Within the ACC we can distinguish:

- 1) a ventral limbic tier, containing BA 24a, 24b and subcallosal area 25. These are connected with ventral OFC (BA13), amygdale and ventral striatum
- 2) a dorsal paralimbic area containing BA 32 and 24c, buried in the cingulate sulcus and extended into the paracingulate gyrus. These are connected with dlPFC (BA46), ventral and polar OFC (BA14, 11, 10)

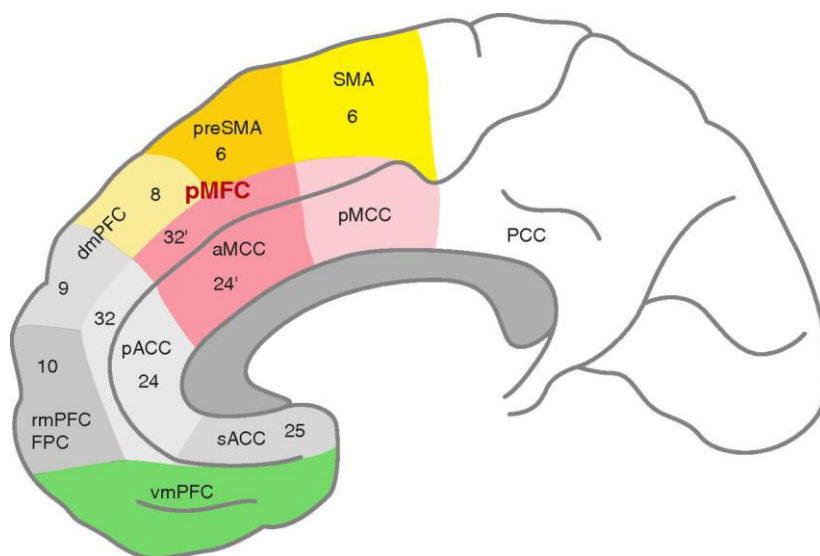


**Figure I.15 : Subregions of the medial frontal wall.**

*The cingulate cortex is divided into anterior, middle, and posterior portions, further subdivided into the subcallosal (sACC) and pregenual (pACC) anterior cingulate cortices, the anterior and posterior midcingulate cortices (aMCC and pMCC, respectively), and the posterior cingulate cortex (PCC) (from Ullsperger et al, 2010).*

Furthermore in the caudal division of the ACC, a qualitatively different region in terms of connections and receptor binding can be identified: the midcingulate cortex (MCC) (Palomero-Gallagher, Vogt, Schleicher, Mayberg, & Zilles, 2009). The MCC contains the human gigantopyramidal fields, which correspond to monkey cingulate motor area, and are located in the more posterior part of BA24, in the cingulate sulcus, approximately on the vertical plane passing through the anterior commissure. Within the MCC we can differentiate two cingulate motor areas corresponding to the anterior MCC (aMCC) and a posterior MCC (pMCC) (Picard & Strick, 1996). In addition Picard & Strick (Picard & Strick, 1996) functionally identify, within the cortex adjoining the cingulate sulcus, the rostral cingulate zone (RCZ) and the caudal cingulate zone (CCZ) based on focal activations during various experimental conditions. The whole cingulate region begins with the pregenual BA32 and continues caudally up to the posterior border of BA24. The CCZ is defined by activations associated with simple motor tasks, and is located in front and behind the VCA line, that is in BA24a corresponding to the pMCC. The RCZ, in rostral area 24 and area 32, is activated by more complex tasks requiring response selection and generation of different motor behavior, and is activated in conjunction with the PFC (Picard & Strick, 1996).

These motor fields receive inputs from the primary motor cortex, the SMA and pre-SMA, the premotor cortex and parietal cortex and send direct corticospinal projections. Electrical stimulation of MCC evokes complex and context-dependent motor responses (J Talairach et al., 1973). Posner et al (Posner, Petersen, Fox, & Raichle, 1988) provided the concept “attention for action”, which integrates premotor function orientation more specific to pMCC, with the potential role of this region in cognitive control, and with the affective/emotional processing of action, which seems more specific to aMCC. These functions include mismatch/conflict resolution (Carter et al., 1998), response selection toward punishment/reward outcome (Shima & Tanji, 1998), error detection (Carter et al., 1998), anticipation/expectancy (Critchley, Mathias, & Dolan, 2001), prediction error (C. B. Holroyd & Coles, 2002), feedback mediated decision making (Kennerley, Walton, Behrens, Buckley, & Rushworth, 2006), nociception (Hutchison, Davis, Lozano, Tasker, & Dostrovsky, 1999) and emotion (Lane et al., 1998). To sum up the MCC seems to provide a cognitive interface with motor system via its prefrontal connections with dlPFC, BA25 and 32 and via its motor projections to motor/premotor areas, dorsal striatum and spinal cord.

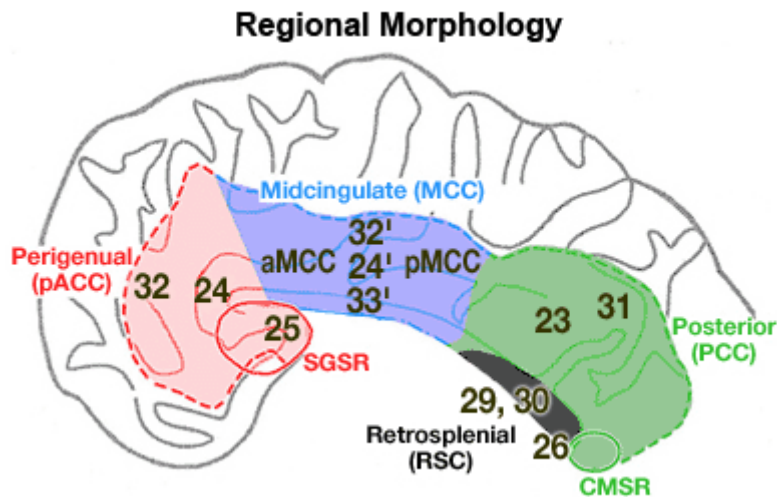


**Figure I.16 : Human cingulate cortex.**

Four region neurobiological model of human cingulate cortex (from Vogt, <http://www.cingulumneurosciences.org/images/regional-morphology.gif>).

### *The Orbito-frontal cortex (OFC)*

The OFC consists of BA14 medially, BA13 ventrally, BA11 ventrally and anterior to BA13, and extends laterally to BA47/12 and rostrally to frontopolar BA10. All these area are considered to be part of the so-called “orbital and medial prefrontal network” (Carmichael & Price, 1996; Ongür & Price, 2000), which distinguish: 1) the orbital network, receiving afferents from all sensorial and visceral modalities, 2) the medial network, visceromotor, also including BA25, rostral BA32 and 24, with no sensorial afferents but connected to PCC, the amygdala, the superior temporal gyrus and the hypothalamus. Both orbital and medial networks are connected to the LPFC. The orbital network, which comprises a striato-pallidus-thalamo-cortical loop, seems to evaluate stimulus-reward/punishment associations leading to behavioural change; the medial network, with its connections, would participate in the limbic system (Kringelbach & Rolls, 2004).

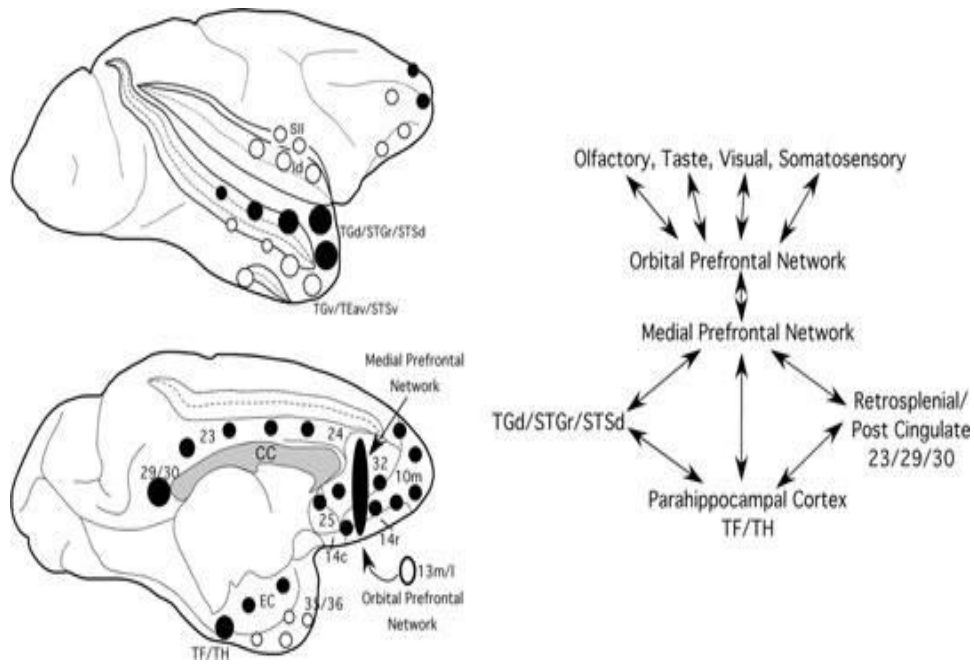


**Figure I.17 : *Orbito-medial cortex***

*Connectional network within the orbital and medial prefrontal cortex of macaque monkeys (from Carmichael & Price, 1996)*

***The lateral pre-frontal cortex (OFC)***

The LPFC can be further divided into:

- ventro-lateral PFC (vlPFC) located in the pars opercularis and pars triangularis of inferior frontal gyrus, corresponding to BA44 and BA45 respectively, and connected with the SMA via the Aslant tract
- dorso-lateral PFC (dlPFC), comprising BA9/46, BA46 and BA8a. It is connected with frontopolar OFC (BA10) and, specifically BA46 is connected with pre-SMA>SMA, lateral BA6 and FEF (BA8)

dlPFC is thus a richly interconnected region, with intrinsic and extrinsic interactions with frontal and extra-frontal associative, as well as with premotor regions, representing a critical “hub” in the control of various aspects of behaviour.

## 4.2 The role of medial frontal cortex in action monitoring

### 4.2.1 *The Anterior Cingulate Cortex*

The anterior cingulate cortex, and particularly the functional region called RCZ (Picard & Strick, 1996), represents *the* structure that is brought to mind when talking about error and/or conflict (that is the competition between two or more alternative responses). These questions have been extensively investigated by means of functional neuroimaging – namely fMRI -, scalp EEG, and direct intracerebral recordings in monkey. A large number of studies in human and primates describe the activation of largely overlapping medio-frontal areas, clustering in the RCZ, during monitoring of response error, negative feedback, response conflict and decision uncertainty (Ridderinkhof, Ullsperger, Crone, & Nieuwenhuis, 2004).

***Monitoring response error.*** fMRI studies in humans have shown an increase of BOLD signal in the ACC in the case of errors compared to correct responses during choice RT tasks. Carter et al (Carter et al., 1998) reported that this region is active during erroneous responses and when there is increased response competition. Moreover, ACC is active when error risk is unexpected, for example, on incongruent trials occurring in a series of congruent trials. The authors thus conclude that the ACC may have an evaluative role, by detecting conditions under which errors are likely to occur, rather than error themselves.

Ullsperger & Von Cramon (Markus Ullsperger & Cramon, 2001a) studied the hemodynamic and electrophysiological (namely the Ne) correlates of response competition and error processing during a two-alternative forced-choice task. The authors found that pre-SMA and medial BA8 were preferentially activated by response competition. On the other hand the MCC, in the depth of anterior cingulate sulcus, was preferentially activated for erroneous responses. The authors thus suggest that the ACC has a major role in error processing and that it is involved in the generation of the Ne. On the other hand they conclude that pre-SMA is involved in conflict detection and/or resolution between alternative responses, a role which is habitually attributed to the ACC.

Nonetheless it is quite problematic to relate a metabolic/hemodynamic activity to an EEG activity. For this reason Debener et al (Debener et al., 2005) conducted a study coupling EEG and fMRI measures of performance monitoring in humans. These authors found that single trial Ne was able to predict the BOLD fMRI activity in the RCZ and proposed the RCZ as the source of the Ne.

Indeed, irrespective of the functional significance of the Ne, several electrophysiological studies have applied source localization approaches in order to uncover the generator of this ERP. Dehaene et al (Dehaene et al., 1994) first identified the ACC as a probable source of the Ne (but discussed that the SMA could also be a possible generator). This result has been subsequently reproduced by means of different models of source localization (M. J. Herrmann et al., 2004; Phan Luu, Tucker, Derryberry, Reed, & Poulsen, 2003; Markus Ullsperger & Cramon, 2001b; Van Veen & Carter, 2002).

***Monitoring response conflict.*** Another hypothesis about the role of the ACC in cognitive control is that this region is in charge of monitoring response conflict in order to improve cognitive control and subsequent behavioural adjustment (Botvinick et al., 2001). Response conflict occurs when a stimulus activates more than one response tendency, as for example during incongruent trials in choice RT tasks. Kerns et al (Kerns, 2006) performed an fMRI study during tasks with high level of conflict in the required response (Simon task and Stroop task) and found that ACC was activated in trials preceding behavioural adjustment. Furthermore, post-conflict and post-error behavioural adjustments were associated with LPFC activity and this PFC activity was predicted by conflict-related ACC activity on the previous trial. In other words, the ACC would be responsible for conflict monitoring and thus for signalling the need for greater cognitive control.

***Monitoring negative feedback.*** Finally some source localization studies and functional neuroimaging studies have focused on the role of MPFC in the evaluation of external information regarding error commission, that is, of externally delivered negative feedback. Some electrophysiological studies have identified the ACC as the most likely generator of the FRN during time-estimation tasks or choice RT tasks (Phan Luu et al., 2003; W.H.R. Miltner et al., 1997). In the context of a gambling task, Gehring & Willoughby (William J Gehring & Willoughby, 2002) localized the FRN evoked 250 msec after a monetary loss, in the ACC. In accordance, several fMRI studies have shown increased ACC activation when negative feedback is delivered (Amiez et al., 2016; C. B. Holroyd et al., 2004; Ullsperger & von Cramon, 2003), suggesting that this region is sensitive to external sources of information on errors. Yet, fMRI studies have shown that hemodynamic responses to negative feedback is not only limited to the ACC but, instead, involves a larger network including medial PFC (Ullsperger & von Cramon, 2003), dlPFC (van Duijvenvoorde, Zanolie, Rombouts, Rajmakers, & Crone, 2008), OFC, and insula, depending on the studies (Rushworth, Noonan, Boorman, Walton, & Behrens, 2011).

*Non-human primates' recordings.* Animal studies allow a direct appraisal of cerebral activity thanks to the possibility of direct recordings in regions of interest. Microelectrodes allow measurement of both adjacent neuronal unit activity, that is, the action potentials, and local field potentials (LFPs) issued from a neuronal population located a few millimetres away.

In a now classical experiment conceived to study action monitoring, monkeys performed a saccade countermanding task, that is, they had to cancel a partially prepared saccade to the target in the context of stop signal. In the case of successfully cancelled saccades, monkeys received a positive reinforcement. Ito et al (Ito, Stuphorn, Brown, & Schall, 2003) recorded single-unit activity in the ACC (dorsal bank of the anterior cingulate sulcus, area 24c) and found two populations of neurons: 1) error-related neurons discharging after non-cancelled saccades, and 2) reinforcement-learning neurons discharging at the presentation of the juice reinforcement in correctly cancelled trials. However, no ACC signalling conflict neurons were found. Authors thus concluded that the ACC monitors the consequences of actions and signals a comparison of predicted and actual outcomes, but it does not signal the amount of conflict engendered by the co-activation of two mutually exclusive responses. Nakamura et al (Nakamura et al., 2005) instructed monkeys to perform a rightward or leftward saccade as a function of cue colour, both in spatially compatible and incompatible conditions. Similarly to Ito et al, the authors found no conflict-related enhancement of activity neither in the ACC nor in the SEF.

Other data support the idea that the ACC is involved in action monitoring, particularly in feedback evaluation. Michelet et al (Michelet, Bioulac, Guehl, Escola, & Burbaud, 2007; Michelet, Bioulac, Guehl, Goillandeau, & Burbaud, 2009), similarly to Amiez et al (C Amiez, Joseph, & Procyk, 2005), actually found ACC neurons responding to both positive and negative feedback, with increased firing for negative outcomes. Furthermore, in another experiment, they found that ACC activity during a warning stimulus following an erroneous trial, is correlated with a decrease in error rate in the next trial (Michelet et al., 2009), suggesting that both error detection and subsequent behavioural adjustment are processed in the ACC.

Looking for the equivalent of the Ne in monkeys, Emeric et al (Emeric et al., 2008) recorded the LFP elicited in the ACC of monkeys performing a saccade stop signal task. They found that LFPs elicited by erroneous non-stopped saccades were larger than LFPs elicited by

correctly stopped saccades. They also found negative feedback-related LFPs signalling the absence of reinforcement after an error, but they found no LFP signalling response conflict. Similarly, the same research team (Godlove et al., 2011) found that monkeys exhibit scalp ERPs corresponding to the Ne and the Pe, when they commit an error during saccade countermanding tasks. The authors concluded that evoked activity in macaque ACC is modulated by error and feedback, but not by conflict.

#### **4.2.2 *The Supplementary Motor Area(s)***

Although less often mentioned than the ACC in human or monkey studies on performance monitoring, the SMA represents another possible candidate as the generator of the Ne and thus as the supervisor of sensori-motor operations. Luu et al (Phan Luu et al., 2003) performed source analysis of the Ne and the FRN using a theta source model, and found activation of multiple regions during error monitoring. They reported a common dorsal source for both negativities, likely corresponding to an activation of area 24 of the dorsal ACC and/or the supplementary motor area, and a second, specific source for the FRN, in the rostral ACC. Moreover, studying the temporal dynamics of theta (4-7 Hz) oscillations for the Ne, the activation of the dorsal source guided the activation of the rostral source. The authors thus hypothesized that the dorsal ACC (and/or the SMA), the common generator of both the Ne and FRN, tracks the parameters of the task (i.e. feedback, conflict) while the rostral ACC, specific to the FRN, tracks the affective evaluation of action outcome. Herrmann et al (M. J. Herrmann et al., 2004), using a different source localization technique, found significantly higher electrophysiological activity for the Ne in the medial and middle frontal gyrus, corresponding to BA 6, that is, to the SMA/pre-SMA and, to a lesser extent, in the caudal part of the ACC adjacent to BA 8.

Similarly, other source localization studies, found a Ne source in the SMA or pre-SMA (Roger et al., 2010), while an fMRI study found an activation of the pre-SMA for response competition rather than for error processing (Markus Ullsperger & Cramon, 2001a).

Likewise in non-human primate studies on performance monitoring, an involvement of the SMA has been reported. Stuphorn et al (Stuphorn, Taylor, & Schall, 2000) recorded neuronal activity in macaque monkey while performing an eye movement countermanding task. Distinct groups of neurons were found in the supplementary eye field: 1) active after

errors, 2) after successful withholding of a partially prepared saccade, or 3) in association with reinforcement. In another experiment, Scangos et al (Scangos et al., 2013) trained monkeys to perform a variant of the movement countermanding paradigm accomplished with the arm, and recorded neurons in the SMA and in the pre-SMA. The majority of cells were differentially active for three types of evaluative signals, that is, errors, reward expectation and reward signals. Furthermore a small group of neurons (called by authors “surprise cells”) responded to unexpected outcome, irrespective to its valence. Finally, LFPs evoked and modulated by errors and conflict but not by reinforcement feedback have been found in primates’ SEF (Emeric et al., 2010).

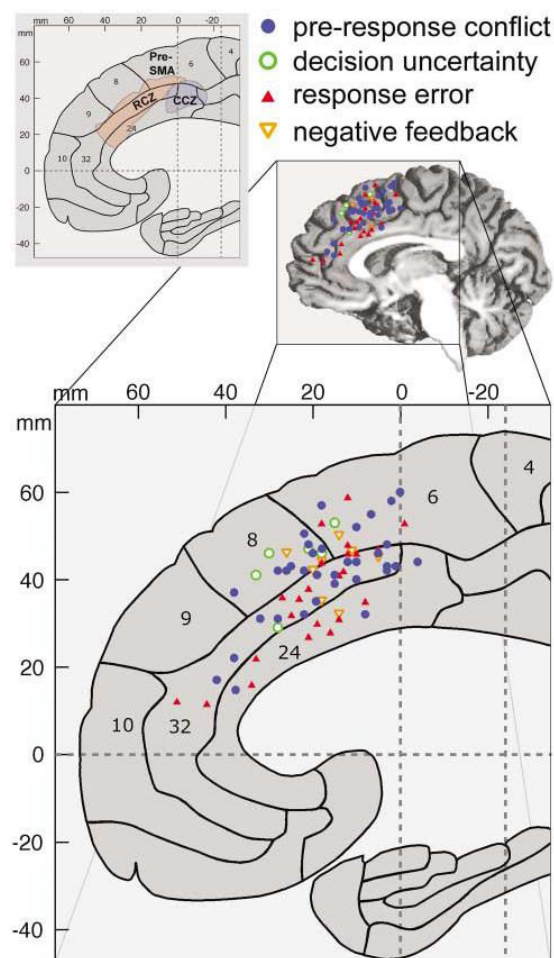


**Figure I.18 : Medial frontal cortex in action monitoring**

*Regions of the human medial frontal cortex as resulted from a meta-analysis of fMRI studies investigating brain activity related to pre-response conflict, decision uncertainty, response errors, and negative feedback (from Ridderinkhof et al, 2004)*

## 5 ASSESSMENT OF CURRENT LITERATURE AND OPEN QUESTIONS

The existence of an action monitoring system as part of cognitive control is now widely accepted. A vast literature exists, based on neuropsychological, metabolic and electrophysiological studies in humans, as well as direct electrophysiological recordings in primates. The wealth of current data helps constrain hypotheses about how action monitoring is implemented in the brain and about the neuronal networks underlying this executive function. Behavioural and EMG data have provided evidence that action monitoring operates on a trial by trial basis but also on-line within a trial. This allows re-organization of sensorimotor processing via speed-accuracy changes and re-focalizing selective attention.

Scalp EEG recordings have supplied the key electrophysiological markers of executive control, that is, the Ne, the Pe and the FRN. These event-related potentials have been integrated in different hypotheses about the functioning of cognitive control. fMRI studies have contributed to these theories and to interpretation of these ERPs. Particular attention has been dedicated to the Ne, which has been interpreted in different and somehow divergent ways, i.e. as reflecting error detection, as indicating conflict between competitive responses, or as a signal of a reward-prediction error, or even as reflecting emotional arousal associated with errors. Subsequently, the discovery of the FRN has lead some to assume that these two negativities reflect a common broad system of error evaluation, the Ne resulting from internal feedback, the FRN resulting from external feedback. Indeed, these two ERPs present the same topography, which has been interpreted to reflect a common cortical generator located somewhere in the medial wall of the frontal lobe. fMRI and source localization studies have pointed mostly to the ACC, as have direct recording in monkeys. Nonetheless, there is lack of intracerebral recording in humans and inference from monkey findings must be taken cautiously, since functional and anatomical homologies between monkey and human ACC has been questioned. Indeed, comparative cytoarchitecture studies have shown differences particularly in the ACC and in the MCC: in humans, four distinct area 32's can be recognized while monkey has only one area d32, and in monkey area 24 does not extend onto the dorsal

bank of the cingulate sulcus (A. Vogt, 2009). Based on cytoarchitectural differences in medial frontal cortex between the two species, some authors have queried the possibility that monkeys generate performance-monitoring ERPs similar to those observed in humans (Cole, Yeung, Freiwald, & Botvinick, 2010; Schall & Emeric, 2010).

To conclude, present data, whether metabolic, electrophysiological or resulting from monkey recordings, do not allow firm conclusions to be drawn about the cortical generator of the Ne.

In the experimental part of this thesis we have tried to respond to several questions that are still unsolved:

- 1) What is the cortical network underlying action monitoring? More specifically, where is the Ne generated in the brain?
- 2) Are the Ne and the Ne-like generated by the same structure?
- 3) As a consequence, what is the functional meaning of this EEG component and what does it tell us about functioning of the monitoring system?
- 4) How can we constrain the source of the Ne based on surface EEG and MEG recordings?
- 5) Do the Ne and the FRN have the same generator?
- 6) Are intrinsic and extrinsic errors treated in the same way by the same structure? That is, from a physiological standpoint, do these two negativities reflect the same monitoring process?

## **II. EXPERIMENTAL WORK**

### **6 COMMON METHODS TO EXPERIMENTAL PARTS 1 & 2**

#### **6.1 Subjects and recording procedure**

Nine subjects (7 females, 2 males, mean age  $25 \pm 8.1$ ) undergoing presurgical evaluation of drug-resistant epilepsy participated in this study. Data from first 5 patients were included in study 1, while data from all but one patients were included in study 2. General and clinical characteristics, as well as electrodes implantation are reported in the methods chapter of each study. All patients gave their informed consent prior to their participation. This study was approved by the Institutional Review Board of the French Institute of Health.

Intracerebral multiple contacts electrodes (10 to 15 contacts, length: 2 mm, diameter: 0.8 mm, 1.5 mm apart) were implanted using a stereotactic method (Jean Talairach et al., 1992). The precise anatomical position of electrode contacts was determined on individual MRIs through the superposition of anatomical MRI and computed tomography scan showing electrodes and based on anatomical landmarks as defined in the literature (Picard & Strick, 1996).

IIEG signals were acquired with a sampling frequency of 1000 Hz. No filter was applied to SEEG data. EEG was subsequently processed off-line. IIEG traces were visually inspected and segments containing artefacts were manually rejected.

#### **6.2 Simon Task**

Subjects had to perform a between-hand choice RT task, the Simon task (Simon, 1979), which is known to induce errors.

Patients were seated in a Faraday cage and stimuli were presented on a display monitor placed 70 cm from patient's eyes with an angular size of  $1.26^\circ$ . Patients had to respond with a right or left thumb keypress as fast as possible as a function of the color (red or

green) of a target stimulus (Figure. II.1). Stimulus could appear in a left or right location which was, however, irrelevant to the task. In congruent trials the target was presented on the same side as the response to be given, while in incongruent trials, target was presented or on the opposite side. A trial began with a white fixation cross in the centre of the screen followed 500 msec later by the target stimulus. Participants had to respond within 1000 msec. If they did not respond, the stimulus disappeared and the white fixation cross of the next trial appeared on the screen. Every block contained 64 trials and every patient performed a training block plus 8 to 11 experimental blocks. Five patients had to respond to a green stimulus by pressing the right key, whilst the others five patients performed the opposite stimulus-response mapping (i.e. responded to a red stimulus by pressing the right key).

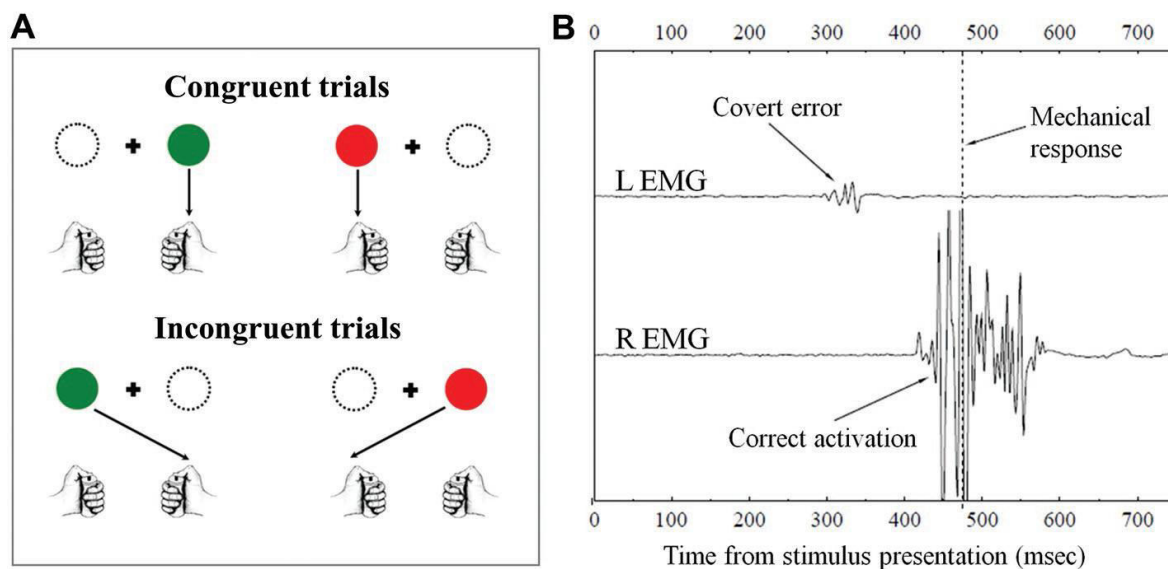


**Figure II.1 : Experimental procedure.**

(A) The Simon task is a between-hand choice reaction time task which induces errors: subjects had to respond with a left or right thumb key-press as a function of the color of a target stimulus. The target could be presented on the same side as the response to be given (congruent trials), or on the opposite side (incongruent trials). (B) Covert errors (often called partial errors) are characterized by a small sub-threshold EMG burst on the incorrect side preceding the correct response.

### 6.3 EMG recordings and trials classification

EMG activity was recorded from *flexor pollicis brevis* of each hand by paired surface electrodes (Figure II.2). EMG signals were acquired with a sampling frequency of 1000 Hz

and an acquisition band-pass filter between 0.1 and 200 Hz. EMG traces were inspected visually, and the onset and offset of EMG activity were marked manually. Visual inspection is thought to be the most accurate technique, as opposed to automated algorithms (Van Boxtel, Geraats, Van den Berg-Lenssen, & Brunia, 1993). Acquired data were analyzed 1) to estimate the intracerebral ERP (first study), and 2) to estimate the power of the gamma-band in the time-frequency domain (second study). Based on EMG onset, we sorted three categories of trials to compare: correct trials; overt error trials; and partial error trials. Partial error trials were defined by the presence of an incorrect EMG burst without any mechanical response, followed by the correct EMG burst and the correct mechanical response (Figure II.1).

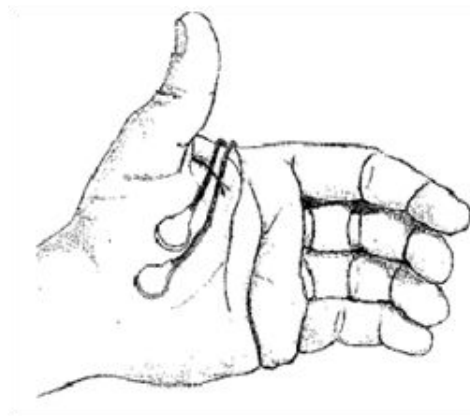


**Figure II.2 :** *EMG recording of the flexor pollicis brevis*

## 6.4 Behavioural Data

Acquired and analysed behavioural data were error rate (ER) and reaction-time (RT), both for congruent and for incongruent condition.

Additionally, distribution analyses were performed. A RT distribution analysis was carried out using the “Vincent averaging technique” (Vincent, 1912). To perform these analyses, we binned the RT distribution in ten classes of equal size (same number of trials). We computed the mean RT and the percentage of correct responses for each class in each condition (congruent and incongruent). Means of each class were then averaged across subjects. From the vincentized distributions of correct trials, the size of the congruency effect (Incongruent minus Congruent) was estimated for each class. This allowed the estimation of the evolution of the congruency effect (also called “delta plots”) to be plotted as a function of reaction time.



## **7 STUDY 1: ACTION MONITORING AND MEDIAL FRONTAL CORTEX: LEADING ROLE OF SUPPLEMENTARY MOTOR AREA**

### **7.1 Introduction**

As indicated above, several functional MRI (fMRI) and electrophysiological human and non-human primates studies indicate that the medial part of the frontal lobe has a critical role in action monitoring and more particularly the rostral cingulate zone (RCZ) has been identified as the leader of the action monitoring system (Ridderinkhof et al., 2004; Van Veen & Carter, 2002). A role of the supplementary motor area (SMA) and pre-SMA in response monitoring has however been hinted by few discordant electrophysiological source analyses of the Error Negativity (Ne), an event-related potential (ERP) considered as the signature of the action monitoring system (Falkenstein et al., 1991; W.J. Gehring et al., 1993; Sven Hoffmann & Falkenstein, 2012; Simons et al., 2010). Nonetheless, the source localization of a scalp EEG activity depends on the *a priori* assumptions about the nature of the source(s) and on the source models used. On the other hand fMRI has a low temporal resolution, and the hemodynamic changes associated to errors processing cannot be easily attributed to a scalp event-related potential (ERP), namely the Ne.

Furthermore error-related signals have been reported also in monkey's supplementary eye fields (SEF) (Emeric et al., 2010; Stuphorn et al., 2000), whose human homologue is situated in the anterior part of the SMA-proper, and more generally inferences from monkey findings must be taken cautiously because the homology of function between monkey and human motor areas must be considered cautiously. Beside, some EEG studies using Laplacian transformation, have showed a small Ne evoked by correct responses (the Ne-like) which is not visible with monopolar montage (Roger et al., 2010; F Vidal et al., 2000; Franck Vidal, Grapperon, & Bonnet, 2003). Considering that Laplacian-transformed are less sensitive to deep generators than surface potential data (Pernier et al., 1988; Pernier, 2007) it seems incongruous, although still possible, that a technique less reliable to detect deep EEG sources compared to surface potential ERPs, could detect such a source if this is located deeply in the ACC. Therefore, available data do not allow concluding firmly about the neuronal network underlying action monitoring in humans, and more specifically about the neuronal generator(s) of the Ne.

A second critical point is as well issued from the discovery of the Ne-like, which presents the same latency, waveform and topography after Laplacian computation (but not in monopolar, cfr (Franck Vidal et al., 2015) as the Ne evoked by errors or partial errors. Indeed if this small Ne-like on correct trials were a (smaller) equivalent of the Ne, this would challenge almost all the actual models accounting for the Ne. Hence, determining whether these two negativities reflect the same functional and physiological mechanism or whether they represent different processes represents a main issue. A way to answer this question is to ascertain whether they originate from the same anatomical structure or not. Different generators for the Ne and the Ne-like would indeed suggest that they represent different processes

Therefore the objective of the present study was to clarify the cortical network underlying action monitoring in humans. Particularly we intended to determine the cortical generator of the Ne and to verify whether or not the Ne-like and the Ne are generated by different structures. Our working hypothesis was that the Ne and the Ne-like are generated by the same structure(s). Since it is always delicate to ascertain an absence of difference we decided to use the most accurate hypothesis-free available method, namely : direct recording of event-related Local Field potentials (LFPs) with intracerebral EEG (iEEG). This technique, which is used for therapeutic purpose in epileptic patients, has a high spatial (millimeters) and temporal (millisecond) resolution and allow direct recording from medial and lateral cerebral cortex. Finally, we decided to use a between-hand choice reaction-time task in order to generate action errors and we chose the Simon task (Simon, 1979) as it easily induces errors, which are needed in sufficient number in order to compare them with correct responses.

## **7.2 Subjects & methods**

Five subjects (3 females, 2 males, mean age  $23 \pm 7.3$ ), undergoing presurgical evaluation of their epilepsy using iEEG, performed a Simon task (Simon, 1979). Subjects were asked to participate to this study because their implantation included electrodes exploring the frontal cortex.

Local field potentials (LFPs) were recorded from a total of 562 contacts on 42 electrodes, which were positioned predominantly in the frontal cortex. Implanted electrodes,

projected on the medial wall of cerebral hemisphere, are schematically represented in Figure II.4

The coordinates of active electrodes were converted from individual Talairach space to normalized Talairach space to allow comparison of electrode positions (reported in Table 2). Normalized MNI coordinates were obtained in order to visualize all patients' electrodes on a Montreal Neurological Institute (MNI) template (Figure II.4).

General characteristics of subjects, their implanted electrodes, as well as the number of overt and partial errors are reported in table 1.

<i>Subject</i>	<i>Sex</i>	<i>Age</i>	<i>Hand laterality</i>	<i>SEEG side</i>	<i>Epileptogenic zone</i>	<i>Electrodes</i>	<i>N° overt and partial errors*</i>
1	F	32	R	L	Rolandic	SC', SA', CC', PM', L', LI'	28/99
2	M	17	L	L	Temporal	SA', SA', LP', CR', OF', PA', OT', GLP', GPH', TP'	0/33
3	F	22	L	L	Not defined	SA', L', OF', CR', OR', A', GPH', TB', TP'	27/46
4	F	15	R	R	Insular	SA, PM, LP, CP, I, OR', H, OP, OF, FT, CCZ, A	16/80
5	M	29	L	R/L	Right Pre-frontal	SA, SA', PM, PM', CCZ', R, FP, OR, TP, OF'	75/29

**Table 1. General characteristics of subjects and of electrode implantation.** Forty seven depth multicontact electrodes were recorded across all patients, 22 of which were located within the frontal lobe, with a total of 628 contacts (42/47 electrodes and 562/628 contacts were included in the analysis as they were located in healthy cerebral tissue). SA: SMA, PM: pre-SMA, OF: Insula/frontal operculum, A: Amygdala, CR: anterior division of the RCZ, OR: orbito-medial prefrontal cortex, CC posterior division of the RCZ., CCZ: caudal cingulate zone, R: rostral inferior frontal gyrus, FP: frontal pole, TP: temporal pole, GPH: para-hippocampal gyrus, TB: temporo-basal region, LP: para-central lobulus, PA: superior parietal lobulus, OP: parietal operculum, H: Heschl's gyrus, CU: Cuneus, FCA: anterior calcarine fissure, C: hippocampus's tail, CP: posterior cingulate gyrus, FT: pars triangularis of inferior frontal gyrus, GLP: posterior lingual gyrus, OT: fusiform gyrus, L: lesion, LI: lesion. Electrodes followed by the apostrophe ' are located in left hemisphere. \*Here we report the number of errors/partial errors committed. The number of errors and partial errors actually analyzed were sometimes lower because of rejection of segments with artifacts (cfr main text for number of analyzed segments containing errors).

With the aim to evaluate action monitoring activity, event-related LFPs were averaged time-locked to EMG onset for three categories of trials: correct trials; errors and partial errors. Let us remember that partial errors are defined by the presence of an incorrect EMG burst without any mechanical response, followed by the correct EMG burst and the correct mechanical response (Michael G.H. Coles, Scheffers, & Fournier, 1995).

For analysis of data, we selected electrodes disclosing LFPs evoked by erroneous actions and modulated by performance. Within the whole responsive electrodes, in order to perform statistics, we selected the contact showing the maximal amplitude and excluded electrodes and contacts showing volume-conducted activity (see results).

Statistics were performed on individual subject data by calculating the between-trials confidence intervals with probability set to 0.05. Differences between conditions were considered significant when their confidence interval did not overlap. In order to analyse trial by trial activities from different cortical regions we performed correlation test with significance set at  $<0.05$ .

Behavioural data were analysed as reported in the previous chapter.

## **7.3 Results**

### **7.3.1 Behavioural results**

Behavioral data show a typical pattern with higher error rates on incongruent trials (8%) and lower on congruent trials (4.9%). Similarly, the partial error rate was 6.9% on congruent trials and 12.1% on incongruent trials. Correspondingly in all subjects, despite the small population, the correct trials RT was significantly longer for incongruent (492 ms) than for congruent conditions (463 ms) (unilateral Wilcoxon test,  $T =$ ;  $p = 0.028$ ), that is, the congruency effect was present in all subjects. A RT distribution analysis was carried out using the “Vincent averaging technique” (Vincent, 1912). This analysis revealed a large drop in correct response rate for fast responses on incongruent conditions, (Figure II.3) indicating that the stimulus, although irrelevant for the task at hand, tend to automatically activate the ipsilateral response (Van Boxtel et al., 1993). From the vincentized distributions of correct trials, the size of the congruency effect (Incongruent minus Congruent) was estimated for each class. This allowed the estimation of the evolution of the congruency effect (also called “delta plots”) to be plotted as a function of reaction time. As shown in Figure II.3 the congruency effect decreases as reaction time increases, as consistently reported in the

literature. This has been interpreted as reflecting the engagement of an active top-down suppression of the automatically activated response (B. Burle, Possamai, Vidal, Bonnet, & Hasbroucq, 2002; Ridderinkhof, 2002). This process takes time to build-up during the course of a trial and is, therefore, most effective for slow responses, hence reducing the size of the Simon effect for those slow responses.

Thus RT and error rate patterns indicated that subjects in the present study behaved as healthy subjects in this task.

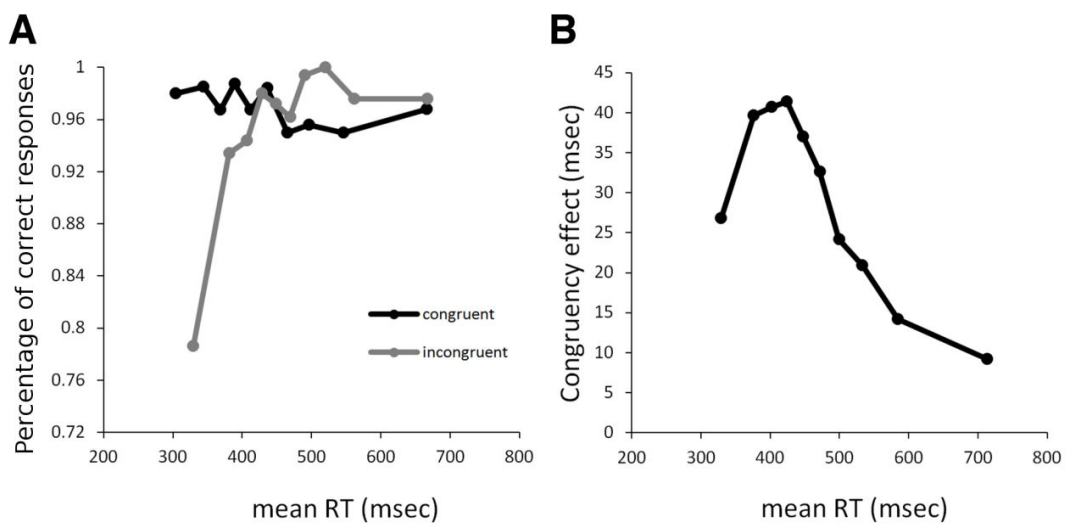


**Figure II.3 : Behavioral pattern.**

(A) Percentage of correct responses on congruent (black line) and incongruent (grey line) condition as a function of reaction time: the two lines show the typical reduction in correct response rate on incongruent trials for short reaction times only. (B) Size of the congruency effect (reaction time on incongruent trials minus reaction time on congruent trials) as a function of reaction time. The curve shows the typical decrease in the congruency effect as a function of reaction time.

### 7.3.2 Electrophysiological results

Error-evoked LFPs were observed exclusively in the medial part of the frontal lobe. One set of electrodes clustered caudally, while other electrodes were more dispersed rostrally (Figure II.4, colored dots and Table 2).

Latencies and amplitudes of averaged LFP of both clusters from each subjects and from each structures for every trial type are reported in table 3, while the time-courses of performance-related LFP are represented in Figure II.4 and II.7.

<i>Subject</i>	<i>Anatomical location</i>	<i>Talairach coordinates</i>		
		<i>x</i>	<i>y</i>	<i>z</i>
1	SMA	-11.1	-21.6	43.4
2	SMA	-9.2	-16.7	53.3
	SMA (rostral part)	-7	-2.4	43.2
3	SMA	-9.3	-2.1	50.2
	pACC	-7.5	41.4	-4.8
	OMPFC	-24.2	18.2	-9.6
4	SMA	4.7	-8.2	48.6
5	SMA	-12.7	-9	48.6
	OMPFC	3.9	29.8	-12.5

**Table 2. Electrophysiological data.** Normalized Talairach coordinates for those electrode contacts exhibiting an LFP. SMA: Supplementary motor area; pACC: pre-genual anterior cingulate cortex; OMPFC: orbito-medial prefrontal cortex

<i>Subject</i>	<i>Latency (ms) Amplitude(V) of SMA LFP for correct responses</i>	<i>Latency (ms) Amplitude (<math>\mu</math>V) of SMA LFP for partial errors</i>	<i>Latency (ms) Amplitude (<math>\mu</math>V) of SMA LFP for overt errors</i>	<i>Latency (ms) Amplitude (<math>\mu</math>V) of MPFC LFP for partial errors</i>	<i>Latency (ms) Amplitude (<math>\mu</math>V) of MPFC LFP for overt errors</i>
1	85 ms 35 $\mu$ V	73 ms 51 $\mu$ V	100 ms 125 $\mu$ V		
2	70 ms 28 $\mu$ V	100 ms 158 $\mu$ V			
3	120 ms 25 $\mu$ V	105 ms 50 $\mu$ V	135 ms 130 $\mu$ V		260 ms (pACC) 295 ms(OMPFC) 48 $\mu$ V (pACC) 77 $\mu$ V (OMPFC)
	170 ms 26 $\mu$ V	150 ms 31 $\mu$ V	190 ms 55 $\mu$ V		
5	125 ms 20 $\mu$ V	82 ms 50 $\mu$ V	125 ms 70 $\mu$ V	110 ms 70 $\mu$ V	355 ms 56 $\mu$ V

**Table 3. Latency and amplitude of averaged LFP for each trial type for each subject**

## **Performance-modulated LFP in the caudal cluster**

In the caudal cluster, all subjects presented a sharp LFP, peaking between 100 and 190 ms after EMG activation (table 3, Figure II.4). The largest LFPs occurred following overt errors, smaller after partial errors, and even smaller, but clearly still present, following correct responses (Figure II.4). Inspection of individual electrode placement showed that none of these active electrodes were positioned within the RCZ, but were clearly located within the SMA, namely above the calloso-marginal fissure and immediately posterior to the vertical commissure anterior (VCA) boundary (Figure II.4). Therefore, we can specify that the responsive structure was SMA proper.

Although intracerebral electrodes are sensitive to current within only a small volume of cerebral tissue, it is possible that the recorded activity may have been volume conducted from a remote generator outside the SMA. However three findings exclude this possibility. First of all, in all patients EMG-locked LFP recorded in the SMA sharply decreased in amplitude over a short distance in a direction leading away from the medial (SMA) and towards the lateral contacts, as shown in Figure II.5A.

Secondly, in one patient with two active electrodes within the SMAp, the LFPs showed a polarity inversion: this indicated a local generator between the two electrodes, i.e. within the SMAp (Figure II.5B)

Lastly, one patient provided a valuable experimental condition in which electrodes were implanted in both the SMA and in neighboring areas including the posterior division of the RCZ. This subject (n° 1) had two electrodes in the SMA (electrodes SC and SA), one in the posterior RCZ (RCZp, electrode CC) and another one situated rostral to the VAC boundary and above the calloso-marginal fissure (electrode PM) (Figure II.6, left panel).

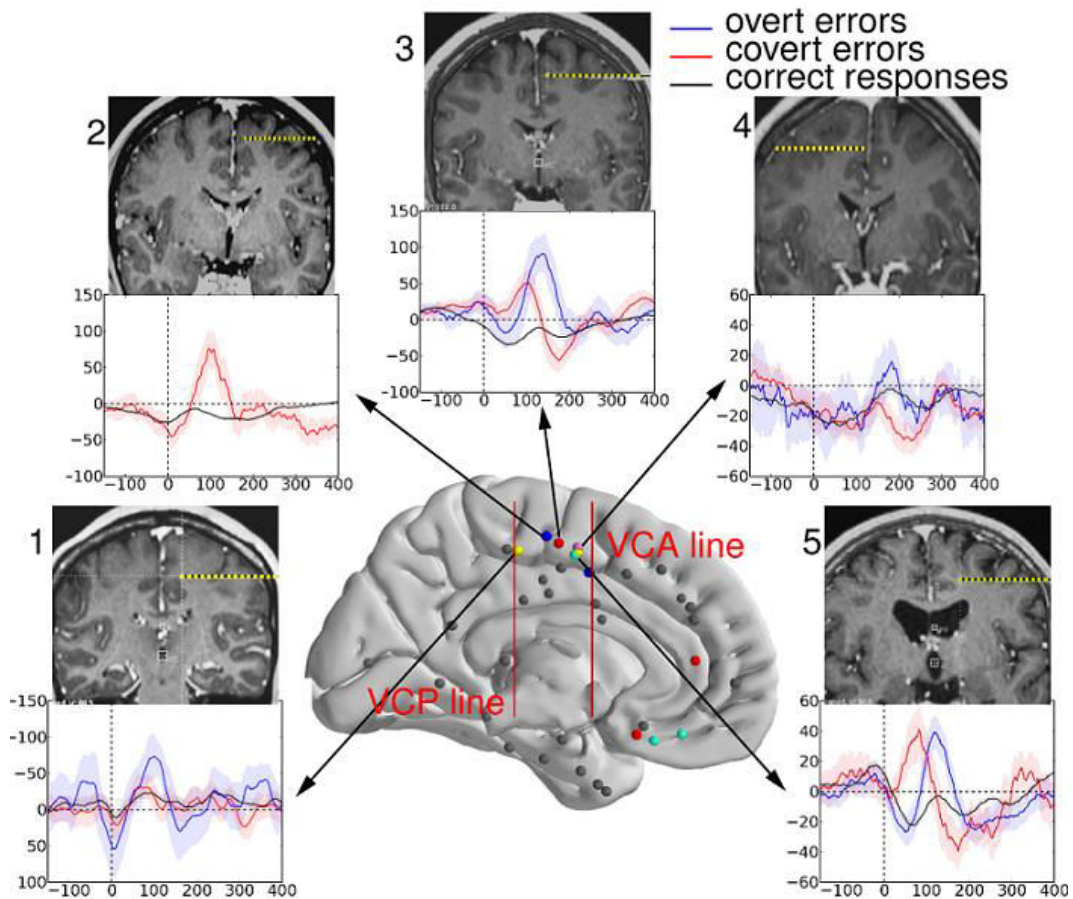


**Figure II.4 : EMG-locked LFPs in the SMA and all recording sites.**

A total of 562 contacts from 42 electrodes were included in the analysis, 34 of whom were implanted up against the medial wall. The anatomical location of these 34 electrodes' internal contacts, converted into normalized MNI brain space to allow comparison across subjects, are shown on a 3D MNI standard brain in its medial aspect. The two red vertical bars represent the VCA (vertical commissure anterior) line and the VCP (vertical commissure posterior) line. A cluster of performance-sensitive electrodes (colored dots) is located in the SMA (caudal cluster, behind VCA line) while other electrodes are more widespread in the rostral part of the medial prefrontal cortex (electrodes anterior to VCA). For each participant averaged EMG-locked LFPs recorded from the SMA are displayed: the largest LFP occurs after overt errors (blue), smaller after partial errors (red) and even smaller LFP after correct responses (black). Lighter enveloping colored bands represent between-trials confidence intervals set to 0.05. For each subject an individual Magnetic Resonance Imaging (MRI) and Computed Tomography (CT) fusion is provided, showing, in a coronal view, the trajectory of the performance-sensitive electrode. All these electrodes were clearly located above the calloso-marginal fissure and behind the VCA line, that is in the SMA.

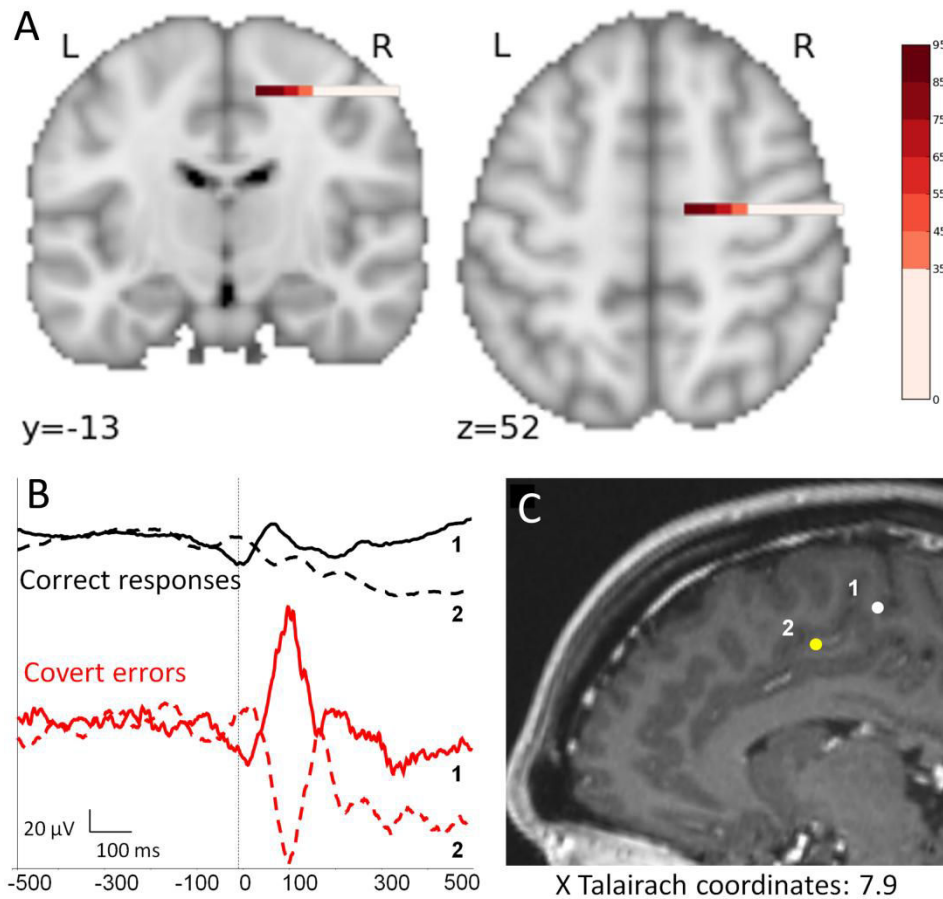


**Figure II.5 : Localization of action monitoring activity in the SMA.**

(A) EMG-locked LFPs showed decreasing amplitude from medial to lateral contacts. The amplitude of error-evoked LFPs recorded along the electrode in the SMA was averaged over subjects and is shown on a coronal and an axial view of an MNI template. The color scale represents these averaged LFPs normalized to the maximum LFP amplitude and expressed as a percentage. (B) LFPs evoked by correct responses and partial errors recorded from two overlying electrodes implanted in the SMA in subject 2. LFPs recorded from these overlying electrodes (electrode 1 and 2 respectively solid and dotted lines) showed the same morphology, the same time course and the same amplitude, but with inverted polarity. The polarity inversion could be ascertained also on single trial data, by measuring latency and amplitude of LFPs on 31 out of the 32 partial-error trials. High correlations were observed for both latencies ( $\rho = 0.94$ ;  $p < .01$ ) and amplitudes ( $\rho = 0.66$ ;  $p < .01$ ) demonstrating that the two recording sites captured the activity of the same source located in the SMA. (C) Sagittal view of patient's MRI/CT fusion scan, showing the anatomical location of electrode 1 in the upper part of the caudal SMA, and of electrode 2, underneath, implanted in the rostral SMA, at the level of VCA boundary.

A triphasic high-amplitude performance-sensitive response was recorded from anterior and posterior parts of SMap (respectively electrode SA and SC), with voltage sharply decreasing from medial to lateral contacts (Figure II.6, right panel). No EMG-locked LFP was detectable in the recording site anterior to the VCA boundary, either for correct responses, or for overt or partial errors. This indicates that the activity recorded in SMap does not arise from a more anterior region, i.e. the pre-SMA. Moreover, the amplitude of LFPs in the electrode located in the RCZp was clearly weaker with respect to SMA's activity and did not show any abrupt decrease from medial to lateral contacts, indicating that the recorded activity arose from a remote source i.e. the SMA.

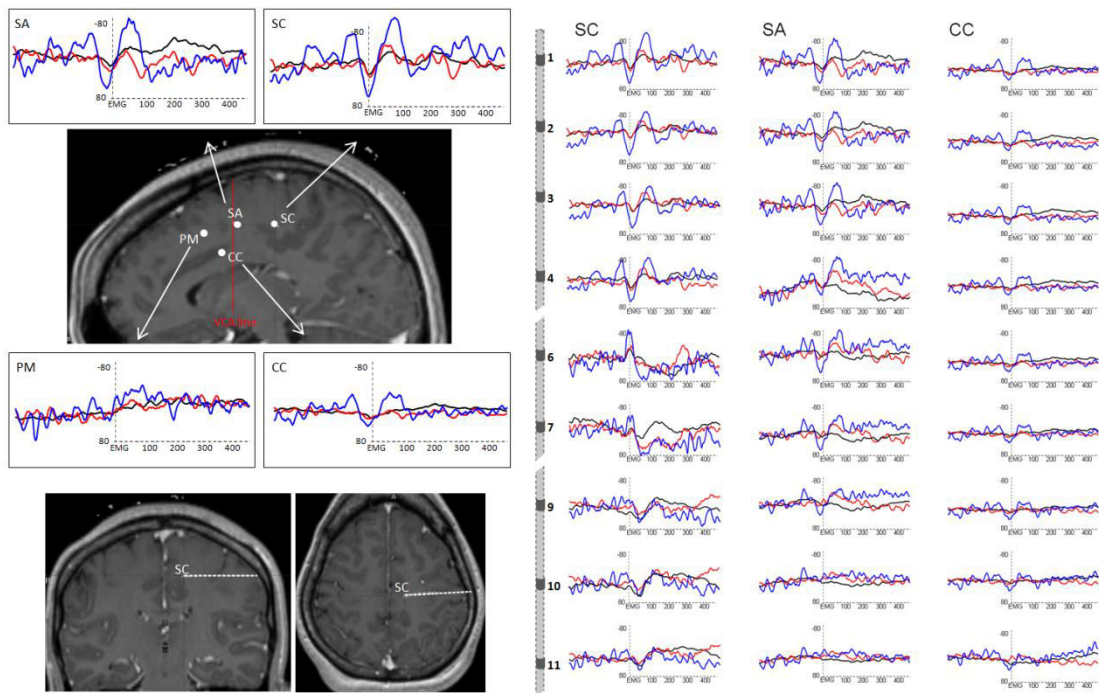


**Figure II.6 :** *Spatial sampling of the caudal part of medial frontal lobe.*

*Left panel: LFPs recorded from the most medial contact of four electrodes implanted in the medial frontal cortex and a reconstruction of the electrodes' trajectory based on individual MRI/CT fusion. Right panel: sketch of an intracerebral electrode (numbers denote contacts from medial to lateral locations) and LFPs recorded from each contact. SC medial: caudal SMA; SC lateral: motor cortex, hand area; SA medial: rostral SMA; SA lateral: premotor cortex, area 6; PM medial: pre-SMA; PM lateral: area 8; CC medial: posterior RCZ; CC lateral: ventral premotor cortex, area 6.*

## LFP in the rostral cluster

Other electrodes disclosing performance-sensitive activity were located more rostrally, in the medial prefrontal region, namely in pre-genual anterior cingulate cortex (pACC, i.e. in the anterior division of the RCZ) in patient 3 and in orbito-medial cortex (OMPFC) in patients 3 and 5 (Figure II.7 and Table 2). The activation profile of those more rostral electrodes differed from that of the caudal cluster in three ways (Figure II.7, II.8 and Table 3): i) the prefrontal activity was delayed and had a longer duration, with a caudo-rostral latency gradient (Figure II.8); ii) it was specific to errors (overt and partial); iii) it was more widespread than the activity within the SMA as demonstrated by recordings from electrodes' lateral contacts.

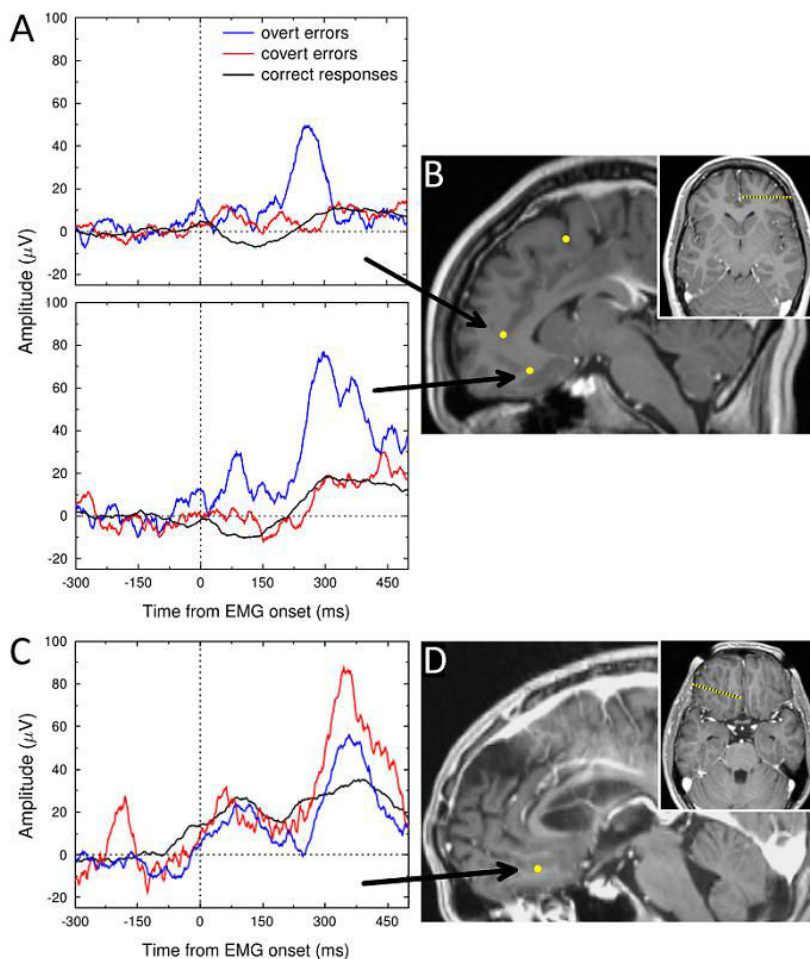


**Figure II.7 : Medial prefrontal LFPs evoked by erroneous activations.**

(A) Averaged LFPs evoked by overt errors peaking at 260 ms in pACC and at 295 ms in OMPFC in subject 3. (B) Individual reconstruction of subject 3's prefrontal electrodes based on MRI/CT fusion scan on an axial and sagittal view (note also the overlying electrode placed in the SMA). (C) Averaged LFPs peaking at 355 ms evoked by partial and overt errors in subject 5. (D) Individual reconstruction of subject 5's prefrontal electrode based on MRI/CT fusion scan on an axial and sagittal view

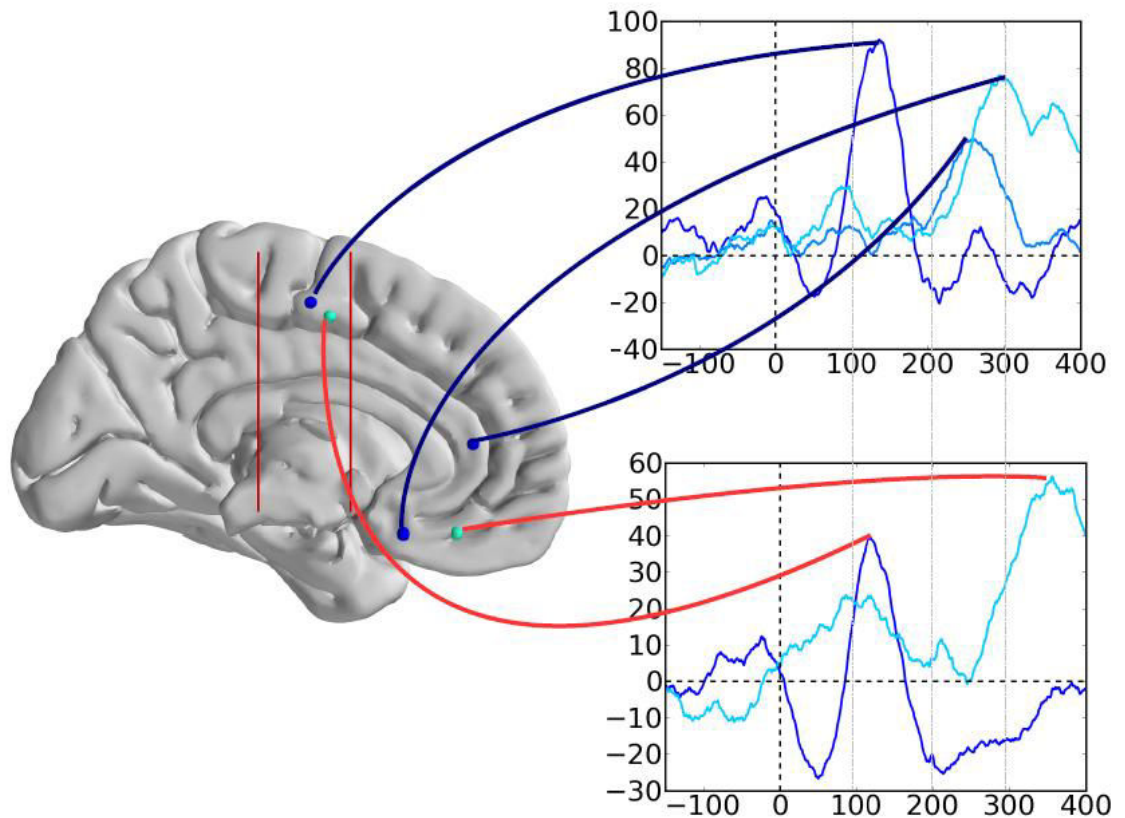


**Figure II.8 :** *Caudo-rostral latency of activation in the medial frontal wall*

*In patient 3 (top) and 5 (bottom). The anatomical location of electrodes placed in SMA, pACC and OMPFC, converted into normalized MNI brain, are shown on a RD MNI standard brain in its medial aspect (left).*

### **Single-trial activity in the SMA and in the medial prefrontal cortex**

In two subjects (subject 3 and 5), the overt error-evoked LFP was detectable on a trial-by-trial basis (Figure II.9). In subject 3 this activity was visible in 21/24 trials and showed the same morphology as the averaged potential, appearing as a phasic activity without any clear oscillatory component. This single trial LFP varied in amplitude from 92 to 414  $\mu\text{V}$ , and it peaked at 100 to 413 ms from EMG onset (this last LFP being related to a longer EMG burst with delayed mechanical response). In subject 5 the error-evoked LFP was clearly identifiable on 64/72 trials in electrode contacts placed in the SMA. As for subject 3, morphology, amplitude (54 to 230  $\mu\text{V}$ ) and latency (peaking at 66 to 191 ms from EMG onset) of this single trial evoked LFP was comparable to those of the averaged potential. Similarly to patient 3, this single trial LFP manifests as phasic activity and does not show any clear oscillation.

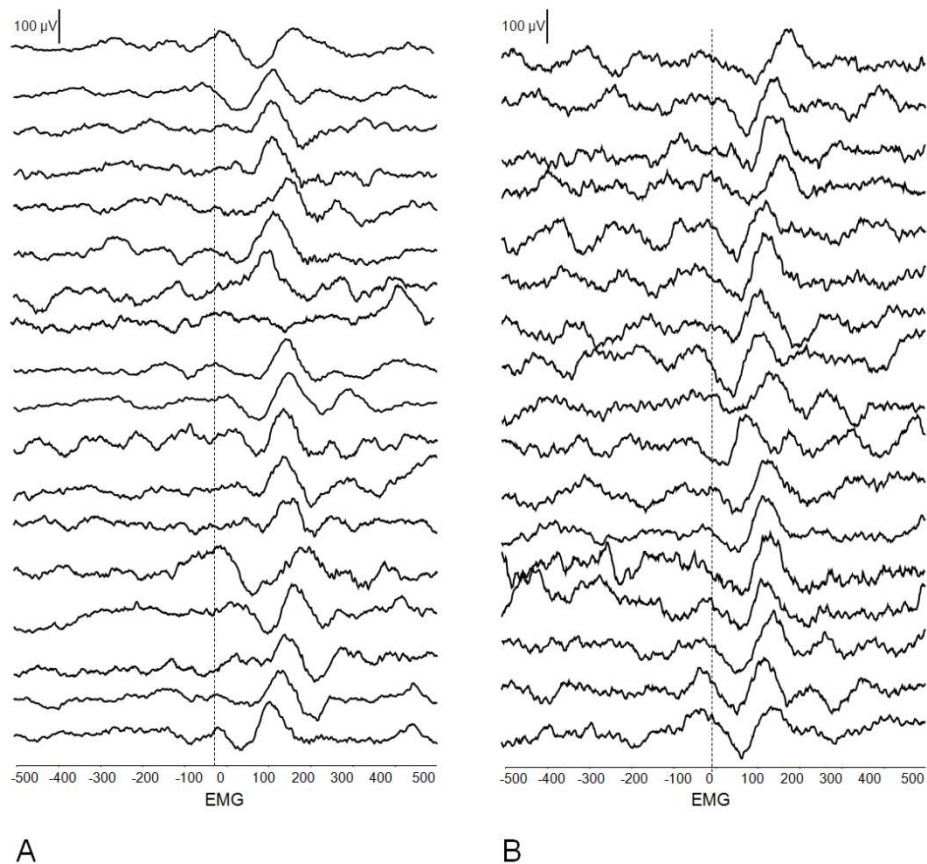


**Figure II.9 :** *Single trial LFPs time-locked to EMG onset in error trials. (A) as an example 18 trials are shown for subject 3 and (B) 17 trials for subject 5.*

### **Relationship between SMA and medial prefrontal activity**

We further investigated the relation between rostral and caudal activity using trial-by-trial analysis (Figure II.10). Single trial LFPs recorded in the SMA and in the medial prefrontal regions were significantly and positively correlated both in terms of latencies ( $\rho = 0.8$ ,  $p < 0.01$  between SMA and pACC on patient 3, and  $\rho = 0.35$ ,  $p < 0.05$  between SMA and OMPFC on patient 5) and, less strongly, amplitudes ( $\rho = 0.63$ ,  $p < 0.01$  and  $\rho = 0.28$ ,  $p < 0.1$ , for patient 3 and 5 respectively, Figure II.1). Medial pre-frontal activity appeared to be contingent upon activity in the SMA because it was always preceded by SMA activity, and importantly it was never present when SMA activity was absent. On the other hand SMA activity can and occasionally did occur without the subsequent pre-frontal activity.

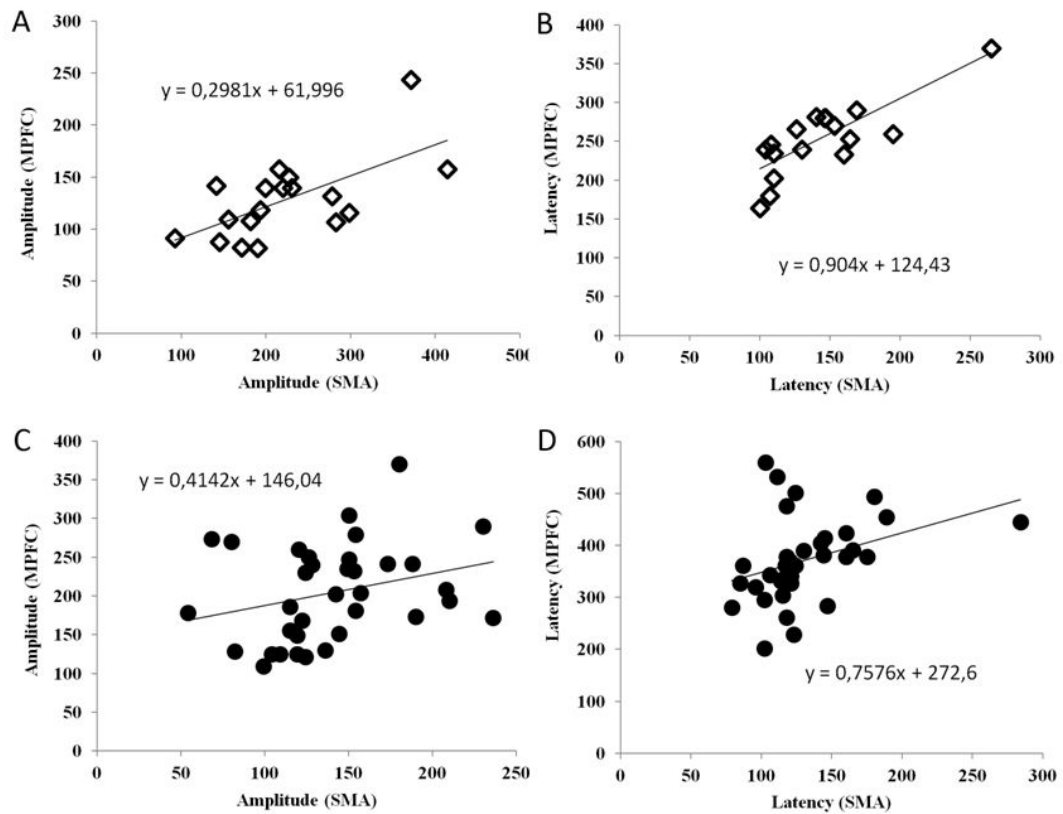


**Figure II.10 : medial prefrontal cortices (MPFC) and SMA activities**

Positive correlations between activities of medial prefrontal cortices (MPFC) and SMA activity in terms of latencies (A and C) and amplitude (B and D). Error-evoked LFPs were detectable on a trial-by-trial basis at both SMA (subject 3: 21 trials out of 24; subject 5: 64 trials out of 72) and medial prefrontal electrodes (pACC for subject 3: 18 trials; OMPFC for subject 5: 35 trials). The intercept of the regression shows the latency shift between SMA and MPFC.

**Relationship between SMA activity and EMG on partial errors**

To further describe the functional significance of the SMA activity we focused on partial errors. These trials are a prototypical case of efficient on-going action control because the incorrect activation is interrupted and corrected (by the opposite “corrective” response). We therefore searched for a functional link between SMA activity and error correction.

We correlated the latencies of LFPs and EMG activity in three patients for whom partial errors LFPs were detectable in the SMA on a trial-by-trial basis (subjects 2, 3 and 5).

We extracted latencies of SMA activity (represented by the onset, peak and end of the LFP of SMA), response interruption (represented by the offset of an incorrect EMG burst) and partial error correction (represented by the onset of the corrective EMG burst) (Figure II.11).

ERP peak was determined by the visual identification of polarity change in the evoked potential (Figure II.11), while LFP onset and end could be identified by slope change at the beginning and respectively at the end of the evoked activity.

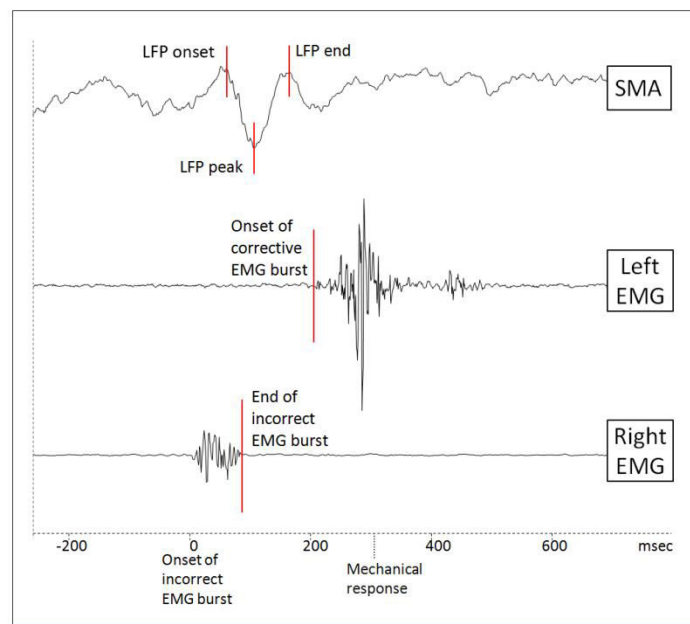


**Figure II.11 : Example of a partial error trial and corresponding SMA LFP.**

*Latencies of SMA activity are represented by the peak and end of the LFP in SMA, partial error interruption is represented by the offset of an incorrect EMG burst and partial error correction is represented by the onset of the corrective EMG burst.*

We found that the peak of the LFP strongly correlated with the offset of the incorrect-trial EMG activation, representing response interruption, (z-score, coefficient correlation of 0.61,  $p < 0.01$ ) (Figure II.11A), while it was less strongly correlated with corrective EMG onset (coefficient correlation 0.27,  $p < 0.01$ ). By contrast, the end of the LFP was strongly correlated with the onset of the corrective EMG activation, and, less strongly, with the offset of the incorrect EMG (coefficient correlation respectively 0.7,  $p < 0.01$  and 0.27,  $p < 0.05$ ) (Figure II.11B).

To resume, on partial errors SMA activity began with the first incorrect muscular activation, culminated when this incorrect action was inhibited, decreased and finally extinguished when the subsequent corrective response was issued.

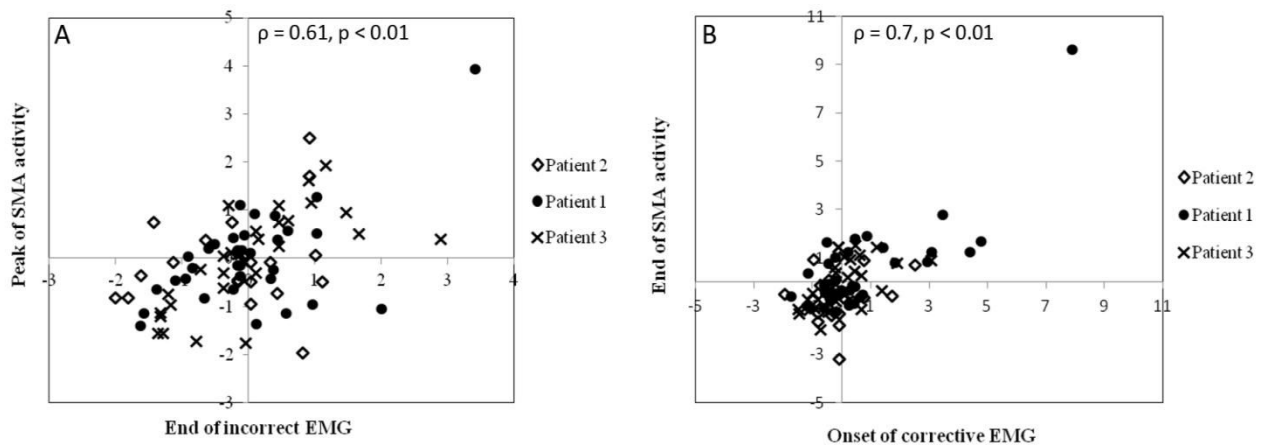


**Figure II.12 : Correlation between LFPs and EMG latencies in partial error.**

*Correlation between the latencies of LFPs and EMG activity during partial error trials.*

*(A) correlation between peak of LFP and partial error interruption. (B) correlation between LFP's offset and onset of corrective response.*

### **A sixth subject**

It should be noted that a sixth subject, a 20 year old left-handed female having electrodes implanted in the medial frontal cortex (one of which was in the caudal part of the SMA and another in the posterior part of the RCZ) performed the Simon task. This subject was not included in the study because iEEG data analysis revealed no EMG-locked LFPs evoked by errors, whether partial or complete, in any of the implanted electrodes. Nevertheless EMG-locked LFPs could be observed on correct responses exclusively in the SMA. In this subject, two surface electrodes were available, allowing a bipolar derivation between Cz and Fz to be obtained. In these surface recordings, EMG-locked ERPs could be observed on correct trials with a time course comparable to that obtained from SMA, but no evoked activity could be observed for either overt or partial errors. The latency of the correct response EMG-locked LFPs was 65 ms, and its amplitude 16  $\mu$ V. A total of 10 electrodes were implanted in the right hemisphere, exploring SMA, posterior RCZ, Insula, parietal operculum, superior parietal lobulus, Heschl's gyrus, Cuneus, anterior calcarine fissure, posterior hippocampus. This subject committed 31 errors and 77 partial errors.

## 7.4 Discussion

Action monitoring is a crucial executive function which is fundamentally grounded on performance evaluation and error processing. How and where error processing is performed is however debated due to a lack of direct investigations in humans. Particularly the neuroanatomical basis of this control process is not yet ascertained, although indirect fMRI (Debener et al., 2005; Ridderinkhof et al., 2004; Markus Ullsperger & Cramon, 2001a) and EEG data (Dehaene et al., 1994; M. J. Herrmann et al., 2004; Van Veen & Carter, 2002) have estimated that the core of this process could take place in the broad RCZ.

In this study LFPs evoked by behavioural relevant responses have been directly recorded in human medial frontal cortex during a task investigating action monitoring and more specifically error processing. The intracerebral activity evoked by motor responses was related to subject's performance and it clearly reflects an action monitoring process. The first main result of this study is that error processing is, to a large extent, carried out by the SMA. The second main finding is that both correct and erroneous action evoked activities are generated in the SMA consequently suggesting that they constitute a same component modulated in amplitude by performance. Indeed a continual ongoing performance monitoring activity was recorded exclusively in this region: here the evoked LFP was early and strongly time-locked to the behavioral relevant muscular activation and it presented an extremely significant characteristic, that is, a progressive modulation of its amplitude as a function of subject's performance. The largest LFPs occurred following overt errors, smaller after partial errors, and even smaller, but clearly still present, following correct responses. Such a pattern of sensitivity to outcome together with the time-course of this LFP makes it similar to the Error Negativity which is assumed to be a neural correlate of the action monitoring system (Falkenstein et al., 1991; W.J. Gehring et al., 1993; Sven Hoffmann & Falkenstein, 2012; Simons et al., 2010). The functional signification of the correct-related ERP, called "Ne-like", is currently debated. However, our intracerebral LFP, exactly as scalp Ne/Ne-like does, become progressively wider larger from correctness to partial errors and from partial errors to errors, and shows comparable time-courses (earlier for partial errors, latest for errors and intermediate for correct responses). This intracerebral LFP can thus be considered as the equivalent of the scalp Ne/Ne-like and it hence reveals an ongoing control process. Therefore the present data clearly demonstrate that the Ne and the Ne-like, in addition to the same latency and the same waveform, have the same cortical generator, thereby indicating that they

represent a unique ERP component, modulated by performance. This finding implies functional consequences for the current models of cognitive control, as none of the current neurocomputational models can account for this unicity.

In one patient however only an activity evoked by correct responses, and not by incorrect responses, was recorded in both SMA intracerebral and fronto-central scalp electrodes. As in some normal subjects a lack of error-related EEG activity is seldom observed, this could explain the absence of intracerebral LFP evoked by errors and of the correspondent scalp Error Negativity in this patient.

Rather unexpectedly, since SMA is not classically assumed to be involved in action monitoring, contrary to the RCZ (as result of several fMRI and EEG studies), the present data show that this control process actually takes place in the SMA proper. Indeed in all patients the only electrodes disclosing such an outcome-modulated activity were situated in the superior frontal gyrus few millimetres behind VCA line (an anatomical landmark commonly used to separate human pre-SMA from SMA-proper (Picard & Strick, 1996)) and the LFPs were visible only in few medial contacts. What is the more, in patient having two neighbouring electrodes in the SMA, the presence of an inverted polarity for both incorrect and correct related LFPs with outcome-modulated amplitude confirms that the neuronal generator of this monitoring activity is local and situated in the SMA proper (at least in this patient). Finally, in all patients the same effect of response lateralization, namely increased amplitude for responses ipsilateral or contralateral to the recording site, was found for correct responses, partial errors and errors, further validating a unique local generator in the SMA for the three trial types. However, this does not allow to estimate the possible participation to action monitoring of the dorsal ACC, which has not completely been explored in this series.

Therefore present data allow to affirm that SMA is strongly implicated in action monitoring and that it plays a pivotal role which was to date attributed mostly to the anterior cingulate cortex. Notwithstanding some electrophysiological studies in monkeys have previously reported activities evoked by behavioural relevant responses in the SEF. Particularly Stephorn et al (Stephorn et al., 2000) describe neurons with increasing firing after errors and Emeric et al (Emeric et al., 2010) report a small correct-related LFP and a higher error-related LFP with latency comparable to the one reported in the present study. The early responsiveness to outcome found in monkey SEF and the human location of SEF in the SMA

region go along with present reports. In addition, these data are in agreement with few recent source-localization EEG studies which have rather suggested an engagement of the medial and middle frontal gyrus corresponding to the SMA (M. J. Herrmann et al., 2004), with the eventual participation of the ACC (Phan Luu et al., 2003; Roger et al., 2010), in performance monitoring and error processing.

Present findings shed new light on human SMA, providing solid arguments for a new function for this area. In fact the SMA is considered to contribute to movement initiation and inhibition, planning action sequences, motor learning and development of automaticity (Nakamura, Sakai, & Hikosaka, 1998). Moreover, as suggested by monkey neuronal recordings (Matsuzaka & Tanji, 1996) and fMRI in humans (Matthew F S Rushworth, Buckley, Behrens, Walton, & Bannerman, 2007; Markus Ullsperger & Cramon, 2001a), it seems to be involved in some executive functions such as task switching and response conflict, most likely with a posterior-anterior grade of implication with increasing cognitive demand from SMA proper to pre-SMA (M F S Rushworth et al., 2002). The present study is a demonstration of a pivotal role for human SMA in action monitoring, and specifically in performance evaluation of required actions.

A better understanding about the functional significance of this response-related activity, and thus of action monitoring carried out in the SMA, can be issued from the analysis of its time-course in partial errors. In this type of incorrect trials LFP begins and reach its peak running parallel to the first incorrect muscular activation, but its ending is rather correlated with the beginning of the following corrective response, i.e. it lasts longer when the correction is later. This could indicate that SMA intervenes in action monitoring by emitting a “default” signal – the LFP here recorded – which may have the functional meaning of an alert or a warning. This signal is released each time a behavioural relevant response is produced and it is early and easily interrupted in correct responses, giving rise to a small LFP. In partial errors this signal extinguishes as a result of the activation of the corrective response and in errors it reaches its highest level, probably indicating the need to enhance cognitive control. Another important consideration is issued from these single trial activities evoked by erroneous activations: contrarily to what is often assumed (Cavanagh, Cohen, & Allen, 2009; Phan Luu, Tucker, & Makeig, 2004; Munneke, Nap, & Schippers, 2015), these phase-locked event-related LFPs do not contain oscillatory activities, i.e. although at a single trial level most of the spectral frequency content occurs in the delta and/or the theta band, no theta nor delta oscillation can be observed. This indicate that the ERPs is not generated by reset of the theta-

delta oscillatory activity, whose increased power observed on EEG (Cavanagh et al., 2009; Phan Luu et al., 2004) might result from an artefact due to bandpass filtering of a transient low frequency non-oscillatory signal (Yeung, Bogacz, Olroyd, & Cohen, 2004).

As a further main result of this study, we observed an additional involvement of the medial pre-frontal cortex, namely the ACC and the OMPFC, which was nonetheless implicated later and only on incorrect responses. This less focal LFP, on account of its latency and its specificity to errors, could be associated to the error positivity (Pe), an error-specific positive deflection following the Ne at about 200-400 ms and presenting a diffuse scalp distribution (Falkenstein et al., 1991) which is considered to reflect diverse evaluative aspects of error processing (Falkenstein et al., 2000; Overbeek et al., 2005). Anyhow, aside from any functional interpretation of this pre-frontal error specific activity, some interesting remarks can be made about the positive correlation found between latency and amplitude of this LFP and the one recorded in the SMA. Their correlation strongly suggests a relationship - or even a hierarchy – between the pre-frontal activity (downstream) and the error negativity produced in the SMA (upstream). In fact latency and amplitude of pre-frontal activity increased in proportion to those of SMA activity. At least two hypotheses can be proposed to explain this correlation from an anatomo-physiological standpoint. 1) LFP arising in the SMA is mandatory for the genesis of the pre-frontal activity and a causal correspondence exists: when, in case of erroneous response, a given threshold is reached in the SMA then a neuronal activity is generated in the medial pre-frontal cortex. Accordingly, there would be a sort of caudo-rostral sequential activation in error processing moving from pre-motor to pre-frontal cortex. 2) The correlation would be less direct and so would be this postero-anterior gradient of involvement, if a third structure would influence both pre-motor and pre-frontal activities. This later ERP would not depend directly upon the SMA activity, but rather upon a structure intervening upstream in the control process

To conclude, this study demonstrates that SMA is primarily involved in action monitoring and error processing. In this control process SMA operates in a continuous and outcome-modulated fashion, ranging incrementally from correctness to errors, rather than in a binary all-or-nothing mode. Differently the medial pre-frontal cortex is engaged only when an erroneous action is produced. In case of negative outcome, the pre-frontal cortex intervenes later and appears to be driven by the SMA, whose “default” activity has reached its peak. SMA turns out to be able to evaluate the outcome of actions it has ordered and, in the event of negative outcome, to drive error processing in relation with medial pre-frontal cortex. The

involvement of the SMA in action monitoring appears functionally grounded, because the SMA is widely considered to be implicated in movement initiation and inhibition (Brinkman & Porter, 1979; Lim, Dinner, & Luders, 1996; Tanji & Kurata, 1982), response selection and motor planning (Chauvel, Rey, Buser, & Bancaud, 1996; Nachev et al., 2008; Sergent et al., 1992; Sergent, 1993). The present study reveals a new function for SMA: the early evaluation of the outcome of actions that it has contributed in initiating.



## **8 STUDY 2: HIGH-GAMMA ACTIVITY INDUCED BY MOTOR RESPONSES IN PERFORMANCE MONITORING: RECORDINGS FROM HUMAN CEREBRAL CORTEX**

### **8.1 Introduction**

Whereas human event-related EEG activity in response to errors or conflict has been extensively investigated, the frequency domain characteristics of performance monitoring have drawn researchers' attention only recently. Time-frequency analysis of brain electrical signals enables differentiation between the evoked or phase-locked activity (that is locked to a response or to a stimulus, namely the ERPs) and the non-phase locked activity, also called induced activity (Basar, 1999; Phan Luu & Tucker, 2001). By analyzing the broad-band energy changes in error-related EEG signals, several authors have reported an increased power in the theta (4-8 Hz) bands just preceding and/or following an incorrect response, compared to a correct response (Cavanagh et al., 2009; Cohen & Cavanagh, 2011; Phan Luu et al., 2004; Phan Luu & Tucker, 2001; Nigbur, Cohen, Ridderinkhof, & Stürmer, 2012; Trujillo & Allen, 2007). Such a modulation, usually called midline frontal theta (Phan Luu et al., 2004), is maximal over the mid frontal electrodes and the cortical source has been localized within the medial frontal cortex comprising the ACC (Phan Luu & Tucker, 2001).

Beside theta band oscillation, higher frequency responses over 30 Hz, the so-called gamma band, are likewise thought to be implicated in a wide range of perceptual, motor and cognitive functions (Hoogenboom, Schoffelen, Oostenveld, Parkes, & Fries, 2006; Lee, 2003; Pantev, 1995). Such faster oscillations can be detected at the scalp of humans by EEG and MEG and also directly from human cortex by means of intracerebral EEG. Neuronal oscillations with broad frequency above 60 Hz, called the "high-gamma" oscillations, have been observed in several cortical areas and under several conditions and states, but their functional meaning, in terms both of neuronal sources and role in cognition, is considered potentially different from the one of lower gamma rhythms (for a review see (Crone, Sinai, & Korzeniewska, 2006). Indeed high-gamma activity (HGA) has been recently found to be tightly correlated to neuronal firing near the recording electrode (Quilichini, Sirota, & Buzsáki, 2010; Ray, Crone, Niebur, Franaszczuk, & Hsiao, 2008; Ray & Maunsell, 2011; Whittingstall & Logothetis, 2009). More specifically, action potentials are correlated with

increase in LFP power at frequencies greater than 50 Hz, while lower frequencies in the gamma band are anti-correlated with these two latter measures (Ray & Maunsell, 2011). Cortical activities modeling have led other authors to admit that the fast oscillations in the high gamma range result from post-synaptic activities induced by inhibitory interneurons on pyramidal neurons, shaping their spiking activities and their synchrony (Suffczynski, Crone, & Franaszczuk, 2014); phase-locked, somatosensory evoked true oscillations have been evidenced in humans even in the very high range (largely over 300 Hz) of the gamma band with EEG (Mochizuki et al., 2003) or MEG recordings (Curio et al., 1994). Therefore, depending on structures, experimental conditions and also on the part of the frequency range considered, it is likely that, in the high gamma band, LFPs record not only true post synaptic oscillations but also a significant amount of action potential activities which transient nature result in broad band activities and spike after depolarization and hyperpolarization components (Belluscio, Mizuseki, Schmidt, Kempter, & Buzsáki, 2012; Buzsáki & Wang, 20012; Scheffer-Teixeira, Belchior, Leão, Ribeiro, & Tort, 2013; Schomburg, Anastassiou, Buzsáki, & Koch, 2012; Waldert, Lemon, & Kraskov, 2013). Furthermore, intracerebral and electrocorticographic recordings in epileptic patients have suggested that broadband increase of signal power at frequencies higher than 60 Hz are more consistent with cortical activation in a variety of functions (Crone et al., 2006; Lachaux et al., 2012). Hence broadband energy increase of gamma activities (including high-gamma) is considered a marker of neural recruitment and have been used to identify the cortical networks underlying several high cognitive processes, such as associative learning (Wolfgang H R Miltner, Braun, ArnoldMatthias, Witte, & Taub, 1999), attention (Engel et al., 2001; Jensen, Kaiser, & Lachaux, 2007), memory (C. S. Herrmann, Munk, & Engel, 2004) and language (Sahin, Pinker, Cash, Schomer, & Halgren, 2009).

Nonetheless, gamma-band responses have not been investigated in performance monitoring until now, neither with surface nor with intracerebral EEG. In the present study we aimed to investigate high gamma-range oscillations in human subjects using direct neuronal recording of cerebral cortex involved in performance monitoring. We choose to study high-gamma oscillations (above 60 Hz) as they could provide supplementary information to LFPs' evoked activities. While the latter are known to mostly reflect synaptic inputs, HGA, which, as discussed above, seems more directly associated with neuronal spiking, could represent a direct and indirect neuronal correlate of synchronized output activity of neurons. High

frequency range (> 60 Hz) thus appears to be well suited for estimating directly and indirectly spiking activity in LFP recordings.

In this study we recorded intracerebral EEG (iEEG) from 9 epileptic patients with implanted depth electrodes for therapeutic purpose while performing a choice reaction-time task. We examined iEEG signals recorded from numerous medial and lateral frontal regions as well as from the insular cortex, as these structures have been found to be involved in action monitoring (C. Amiez, Hadj-Bouziane, & Petrides, 2012; Klein et al., 2007; Ridderinkhof et al., 2004; M Ullsperger & von Cramon, 2004). We assessed the HGA power induced by behavioral relevant responses and searched for a modulation of energy as a function of action outcome.

## **8.2 Materials & Methods**

### **8.2.1 *Participants and task***

Nine subjects (7 females, 2 males, mean age  $25 \pm 8.1$ ), undergoing presurgical evaluation of their epilepsy using iEEG, performed a Simon task (Simon, 1979). Implantation procedure, electrodes reconstruction, task, data acquisition and pre-processing are reported in chapter 2.

General characteristics of subjects, their implanted electrodes, as well as the number of overt and covert errors are reported in table 1.

### **8.2.2 *Spatial Sampling***

Across the nine patients, local field potentials (LFPs) were recorded from 968 contacts on 91 one-dimensional depth electrodes positioned predominantly in the frontal cortex. We included in the analysis data recorded from the electrodes located in the frontal and in the insular cortex, for a total of 93 distinct anatomical sites from 631 contacts and 59 electrodes. For comparison purpose, electrodes' sites were grouped into distinct anatomical clusters, as illustrated in table 2. On account of interindividual anatomical variability, sites were pooled into the same clusters if they belonged to the same anatomical structure, defined on the individual MRI by anatomical (gyri and sulci) or functional landmarks.

<i>Subject</i>	<i>Sex</i>	<i>Age</i>	<i>Hand laterality</i>	<i>SEEG side</i>	<i>Epileptogenic zone</i>	<i>Electrodes</i>	<i>N°overt and partial errors*</i>
1	F	32	R	L	Rolandic	SC', SA', CC', PM', L', LI'	28/99
2	F	22	L	L	Not Defined	SA', L', OF', CR', OR', A', GPH', TB', TP'	27/46
3	F	15	R	R	Right Insular	SA, PM, LP, CP, I, OR', H, OP, OF, FT, CCZ, A	16/80
4	M	29	L	R/L	Right Pre-frontal	SA, SA', PM, PM', CCZ', R, FP, OR, TP, OF'	75/29
5	M	24	R	R	Right Fronto-opercular	SA, PM, CCZ, CR, OF, OC, OP, OR, OR', TP, T, H,	39/18
6	F	20	R	R	Not Defined	SA, CCZ, L, OF, OP, PA, C, H, CU, FCA	29/76
7	F	42	R	L	Left Temporal	PM', CCZ', OR', OR, CR', R', OF', TP', A', B', C'	73/28
8	F	27	R	L	Left Orbito-frontal	CCA', CCZ, CR', R', FP', FT', OR', OR, TB', T'	40/68
9	F	21	R	R	Right Temporal	SA, OR, OR', OF, B, T, H, TP, PCG, PCG', PFG	21/69

**Table 1. General characteristics of subjects and of electrode implantation.** Ninety one depth multicontact electrodes were recorded across all patients, 59 of which were located within the frontal lobe, with a total of 968 contacts (59/91 electrodes and 631/968 were located in the frontal lobe). SA: SMA, PM: pre-SMA, OF: Insula/frontal operculum, A: Amygdala, CR: anterior division of the RCZ, OR: orbito-medial prefrontal cortex, CC posterior division of the RCZ, CCZ: caudal anterior cingulate zone, R: rostral inferior frontal gyrus, FP: frontal pole, TP: temporal pole, GPH: para-hippocampal gyrus, TB: temporo-basal region, LP: para-central lobulus, PA: superior parietal lobulus, OP: parietal operculum, H: Heschl's gyrus, CU: Cuneus, FCA: anterior calcarine fissure, C: hippocampus's tail, CP: posterior cingulate gyrus, FT: pars triangularis of inferior frontal gyrus, GLP: posterior lingual gyrus, OT: fusiform gyrus, L: lesion, LI: lesion, B: Hippocampus, H: Heschl, R: ventral prefrontal cortex, FP: fronto-polar, FT: inferior frontal gyrus, GC: posterior cingulate gyrus, PFG: inferior parietal lobule . Electrodes followed by the apostrophe ' are located in left hemisphere. \*Here we report the number of errors/partial errors committed. The number of errors and partial errors actually analyzed were sometimes lower because of rejection of segments with artifacts.

### **8.2.3 Data Analysis**

iEEG signals were sampled at 1 kHz, low-pass filtered to 250 Hz and then segmented into epochs locked on finger movement (i.e. the EMG burst at the button press). Data were segmented into windows extending from 1100 ms before EMG onset to 700 ms after EMG onset. Epoch segmentation was also performed on the respective stimulus onset and the data from -0.95 ms to 0.6 ms prior to stimulus presentation was taken as a baseline activity for the calculation of the single-trial HGA.

Spectral density estimation was performed using multi-taper method based on discrete prolate spheroidal (slepian) sequences (Mitra & Pesaran, 1999; Percival & Walden, 1993). To extract high-gamma activity from 60 to 120 Hz, iEEG time series were multiplied by  $k$  orthogonal tapers ( $k = 8$ ) (0.15s in duration and 60Hz of frequency resolution, each stepped every 0.005s), centered at 90Hz and Fourier-transformed. Complex-valued estimates of spectral measures, including cross-spectral density matrices, were computed at the contact level (bipolar derivation) for each trial  $n$ , time  $t$  and taper  $k$ . Then, single-trial power estimates in the high-gamma range (60-120Hz) locked on EMG and stimulus onset, were log-transformed and low-pass filtered at 50Hz to reduce noise. Single-trial estimates of high-gamma power were z-transformed with respect to baseline period from -0.5 and -0.1 s prior to stimulus onset.

### **8.2.4 Statistical analysis**

Statistical inference was performed on individual subject data for each time point  $t$  and each bipolar derivation for the analysis of HGAs. The effect of the task on HGA power was evaluated by comparing baseline power values to movement-related power values, using a parametric t-test with statistical threshold set to  $p < 0.05$ . To account for the multiple comparisons problem at the single time-point level, we controlled the false discovery rate (FDR) (Benjamini & Hochberg, 2016). To further assess the validity of our results, we quantified the minimum number of consecutive significant time points required to reject a null hypothesis of absence of a cluster given a chance probability  $p_0 = 0.05$  (two possible outcomes, significant or non-significant). Given the number of test performed by subject we

kept only those clusters whose duration exceeded a given significance level for at least three points (Brovelli, Chicharro, Badier, Wang, & Jirsa, 2015).

With the aim to evaluate action monitoring modulation of the gamma-power, three categories of trials were compared based on response correctness: correct trials; overt error trials; and partial error trials. We identified response specificity by comparing gamma-band responses in the three conditions using a One-Way ANOVA analysis with three levels at each timepoint.

Finally we investigated the possibility of a link between evoked and time-locked phasic activity, namely the LFP's ERP, and the high-gamma induced activity. As in patients 1 and 4 signal-to-noise ratio allowed to detect single-trial error-related potential in both SMA and medial pre-frontal cortex (pre-genual ACC in patient 1 and in the orbito-mesial prefrontal cortex in subject 4; see results of Experimental part I), we compared this time-locked phasic activity with the HGA modulation on a trial by trial basis. We first quantified on how many trials an ERP or an HGA response could be detected. We then evaluate their relationship by comparing their true co-occurrence (trials containing both ERP and LFP) to the expected probability whether they would be independent: in this case the probability of co-occurrence is simply the product of the two probabilities.

Behavioural data were analysed as reported in the previous chapter.

## **8.3 Results**

### **8.3.1 Behavioural Results**

Mean RT was lower for congruent trials (458 ms) than for incongruent trials (479 ms). ANOVA showed an effect of congruency ( $F(1,14) = 3.85$ ;  $p = 0.04$ , one tailed), a trivial effect of quantile ( $F(4,36) = 1.57$ ;  $p < .001$ ) and an interaction between congruency and quantiles ( $F(4,36) = 5.73$ ;  $p < 0.01$ ), as illustrated by RT distributions in Figure II.13. Error rate for congruent trials was 0.95, and for incongruent trials 0.94. Statistical analysis showed no effect of congruency on ER ( $F < 1$ ), an effect of quantiles ( $F(4,36) = 13.15$ ;  $p < .001$ ) and a marginal interaction between quantiles and congruency ( $F(4,36) = 2.37$ ;  $p = .07$ ). Conditional accuracy functions (CAF) are showed in Figure II.13.

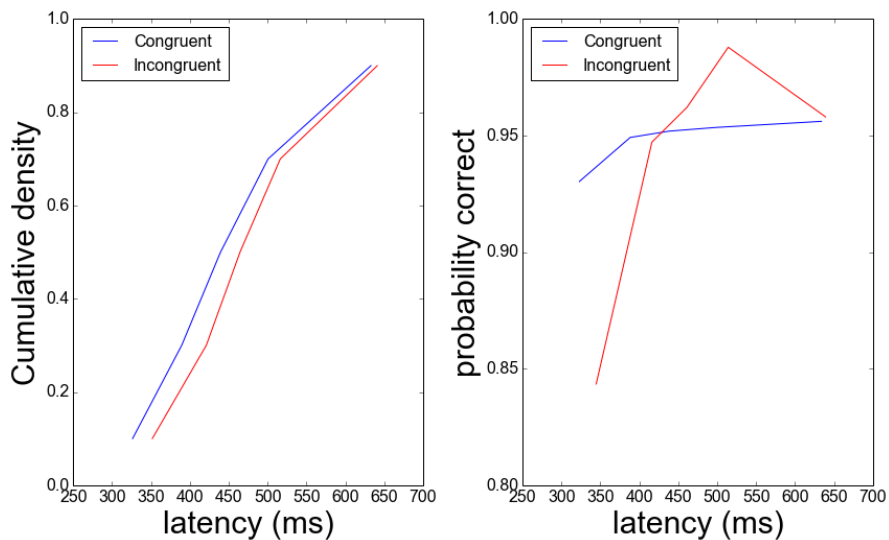


**Figure II.13 : Behavioural pattern.**

**On the Left:** Distribution of RT: difference in RT on congruent (blue line) versus incongruent (red line) trials is greater for short reaction times. **On the right:** CAF: Percentage of correct responses on congruent (blue line) and incongruent (red line) condition as a function of reaction time: the two lines show the typical reduction in correct response rate on incongruent trials for short reaction times only.

### 8.3.2 Task-related High-gamma activity

The high-gamma band time-frequency analysis of LFPs induced by motor responses (namely the EMG), revealed a response to the task in the high-gamma band in a vast frontal network. Indeed, during the Simon-task, 417 bipolar derivations (out of 631 in nine patients, that is, 66.1% of recording contacts) had a significant modulation above 60 Hz after motor response compared to the baseline period (t-test comparison with pre-EMG baseline, corrected for multiple comparison  $p < 0.05$ , cluster of 3 time points). When, on the same electrode, several contiguous active bipolar derivations explored the same anatomical structures (for example 3 contiguous contacts exploring the SMA), they were further considered as exploring only one single site. Accordingly, as different bipolar derivations in the same site could disclose slightly different HGA responses and significant levels, we selected the bipolar derivation with the maximal effect and the minimal p-value as representative of the HGA modulation for that electrode in the given structure. On the other hand, if in the same patient two distinct electrodes explored two close locations within the same structure they were considered as two distinct sites (for example two depth electrodes implanted nearby in the ACC, were considered as two sites exploring that structures). This explains the number of active sites reported below and in table 2.

Overall, along all the active sites on medial and lateral wall of the frontal lobe and in the insulo-opercular regions, a significant modulation in the HGA power with respect to the baseline period was present in 77 anatomical sites out of 93, that is, 82.7% of explored sites. Task-related HGA modulation was detected in all nine anatomical clusters, that is: 1) the SMA, in the medial aspect of the superior frontal gyrus caudal to the vertical plan passing through the anterior commissure (VAC plane); 2) the preSMA, situated in the medial wall rostrally to the VAC plane; 3) the midcingulate cortex (MCC) in the posterior part of the ACC; 4) the rostral division of the ACC (rACC) ; 5) the lateral prefrontal cortex in its dorsal part (DLPFC); 6) the lateral prefrontal cortex in its ventral aspect (VLPFC); 7) the orbito-frontal cortex (OFC); 8) the frontal operculum; 9) and the anterior part of the Insula.

Statistical analysis with One-Way ANOVA revealed three types of possible modulation in the high-gamma band: 1) an increase of HGA for error trials compared to correct trials, 2) an increase of HGA for partial error trials compared to correct trials, and 3) an increase of HGA for error trials compared to partial error trials. These different modulations could coexist in the same site. Overall, HGA power was enhanced for incorrect responses, while in correct trials it showed an absence of increase or a clear decrease after EMG activation (see Figures II.14). Nonetheless in a small number of sites (5.4%), the HGA was significantly increased for correct trials compared to errors (overt or partial). The time course of the HGA and of its power modulation varied to some extent across the anatomical structures. We will now describe the observed induced high-gamma responses in more detail for each anatomical cluster.

### **8.3.3 The supplementary motor area (SMA)**

We observed a HGA power increase during the motor task in all recording sites placed in the SMA and a modulation as a function of subject's performance in all subjects and in 6/7 (85.7%) of electrodes placed in the SMA, in both right (three sites) and left (three sites) hemispheres. On individual MRI all electrodes were located caudal to the VCA line (Figure II.14). HGA modulation was higher for errors compared to correct responses in all sites, for partial errors compared to correct responses in 5 sites (71.4%), and for errors compared to partial errors in 3 sites (41.8%). The time profile of the responses consisted of a sustained energy increase for both types of errors starting at time 0 (in 3 sites) or at 100 ms (in the other 3 sites) and sustained up to 600 ms (Figure II.14). The peak latency of HGA was around 200 ms for all but one patient, disclosing a later peak at 500 ms.

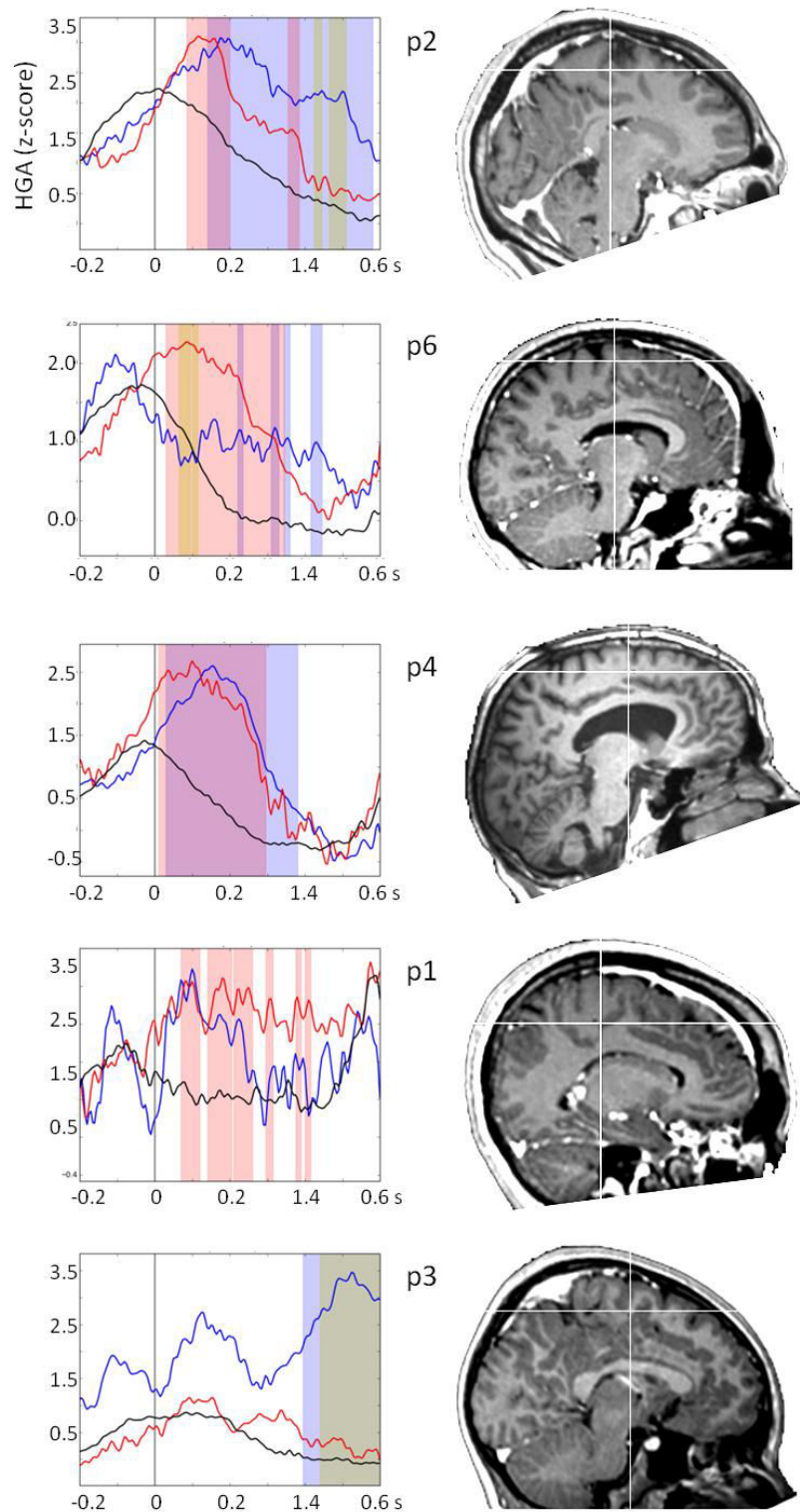


**Figure II.14 : Supplementary motor area (SMA) cluster.**

*Time-course of HGA modulation in the SMA induced by behavioural relevant responses in five patients. Time zero corresponds to the EMG onset. Segments with statistically significant difference between errors and correct responses are shaded in red, between partial errors and correct responses are shaded in blue, and between errors and partial errors are shaded in gray.*

### 8.3.4 The pre-supplementary motor area (preSMA)

Among the 8 sites exploring the preSMA, thus located rostral to the VCA line, six (75.5%) showed a non-specific task-related increase of HGA, while in only two sites (25%) such an increase was specific to errors compared to correct responses (Figure II.15). In both cases the HGA power increase seemed to be less sustained and later (see Figure II.15).

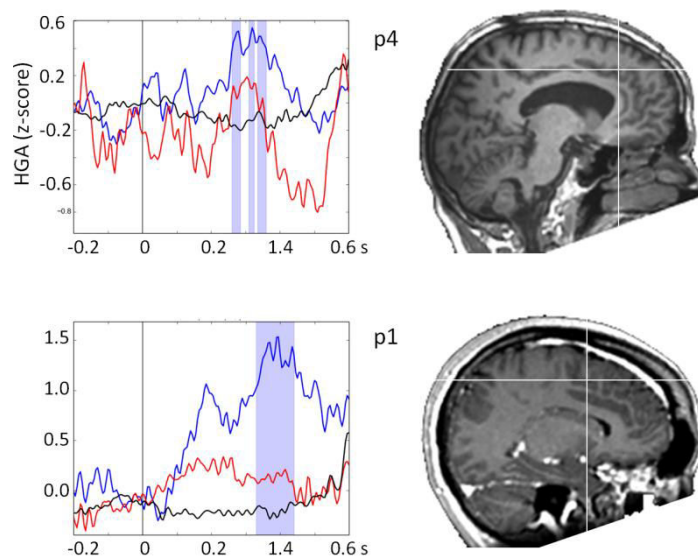


**Figure II.15 : Pre-Supplementary motor area (preSMA) cluster.**

*Time-course of HGA modulation in the preSMA induced by behavioural relevant responses in two patients. Time zero corresponds to the EMG onset. Segments with statistically significant difference between errors and correct responses are shaded in blue, between partial errors and correct responses are shaded in red, and between errors and partial errors are shaded in yellow.*

### 8.3.5 The midcingulate cortex (MCC)

Eight electrodes among seven subjects explored the posterior division of the ACC, that is the MCC, as defined in the Introduction chapter (Picard & Strick, 1996). All but one disclosed a task effect. Three sites showed an increase of HGA for errors, two of them also for partial errors and one site showed a modulation also for overt errors compared to partial errors (Figure II.16). Increase in gamma frequency band started around 100 ms after EMG onset and was sustained in two/ three sites (Figure II.16).

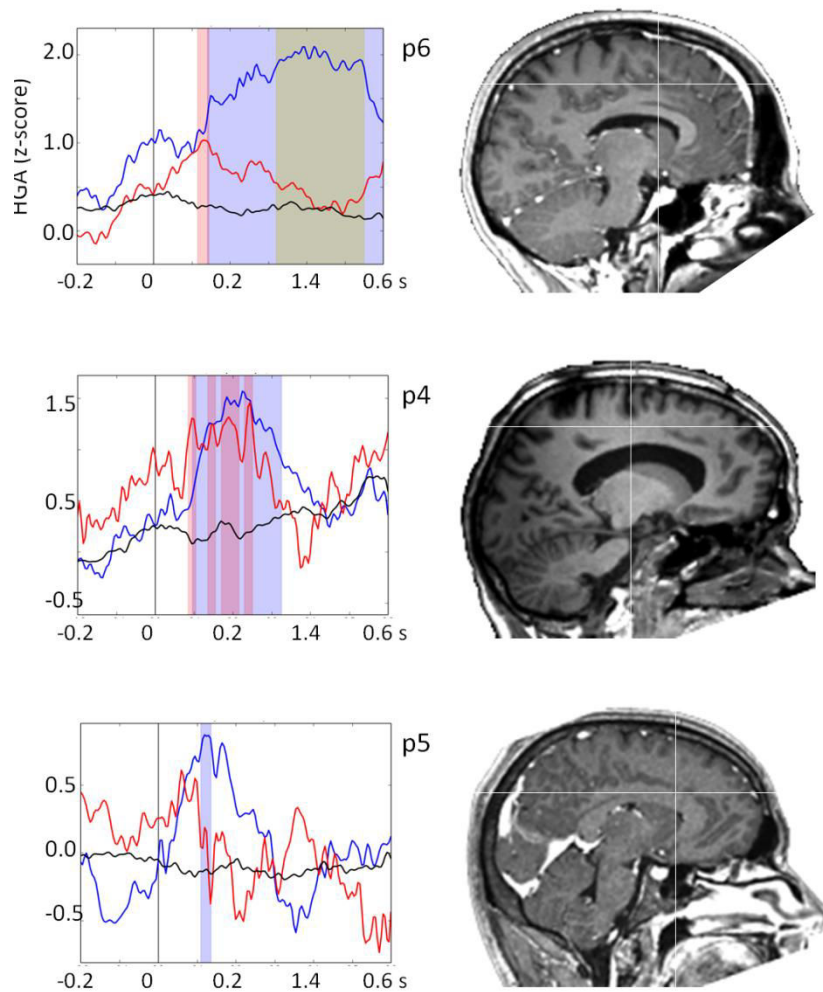


**Figure II.16 : Mid-cingulate cortex (MCC) cluster.**

*Time-course of HGA modulation in the MCC induced by behavioural relevant responses in three patients. Time zero corresponds to the EMG onset. Segments with statistically significant difference between errors and correct responses are shaded in blue, between partial errors and correct responses are shaded in red, and between errors and partial errors are shaded in yellow.*

**8.3.6 The rostral anterior cingulate cortex (rACC)**

Six recording sites among four patients explored this region and were located in the pregenual ACC, including the pregenual BA 32 and BA 24. Within five sites disclosing a non-specific task-related increase of HGA, only two (that is 33.3%) had an enhanced response for errors - overt in one case and partial in the other - compared to correct responses, with different time-courses (See Figure II.17).

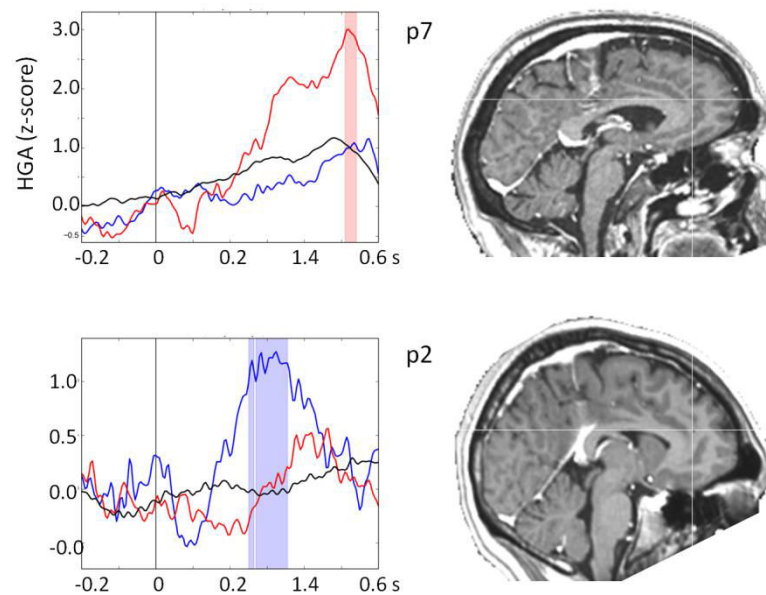


**Figure II.17 : Rostral anterior cingulate cortex (rACC) cluster.**

*Time-course of HGA modulation in the rACC induced by behavioural relevant responses in two patients. Time zero corresponds to the EMG onset. Segments with statistically significant difference between errors and correct responses are shaded in blue, between partial errors and correct responses are shaded in red, and between errors and partial errors are shaded in yellow.*

### **8.3.7 The dorso-lateral prefrontal cortex (DLPFC)**

The DLPFC was extensively explored in all patients with a total of 29 electrodes. Electrodes were placed on the convexity of the frontal lobe in the first and in the second frontal gyrus. The majority of recording sites, 19/29 in eight patients, disclosed a positive modulation of HGA during the task compared to the baseline and 17/29 an enhanced HGA for erroneous trials. As observed in the other regions, HGA for correct trials showed stability or even a clear decrease of gamma power after EMG onset compared to the increase observed for errors and partial errors (see Figure II.18). The time profile of HGA modulation was variable, with some sites disclosing an early (around EMG onset) gamma-band response, and other sites a slightly later response, around 100-180 ms after EMG onset. Typical gamma-band responses from eight subjects are reported in Figure II.18.

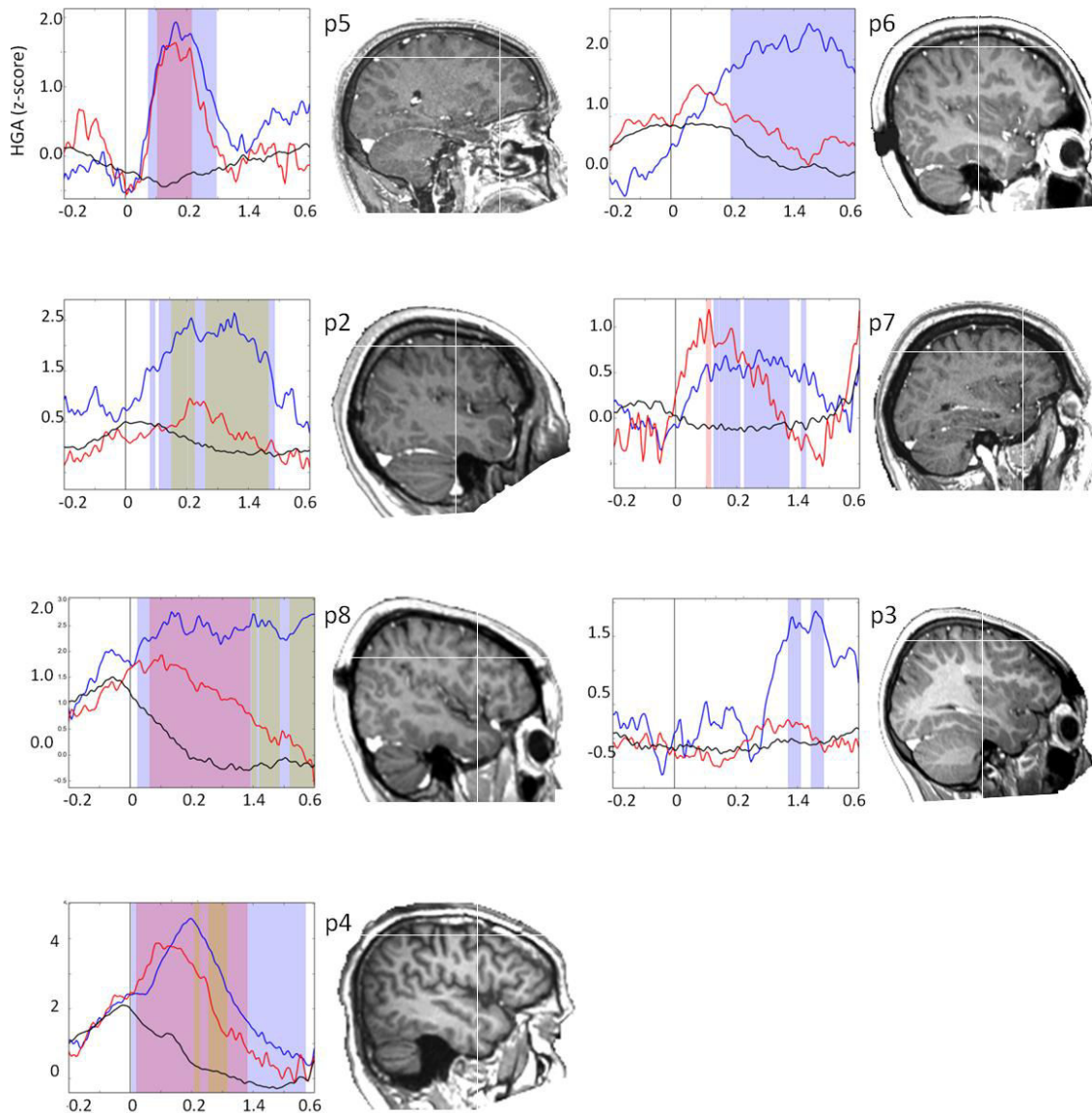


**Figure II.18 : Dorso-lateral pre-frontal cortex (DLPFC) cluster.**

The convexity of prefrontal cortex was largely sampled in all patients with a total of 29 electrodes, and an increased in the HGA was visible in 7 patients. Here we illustrate examples the time-course of HGA modulation in the DLPFC of these subjects induced by behavioural relevant responses. Time zero corresponds to the EMG onset. Time zero corresponds to the EMG onset. Segments with statistically significant difference between errors and correct responses are shaded in blue, between partial errors and correct responses are shaded in red, and between errors and partial errors are shaded in yellow.

### **8.3.8 The ventro-lateral prefrontal cortex (VLPFC)**

Five subjects have electrodes implanted in the rostral third frontal gyrus, that is in the VLPF, for a total of 9 recording electrodes, all disclosing a task-related response in the gamma band. Almost all electrodes (8/9) showed enhanced HGA power for both types of error compared to correct responses, with five sites disclosing a modulation from overt to partial errors and from partial errors to correct responses. Surprisingly, in this cluster, 4 recording sites, three of whom owing to the same patient, disclosed a inverted pattern with an enhanced response for correct responses and a reduced response for incorrect responses, which could somehow vary during the post-response period, as illustrated in Figure II.19.

### **8.3.9 The orbital-frontal cortex (OFC)**

In 7 patients, 11 recording electrodes were implanted in the orbital surface of the frontal lobe, 90.9% of them with enhanced HGA during the motor task compared to the pre-stimulus baseline. Nonetheless, in only four sites we recorded a positive modulation for overt and partial errors compared to correct responses. The time-course of high-gamma power was globally slightly delayed compared to more caudal and dorsal clusters, with sustained HGA beginning around 200 ms after EMG onset or later. In a fifth site we observed an inverse pattern with enhanced HGA for correct responses compared to partial errors. HGA responses in the OFC are reported in Figure II.20.

### **8.3.10 The frontal operculum**

Ten electrodes were implanted in 8 patients in different parts of the frontal operculum, including the central operculum (1 recording site), the *pars opercularis* (7 recording sites), and the *pars triangularis* (2 recording sites). Among all sites, a great majority (9/10) has an enhanced response to the task, the totality of which disclosed a modulation by performance, with HGA power larger for errors than for correct responses. Several sites showed an enhanced response for overt compared to partial errors and in one site we observed an inversed pattern of HGA modulation, similar to the ones observed in then VLPFC. High-gamma power modulations are illustrated for seven patients in Figure II.21.

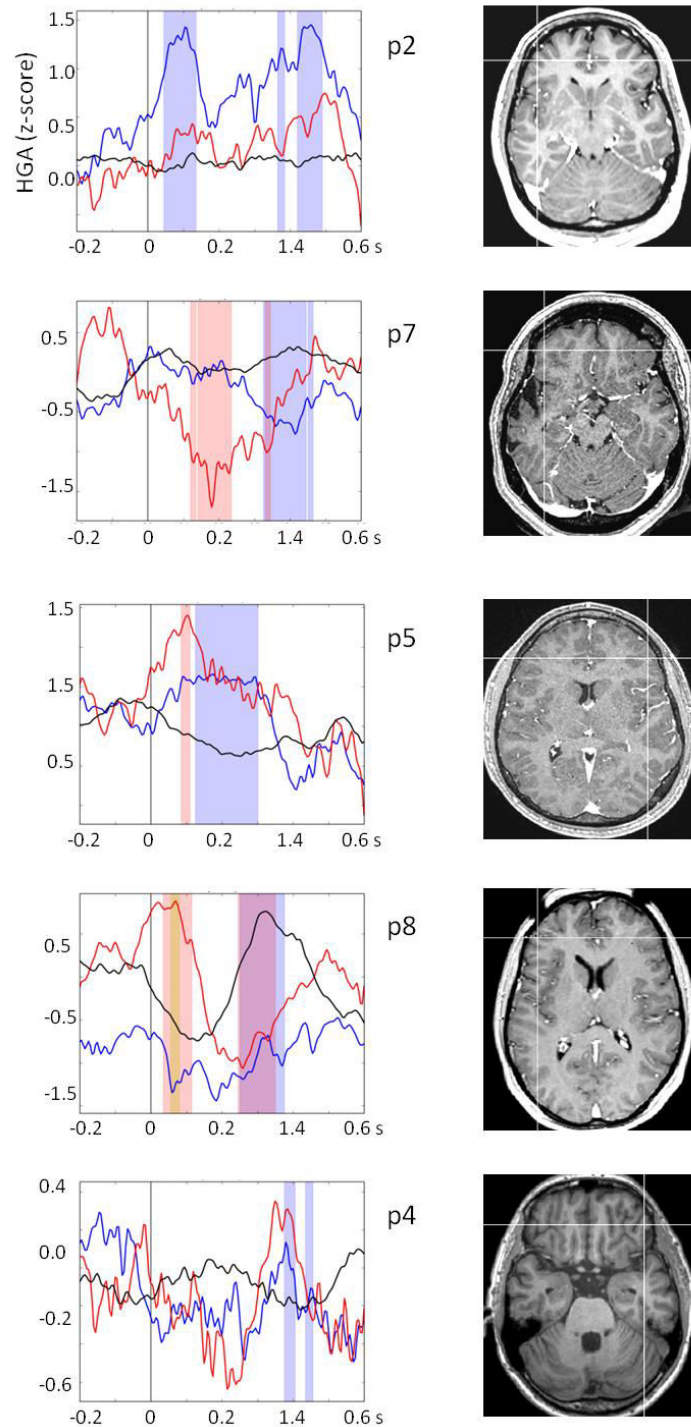


**Figure II.19 : Ventro-lateral prefrontal cortex (VLPFC) cluster.**

The inferior frontal gyrus sampled in 5 patients, all showing an increased in the HGA. The time-course of HGA modulation in the VLPFC of these subjects induced by behavioural relevant responses is illustrated. Time zero corresponds to the EMG onset. Segments with statistically significant difference between errors and correct responses are shaded in blue, between partial errors and correct responses are shaded in red, and between errors and partial errors are shaded in yellow. Note that in four recording sites HGA power was higher in correct response compared to incorrect response trials, as illustrated as an example for patient7 and 8.

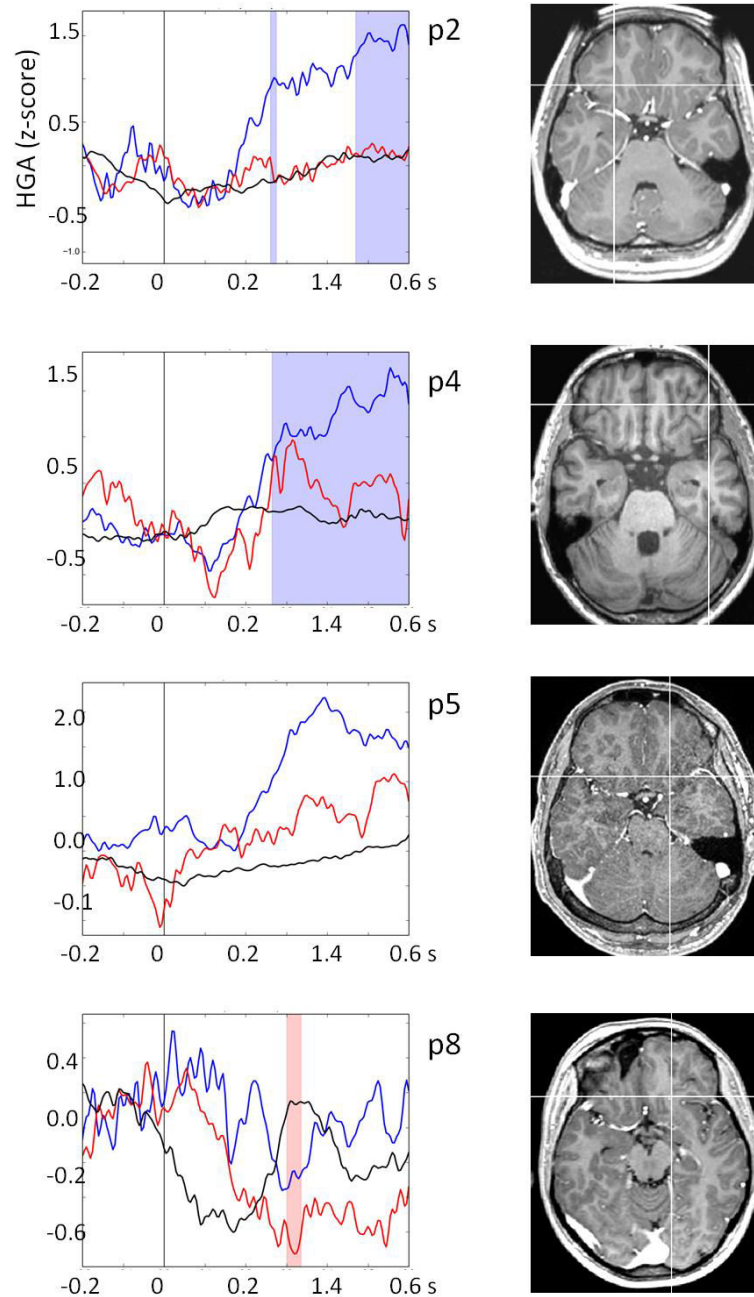


**Figure II.20 : Orbito-frontal cortex (OFC) cluster.**

*Time-course of HGA modulation in the OFC induced by behavioural relevant responses in four patients. Time zero corresponds to the EMG onset. Time zero corresponds to the EMG onset. Segments with statistically significant difference between errors and correct responses are shaded in blue, between partial errors and correct responses are shaded in red, and between errors and partial errors are shaded in yellow. As illustrated in the figure, one patient (8) disclosed enhanced HGA power for correct response compared to incorrect response trials.*

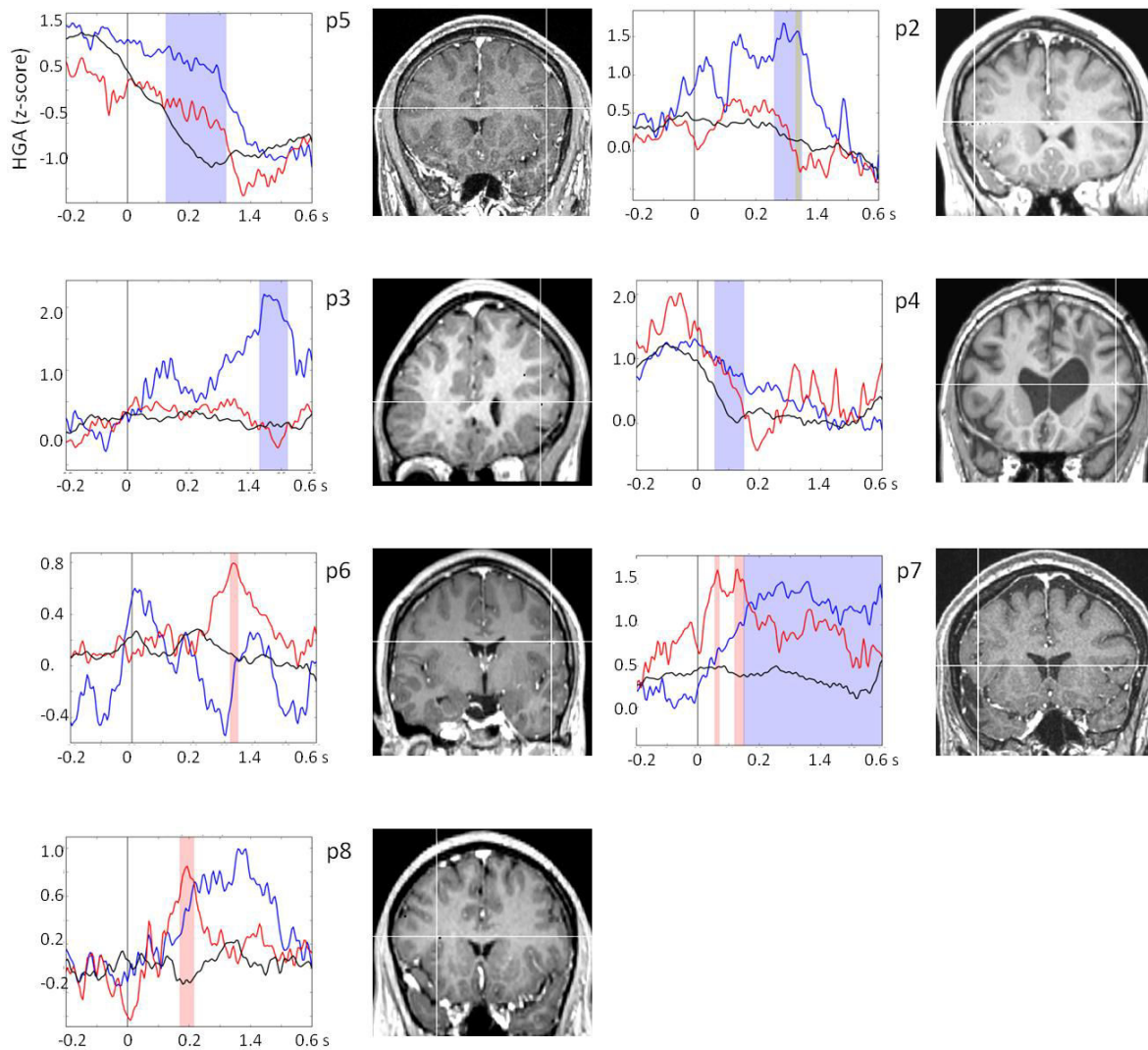


**Figure II.21 : Frontal operculum cluster.**

*Time-course of HGA modulation in the frontal operculum induced by behavioural relevant responses was detected in seven patients. Time zero corresponds to the EMG onset. Time zero corresponds to the EMG onset. Segments with statistically significant difference between errors and correct responses are shaded in blue, between partial errors and correct responses are shaded in red, and between errors and partial errors are shaded in yellow.*

### 8.3.11 The anterior insula

Three patients have an exploration of anterior insular cortex (mostly in its dorsal part) for evaluation of their epilepsy. All five recording sites showed a non-specific task-related increase of HGA, and four of them an specific increase for incorrect responses (both errors and partial errors) consisting in a sustained energy increase from around 100 ms to 400-500 ms (Figure II.22).

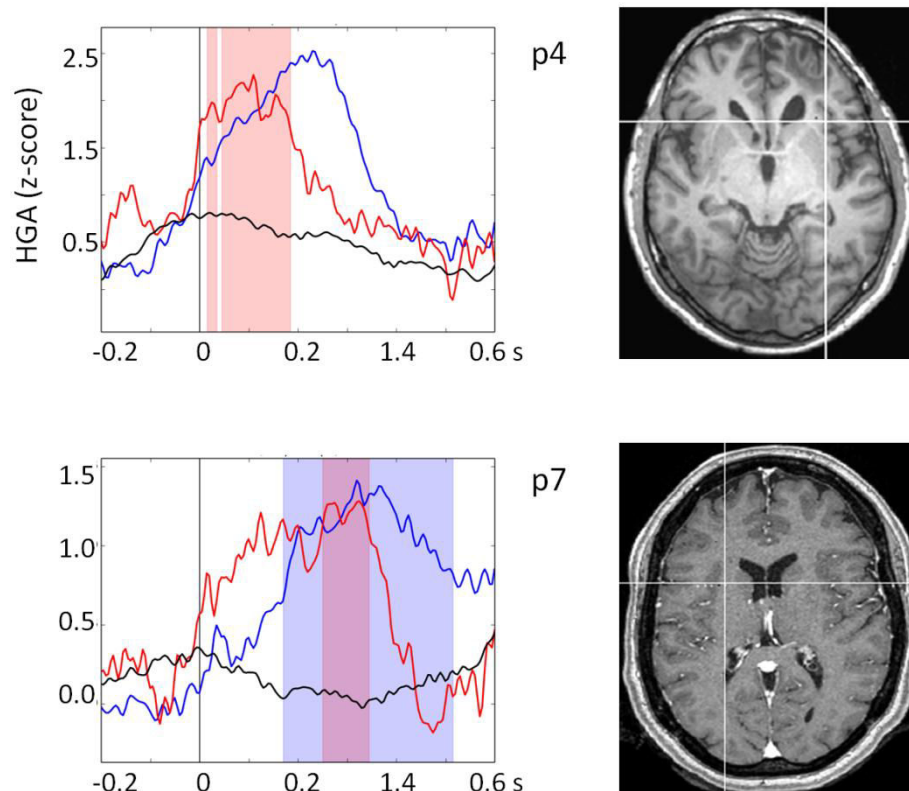


**Figure II.22 : Anterior Insula cluster.**

*The anterior-dorsal insula was explored in with five recordings sites in three patients, and HGA modulation in the rACC induced by behavioural relevant responses was visible in four recording sites in two patients. Time zero corresponds to the EMG onset. Time zero corresponds to the EMG onset. Segments with statistically significant difference between errors and correct responses are shaded in blue, between partial errors and correct responses are shaded in red, and between errors and partial errors are shaded in yellow.*

### **8.3.12 *Single-trial HGA and ERPs***

For patient 1 in the SMA error-related potentials were visible in 21/23 trials (91.3% of trials), while single trials HGA modulation was present in 20/23 trials (86.95% of trials). As the ERP and the HGA co-occurred in the SMA in 82.6% of cases (19/23 trials), which is very close to their odds' product (79.4%), single trial ERPs and HGA can be considered independent. A same independency has been found between ERPs and HGA in the ACC, which occurred respectively in 73.9% (17/23 trials) and 52.2% of cases (12/23 trial), leading a probability of co-occurrence at 38.5%, which was very similar to the observed co-occurrence (39.1%, that is in 9/23 trials).

For patient 4 we obtained similar results concluding for an independency between the occurrence of the ERP and the HGA both for the SMA and for the OMPFC. The probability to observe an ERP and HGA in the same trial was 44.6% in the SMA (ERP visible on 54/77 trials, that is 70.1%, and HGA increase detected on 49/77 trials, that is on 63.6%), while we actually observed both phasic and induced activities on 35/77 trials, that is in 45.4% of cases. In the OMPFC, ERPs and HGA occurred respectively in 49.3% (38/77 trials) and 53.2% of cases (41/77 trial), leading a probability of co-occurrence at 26.3%, which was very close to the observed co-occurrence (27.3%, that is in 21/77 trials).

	SMA	preSMA	MCC	rACC	DLPFC	VLPFC	OFC	Frontal Operculum	Insula	Total
N° patients	5	6	7	4	9	5	7	8	3	93 (9)
N° recorded sites	7	8	8	6	29	9	11	10	5	
N° non-specific (task-related) (%)	7 (100%)	6 (75.5%)	7 (85.7%)	5 (83%)	19 (65.5%)	9 (100%)	10 (90.9%)	9 (90%)	5 (100%)	77 (82.7)
N° (Partial) Error > Correct (%)	6 (85.7%)	2 (25%)	3 (37.5%)	2 (33.3%)	17 (58.6%)	8 (88.8%)	4 (36.4%)	9 (90%)	4 (80%)	55 (59.1%)
N° Overt Error > Correct (%)	6 (85.7%)	2 (25%)	3 (37.5%)	1 (16.6%)	15 (51.7%)	5 (55.5%)	4 (36.4%)	8 (80%)	4 (80%)	55 (59.1%)
N° Partial Error > Correct (%)	5 (71.4%)	0 (0%)	2 (25%)	1 (16.6%)	9 (31%)	5 (55.5%)	4 (36.4%)	6 (60%)	3 (60%)	35 (37.6%)
N° Overt Error > Partial Error (%)	3 (42.8%)	0 (0%)	1 (12.5%)	0 (0%)	2 (6.9%)	2 (22.2%)	1 (9.1%)	2 (20%)	0 (0%)	11 (11.8%)
N° Correct > (Partial) Error (%)	0 (0%)	0 (0%)	0 (0%)	0 (0%)	0 (0%)	4 (44.4%)	1 (9.1%)	1 (10%)	0 (0%)	6 (6.4%)

**Table 2.** Overview of anatomical regions exhibiting significant HGA power modulation induced by motor response during the task. For each anatomical cluster, the total number of recording sites is reported, as well as the number and the percentage of sites with task-related and outcome-modulated significant HGA modulation.

## 8.4 Discussion

In the present study we assessed, to our knowledge for the first time, high-gamma neuronal oscillations induced by motor responses during action monitoring using direct recordings of LFPs of human cerebral cortex. As a first major result we found that behavioural relevant motor responses during the task activate a large-scale network of fronto-insular brain regions indexed by widely distributed HGA (> 60 Hz) power modulations. Indeed a large majority of recording sites (82.7%), including all explored structures among the whole patients population, disclosed increased high-gamma energy at the time of the motor response as defined by the EMG onset. Furthermore, this increase of HGA was modulated by subjects' performance in almost 60% of sites and in all anatomical clusters, that is, in the SMA, the preSMA, the MCC, the rACC, the DLPFC, the VLPFC, the OFC, the frontal operculum and in the anterior Insula. Nonetheless, only in certain structures the HGA was systematically (that is in almost all recording sites) modulated by action outcome, namely the SMA, the VLPFC including the opercular region and the anterior insula. In these regions enhanced high-gamma responses for erroneous responses were detected on 80% of sites (insula), 86% (SMA) and around 90% in VLPFC and frontal operculum, while in the other structures this was observed only on about 35% of recording sites. Additionally, for almost all recording sites, the high-gamma power was modulated by outcome in a binary manner: as reported in results and Figures II.14-22, HGA power was markedly enhanced for incorrect responses (whether partial or full-blown), while on correct trials its time-course showed an absence of increase or a clear decrease after EMG activation.

Taken as a whole our results point out a clear (and double) dissociation between present high-frequency oscillatory responses and the well-known classical electrophysiological signature(s) of the action monitoring system, above-all the Error Negativity (Ne) (Falkenstein et al., 1991; W.J. Gehring et al., 1993) on the other hand low-frequency oscillatory induced activity known as the midline frontal theta (Phan Luu & Tucker, 2001; Nigbur et al., 2012). Indeed, beyond the controversy about the artifactual origin of the midline theta and of its relationship with the Ne (Yeung, Bogacz, et al., 2004), both these activities are assumed to originate in limited cortical structure(s) within the medial frontal cortex (Cohen & van Gaal, 2014; Dehaene et al., 1994; M. J. Herrmann et al., 2004; Roger et al., 2010; Van Veen & Carter, 2002). More specifically, as revealed by our previous study, the Ne has found to originate in the SMA, while more delayed and specific to errors ERPs are generated in the rostral part of the medial pre-frontal cortex. Thus, the first dissociation is

fundamentally anatomical: while outcome modulated ERPs are generated in limited and well-defined cortical areas within the medial frontal cortex, HGA modulation in response to action outcome spread widely in all explored regions, encompassing the whole medial, lateral and orbital aspects of the frontal lobe and involving extra-frontal structures such as the anterior insula. Secondly, a functional dissociation exists between non-oscillatory time-locked activity and the HGA in action monitoring: the first responds in a continuous manner with gradual increase from correct responses (the Ne-like on scalp EEG data but refer also to our previous results), to partial then to overt errors (Scheffers et al., 1996; F Vidal et al., 2003, 2000), while the second mainly respond in a binary manner disclosing an increasing energy only for incorrect responses, even in the SMA.

It is now natural to wonder about the anatomo-functional grounds of the patent divergent behaviours of these two electrophysiological measures assessed during action monitoring, which evidently reflect different neuronal processes, both in terms of neuronal sources of electrical activities and in terms of role in more large-scale neuronal communication and function.

A possible lens to interpret the present data is offered from the data itself and from rather recent advances in human anatomical connectivity. Indeed, as above mentioned, although all structures disclosed enhanced HGA in response to subject's performance, this was systematically observed only in the SMA, in the VLPFC including the frontal operculum, and in the insula. Such finding in the SMA is not surprising, since this structure has demonstrated to play a key role in action monitoring by emitting a continuous outcome-modulated signal (the Ne, see the previous study) each time a behaviourally relevant response is produced. Concerning the VLPFC, recent diffusion tractography and post-mortem dissections study allowed discovering of a short frontal intralobar tract directly connecting the SMA and the preSMA with the posterior part of the inferior frontal gyrus (IFG), namely the *pars opercularis*, but also the *pars triangularis* and the inferior region of the pre-central gyrus, that is the central operculum (Catani et al., 2011). This direct system of fibers, called the "frontal aslant tract", could therefore represent the anatomical pathway through which the SMA, henceforth recognised as a fundamental node in the network underlying action monitoring, communicate with the VLPFC and the frontal operculum via high-gamma neuronal oscillations. Concerning the Insula, its dorsal dysgranular and granular cortex have shown to be connected in the macaque with both areas F3 and F6 on the medial frontal wall, whose human homologous are the SMAs (M Matelli & Luppino, 1991; Zilles et al., 1995),

and coherently, a recent study found tractography samples from the dysgranular and granular insula in the most dorsal extent of the premotor cortex as well as in the supplementary motor area (Cerliani et al., 2012). These anatomical-connectivity data could thus explain, at least in part, why the VLPFC with the frontal operculum and the antero-dorsal insula, which are strongly interconnected with the SMA, disclose together a systematic modulation of their high-gamma oscillatory activity for incorrect motor actions.

Additionally, whereas lower frequency LFPs activities (as the ERPs) are thought to represent the synaptic activity of a large population of neurons (a few thousand) (Nunez, 1981), HGA are considered to reflect the activity of smaller population of neurons (Nunez, 1981), as higher frequencies are probably largely influenced by currents associated with action potentials (Ray et al., 2008; Ray & Maunsell, 2011). In fact action potentials can be modeled as a quadrupole along the axonal axis (Pernier, 2007) and consequently the resulting potential decreases proportionally to the cube of its distance to the source and it can be recorded only at small distance. Thus it is likely that HGA from LFP recordings allow estimating (either indirectly or directly) spiking activity in a relatively small population of neurons (Ray et al., 2008). This could explain the non-systematic HGA responses observed in the other frontal regions, namely the preSMA, the cingulate cortex, the DLPFC and the OFC, where recording sampling would allow detection only of “islets” of neuronal activity. On the other hand, in a region massively and constantly activated during the task, like the SMA or the VLPFC, it would be easier to observe HGA wherever the electrode is placed.

In sum HGA and ERPs have quite different neuronal origins and thus they can be relatively independent to each other. This has been confirmed in this study by the absence of correlation between single trial ERP and single-trial HGA responses, both in the SMA and in the medial prefrontal cortex in both patients with error-evoked potentials visible on a trial-by-trial basis. A consequent question is: what is the functional meaning of the high-gamma binary response recorded in the SMA, the VLPF with operculum and in the Insula? More particularly, which information is supplied by high-gamma responses activated through a frontal network partially different from the network underlying the error negativity? Detection of HGA in the VLPFC is not incoherent, since a role for the VLPFC in cognitive control has been largely established thanks to numerous fMRI studies (Aron, Robbins, & Poldrack, 2004; Miller & Cohen, 2001; Wagner, Maril, Bjork, & Schacter, 2001). Particularly, the inferior frontal gyrus, has been associated to suppression of inappropriate responses, that is to response inhibition, possibly via subcortical projections to the subthalamic nucleus (Aron et

al., 2004; Aron, Robbins, & Poldrack, 2014; Hampshire, Chamberlain, Monti, Duncan, & Owen, 2010; Wery P M van den Wildenberg et al., 2006). Thus the enhanced HGA for errors in the VLPFC might represent an inhibitory activity of this region since: 1) HGA is compatible with a neuronal output, and 2) the binary modulation of the HGA (absence of increase for correct responses) is coherent with the need to produce an inhibitory output only in case of incorrect association. An implication of frontal operculum and of anterior insula have also been claimed for feedback processing and action monitoring (Céline Amiez et al., 2016; Céline Amiez, Sallet, Procyk, & Petrides, 2012; Dosenbach et al., 2006), which is in agreement with present findings. As well, a similar mechanism can be hypothesized for the SMA, whose major role in movement inhibition is well established (Spieser, van den Wildenberg, Hasbroucq, Ridderinkhof, & Burle, 2015; Sumner et al., 2007). Alternatively, HGA in the SMA could indicate that this region “sends” the acquired information about ongoing actions (namely the incorrect ones) to other higher-order structures, charged to enhance cognitive control. Certainly, if one admits that the LFPs indicate neuronal input, it remains to understand how the VLPFC has been informed about action performance since, as observed in the first study, contrarily to the MPFC, no LFP have been recorded in this region. Similarly, one could question why the MPFC, which has found to present a single trial evoked activity directly correlated to the one of the SMA (see first study), demonstrates to be relatively “silent” in terms of HGA. However, all this remains speculative since, even admitting that HGA represents neuronal output it is not possible at present to establish the nature of such an output (inhibitory or excitatory) nor the target of the output.





## **9 STUDY 3: DOES ERROR NEGATIVITY AND FEEDBACK-RELATED NEGATIVITY HAVE THE SAME CORTICAL GENERATOR? EVIDENCE FROM SIMULTANEOUS EEG/MEG RECORDINGS OF ERROR RELATED ACTIVITIES**

### **9.1 Introduction**

Whether interpreted as reflecting error detection, or conflict between competitive responses (Yeung, Botvinick, et al., 2004), or as representing a signal of a reward-prediction error (C. B. Holroyd & Coles, 2002), or even the emotional arousal associated with errors (Phan Luu et al., 2003), the Error Negativity (Ne) evoked by behaviourally relevant responses in choice reaction-time (RT) task is always generated on the basis of internal information, even in the absence of reafferences (S Allain, Hasbroucq, Burle, Grapperon, & Vidal, 2004).

When information on response correctness is unavailable until provided by an external feedback, another ERP component related to the Ne, the feedback-related negativity (FRN) is elicited around 270 ms after feedback presentation (William J Gehring & Willoughby, 2002; W.H.R. Miltner et al., 1997; Ruchow et al., 2002). The Ne and the FRN both show negative polarities, fronto-central topography and sensitivity to bad outcome, and are therefore usually considered as reflecting the same underlying cognitive process of error evaluation, in the first case as a consequence of an internally generated information, in the second as a consequence of an externally provided information (W.H.R. Miltner et al., 1997).

The hypothesis that a single error-processing mechanism produces both an ERN associated with error commission and an FRN associated with negative feedback presentation has been significantly developed by Holroyd & Coles (C. B. Holroyd & Coles, 2002) in the context of the reinforcement-learning theory. According to this model, in case of a discrepancy between expected and actual outcome – as in case of erroneous responses – the mesencephalic dopaminergic system conveys a prediction error signal through its dopaminergic projections to the medial frontal cortex. This, in turns, emits a “learning” signal which is necessary to update the response production system (C. B. Holroyd & Coles, 2002; Nieuwenhuis et al., 2004). Such a signal would be represented either by the Ne or by the

FRN, depending on the origin, internally or externally delivered, of the information about response outcome, and the medial frontal structure generating that signal is assumed to be the anterior cingulate cortex (ACC). Indeed, source - localization studies of the Ne and the FRN (Dehaene et al., 1994; M. J. Herrmann et al., 2004; C. B. Holroyd & Coles, 2002; Nieuwenhuis et al., 2004; Ruchow et al., 2002; Van Veen & Carter, 2002) have pointed to this region as the generator of both Ne and FRN. Similarly fMRI studies (Céline Amiez et al., 2013, 2012; Debener et al., 2005; C. B. Holroyd et al., 2004; Monchi, Petrides, Petre, Worsley, & Dagher, 2001; Ridderinkhof et al., 2004; Markus Ullsperger & Cramon, 2001a; Markus Ullsperger & von Cramon, 2003) have shown increased activation of the ACC after both erroneous motor responses and presentation of a negative feedback. Furthermore, single-cell recordings in nonhuman primates indicate that feedback evaluation leads to modulation of neuronal firings in the ACC (C Amiez et al., 2005; Ito et al., 2003; Michelet et al., 2007).

However, in our first study we found that the Ne was generated in the SMA. This result is clearly in contradiction with the above mentioned hypothesis of a unique generator in the ACC for the two negativities underlying the same evaluation process. Therefore two alternative hypotheses could explain such a apparent incongruence: either 1) both negativities, with the same functional meaning, originate in the same structure which would be, in that case, the SMA rather than the ACC; or 2) the Ne and the FRN have distinct cortical sources. This last hypothesis implies that they thus reflect distinct cognitive processes. The first hypothesis seems the less likely, since there are numerous strong data supporting the idea of an important role of human and monkey ACC in feedback processing (C Amiez et al., 2005; Céline Amiez et al., 2013; Michelet et al., 2007). To reconcile our previous results findings pointing to the SMA as the source of the Ne with converging evidence of a main involvement of the ACC in feedback evaluation, we rather hypothesized that the Ne and the FRN, contrary to what is often assumed, are not generated by the same cortical structure.

To test this hypothesis we designed an experimental task in which participants use feedback stimuli to learn, by trial-and-error, the association rules between stimulus and response side. In such a task, the amplitude of the FRN is usually sensitive to performance in the learning phase while the amplitude of the Ne is usually sensitive to performance when the rule has been learnt (C. B. Holroyd & Coles, 2002; Nieuwenhuis et al., 2002).

In Experiment 1, we have observed that the Ne was elicited in both SMAs for unimanual responses. Therefore, we suspected that the activities generated by the parts of the

SMA<sub>s</sub> situated in the banks of the interhemispheric fissure might cancel each other while, given that SMA<sub>s</sub> in humans partly extend on the dorsal convexity, activities generated by this most superficial part of the SMA<sub>s</sub> would add up and generate the surface-recorded Ne. Indeed, as indicated in the introduction section, if we accept to model cortical activities by equivalent dipoles, those elicited in the banks of the interhemispheric fissure are tangential. MEG, being essentially sensitive to tangential generators, should, in principle, easily pick them up, but if these dipoles are generated bilaterally (that is if their directions are opposite) they will cancel each other, and MEG (as well as EEG) will be blind to them.

Activation of the part of the SMA<sub>s</sub> situated on the convexity can be accounted by a radial dipole. If both SMA<sub>s</sub> are active, these dipoles being parallel, instead of cancelling each other, as in the case of tangential dipoles, will add up and will easily show up on EEG recordings, while MEG, being less sensitive to radial generators, should be almost blind to these activities.

Keeping in mind this possibility, we decided to record simultaneous EEG and MEG in the same task. In case of absence of an identifiable Ne with MEG recordings, it would be mandatory to demonstrate with EEG that the Ne is actually present but not visible.

Finally, since previous studies have shown a magnetic analogue of the FRN (Talmi, Fuentemilla, Litvak, Duzel, & Dolan, 2012), our working hypothesis was that the Ne and the FRN are elicited by different generators and that this hypothesis could be tested by comparing the patterns of activities evoked (or not evoked) on MEG and EEG signals, by the FRN during learning, on the one hand, and by the Ne once the rule is learnt, on the other hand

## **9.2 Materials and Methods**

### **9.2.1 Subjects**

Sixteen subjects aged from 20 to 36 years (mean age  $26,1 \pm 4,4$ ), 8 male, 8 female, participated in the study. All of them were right-handed and had normal or corrected-to-normal vision. Accordingly to the declaration of Helsinki, a written informed consent before starting the experiment was obtained from each of them.

### **9.2.2 Task**

The subjects performed a between-hand choice reaction-time (RT) task. Initially subjects learned by trial and error and thanks to a feedback stimulus, which of two buttons to press after the presentation of response signals. An experimental block was composed of three parts. Participants executed three experimental blocks of 176 trials each. Stimuli were different from one block to the other.

In the first part of the block, which was called Learning phase, subjects had to learn the association between a visual target and the response side. The requested response was a left or right thumb keypress. A trial started with a fixation cross. The visual target was a centred, white, geometric shape, presented for 1000 ms. Following an 800 ms intra-trial interval, a visual feedback lasting 800 ms informed if the given response was correct (“Oui”) or not (“Non”), or if the response was delivered too late, that is after 1000 ms (“Tard”). Following an inter-trial interval lasting 1200 to 2500 ms, a second stimulus appeared. During this first Learning phase, which consisted of 48 trials, eight different stimuli to be learned were presented.

In a second intermediary part, called Consolidation phase, only four within the eight stimuli were presented, in order to consolidate the stimulus-response association. The Consolidation phase was necessary to assure that subjects had correctly learned these four stimuli which would be presented in the subsequent phase. It consisted of 16 trials.

The following third phase had been called Simon phase as it was characterized by a manipulation of spatial congruency as in the classical Simon task (Craft & Simon, 1970), with the aim of facilitate errors. Stimulus-response association was the same than in the preceding phases but the four stimuli (the same than in the Consolidation phase) were presented on left or right location with respect to a fixation cross. Location was an irrelevant attribute, so that on incongruent trials stimulus was presented on the side opposite to the response to be given, while on congruent trial it was presented on the same side as that of the required response. Furthermore, in order to facilitate errors, time pressure was enhanced by reducing stimulus presentation at 150 ms and by reducing maximum RT to 700 ms. The other parameters of the task (intra- and inter-trial interval, feedback duration) were the same as those of the two previous phases; number of trial was 112. Presentation software was used for stimulus delivery and experimental control during MEG/EEG acquisition.

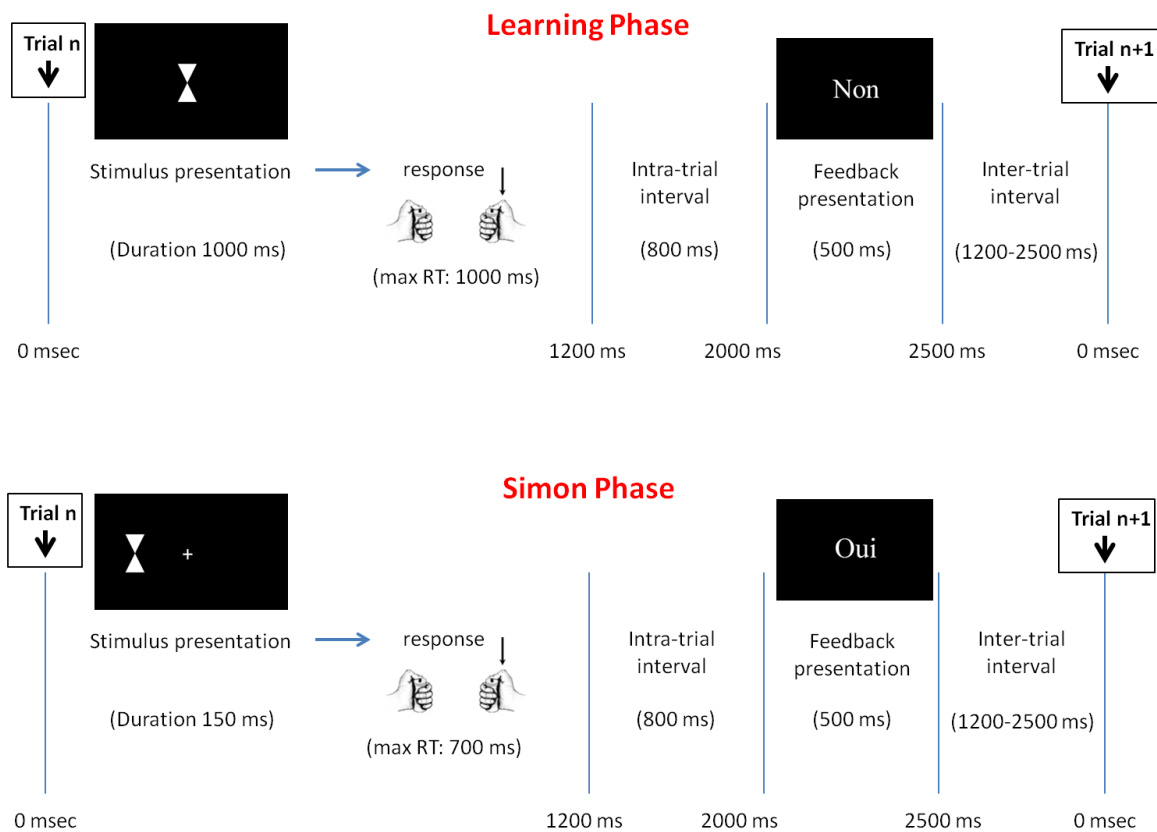


**Figure II.23 : Performance-monitoring and feedback evaluation paradigm.**

The Learning and the consolidation phases are illustrated on top panel. The Simon phase is illustrated in the bottom panel. As showed in the figure, stimulus is presented in a central location during the two first phases, while it is presented in a right or left location (irrelevant for the task at hand) in the third phase, in order to facilitate errors. Additionally, duration of stimulus presentation as well as maximal RT were reduced in the Simon phase.

### 9.2.3 EEG and MEG data recordings and pre-processing

The data were acquired at La Timone hospital in Marseille on a 4D Neuroimaging MEG/EEG system at a sampling rate of 2035 Hz (for EEG/EMG) and 2034.51 Hz for MEG (bandwidth DC-800 Hz). A total of 248 MEG magnetometers were recorded with an online correction based on reference channels. Scalp EEG was recorded from sixty-four sintered Ag/AgCl metal electrodes conformed to the 10–20 positioning system. A scalp reference (between Cz and CPz) was used for EEG acquisition.

Recordings included 30 seconds of baseline background activity before starting each block.

The electromyographic activity of the *flexor pollicis brevis* of both hands was recorded with two electrodes placed on the thenar eminences. Motor responses were acquired using a LUMItouch optical response keypad.

The electrooculography (EOG) and the Electrocardiography (EKG) were recorded by paired surface electrodes in order to correct for eye movement and EKG artifacts.

A subject-specific headframe coordinate reference was obtained thanks to three anatomical landmarks (nasion, left and right tragus), which were subsequently digitalized (Polhemus Digitization System), together with five coils and subject's head shape at the start of the recording session. Before and after each block subject's head position with respect to the five coils and the MEG sensors was estimated in order to verify the absence of large dislocation during data acquisition.

Subjects were comfortably installed in a half-seated position in the magnetically shielded room and were monitored by a video-camera during the session. Subjects were instructed to avoid movements as much as possible. Before starting the experimental and data acquisition sessions, subjects run a shorter training version of the task in order to familiarize with it.

#### **9.2.4 EEG and MEG data analysis**

The onset of EMG activity was marked manually after visual inspection as this is considered the more accurate technique (Van Boxtel et al., 1993).

Eye blinks were isolated and removed from EEG traces using an Independent Component Analysis (ICA). Similarly, ICA was used to remove eye blinks as well as EKG activity from MEG signals.

All other artefacts were manually rejected after visual inspection on continuous MEG and EEG traces. We re-referenced off line EEG monopolar recordings into average reference data, which considerably increased the quality of the data. In order to process as similarly as possible EEG and MEG data, visual inspection of MEG data was performed as on EEG data: MEG signals of each group of 4 contiguous sensors in the 248 channels were averaged and subsequently, artefacts rejection was manually performed on 62 virtual (averaged) channels,

on MEG continuous data. EMG marking procedure and EEG/MEG artefact rejection were performed using AnyWave software (Colombet, Woodman, Badier, & Bénar, 2015).

Data were analysed from the Learning phase and from the Simon phase, using the FieldTrip MATLAB software toolbox (Oostenveld, Fries, Maris, & Schoffelen, 2011). For each phase, trials were grouped into three categories based on response correctness and EMG pattern: pure correct, error and partial error trials. EEG and MEG traces were epoched time locked to the EMG onset leading to the mechanical response for pure correct and overt error trials, and time-locked to the small incorrect EMG burst for partial error trials. Epochs of 1000 ms (-500 ms, +500 ms) were obtained around EMG onset. Epochs of 700 ms (-100, +600 ms) around feedback presentation were extracted from EEG and MEG traces.

Monopolar EEG data were set up in averaged reference montage. We computed a Laplacian transformation of the monopolar EEG data to improve detection of negativity on correct trials (note that the reference, whether monopolar or averaged, has strictly no influence on the outcome of the Laplacian transformation). EEG signals were first interpolated with spherical spline interpolation (Pernier et al., 1988), and afterward, the second derivatives in the two dimensions of space were calculated. The chosen degree of the spline was three as this value minimizes errors (Pernier et al., 1988), and the interpolation was computed with a maximum of 15 degrees for the Legendre polynomial.

Averaged MEG data were visually analyzed in order to appreciate the time-course and the waveform of the evoked fields and to compare them to the well-known equivalent evoked potentials.

Considering that there is no effect of the responding hand in this type of situations, regardless of the responding hand, all central contralateral and ipsilateral EEG activities have been averaged together. This, of course, could not be done with MEG signals since symmetrical dipolar activities at cortical level result in asymmetrical magnetic fields at scalp level.

### **9.2.5 Statistical Analysis:**

First, we aimed at determining the maximal amplitudes of the evoked activities on averaged data while avoiding artefactual differences due to larger noise contamination of error

data, as compared to correct data: the signal to noise ratio is lower on errors than on correct trials because errors are fewer. To do so, for the Ne we took a time window of 40 ms centred both on the positive dip preceding the Ne and its negative peak and we computed the mean amplitude in these time-windows. Subsequently we calculated the difference between the two means (of the dip and the peak) to obtain the amplitude of the evoked potential (F Vidal et al., 2000). For the FRN, we compared the mean amplitude of its peak (relative to a 100 ms prestimulus baseline) in a 40 ms time window centred on the peak (270 ms) for correct and error FRN.

Probably because the keypad used in this experiment was extremely sensitive, there was an unusual small number of partial errors and, although these trials have been separated from pure correct and error trials, they were too few to allow further reliable analysis.

Analysis of behavioural data was performed as reported in chapter 2.

### **9.2.6 Source Localisation:**

Source localisation off MEG grand-average data was computed on a default anatomy (ICBM 152, <http://www.sciencedirect.com/science/article/pii/S1053811910010062>) using the Brainstorm software (Tadel, Baillet, Mosher, Pantazis, & Leahy, 2011). For inverse modelling, we used the whitened and depth-weighted linear L2-minimum norm estimates, implemented in Brainstorm. We used a data-based average subject-specific headframe coordinate reference. Noise covariance for the inversion was estimated on the baseline window of recorded data (-100 to 0 ms for FRN and -500 to -100 ms for Ne). Source time-courses were standardized on those baseline windows.

## **9.3 Results**

### **9.3.1 Behavioural data**

Behavioural and EMG data replicated previous data: the error rate was higher in incongruent trials (8.8%) than in congruent trials (6.1%,  $F(1,14) = 20.77$ ,  $p < .00$ ). Similarly RT in congruent trials was shorter (497 ms) than in incongruent trials (514 ms) ( $F(1,14) = 11.84$ ,  $p < .00$  one tailed). Partial error rate was low, (probably because of keypad sensitivity,

both in congruent (0.21) and incongruent (0.22) trials, with no significant difference between trial type ( $F(1,14) = 1.64, p = 0.22$ ).

### **9.3.2 EEG and MEG results**

In this session we will first present data averaged on EMG onset for the Simon Phase followed by data averaged on feedback in the learning phase. We will show electrophysiological data for errors and correct trials only. Since we clearly predict the direction of the tested effects, for the Ne and for the FRN (namely that activities are larger on errors than on correct responses), we resorted to one-tailed Student's  $t$  tests in the following.

#### *Error Negativity in the Simon phase*

**EEG:** Figure II.24 shows, respectively on the top and on the bottom panel, the averaged reference montage and the Laplacian grand average obtained over FCz electrode for errors (red line) and correct responses (blue line), time-locked to the relevant EMG activity onset, as well as their topography. The present data replicate published data (Falkenstein et al., 2000; S Hoffmann & Falkenstein, 2010; F Vidal et al., 2003, 2000) with a negative wave peaking shortly after errors and a smaller but highly visible negativity after correct responses. Statistical analysis of average reference and Laplacian-transformed data confirms that the amplitude of the negativity evoked by errors was significantly higher than the amplitude of the negativity on correct trials: averaged reference:  $t(14) = 4,604, p = 0,0002$  (one-tailed); Laplacian  $t(14) = 2,6283, p = 0,0099$  (one-tailed). Both error and correct related negativities present typical and identical fronto-central topography after Laplacian transformation. Thus, this activity corresponds to the Error negativity.

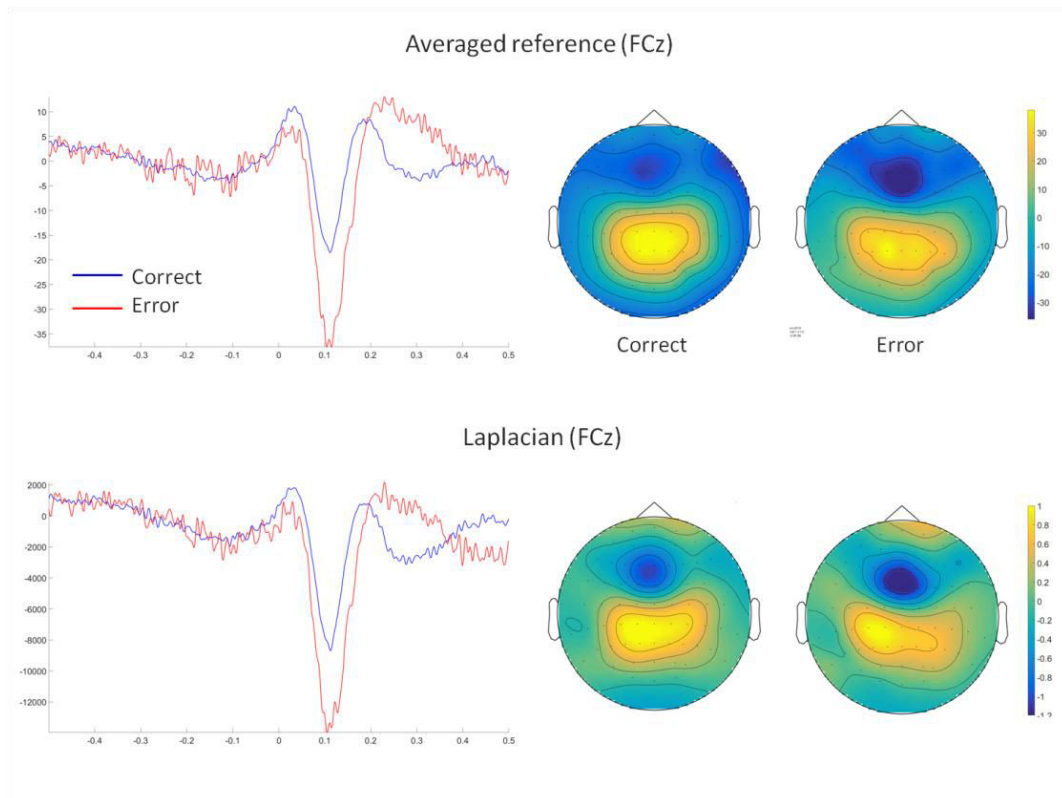


**Figure II.24 : The Ne on EEG data in the Simon phase.**

*EEG grand-averages (FCz) time-locked to EMG onset in the Simon phase, for error trials (red line) and correct trials (blue line). Top panel illustrates Averaged Reference data and corresponding topographies for correct and error trials. Bottom panel illustrates Laplacian transformed data and corresponding topographies for correct and error trials. Time zero corresponds to the EMG onset. The negative wave, as the Ne reported in the literature, shows higher amplitude for errors compared to correct trials in both Averaged reference and Laplacian data.*

**MEG:** A careful examination of the grand-averaged MEG data time-locked to EMG onset in the Simon phase did not demonstrate a magnetic equivalent of the Ne. On the contrary, at the same latency as that of the Ne observed on EEG data, we observed an evoked field which was clearly lateralized, contralateral to the responding hand and which was not modulated by subjects' performance, that is to say, it clearly showed the same amplitude for errors and for corrects responses. Consequently, since 1) it is insensitive to performance and 2) its response-dependent topography is clearly incompatible with a medial generator, this component cannot be considered as a magnetic analogue of the Ne. Furthermore, the source localization of this activity, found a source contralateral to the responding hand on the fronto-central convexity, approximately located on the primary sensori-motor cortex (Figure II.26).

The time-course of such evoked field and its lateralized fronto-central topography are shown on Figure II.25.

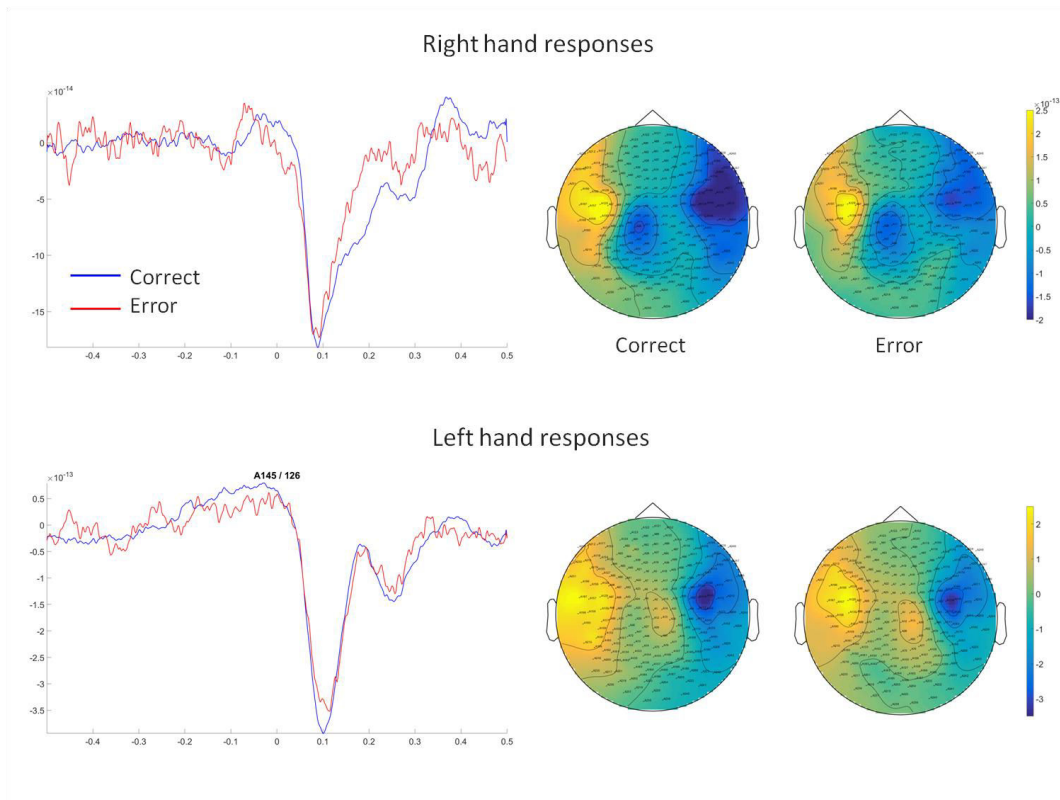


**Figure II.25 : Response-related MEG data in the Simon phase.**

Grand-averaged MEG data time-locked to EMG onset in the Simon phase are presented for right hand responses (top panel) as well as for left hand responses (bottom panel). Time zero corresponds to the EMG onset. As illustrated in the two figures corresponding to the time course of MEG data, an evoked field peaks, around 100 ms second after EMG onset, that is, at the same latency as the Ne on EEG data, disclosing the same amplitude for correct and erroneous trials. This field is contralateral to the responding hand and shows comparable topographies for both trial types.

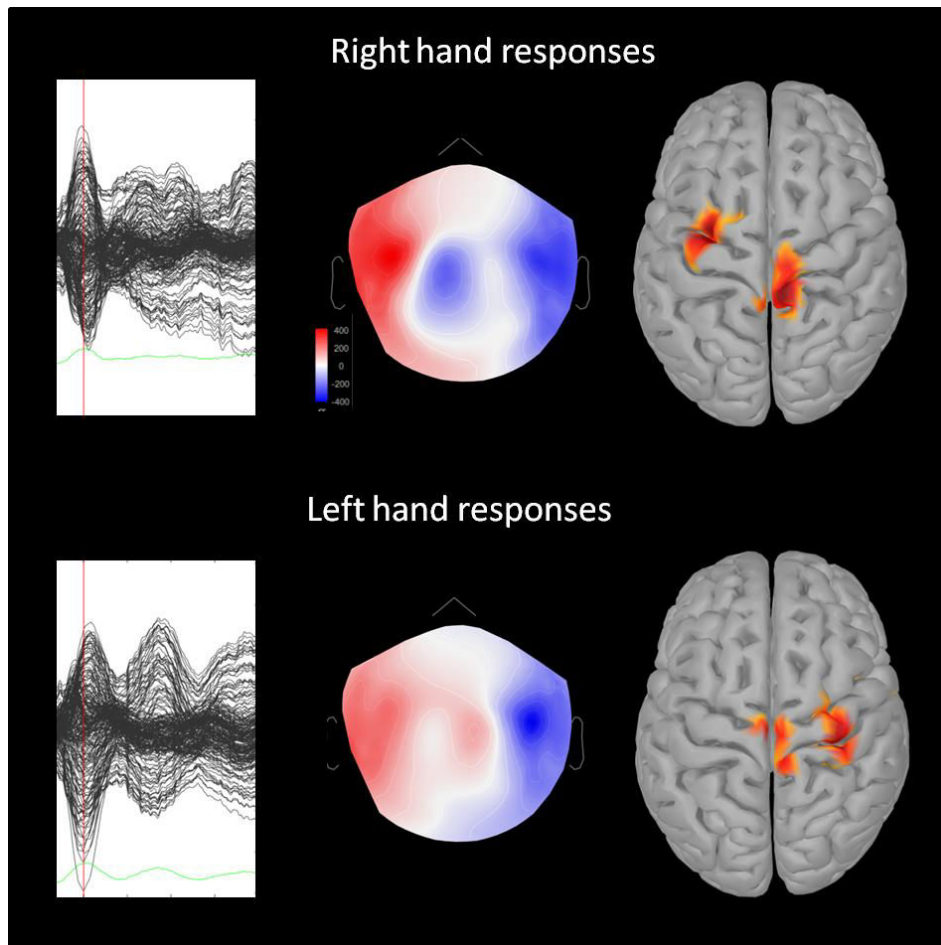


**Figure II.26 : Source localization of response-related MEG data.**

*Minimum norm constraint has been applied to estimate the sources of the evoked-field time-locked to EMG onset. For right hand responses, a cortical source is visible over the left precentral gyrus, while for left hand responses a cortical source is visible slightly posterior over the right precentral gyrus. For both right and left hand responses, an additional source is visible over the top of the precentral gyrus, lateralized to the right. According to the topographies, any source would be found on the medial wall.*

### **9.3.3 Feedback Related Negativity in the learning phase.**

**EEG:** Grand averages time-locked to stimulus presentation (that is, negative and positive feedback), obtained both on averaged reference montage and Laplacian data, show a small feed-back related negativity. Although a late median negative deflection was observed peaking around 300 ms, this wave was not modulated in amplitude as a function of feedback value (Figure II.27).

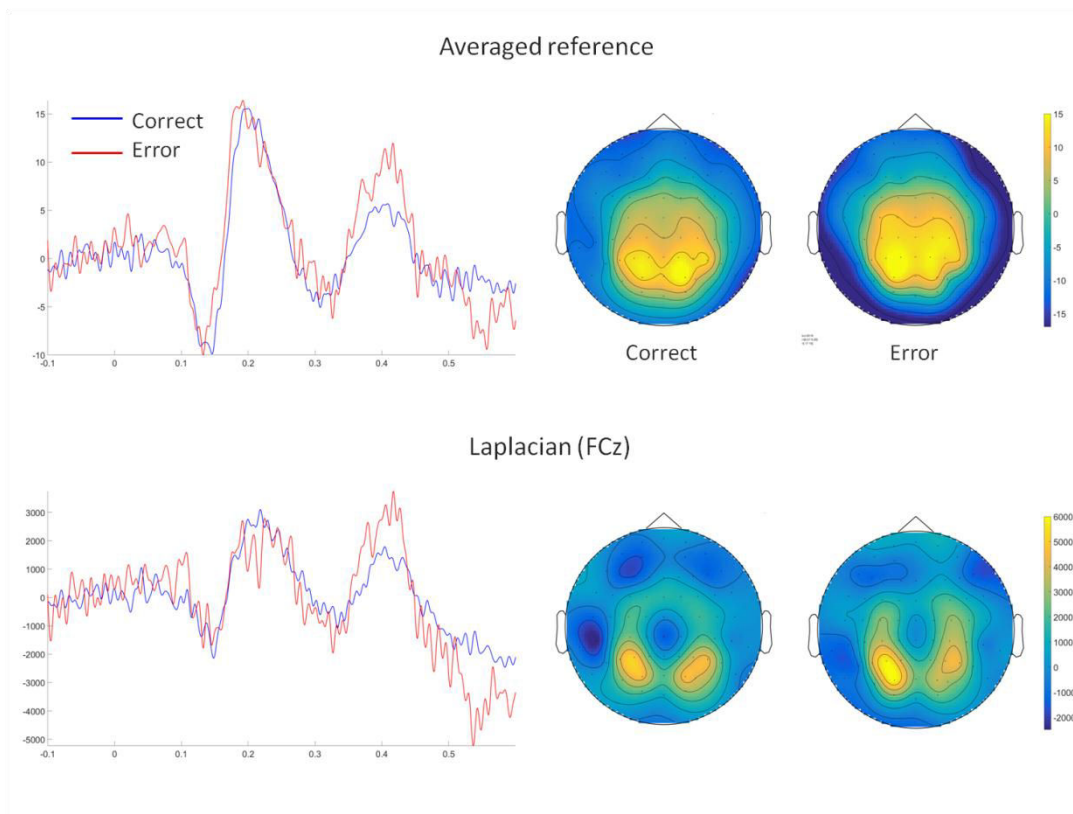


**Figure II.27 : Time-courses and topography of feedback related EEG data.**

*EEG grand-averages (FCz) time-locked to feedback presentation in the Learning phase for error trials (red line) and correct trials (blue line). Top panel illustrates Averaged Reference data and corresponding topographies for correct and error trials. Bottom panel illustrates Laplacian transformed data and corresponding topographies for correct and error trials. Time zero corresponds to feedback presentation. As illustrated in the figure, a negative deflection occurs around 300 ms after feedback presentation, showing a fronto-median topography, and with a comparable amplitude for correct and for error trials.*

**MEG:** A clear evoked field time-locked to feedback presentation was observed at fronto-central sensors on grand-averaged MEG traces. The waveform of this symmetric evoked field, which topography was independent of the responding hand, was obtained for both negative (red line) and positive (blue line) feedback. This field is illustrated in Figure II.28, as well as its topography. This activity peaked around 270 ms and, importantly its amplitude was significantly higher for negative feedback than for positive feedback  $t(14) = 2,098$ ,  $p = 0,0273$  (one-tailed). Furthermore, source localization of this activity showed a fronto-medial source (Figure II.29), approximately located in the caudal part of the ACC. On account of its latency, its topography, its source and of its sensitivity to feedback value, we conclude that this activity represents the magnetic equivalent of the FRN.

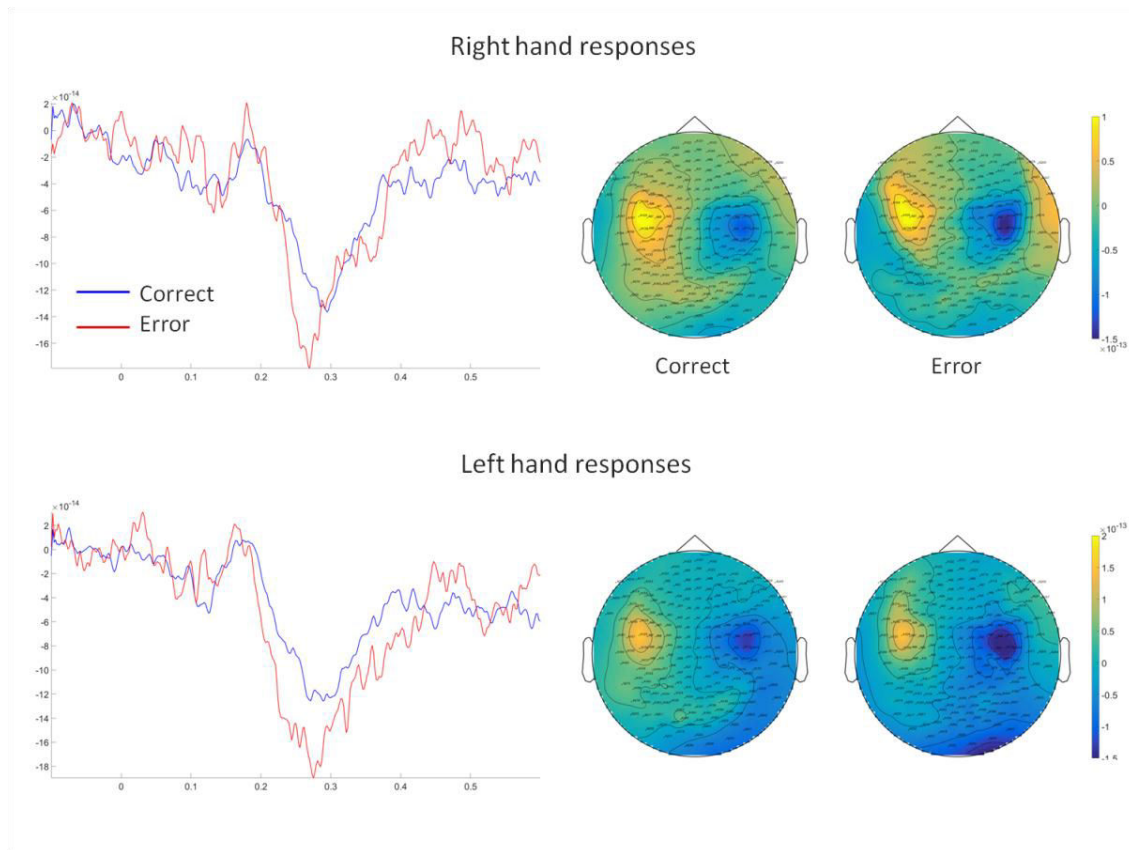


**Figure II.28 : Time-courses and topography of feedback related MEG data.**

*MEG grand-averages time-locked to feedback presentation in the Learning phase for error trials (red line) and correct trials (blue line) are illustrated for right hand responses (top panel) and for left hand response (bottom panel). The zero on time indicates feedback presentation. An activity evoked by feedback presentation, presenting higher amplitude for negative feedback compared to positive feedback is clearly visible, showing very similar median topography for both right and left hands, as well as for correct and erroneous trials.*

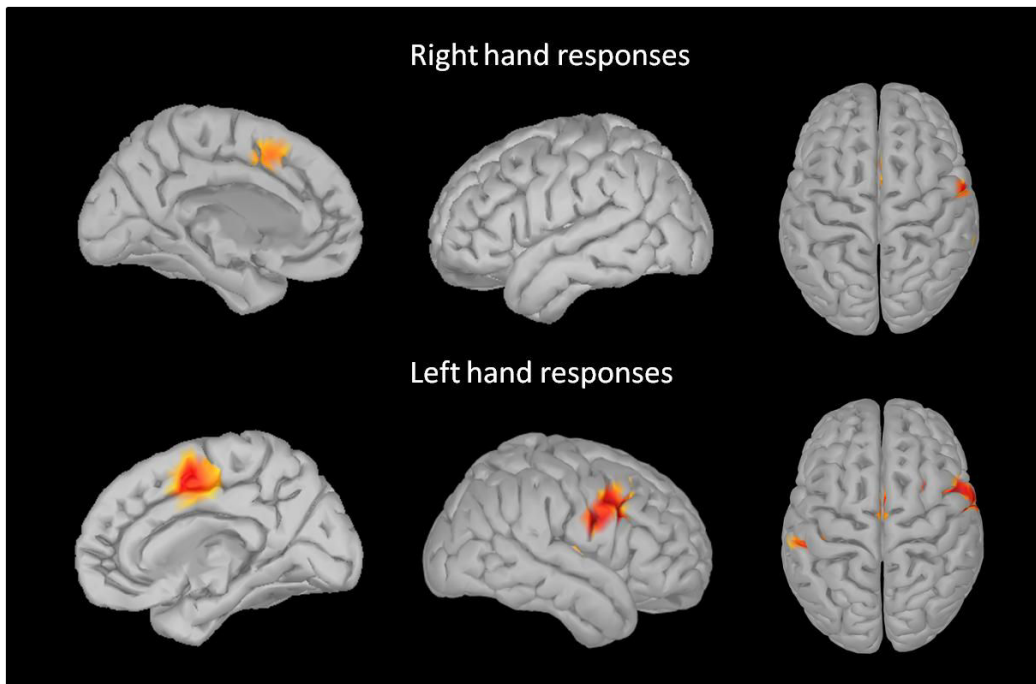


**Figure II.29 : Source localization of feedback-related MEG activity.**

*Minimum norm constraint has been applied to estimate the sources of the magnetic field evoked by feedback presentation in the Learning phase. A fronto-medial generator, approximately located in the caudal part of the ACC, is found for both left and right responses.*

## 9.4 Discussion

In this study we aimed at assessing the identity of the source of the Ne and the FRN using EEG/MEG simultaneous recording during a task evolving from a learning by trial-and-error task to a choice RT task. We assumed that, if the FRN is generated by a cortical structure other than the one which generates the Ne, EEG and MEG data should display different sensitivities to these two components.

As expected, in the Simon phase, we observed a Ne on scalp EEG, peaking early after EMG onset, modulated by outcome (namely larger for errors as compared to correct trials), which replicates previously published results (S Hoffmann & Falkenstein, 2010; Roger et al., 2010; F Vidal et al., 2003, 2000). On MEG grand-averaged data, despite careful examination of the activity time-locked to the motor response during the Simon phase, no evoked field corresponding to the Ne could be identified. On the contrary, the evoked field observed at the same latency as the Ne was 1) contralateral to the responding hand, and 2) not modulated by

response outcome as its amplitude was identical for both correct and erroneous responses. In account of these characteristics, such an evoked field is neither compatible with a generator located in the medial frontal wall, nor with a performance monitoring activity, since it does not show any sensitivity to performance. Therefore, this evoked field cannot represent the magnetic equivalent of the Ne. Two previous studies (Keil, Weisz, Paul-jordanov, & Wienbruch, 2010; W.H.R. Miltner et al., 1997) attempted to detect the Ne using MEG recordings, but, in our opinion, the magnetic activity observed in both experiments present neither topography nor sensitivity to performance comparable to those of the EEG Ne. These are important points since both MEG and EEG signals are due to the same primary currents which are responsible for intracellular and extracellular currents that generate variations of surface magnetic fields and variations of surface potentials, respectively. Therefore if a given MEG component is supposed to represent the magnetic counterpart of a given EEG component, they should exhibit very similar properties in terms of generators and sensitivity to experimental manipulations.

Instead, because of its fronto-central location contralateral to the response, its source estimated on the central region approximately over the primary sensory-motor cortex, its absence of modulation by performance and its short latency, the magnetic activity observed in our study resembles a similar EEG lateralized negative component, observed by Roger et al (Roger et al., 2010) at similar topographies. We speculate that it arises from the somatosensory cortex and that it could represent hypothetically late backward afferent activity. However, investigating the anatomical and functional origin of this lateralized magnetic activity was beyond the aim of this study. Whatever the functional significance of this evoked field, its high signal-to-noise time course attest to the reliability of present MEG data and suggest that it is unlikely the Ne would have gone unnoticed because of a possible poor quality of the MEG recordings.

A first important question arises spontaneously from these data: why is the Ne so apparent on scalp EEG while it cannot be detected by MEG? The simplest and most likely explanation issues from cytoarchitectonics and electrophysiology. We have previously seen in Experiment 1 that the Ne is generated by the SMA in humans. As both right and left SMA are active during action monitoring, two equivalent dipoles are created in the medial frontal wall, oriented towards one another and tangentially to the scalp: in such a symmetric dipole configuration, the dipole moment vectors cancel. Advances in cytoarchitectonical anatomy have demonstrated that the human SMA leaves the medial wall and extends on the top of the

gyrus (Zilles et al., 1995). Therefore, this part of the SMA on the top of the gyrus would generate two equivalent dipoles radial to the scalp giving rise to the Ne detected by the EEG; on the other hand MEG being almost blind to radial sources, this part of performance-related SMA activity would not be detected either.

Concerning the Feedback Related Activity, we observed different findings on EEG and on MEG data. Indeed in the Learning phase we observed a time-locked stimulus evoked field peaking around 270 ms after feedback presentation, which is neither lateralised nor depending on response side, and whose amplitude is higher for negative as compared to positive feedback. Furthermore, although approximate as not performed on individual MRI, the source localization of this activity is in the medial frontal cortex, nearby the ACC. For these characteristics, analogous to those previously reported for EEG and MEG data (William J Gehring & Willoughby, 2002; W.H.R. Miltner et al., 1997; Ruchow et al., 2002; Talmi et al., 2012), we conclude that it represents the magnetic equivalent of the FRN.

As shown in Figure II.27, corresponding EEG grand-averaged evoked activity on the Learning phase, although showing a negative deflection in the same range latency and a similar fronto-central median topography, do not allow identifying a clear FRN, mostly as this EEG component is not modulated by the feedback value. This could be partially explained by task design, which do not allow, in the learning phase, to ensure that all errors are due to not yet learned stimulus-response associations. That is to say, some of the presented feedback, namely the ones delivered at the end of that phase, could have been not informative since (some) subjects may have already learnt the association rules. Further data analysis should answer this question. Nonetheless, this does not explain completely why a modulation as a function of feedback (i.e. higher amplitude for negative feedback) is observed for the FRN on MEG data but not on EEG data. It could be due to the fact that we used Laplacian-transformed data and average reference data which are less sensitive to deep sources than monopolar recordings, although MEG recordings are not very sensitive to deep sources.

However, it is undeniable that a large feedback-related field can be recorded by MEG, while an error-related activity, well visible on scalp EEG signals, cannot. As a consequence, there cannot be a unique and sole anatomical source for these two negativities, which necessarily originate from distinct cortical regions, the Ne from the SMA and the FRN most probably from the ACC as has been regularly found in the literature and as roughly estimated by the source localization in our study. Indeed the highly folded anterior cingulate cortex,

which presents inter-individual variability (Céline Amiez et al., 2013; B. A. Vogt, Nimchinsky, Vogt, & Hof, 1995) can generate an oblique equivalent dipole, whose tangential component could generate a magnetic field detectable by MEG.

The results of the present study contradict the idea that the same system of performance evaluation is active during processing of internally generated and externally provided feedback, since this theory is based on the assumption that the same structure processes both type of information (C. B. Holroyd & Coles, 2002; Nieuwenhuis et al., 2004). Many fMRI (Céline Amiez et al., 2013; C. B. Holroyd et al., 2004), human (Phan Luu et al., 2003; W.H.R. Miltner et al., 1997; Ruchsow et al., 2002) and monkey (C Amiez et al., 2005; Emeric et al., 2008; Michelet et al., 2007) electrophysiological studies indicate an important role of the ACC in feedback processing. On the other hand, the feedback- and response-related ERNs neither share identical waveform nor identical scalp distributions (although they are similar), and thus it would be quite summary to consider them as identical phenomena. Furthermore, our results corroborated previous studies suggesting that internal error processing is supported by different, possibly partially overlapping, neuronal network centred on more caudal medial regions, that is the SMAs, while external negative feedback would be processed by more rostral regions (Akkal et al., 2002; Dehaene et al., 1994; Garavan et al., 2002; M. J. Herrmann et al., 2004; Ito et al., 2003; Phan Luu et al., 2003; Roger et al., 2010).

The possible different roles of the SMA and of more rostral medial regions, as they can be inferred from results of this and of two previous studies, will be further discussed in the next chapter.





### III. GENERAL DISCUSSION

Action monitoring is a fundamental executive function for adapting and optimizing behavior. Outcome evaluation, a sub-function of action monitoring, is essential for experience-based learning, and, as well, improvement of performance. The error negativity (Ne) is considered as an electrophysiological signature of the action monitoring system, but its functional significance is still debated and its specificity to errors is questioned. Besides, the anatomical source of the Ne is not ascertained, although most available human and monkey data point to the medial frontal cortex, namely to the ACC. This structure, largely assumed to be implicated in feedback processing, is considered as the cortical source of the feedback-related negativity (FRN) and most often, of the Error Negativity. Moreover, the Ne and the FRN are often supposed to represent the same evaluative process (C. B. Holroyd & Coles, 2002; Nieuwenhuis et al., 2004) and, thus, to be subserved by the same structure. In this chapter we will discuss the results of our three studies in the context of the current literature in the following order: we will address the questions of 1) the role of the SMA in action monitoring, 2) the unity of the Ne/Ne-like; 3) SMA activity *vis à vis* the medial and lateral prefrontal cortex through an anatomo-functional hierarchic framework; 4) the role of the ACC in outcome evaluation; and 5) current knowledge about action monitoring dysfunction in brain pathologies in the light of present results.

#### 10 The SMA as a key node in action monitoring in humans

As demonstrated in the first study, action monitoring is, at least to a large extent, carried out by the SMA. Although somehow unexpected, this finding was not totally unpredictable (since a minority of previous studies had already pointed to the SMA as a possible source for the Ne). Particularly, Herrmann et al (M. J. Herrmann et al., 2004), Luu et al (Phan Luu et al., 2003) and Roger et al (Roger et al., 2010) using different source localization methods, found electrical activity in medial BA 6, corresponding to the preSMA/SMA. Moreover, Vidal et al. (F Vidal et al., 2000) indirectly reasoned that since Laplacian was relatively insensitive to deep sources, it would be paradoxical for it to show up

so clearly on Laplacian-transformed recordings, and even unmask the Ne-like on correct responses, if its generator was the ACC and not the SMA.

More interesting are direct recordings from non-human primates executing various tasks in which action monitoring was necessarily operating. Nakamura et al (Nakamura et al., 2005), but also Emeric et al, (Emeric et al., 2010) found neurons with error-related activity in the supplementary eye field (SEF), whose human homologue is located in the SMA (Picard & Strick, 1996). Stuphorn et al, (Stuphorn et al., 2000) recorded in the SEF neurons active after errors and, additionally, during successful withholding of prepared movements. Scangos et al (Scangos et al., 2013) evaluated performance monitoring using an arm movement countermanding task and found neurons responsive to both errors and reward in monkeys' SMA and preSMA. Finally, Godlove et al, (Godlove et al., 2011), in order to evaluate the relationship between single-unit activity in monkeys' medial frontal neurons and the observed Ne in humans, performed scalp ERP in monkeys and found analogous error-related fronto-medial potentials. Nonetheless, numerous primate single-unit recording studies predominantly found signals encoding unfavorable outcomes in the ACC (Akkal et al., 2002; Bioulac, Michelet, Guehl, Aouizerate, & Burbaud, 2005; Emeric et al., 2008; Ito et al., 2003; Michelet et al., 2007, 2009). If, on the one hand, the role of the anterior cingulate cortex in action monitoring had not been completely assessed in the first study because of an incomplete sampling of this region, on the other hand the presence of a performance monitoring activity in monkey ACC neurons does not necessarily mean that human ACC is as involved in the same performance monitoring operations as monkey ACC. Indeed, since SMA has been assumed to be phylogenetically derived from the anterior cingulate periarchicortical limbic cortex (Goldberg, 1985), one may wonder whether some functions, which are implemented in the ACC in monkeys, could be supported by the SMA in humans.

## **11 Ne/Ne-like: a unique generator for a unique mechanism**

The action monitoring system is known to be a generic system evaluating all types of responses, whatever the effector (i.e. hand, finger, foot and eyes), the stimulus modality (Falkenstein et al., 1991, 2000; C. Holroyd et al., 1998; Nieuwenhuis et al., 2001), or the type of controlled parameters, since continuous responses parameters such as force or response duration seem to affect the Ne/Ne-like (C Meckler, 2010). Nor does the action monitoring

system distinguish the source of an error, as it responds to both selection errors and fast-guess errors (Cedric Meckler, Carbonnell, Hasbroucq, Burle, & Vidal, 2013). Additionally we have shown that the action monitoring system can actually act in a continuous manner, processing both correct and erroneous responses.

The LFPs recorded in the SMA, for each type of behaviorally relevant response, whatever their outcome, cannot be anything but the Ne. Therefore, the Ne and the Ne-like are generated in the same structure. This indicates that the Ne and the Ne-like do not correspond to different components but represent a unique activity whose amplitude depends on response correctness.

The nature of the Ne-like, first disclosed by Vidal et al (F Vidal et al., 2000) using density Laplacian transformation, has long been debated. As an enhanced Ne for correct responses was observed by Ford et al (Ford, 1999) in schizophrenic patients, the Ne-like activity was thus initially interpreted as reflecting a perturbed error detection in these patients and a false error detection process in normal subjects. It has also been attributed to an artifact caused by the temporal overlap between stimulus-locked and response-locked activities by Coles et al (M.G.H. Coles, Scheffers, & Holroyd, 2001), though this view has since been disproven by Vidal et al (F Vidal et al., 2003).

Later, the Ne-like was then observed in several other reports (Bartholow et al., 2005; Falkenstein et al., 2000; P Luu, Flaisch, & Tucker, 2000; Mathalon, Whitfield, & Ford, 2003). Although its existence is now consensually accepted, its nature is still debated. Specifically it has been discussed as to whether the correct- and error-related negativities reflect the same functional mechanism, modulated in amplitude, or whether they reflect completely distinct processes. This has important implications because most of the models accounting for the functional significance of the Ne are incompatible with the existence of a true Ne on correct responses after response activation onset.

Results of the first study, showing that the Ne/Ne-like are emitted by the same structure whatever the response correctness, demonstrating that the action monitoring system operates in a continuous and graded manner from correctness to errors, opens up new perspective of modeling cognitive control. Indeed almost all models of cognitive control are unable to account for the Ne-like as being just a small Ne. The initial view of the Ne as an error detection mechanism (M.G.H. Coles et al., 2001; Falkenstein et al., 1991; Scheffers et al., 1996), faced with the presence of a Ne on correct trials, cannot be retained for obvious

reasons. The conflict monitoring model (Botvinick et al., 2001; Braver, Barch, Gray, Molfese, & Snyder, 2001; Yeung, Botvinick, et al., 2004) states that the medial frontal cortex measure a “response conflict” represented by the Ne, defined as the product of the activation of the competitive responses weighted by the inhibitory connections between these responses. This model forecasts the presence of a Ne on correct trials as a measure of conflict between competitive responses, but, since the degree of conflict increases as the temporal overlap between incorrect and correct response activation increases, the conflict would be maximal after the response on errors but *before* responses in the case of correct trials (B Burle, Roger, Allain, Vidal, & Hasbroucq, 2008). Thus, according to this model, the occurrence of the Ne-like, as a measure of such conflict, is predicted *before* the response, although it actually occurs later. Note that, to our knowledge, the conflict model cannot be easily modified to account for a Ne on correct responses after response activation onset. As a consequence, the conflict theory cannot be retained as a valid explanation for the Ne/Ne-like (B Burle et al., 2008).

Reinforcement-learning theory is grounded on a double anatomo-physiological and functional basis: it states that the mesencephalic dopaminergic system measures differences between expected and actual outcome: in this framework if an outcome is “worse than expected” (i.e. an error), dopaminergic release activates the ACC which, in turns, emits a signal corresponding to this prediction error, represented by the Ne (C. B. Holroyd & Coles, 2002; Nieuwenhuis et al., 2004). Indeed it has been explicitly assumed that “... the ERN is elicited when a neural system first detects that the consequences of an action are worse than expected.” (Holroyd & Coles, 2002, page 680). If one accepts the dopaminergic mesencephalic system as a “modulator” of the ACC (or rather the SMA), which would emit a “default” signal for every produced response, the dopaminergic projections could enhance or reduce this signal as a function of prediction errors, thus explaining both the Ne and the Ne-like. However, although from an anatomo-physiological standpoint this represents a plausible hypothesis, it cannot be valid from a functional standpoint, since, as shown by Meckler et al, (2010), the Ne-like is greatly increased when the actual correct response is unexpected, that is when the outcome is actually “better than expected”. Indeed, in Meckler et al., (2010) study, in certain experimental conditions, a response bias was introduced: one of the two possible responses was highly probable (80%: expected) while the other response was highly improbable (20%: unexpected). While a high error rate occurred in the unexpected conditions, most responses were still correct but yielded high amplitude Ne’s although response outcome was better than expected, at least in comparison to correct response in the expected condition.

Finally the emotional hypothesis (Hajcak, McDonald, & Simons, 2004, 2003; Vocat, Pourtois, & Vuilleumier, 2008) could account for a Ne on correct trials, since it postulates that the Ne reflects emotional arousal associated with the execution of a behaviourally relevant response, which is obviously greater for errors and which would still be present even in case of correct responses. Although this hypothesis has not received strong experimental support, it has been shown, for example that the Ne was sensitive to the value of errors (Hajcak, Moser, Yeung, & Simons, 2005) and that the Ne as well as the Ne/like was enhanced in obsessional compulsive patients (Endrass, Klawohn, Schuster, & Kathmann, 2008). Nonetheless, if this model is theoretically functionally compatible with the generation of a Ne for both correct and incorrect responses by the same structure, from a physiological point of view it is less plausible to ascribe an emotional function to the SMA than to the ACC.

We propose, as discussed above and as issued from trial-by-trial analysis of the Ne on partial errors, that the Ne represents a “default” signal, emitted for any behaviourally relevant response, acting as an alerting or warning signal, able to induce on-line response control. This signal would be interrupted early (corresponding to the small Ne-like) on correct responses since subjects have already reached the desired goal state; it would be interrupted once the correct response is activated in the case of partial errors (resulting in a slightly higher Ne); and it would rise to its maximum level for errors (giving rise to the highest Ne), here signalling the need to enhance cognitive control. Action monitoring, as implemented in the SMA would thus be a continuous system, gradually evaluating all performed actions, which would eventually turn into a binary function to allow differentiation of incorrect actions. This would appeal the intervention of a more rostral structure in the medial and lateral prefrontal cortex for the subsequent necessary behavioural adjustment.

## **12 Prefrontal cortex and SMA in action monitoring**

In the first experiment we observed an involvement of the MPFC, namely the OFC and the pregenual ACC, exclusively in case of erroneous responses, and with a delayed implication of the SMA. Furthermore, in the second study, we assessed HGA in a large sampling of frontal structures, and found an outcome modulation in the high-gamma power in a large-scale fronto-insular network. Particularly, the high-gamma activity disclosed a

systematically enhanced response for incorrect responses, in addition to the SMA, also in the VLPFC and in the fronto-opercular region, as well as in the anterior-dorsal insula.

These results thus demonstrate, according to current literature, an involvement of different prefrontal and extra-frontal (namely insular) regions in action monitoring (for reviews see (Kok, Ridderinkhof, & Ullsperger, 2006; Ridderinkhof et al., 2004). Nonetheless, the characteristics of such an involvement markedly differs from the SMA to more rostral structures, and can be resumed as follows: 1) the SMA is activated early and constantly for each behaviourally relevant action if we consider phase locked activity, and activated only in case of errors if we select the HGA non-phase locked activity 2) the MPFC is mainly activated later, only in the case of errors and probably as a consequence (direct or indirect) of SMA activation if we consider phase-locked activity. If we select the HGA non-phase locked activity it is also activated in the case of errors, although less systematically; and 3) the systematic activation of the SMA, the VLPFC (whose phase-locked activity does not respond to performance) and the Insulo-opercular region as revealed by HGA, is binary as it is in the MPFC (enhanced high-gamma power for incorrect but not for correct responses).

Taken as a whole, these findings seem to indicate a hierarchical organization within the action monitoring system. This organization is supported by a well-known gradient of anatomic-connectivity going from more caudal pre-motor, to medial prefrontal to rostral regions, as well as from medial to lateral cortices (Medalla & Barbas, 2010; M Petrides & Pandya, 1999; Michael Petrides & Pandya, 2007). In particular, connectivity between the inferior and lateral frontal cortex with premotor areas, the anterior insula and the ACC are supported by well established streams of fibers, reciprocally connecting these regions (Barbas, 1988; Cipolloni & Pandya, 1999; Goldman-Rakic, Cools, & Srivastava, 1996).

The lateral prefrontal cortex guides goal-directed behavior through selection of relevant stimuli mediated by bidirectional pathways towards secondary sensori-motor structures, that is, by exercising top-down control (Miller & Cohen, 2001). Furthermore the prefrontal cortex, and particularly the ventro-lateral region, has a key role in action inhibition and suppression of irrelevant stimuli (Aron et al., 2004, 2014; Fonken et al., 2016; Hampshire et al., 2010; Wery P M van den Wildenberg et al., 2006), and is directly connected with the SMA by a specific “aslant” tract (Catani et al., 2011).

In goal-directed behaviour, top-down information flows from supramodal prefrontal areas to the effector’s primary motor cortex via intermediate premotor areas. This rostro-

caudal stream integrates motivational states and transforms relatively abstract goals in prefrontal cortex, into motor command and motor plans in the premotor system, to finally activate concrete movement representation in the primary motor system (Passingham, 1995; Ramnani & Owen, 2004). Such a hierarchy in the control of goal-directed action, and such a cascade of information, could follow the opposite direction during monitoring of ongoing action: as suggested by results of our studies (and others), the SMA would monitor ongoing action in a continuous and gradual manner (as evidenced by LFP ERPs). Then, when the SMA reaches a threshold, as in case of incorrect action, it would inform downstream structures, that is, the prefrontal cortex (as evidenced by the LFP ERP). The prefrontal structures would process information in a more abstract and binary fashion, that is, by classifying them into correct and incorrect, as possibly indicated by error-evoked LFP in the MLPFC and by enhanced HGA in a vast prefrontal-insular network. The prefrontal cortex, and particularly the VLPFC and the insulo-opercular regions, could in turn reorient attention and inhibit irrelevant responses and/or stimuli and settles the framework from which SMA would “read” response outcome. However, following this hypothesis, the VLPFC should be informed about the outcome of ongoing action, whether directly or indirectly through the SMA. Nonetheless these regions in the inferior frontal gyrus do not seem to respond to performance as explored by phase-locked activity. Nonetheless, although the Ne is not generated in the prefrontal cortex, healthy prefrontal functioning is a mandatory condition for sensitivity of the Ne to response correctness since patients with unilateral prefrontal lesions present equal Ne amplitudes whether the response is correct or not (William J Gehring & Knight, 2000); we will thus discuss later the role of the prefrontal cortex and its alteration in brain pathologies. To summarize, there would be a bidirectional hierarchical organization, with rostro-caudal gradient of activation for the motor command of goal-directed action, and, in return, a caudo-rostral activation for evaluation of the executed (or ongoing) action.

### **13 Outcome evaluation: from internally generated to externally delivered feedback**

The third study showed that, since the Ne is not visible with MEG recordings while the FRN is, these two error-related signals, contrarily to what is often assumed, cannot originate from the same structure. At the very least, there would be an additional generator

which would be responsible for an additional component represented by the feedback-related field observed on MEG. Hence, these results disagree with the idea that the Ne and the FRN represent the same mechanisms and with models that account in a similar manner for their generation (C. B. Holroyd & Coles, 2002).

The Ne is sensitive to performance. The FRN, sensitive to informative feedback on performance, is elicited by “bad” feedback (e.g. loss of money) (William J Gehring & Willoughby, 2002; Hajcak, Moser, Holroyd, & Simons, 2006) whatever the correctness of the response. In other words, the FRN is sensitive to the “utilitarian” (gain or loss) value of feedback, rather than to the “performance” (correct or incorrect) value of the feedback. Holroyd & Coles (2002) in reinforcement-learning theory unify the distinction between utilitarian and performance value of feedback through a common property represented by the reinforcement adaptive values carried by the feedback (internal or external) itself. When “the consequences are worse than expected”, the ACC, by dopaminergic projections, would emit a signal, i.e. the Ne or the FRN as a function of the feedback’s origin.

This model is thus able to predict an inverse relationship between the amplitude of the Ne and the FRN. Nonetheless, when applied to the Ne, as reported in a previous study, reinforcement-learning theory, although physiologically grounded, cannot account for the presence of a Ne on correct trials, since an enhanced Ne appears in correct trials when such a response is unexpected (Meckler et al, 2010). Present findings further support the idea that this theory is inadequate for modeling the processing of internally generated information about sensory-motor actions. However there are several lines of evidence that expectancy modulates FRN amplitude (Hajcak et al., 2006; Moser & Simons, 2009) and that in human and non-human primates ACC is highly sensitive to feedback delivery (Céline Amiez et al., 2013; Michelet et al., 2007, 2009; Matthew F S Rushworth et al., 2007).

In our third study we found that the ACC, as shown by a first crude source localization, is a likely generator of the FRN. Furthermore, as showed by error-related ERPs in the first study and by the induced HGA increase in the second study, the ACC turns out to be active only in the case of erroneous responses. Additionally its activity is correlated with the earlier continuous activity in the SMA. We have already proposed that action monitoring could be a two-step process: a first step of continuous monitoring could take place in the SMA, and a second step of binary categorization (good versus bad outcome) driven by the SMA could be performed in the ACC. It would thus be conceivable that performance

evaluation and error detection, in the absence of internal information upon which SMA activity relies, would be processed directly in the ACC since externally provided feedback would bypass needless intermediate premotor areas. In this light, the ACC would represent a sort of hub structure for a single computation of different sources of feedback. This remains a very hypothetical although tempting interpretation of present and previously reported findings, since the localization of ACC activity in the various studies (including ours) can vary from more rostral to more caudal sites.

## **14 Pathologies and altered action monitoring**

Adaptive and flexible behaviour can be altered in several neuropsychiatric disorders in which maladaptive, rigid and repetitive behaviours are observed, and not appropriately modified by action outcome. Accumulating evidence suggests that defective error processing contributes to such inability to dynamically adjust performance, which results in rigid behaviours. As a neuronal marker of error processing and performance evaluation, the Ne has been extensively studied in different brain pathologies, and its alteration has been recently proposed as a potential sensitive endophenotype of neuropsychiatric disorders (Manoach & Agam, 2013; Olvet & Hajcak, 2008). Alteration of cognitive control as revealed by Ne abnormalities has been observed in anxiety disorders, depression, obsessive-compulsive disorder (OCD), Parkinson disease (PD), autism spectrum disorders, and schizophrenia. Schematically, we can observe pathologies disclosing either a hyper- or hypo-functioning of cognitive control.

Within the pathologies showing an hyper-functioning, schizophrenia is characterized by a reduction of the Ne amplitude, while the Ne-like is augmented (Bates, Kiehl, Laurens, & Liddle, 2002; Mathalon et al., 2002). Additionally, schizophrenic patients show reduced ACC error-related activity in fMRI studies (Carter et al., 2001; Laurens et al, 2003). Furthermore, reduced Ne amplitude is observed in normal siblings of schizophrenic patients and, together with reduced ACC activity, it is considered as a trait marker of genetic vulnerability to schizophrenia that predates illness onset (Perez et al., 2014). Altered error processing and learning in schizophrenic patients may play an important role in the perseverative and rigid patterns of behaviour and thinking that characterize this pathology.

Autistic children, often presenting stereotyped and repetitive patterns of activity, interests and behaviours, which could potentially be related to a deficient error detection process, have shown a reduction in post-error slowing (Bogte, Flamma, van der Meere, & van Engeland, 2007), or reduced error self-correction (Russell & Jarrold, 1998). Accordingly, the Ne is significantly reduced in these patients (South et al, 2010; Vlamings et al, 2008), but ACC bold activity has been found to be reduced (Thakkar et al., 2008). This could suggest that altered discrimination between correct and incorrect action may contribute to restricted stereotyped behaviours in autism.

As dopaminergic projections to the ACC are considered to be responsible for the modulation of the Ne, this marker has been tested in Parkinson's disease (PD), characterized by dopamine depletion in the midbrain dopaminergic system. Indeed, patients with PD show reduced Ne, even in the early stage of the disease (Beste et al, 2009; Stemmer et al, 2007; Willemsen et al, 2008).

Other neuropsychiatric diseases show a different pattern of altered neuronal markers of error processing. For instance patients affected by OCD, who have repetitive, ritualized and compulsive thoughts and behaviours, demonstrate augmented activity in the ACC (Ursu et al., 2003), together with an enhanced Ne for both correct and erroneous trials (Endrass et al., 2008), and their unaffected siblings also show a higher Ne (Carrasco et al., 2013). These exaggerated error signals in response to outcome could provoke a pervasive sense of dissatisfaction and self-doubt (Pitman, 1987) triggering the compulsion to repeat behaviours and actions, even if successfully completed. One could imagine, for example, that an OCD patient having correctly locked the door compulsively checks and repeats this action because of persistent and excessive error signals (Aouizerate et al., 2004).

Similar to OCD patients, subjects affected by generalized anxiety disorders, as well as depressed individuals, exhibit increased sensitivity to mistakes and negative feedback, as demonstrated by an abnormally high Ne for incorrect trials (Holmes & Pizzagalli, 2008). Nonetheless, the enhanced sensitivity to errors in anxiety and depression may not be specific to these pathologies, but rather reflect an underlying common characteristic that would predominate in both disorders (Hajcak et al., 2004).

Overall, the existing literature on error processing dysfunction in neuropsychiatric pathologies could offer a key for interpreting some aspects of these disorders, and to understand a part of their underlying physiopathological processes and their anatomical

substrates. Since the ACC has been considered to be the generator of the Ne, and since pathological alterations in metabolism as well as anatomy and connectivity have been observed in the ACC in these neuropsychiatric disorders, error processing dysfunction in these diseases is commonly interpreted as a cingulate problem. A disturbance in the anterior cingulate cortex activity is obviously probable in these pathologies all characterized by a general “prefrontal” dysfunction.

Nonetheless, in this clinical context, some of our findings deserve some consideration. Indeed, although the ACC is probably altered in these pathologies, the error signal which is utilised to model its functioning (or dysfunctioning) actually does not originate from the ACC. Therefore, the alteration of cognitive control as evidenced by the Ne cannot be a primary cingulate deficit. One possibility is that, at least in some pathologies, this could instead be an SMA deficit, and that cingulate alteration could eventually be a consequence of SMA dysfunction. For instance, this hypothesis is plausible for Parkinson’s disease, where dopamine depletion could induce hypoactivity of premotor structures, namely the SMA. Indeed, in a monkey model of PD, neuronal firing in the SMAs after a Go signal is markedly decreased (Escola et al., 2003). If one admits that striatal projections to the SMA via the thalamus modulate SMA activity and thus the Ne amplitude, the reduced Ne found in PD patients could be a direct consequence of decreased dopaminergic modulation of action monitoring activity in this structure. Another possible interpretation derives from the statement that all these are “prefrontal” disorders, and that the prefrontal cortex may be another possible candidate for a modulator of SMA activity. Therefore, pathologically reduced activity of prefrontal cortex (as in prefrontal cortex lesions, or in schizophrenic patients) would result in a disruption of this modulatory process and thus of the Ne amplitude. Furthermore, in normal subjects the Ne amplitude is modified as a function of expectancy (Cedric Meckler et al., 2011), being higher if the response is unexpected even though correct, and this expectancy modulation might likely be top-down, performed by the prefrontal cortex. Hence, in some prefrontal dysfunction disorders this modulation would be disrupted and each response would be “unexpected”, giving rise to higher Ne for both correct and incorrect actions.

## IV. CONCLUSIONS

Some principal points can be drawn from the studies conducted in this thesis.

First of all, the physiological process reflected by the Ne is a generic, continuous process, operating on-line for each behaviourally relevant action. This action monitoring process is gradually modulated as a function of outcome. Therefore, in this context and in this phase of cognitive control, errors and corrects responses should not be opposed, since errors appear as the extreme point of a continuum.

Specific error processing emerges as a secondary process, driven by a more generic, “default mode” action monitoring process. When a negative outcome occurs, the signal emitted by the action monitoring system would reach a threshold and, possibly acting as a warning signal, would make the cognitive control shift to a binary mode (even in the SMA if we consider HGA), which classes outcomes as favourable or unfavourable, and signals the need to enhance cognitive control.

This process would follow a caudo-rostral gradient within a large-scale frontal network including extra-frontal structures, such as the anterior insula, with generic action monitoring being implemented in the SMA in a continuous manner, and with a more abstract binary error detection process implemented in prefrontal structures including the rostral ACC, the VLPFC and the operculo-insular region, which might possibly intervene in modifying behaviour. On the other hand, a rostro-caudal modulation of the action monitoring activity in the SMA could be performed by the prefrontal cortex, as possibly suggested by HGA, and/or, alternatively, by the dopaminergic mesencephalic system. The SMA is a critical node within this neuronal network underlying action monitoring and error processing, and even plays a leading role, as its activity seems to drive the activity of more rostral regions. In this sense, according to Orgogozo & Larsen (Orgogozo & Larsen, 1979) the SMA would represent a “supramotor” area, with higher monitoring function for sensori-motor actions.

When internal information, upon which SMA activity relies, is not available, the ACC may directly process the value of externally provided feedback, which could by-pass the redundant motor-premotor system. This process is reflected by the FRN, which thus would

not represent processes similar to the Ne, since it is hard to imagine, on the basis on MEG data, that they are generated by the same structure

Finally, since the Ne has been found to be primarily generated in the SMA and not in the ACC, the physiological and functional interpretation of the alteration of its amplitude and modulation by experimental conditions which have been observed in different human pathologies needs to be reconsidered, since they cannot be ascribed (at least directly) to a dysfunction of the cingulate cortex.



## V. REFERENCES

- Akkal, D., Bioulac, B., Audin, J., Burbaud, P., Segalen, Â. V., & Saignat, Â. (2002). Comparison of neuronal activity in the rostral supplementary and cingulate motor areas during a task with cognitive and motor demands. *European Journal of Neuroscience*, *15*(5), 887–904.
- Akkal, D., Dum, R. P., & Strick, P. L. (2007). Supplementary Motor Area and Presupplementary Motor Area: Targets of Basal Ganglia and Cerebellar Output. *Journal of Neuroscience*, *27*(40), 10659–10673. <http://doi.org/10.1523/JNEUROSCI.3134-07.2007>
- Allain, S., Carbonnell, L., Falkenstein, M., Burle, B., & Vidal, F. (2004). The modulation of the Ne-like wave on correct responses foreshadows errors. *Neuroscience Letters*, *372*(1), 161–166. <http://doi.org/10.1016/j.neulet.2004.09.036>
- Allain, S., Hasbroucq, T., Burle, B., Grapperon, J., & Vidal, F. (2004). Response monitoring without sensory feedback. *Clinical Neurophysiology*, *115*(9), 2014–2020. <http://doi.org/10.1016/j.clinph.2004.04.013>
- Amiez, C., Hadj-Bouziane, F., & Petrides, M. (2012). Response selection versus feedback analysis in conditional visuo-motor learning. *NeuroImage*, *59*(4), 3723–3735. <http://doi.org/10.1016/j.neuroimage.2011.10.058>
- Amiez, C., Joseph, J., & Procyk, E. (2005). Anterior cingulate error-related activity is modulated by predicted reward. *European Journal of Neuroscience*, *21*, 3447–3452. <http://doi.org/10.1111/j.1460-9568.2005.04170.x>
- Amiez, C., Neveu, R., Warrot, D., Petrides, M., Knoblauch, K., & Procyk, E. (2013). The Location of Feedback-Related Activity in the Midcingulate Cortex Is Predicted by Local Morphology. *The Journal of Neuroscience*, *33* (5), 2217–2228. <http://doi.org/10.1523/JNEUROSCI.2779-12.2013>
- Amiez, C., Sallet, J., Procyk, E., & Petrides, M. (2012). Modulation of feedback related activity in the rostral anterior cingulate cortex during trial and error exploration. *NeuroImage*, *63*(3), 1078–1090. <http://doi.org/10.1016/j.neuroimage.2012.06.023>
- Amiez, C., Wutte, M. G., Faillenot, I., Petrides, M., Burle, B., & Procyk, E. (2016). NeuroImage Single subject analyses reveal consistent recruitment of frontal operculum in performance monitoring. *NeuroImage*, *133*, 266–278. <http://doi.org/10.1016/j.neuroimage.2016.03.003>
- Amzica, F., & Steriade, M. (2000). Neuronal and glial membrane potentials during sleep and paroxysmal oscillations in the neocortex. *Journal of Neuroscience*, *20*, 6648–6665.
- Aouizerate, B., Guehl, D., Cuny, E., Rougier, A., Bioulac, B., Tignol, J., & Burbaud, P. (2004). Pathophysiology of obsessive-compulsive disorder: A necessary link between phenomenology, neuropsychology, imagery and physiology. *Progress in Neurobiology*, *72*(3), 195–221. <http://doi.org/10.1016/j.pneurobio.2004.02.004>
- Aron, A. R., Robbins, T. W., & Poldrack, R. A. (2004). Inhibition and the right inferior frontal

cortex, 8(4). <http://doi.org/10.1016/j.tics.2004.02.010>

- Aron, A. R., Robbins, T. W., & Poldrack, R. A. (2014). Inhibition and the right inferior frontal cortex : one decade on. *Trends in Cognitive Sciences*, 18(4), 177–185. <http://doi.org/10.1016/j.tics.2013.12.003>
- Barbas, H. (1988). Anatomic organization of basoventral and mediodorsal visual recipient prefrontal regions in the rhesus monkey. *The Journal of Comparative Neurology*, 276(3), 313–342. <http://doi.org/10.1002/cne.902760302>
- Bartholow, B. D., Pearson, M. A., Dickter, C. L., Sher, K. J., Fabiani, M., & Gratton, G. (2005). Strategic control and medial frontal negativity : Beyond errors and response conflict. *Psychophysiology*, 42(1), 33–42. <http://doi.org/10.1111/j.1469-8986.2005.00258.x>
- Basar, E. (1999). *Brain Function and Oscillations. II. Integrative Brain Function. Neurophysiology and Cognitive Processes*. Springer Verlag Berlin Heidelberg.
- Bates, A. T., Kiehl, K. A., Laurens, K. R., & Liddle, P. F. (2002). Error-related negativity and correct response negativity in schizophrenia. *Clinical Neurophysiology*, 113(9), 1454–1463. [http://doi.org/10.1016/S1388-2457\(02\)00154-2](http://doi.org/10.1016/S1388-2457(02)00154-2)
- Belluscio, M. A., Mizuseki, K., Schmidt, R., Kempter, R., & Buzsáki, G. (2012). Cross-Frequency Phase–Phase Coupling between Theta and Gamma Oscillations in the Hippocampus. *The Journal of Neuroscience*, 32(2), 423–435. <http://doi.org/10.1523/JNEUROSCI.4122-11.2012>
- Benjamini, Y., & Hochberg, Y. (2016). Controlling the False Discovery Rate : A Practical and Powerful Approach to Multiple Testing Author ( s ): Yoav Benjamini and Yosef Hochberg Source : Journal of the Royal Statistical Society . Series B ( Methodological ), Vol . 57 , No . 1 ( 1995 ), Publi. *Journal of the Royal Statistical Society.*, 57(1), 289–300.
- Berger, H. (1929). Über das Elektrenkephalogramm des Menschen (On the human electroencephalogram). *Archiv F. Psychiatrie U. Nervenkrankheiten*, 87, 527–570.
- Beste, C., Willemsen, R., Saft, C., & Falkenstein, M. (2009). Error processing in normal aging and in basal ganglia disorders. *Neuroscience*, 159(1), 143–149. <http://doi.org/10.1016/j.neuroscience.2008.12.030>
- Bioulac, B., Michelet, T., Guehl, D., Aouizerate, B., & Burbaud, P. (2005). The anterior cingulate cortex in error detection and conflict monitoring. Unitary neuronal activity in monkeys. *Bulletin de L'Academie Nationale de Medecine*, 189, 1529–1538.
- Birmauer, N., Elbert, T., Canavan, A., & Rockstroh, B. (1990). Slow Potentials of the Cerebral Cortex and Behavior. *Physiological Reviews*, 70, 1–41.
- Bogte, H., Flamma, B., van der Meere, J., & van Engeland, H. (2007). Post-error adaptation in adults with high functioning autism. *Neuropsychologia*, 45(8), 1707–1714. <http://doi.org/10.1016/j.neuropsychologia.2006.12.020>
- Botvinick, M. M., Braver, T. S., Barch, D. M., Carter, C. S., & Cohen, J. D. (2001). Conflict Monitoring and Cognitive Control. *Psychological Review*, 108(3), 624–652. <http://doi.org/10.1037//0033-295X.108.3.624>

- Braver, T. S., Barch, D. M., Gray, J. R., Molfese, D. L., & Snyder, A. (2001). Anterior Cingulate Cortex and Response Conflict: Effects of Frequency, Inhibition and Errors. *Cerebral Cortex*, *11* (9), 825–836. <http://doi.org/10.1093/cercor/11.9.825>
- Brázdil, M., Roman, R., Daniel, P., & Rektor, I. (2005). Intracerebral Error-Related Negativity in a Simple Go / NoGo Task. *Journal of Psychophysiology*, *19*, 244–255. <http://doi.org/10.1027/0269-8803.19.4.244>
- Bressler, S., & Freeman, W. (1980). Frequency analysis of olfactory system EEG in cat, rabbit and rat. *Electroencephalogr Clin Neurophysiol*, *50*, 19–24.
- Brewer, N., & Smith, G. (1989). Developmental changes in processing speed: influence of speed-accuracy regulation. *Journal of Experimental Psychology General*, *118*, 298–310.
- Brinkman, C., & Porter, R. (1979). Supplementary motor area in the monkey: activity of neurons during performance of a learned motor task. *Journal of Neurophysiology*, *42*(3), 681–709. Retrieved from <http://jn.physiology.org/content/42/3/681.abstract>
- Brodmann, K. (1909). *Vergleichende Lokalisationslehre der Grosshirnrinde*. (J. A. Bart, Ed.). Leipzig.
- Brovelli, A., Chicharro, D., Badier, J.-M., Wang, H., & Jirsa, V. (2015). Characterization of Cortical Networks and Corticocortical Functional Connectivity Mediating Arbitrary Visuomotor Mapping. *The Journal of Neuroscience*, *35* (37), 12643–12658. <http://doi.org/10.1523/JNEUROSCI.4892-14.2015>
- Burle, B., Possamai, C., Vidal, F., Bonnet, M., & Hasbroucq, T. (2002). Executive control in the Simon effect: an electromyographic and distributional analysis. *Psychological Research*, *66*, 324–336. <http://doi.org/10.1007/s00426-002-0105-6>
- Burle, B., Roger, C., Allain, S., Vidal, F., & Hasbroucq, T. (2008). Error Negativity Does Not Reflect Conflict: A Reappraisal of Conflict Monitoring and Anterior Cingulate Cortex Activity. *Journal of Cognitive Neuroscience*, *20*(9), 1637–1655.
- Burle, B., Spieser, L., Roger, C., Casini, L., Hasbroucq, T., & Vidal, F. (2015). Spatial and temporal resolutions of EEG: Is it really black and white? A scalp current density view. *International Journal of Psychophysiology*, *97*(3), 210–220. <http://doi.org/10.1016/j.ijpsycho.2015.05.004>
- Buzsáki, G., Anastassiou, C. A., & Koch, C. (2012). The origin of extracellular fields and currents—EEG, ECoG, LFP and spikes. *Nature Reviews Neuroscience*, *13*, 407–420.
- Buzsáki, G., & Wang, X. J. (20012). Mechanisms of gamma oscillations. *Annual Review of Neuroscience*, *35*, 203–225.
- Carmichael, S. T., & Price, J. L. (1996). Connectional networks within the orbital and medial prefrontal cortex of macaque monkeys. *The Journal of Comparative Neurology*, *371*(2), 179–207. [http://doi.org/10.1002/\(SICI\)1096-9861\(19960722\)371:2<179::AID-CNE1>3.0.CO;2-#](http://doi.org/10.1002/(SICI)1096-9861(19960722)371:2<179::AID-CNE1>3.0.CO;2-#)
- Carrasco, M., Harbin, S. M., Nienhuis, J. K., Fitzgerald, K. D., Gehring, W. J., & Hanna, G. L. (2013). Increased error-related brain activity in youth with obsessive-compulsive disorder and unaffected siblings. *Depression and Anxiety*, *30*(1), 39–46. <http://doi.org/10.1002/da.22035>

- Carter, C. S., Braver, T. S., Barch, D. M., Botvinick, M. M., Noll, D., & Cohen, J. D. (1998). Anterior Cingulate Cortex, Error Detection, and the Online Monitoring of Performance. *Science*, 280(5364), 747–749. Retrieved from <http://science.sciencemag.org/content/280/5364/747.abstract>
- Carter, C. S., MacDonald, A. W., Ross, L. L., Stenger, V. A., MacDonald III, A. W., Ross, L. L., & Stenger, V. A. (2001). Anterior cingulate cortex activity and impaired self-monitoring of performance in patients with schizophrenia: an event-related fMRI study. *American Journal of Psychiatry*, 158(9), 1423–1428. <http://doi.org/10.1176/appi.ajp.158.9.1423>
- Catani, M., Dell, F., Vergani, F., Malik, F., Hodge, H., Roy, P., ... Schotten, D. (2011). Short frontal lobe connections of the human brain. *Cortex*, 48(2), 273–291. <http://doi.org/10.1016/j.cortex.2011.12.001>
- Cavanagh, J. F., Cohen, M. X., & Allen, J. J. B. (2009). Prelude to and Resolution of an Error: EEG Phase Synchrony Reveals Cognitive Control Dynamics during Action Monitoring. *Journal of Neuroscience*, 29(1), 98–105. <http://doi.org/10.1523/JNEUROSCI.4137-08.2009>
- Cerliani, L., Thomas, R. M., Jbabdi, S., Siero, J. C. W., Nanetti, L., Crippa, A., ... Keysers, C. (2012). Probabilistic Tractography Recovers a Rostrocaudal Trajectory of Connectivity Variability in the Human Insular Cortex. *Human Brain Mapping*, 33(9), 2005–2034. <http://doi.org/10.1002/hbm.21338>
- Chauvel, P., Rey, M., Buser, P., & Bancaud, J. (1996). What stimulation of the supplementary motor area in humans tells about its functional organization. In H. O. Luders (Ed.), *Advances in neurology* (pp. 199–209). Philadelphia: Lippincott-Raven Publishers.
- Cipolloni, P. B., & Pandya, D. N. (1999). Cortical connections of the frontoparietal opercular areas in the rhesus monkey. *Journal of Comparative Neurology*, 403(4), 431–458. [http://doi.org/10.1002/\(SICI\)1096-9861\(19990125\)403:4<431::AID-CNE2>3.0.CO;2-1](http://doi.org/10.1002/(SICI)1096-9861(19990125)403:4<431::AID-CNE2>3.0.CO;2-1)
- Cohen, M. X., & Cavanagh, J. F. (2011). Single-trial regression elucidates the role of prefrontal theta oscillations in response conflict. *Frontiers in Psychology*, 2(FEB), 1–12. <http://doi.org/10.3389/fpsyg.2011.00030>
- Cohen, M. X., & van Gaal, S. (2014). Subthreshold muscle twitches dissociate oscillatory neural signatures of conflicts from errors. *NeuroImage*, 86, 503–513. <http://doi.org/10.1016/j.neuroimage.2013.10.033>
- Cole, M. W., Yeung, N., Freiwald, W. A., & Botvinick, M. (2010). Conflict over cingulate cortex: Between-species differences in cingulate may support enhanced cognitive flexibility in humans. *Brain, Behavior and Evolution*, 75(4), 239–240. <http://doi.org/10.1159/000313860>
- Coles, M. G. H., Scheffers, M. K., & Fournier, L. (1995). Where did you go wrong? Errors, partial errors, and the nature of human information processing. *Acta Psychologica*, 90(1), 129–144. [http://doi.org/10.1016/0001-6918\(95\)00020-U](http://doi.org/10.1016/0001-6918(95)00020-U)
- Coles, M. G. H., Scheffers, M. K., & Holroyd, C. B. (2001). Why is there an ERN / Ne on correct trials? Response representations, stimulus-related components, and the theory of error-processing, 56, 173–189.

- Coles, M. G. H., Scheffers, M. K., & Holroyd, C. B. (2001). Why is there an ERN/Ne on correct? TrialsResponse representations, stimulus-related components, and the theory of errorprocessing. *Biological Psychology*, *56*(3), 173–189.
- Colombet, B., Woodman, M., Badier, J. M., & Bénar, C. G. (2015). AnyWave: A cross-platform and modular software for visualizing and processing electrophysiological signals. *Journal of Neuroscience Methods*, *242*, 118–126. <http://doi.org/10.1016/j.jneumeth.2015.01.017>
- Craft, J. L., & Simon, J. R. (1970). Processing symbolic information from a visual display : interference from irrelevant directional cue. *Journal of Experimental Psychology*, *83*, 415–420.
- Critchley, H. D., Mathias, C. J., & Dolan, R. J. (2001). Neural Activity in the Human Brain Relating to Uncertainty and Arousal during Anticipation. *Neuron*, *29*(2), 537–545. [http://doi.org/10.1016/S0896-6273\(01\)00225-2](http://doi.org/10.1016/S0896-6273(01)00225-2)
- Crone, N. E., Sinai, A., & Korzeniewska, A. (2006). High-frequency gamma oscillations and human brain mapping with electrocorticography. *Progress in Brain Research*, *159*, 275–295. [http://doi.org/10.1016/S0079-6123\(06\)59019-3](http://doi.org/10.1016/S0079-6123(06)59019-3)
- Cunnington, R., Windischberger, C., Deecke, L., & Moser, E. (2002). The Preparation and Execution of Self-Initiated and Externally-Triggered Movement: A Study of Event-Related fMRI. *NeuroImage*, *15*(2), 373–385. <http://doi.org/10.1006/nimg.2001.0976>
- Curio, G., Mackert, B.-M., Burghoff, M., Koetitz, R., Abraham-Fuchs, K., & Härer, W. (1994). Localization of evoked neuromagnetic 600 Hz activity in the cerebral somatosensory system. *Electroencephalography and Clinical Neurophysiology*, *91*(6), 483–487. [http://doi.org/10.1016/0013-4694\(94\)90169-4](http://doi.org/10.1016/0013-4694(94)90169-4)
- Dagenbach, D., & Carr, T. H. (1994). Inhibitory processes in attention, memory, and language. In D. C. T. Dagenbach (Ed.), *Inhibitory processes in attention, memory, and language* (Academic P, pp. 189–239). San Diego.
- De Jong, R., Liang, C. C., & Lauber, E. (1994). Conditional and un-conditional automaticity: A dual-process model of effects of spatial S–R correspondence. *Journal of Experimental Psychology: Human Perception & Performance*, *20*, 731–750.
- Debener, S., Ullsperger, M., Siegel, M., Fiehler, K., von Cramon, Y., & Engel, A. K. (2005). Trial-by-trial coupling of concurrent electroencephalogram and functional magnetic resonance imaging identifies the dynamics of performance monitoring. *Journal of Neuroscience*, *25*(50), 11730–11737.
- Dehaene, S., Posner, M. I., & Tucker, D. M. (1994). Localization of a neuronal system for error detection and compensation. *Science*, *5*(5), 303–305.
- Dosenbach, N. U. F., Visscher, K. M., Palmer, E. D., Miezin, F. M., Wenger, K. K., Kang, H. C., ... Petersen, S. E. (2006). A Core System for the Implementation of Task Sets. *Neuron*, *50*(5), 799–812. <http://doi.org/10.1016/j.neuron.2006.04.031>
- Dutilh, G., & Vandekerckhove, J. (2012). Testing theories of post-error slowing. *Attention, Perception, & Psychophysics*, *74*(2), 454–465. <http://doi.org/10.3758/s13414-011-0243-2>
- Emeric, E. E., Brown, J. W., Leslie, M., Pouget, P., Stuphorn, V., Schall, J. D., ... Schall, J. D.

- (2008). Performance Monitoring Local Field Potentials in the Medial Frontal Cortex of Primates : Anterior Cingulate Cortex Performance Monitoring Local Field Potentials in the Medial Frontal Cortex of Primates: Anterior Cingulate Cortex. *Journal of Neurophysiology*, *99*, 759–772. <http://doi.org/10.1152/jn.00896.2006>
- Emeric, E. E., Leslie, M., Pouget, P., Schall, J. D., Emeric, E. E., Leslie, M., ... Schall, J. D. (2010). Performance Monitoring Local Field Potentials in the Medial Frontal Cortex of Primates : Supplementary Eye Field Performance Monitoring Local Field Potentials in the Medial Frontal Cortex of Primates: Supplementary Eye Field. *Journal of Neurophysiology*, *104*, 1523–1537. <http://doi.org/10.1152/jn.01001.2009>
- Endrass, T., Klawohn, J., Schuster, F., & Kathmann, N. (2008). Overactive performance monitoring in obsessive-compulsive disorder: ERP evidence from correct and erroneous reactions. *Neuropsychologia*, *46*(7), 1877–1887. <http://doi.org/10.1016/j.neuropsychologia.2007.12.001>
- Engel, A. K., Fries, P., & Singer, W. (2001). DYNAMIC PREDICTIONS : OSCILLATIONS AND SYNCHRONY IN TOP – DOWN PROCESSING. *Nature Reviews Neuroscience*, *2*(October), 704–716.
- Escola, L., Michelet, T., Macia, F., Guehl, D., Bioulac, B., & Burbaud, P. (2003). Disruption of information processing in the supplementary motor area of the MPTP-treated monkey. *Brain*, *126*(1), 95–114. Retrieved from <http://brain.oxfordjournals.org/content/126/1/95.abstract>
- Falkenstein, M. (2004). ERP correlates of erroneous performance. In M. Ullsperger & M. Falkenstein (Eds.), *Errors, Conflicts, and the Brain. Current Opinions on Performance Monitoring* (pp. 5–12). Leipzig: MPI of Cognitive Neuroscience.
- Falkenstein, M., Hohnsbein, J., Hoormann, J., & Blanke, L. (1991). Effects of crossmodal divided attention on late ERP components. II. Error processing in choice reaction tasks. *Electroencephalography and Clinical Neurophysiology*, *78*, 447–455.
- Falkenstein, M., Hoormann, J., Christ, S., & Hohnsbein, J. (2000). ERP components on reaction errors and their functional significance: A tutorial. *Biological Psychology*, *51*, 87–107.
- Fonken, Y. M., Rieger, J. W., Tzvi, E., Crone, N. E., Chang, E., Parvizi, J., ... Krämer, U. M. (2016). Frontal and motor cortex contributions to response inhibition : evidence from electrocorticography. *Journal of Neurophysiology*, *115*(4), 2224–2236. <http://doi.org/10.1152/jn.00708.2015>
- Ford, M. J. (1999). Schizophrenia : The broken P300 and beyond. *Psychophysiology*, *36*, 667–682.
- Fries, P., Reynolds, J., Rorie, A., & Desimone, R. (2001). Modulation of oscillatory neuronal synchronization by selective visual attention. *Science*, *291*(5508), 1560–1563.
- Friston, K., Frith, C., Passingham, R., Liddle, P., & Frackowiak, R. (1992). Motor practice and neurophysiological adaptation in the cerebellum: a positron emission tomography study. *Proc R Soc Lond*, *248*, 223–228.
- Garavan, H., Ross, T., Murphy, K., Roche, R., & Stein, E. (2002). Dissociable executive functions in the dynamic control of behavior: inhibition, error detection, and correction.

- Neuroimage*, 17(4), 1820–1829.
- Gehering, W. J., & Fencsik, D. E. (2001). Functions of the medial frontal cortex in the processing of conflict and errors. *Journal of Neuroscience*, 21, 9430–9437.
- Gehring, W. J., Goss, B., Coles, M. G. H., Meyer, D. E., & Donchin, E. (1993). A neural system for error detection and compensation. *Psychological Science*, 4, 385–390.
- Gehring, W. J., & Knight, R. T. (2000). Prefrontal-cingulate interactions in action monitoring. *Nat Neurosci*, 3(5), 516–520. Retrieved from <http://dx.doi.org/10.1038/74899>
- Gehring, W. J., & Willoughby, A. R. (2002). The Medial Frontal Cortex and the Rapid Processing of Monetary Gains and Losses. *Science*, 295(5563), 2279–2282. Retrieved from <http://science.sciencemag.org/content/295/5563/2279.abstract>
- Godlove, D. C., Emeric, E. E., Segovis, C. M., Young, M. S., Schall, J. D., & Woodman, G. F. (2011). Event-Related Potentials Elicited by Errors during the Stop-Signal Task . I . Macaque Monkeys. *Journal of Neuroscience*, 31(44), 15640–15649. <http://doi.org/10.1523/JNEUROSCI.3349-11.2011>
- Goldberg, G. (1985). Supplementary motor area structure and function: Review and hypotheses. *Behavioral and Brain Sciences*, 8, 567–588.
- Goldman-Rakic, P. S., Cools, A. R., & Srivastava, K. (1996). The Prefrontal Landscape: Implications of Functional Architecture for Understanding Human Mentation and the Central Executive [and Discussion]. *Philosophical Transactions of the Royal Society of London B: Biological Sciences*, 351(1346), 1445–1453. Retrieved from <http://rstb.royalsocietypublishing.org/content/351/1346/1445.abstract>
- Gorsuch, R. L. (1983). *Factor Analysis (2nd edition)*. Hillsdale, NJ: Erlbaum.
- Grafton, S., Mazziotta, J., Presty, S., Friston, K., Frackowiak, R., & Phelps, M. (1992). Functional anatomy of human procedural learning determined with regional cerebral blood flow and PET. *Journal of Neuroscience*, 12, 2542–2548.
- H Rosvold, A Mirsky, I Sarason, E.D Bransome Jr., L. . B. (1956). A continuous performance test of brain damage. *Journal of Consulting Psychology*, 20, 343–350.
- Hajcak, G., Donald, N. M. C., & Simons, R. F. (2003). To err is autonomic : Error-related brain potentials , ANS activity , and post-error compensatory behavior. *Psychophysiology*, 40, 895–903. <http://doi.org/10.1111/1469-8986.00107>
- Hajcak, G., McDonald, N., & Simons, R. F. (2003). Anxiety and error-related brain activity. *Biological Psychology*, 64(1), 77–90. [http://doi.org/10.1016/S0301-0511\(03\)00103-0](http://doi.org/10.1016/S0301-0511(03)00103-0)
- Hajcak, G., McDonald, N., & Simons, R. F. (2004). Error-related psychophysiology and negative affect. *Brain and Cognition*, 56(2), 189–197. <http://doi.org/10.1016/j.bandc.2003.11.001>
- Hajcak, G., Moser, J. S., Holroyd, C. B., & Simons, R. F. (2006). The feedback-related negativity reflects the binary evaluation of good versus bad outcomes. *Biological Psychology*, 71(2), 148–154. <http://doi.org/10.1016/j.biopsycho.2005.04.001>
- Hajcak, G., Moser, J. S., Yeung, N., & Simons, R. F. (2005). On the ERN and the significance

- of errors. *Psychophysiology*, 42(2), 151–160. <http://doi.org/10.1111/j.1469-8986.2005.00270.x>
- Hajcak, G., & Simons, R. F. (2008). Oops !.. I did it again : an ERP and behavioral study of double-errors. *Brain & Cognition*, 68(1), 15–21.
- Hampshire, A., Chamberlain, S. R., Monti, M. M., Duncan, J., & Owen, A. M. (2010). NeuroImage The role of the right inferior frontal gyrus : inhibition and attentional control. *NeuroImage*, 50(3), 1313–1319. <http://doi.org/10.1016/j.neuroimage.2009.12.109>
- Hasbroucq, T., Akamatsu, M., Mouret, I., & Seal, J. (1995). Finger pairings in two-choice reaction time tasks : Does the between-hands advantage reflect response preparation ? *Journal of Motor Behavior*, 27, 251–262.
- Hasbroucq, T., Possamaï, C. A., Bonnet, M., & Vidal, F. (1999). Effect of the irrelevant location of the response signal on choice reaction time : An electromyographic study in humans. *Psychophysiology*, 36, 522–526.
- Herrmann, C. S., Frund, I., & Lenz, D. (2010). Human gamma-band activity : A review on cognitive and behavioral correlates and network models. *Neuroscience and Biobehavioral Reviews*, 34, 981–992. <http://doi.org/10.1016/j.neubiorev.2009.09.001>
- Herrmann, C. S., Munk, M. H. J., & Engel, A. K. (2004). Cognitive functions of gamma-band activity : memory match and utilization. *Trends in Cognitive Sciences*, 8(8), 347–355. <http://doi.org/10.1016/j.tics.2004.06.006>
- Herrmann, M. J., Ro, J., Ehlis, A., Heidrich, A., & Fallgatter, A. J. (2004). Source localization ( LORETA ) of the error-related-negativity ( ERN / Ne ) and positivity ( Pe ). *Cognitive Brain Research*, 20(2), 294–299. <http://doi.org/10.1016/j.cogbrainres.2004.02.013>
- Hjorth, B. (1975). An on-line transformation of EEG scalp potentials into orthogonal source derivations. *Electroencephalography and Clinical Neurophysiology*, 39, 526–530.
- Hoffmann, S., & Falkenstein, M. (2010). Independent component analysis of erroneous and correct responses suggests online response contro. *Human Brain Mapping*, 31(9), 1305–1315.
- Hoffmann, S., & Falkenstein, M. (2012). Predictive information processing in the brain : Errors and response monitoring. *International Journal of Psychophysiology*, 83(2), 208–212. <http://doi.org/10.1016/j.ijpsycho.2011.11.015>
- Holmes, A. J., & Pizzagalli, D. A. (2008). Response conflict and frontocingulate dysfunction in unmedicated participants with major depression. *Neuropsychologia*, 46(12), 2904–2913. <http://doi.org/10.1016/j.neuropsychologia.2008.05.028>
- Holroyd, C. B., & Coles, M. G. H. (2002). The Neural Basis of Human Error Processing : Reinforcement Learning , Dopamine , and the Error-Related Negativity, 109(4), 679–709. <http://doi.org/10.1037//0033-295X.109.4.679>
- Holroyd, C. B., Nieuwenhuis, S., Yeung, N., Nystrom, L., Mars, R. B., Coles, M. G. H., & Cohen, J. D. (2004). Dorsal anterior cingulate cortex shows fMRI response to internal and external error signals, 7(5), 497–498. <http://doi.org/10.1038/nn1238>

- Holroyd, C., Dien, J., & Coles, M. G. . (1998). Error-related scalp potentials elicited by hand and humans foot movements: Evidence for an output-independent error-processing system. *Neuroscience Letters*, *242*, 65–68.
- Hoogenboom, N., Schoffelen, J.-M., Oostenveld, R., Parkes, L. M., & Fries, P. (2006). Localizing human visual gamma-band activity in frequency, time and space. *NeuroImage*, *29*(3), 764–773. <http://doi.org/10.1016/j.neuroimage.2005.08.043>
- Hutchison, W. D., Davis, K. D., Lozano, A. M., Tasker, R. R., & Dostrovsky, J. O. (1999). Pain-related neurons in the human cingulate cortex. *Nat Neurosci*, *2*(5), 403–405. Retrieved from <http://dx.doi.org/10.1038/8065>
- Ito, S., Ito, S., Stuphorn, V., Brown, J. W., & Schall, J. D. (2003). Performance Monitoring by the Anterior Cingulate Cortex During Saccade Countermanding. *Science*, *320*(5642), 120–122. <http://doi.org/10.1126/science.1087847>
- Jensen, O., Kaiser, J., & Lachaux, J. (2007). Human gamma-frequency oscillations associated with attention and memory. *Trends in Cognitive Sciences*, *30*(7), 317–324. <http://doi.org/10.1016/j.tins.2007.05.001>
- Keil, J., Weisz, N., Paul-jordanov, I., & Wienbruch, C. (2010). NeuroImage Localization of the magnetic equivalent of the ERN and induced oscillatory brain activity. *NeuroImage*, *51*(1), 404–411. <http://doi.org/10.1016/j.neuroimage.2010.02.003>
- Kennerley, S. W., Walton, M. E., Behrens, T. E. J., Buckley, M. J., & Rushworth, M. F. S. (2006). Optimal decision making and the anterior cingulate cortex. *Nat Neurosci*, *9*(7), 940–947. Retrieved from <http://dx.doi.org/10.1038/nn1724>
- Kerns, J. G. (2006). Anterior cingulate and prefrontal cortex activity in an FMRI study of trial-to-trial adjustments on the Simon task. *NeuroImage*, *33*(1), 399–405. <http://doi.org/10.1016/j.neuroimage.2006.06.012>
- Klein, T. A., Endrass, T., Kathmann, N., Neumann, J., von Cramon, D. Y., & Ullsperger, M. (2007). Neural correlates of error awareness. *NeuroImage*, *34*(4), 1774–1781. <http://doi.org/10.1016/j.neuroimage.2006.11.014>
- Kok, A., Ridderinkhof, K. R., & Ullsperger, M. (2006). The control of attention and actions: Current research and future developments. *Brain Research*, *1105*(1), 1–6. <http://doi.org/10.1016/j.brainres.2006.03.027>
- Kringelbach, M. L., & Rolls, E. T. (2004). The functional neuroanatomy of the human orbitofrontal cortex: Evidence from neuroimaging and neuropsychology. *Progress in Neurobiology*, *72*(5), 341–372. <http://doi.org/10.1016/j.pneurobio.2004.03.006>
- Lachaux, J., Axmacher, N., Mormann, F., Halgren, E., Crone, N. E., & Lyon, C. B. (2012). Progress in Neurobiology High-frequency neural activity and human cognition : Past , present and possible future of intracranial EEG research. *Progress in Neurobiology*, *98*(3), 279–301. <http://doi.org/10.1016/j.pneurobio.2012.06.008>
- Laming, D. (1979). Choice reaction performance following an error. *Acta Psychologica*, *43*, 199–224.
- Lane, R., Reiman, E. M., Axelrod, B., Yun, L. S., Holmes, A., & Schwartz, G. E. (1998). Neural Correlates of Levels of Emotional Awareness: Evidence of an Interaction between

- Emotion and Attention in the Anterior Cingulate Cortex. *Journal of Cognitive Neuroscience*, 10(4), 525–535.
- Laurens, K. R., Ngan, E. T. C., Bates, A. T., Kiehl, K. A., & Liddle, P. F. (2003). Rostral anterior cingulate cortex dysfunction during error processing in schizophrenia. *Brain*, 126(3), 610–622. Retrieved from <http://brain.oxfordjournals.org/content/126/3/610.abstract>
- Lee, D. (2003). Coherent Oscillations in Neuronal Activity of the Supplementary Motor Area during a Visuomotor Task. *Journal of Neuroscience*, 23(17), 6798–6809.
- Lim, S. H., Dinner, D. S., & Luders, H. O. (1996). Cortical stimulation of the supplementary sensorimotor area. In H. O. Luders (Ed.), *Advances in neurology* (pp. 187–197). Philadelphia: Lippincott-Raven Publishers.
- Llinas, R. R. (1988). The intrinsic electrophysiological properties of mammalian neurons: insights into central nervous system function. *Science*, 242, 1654–1664.
- Llinás, R. R. (2014). Intrinsic electrical properties of mammalian neurons and CNS function : a historical perspective TYPES. *Frontiers Cellular Neuroscience*, 8(November), 1–14. <http://doi.org/10.3389/fncel.2014.00320>
- Logan, G., & Cowan, W. (1984). On the ability to inhibit thought and action: A theory of an act of control. *Psychological Review*, 91, 295–327.
- Lopes da Silva, F. (2010). EEG : Origin and Measurement. In C. Mulert & L. Lemieux (Eds.), *EEG-fMRI* (pp. 19–39). Berlin: Springer Verlag Berlin Heidelberg. <http://doi.org/10.1007/978-3-540-87919-0>
- Lopes da Silva, F. (2011). *Computer-Assisted EEG Diagnosis: Pattern Recognition and Brain Mapping*. (D. Schomer & F. Lopes da Silva, Eds.).
- Lopes da Silva, F., & Schomer, D. L. (2012). *Niedermeyer's Electroencephalography. Basic Principles, clinical applications, and related fields* (Lippincott).
- Lorente De No, R. (1947). Action potential of the motoneuron of the hypoglossus nucleus. *Journal of Cellular and Comparative Physiology*, 29, 207–287.
- Luu, P., Flaisch, T., & Tucker, D. M. (2000). Medial frontal cortex in action monitoring. *The Journal of Neuroscience : The Official Journal of the Society for Neuroscience*, 20(1), 464–469.
- Luu, P., & Tucker, D. M. (2001). Regulating action : alternating activation of midline frontal and motor cortical networks. *Clinical Neurophysiology*, 112(7), 1295–1306.
- Luu, P., Tucker, D. M., Derryberry, D., Reed, M., & Poulsen, C. (2003). Electrophysiological responses to errors and feedback in the process of action regulation. *Psychological Science*, 14(1), 47–53.
- Luu, P., Tucker, D. M., & Makeig, S. (2004). Frontal midline theta and the error-related negativity : neurophysiological mechanisms of action regulation. *Clinical Neurophysiology*, 115(8), 1821–1835. <http://doi.org/10.1016/j.clinph.2004.03.031>
- Macar, F., Coull, J., & Vidal, F. (2006). The supplementary motor area in motor and

- perceptual time processing: fMRI studies. *Cognitive Processing*, 7(2), 89–94. <http://doi.org/10.1007/s10339-005-0025-7>
- Maier, M. a, Armand, J., Kirkwood, P. a, Yang, H.-W., Davis, J. N., & Lemon, R. N. (2002). Differences in the corticospinal projection from primary motor cortex and supplementary motor area to macaque upper limb motoneurons: an anatomical and electrophysiological study. *Cerebral Cortex*, 12(3), 281–296. <http://doi.org/10.1093/cercor/12.3.281>
- Manoach, D. S., & Agam, Y. (2013). Neural markers of errors as endophenotypes in neuropsychiatric disorders. *Frontiers in Human Neuroscience*, 7(JUL), 350. <http://doi.org/10.3389/fnhum.2013.00350>
- Masaki, H., & Segalowitz, S. (2004). Error negativity : A test of the response conflict versus error detection hypotheses. In M. Ullsperger, M. et Falkenstein (Ed.), *Errors, Conflicts, and the Brain. Current Opinions on Performance Monitoring* (pp. 76–83). Leipzig: MPI of Cognitive Neuroscience.
- Matelli, M., & Luppino, G. (1991). Architecture of Superior and Mesial Area 6 and the Adjacent Cingulate Cortex in the Macaque Monkey. *Journal of Comparative Neurology*, 462, 445–462.
- Matelli, M., & Luppino, G. (2001). Parietofrontal circuits for action and space perception in the macaque monkey. *NeuroImage*, 14(1 Pt 2), S27–32. <http://doi.org/10.1006/nimg.2001.0835>
- Matelli, M., Luppino, G., & Rizzolatti, G. (1985). Patterns of cytochrome oxidase activity in the frontal agranular cortex of the macaque monkey. *Behavioural Brain Research*, 18(2), 125–136.
- Mathalon, D. H., Fedor, M., Faustman, W. O., Gray, M., Askari, N., & Ford, J. M. (2002). Response-monitoring dysfunction in schizophrenia: An event-related brain potential study. *Journal of Abnormal Psychology*, 111(1), 22–41. <http://doi.org/10.1037//0021-843X.111.1.22>
- Mathalon, D. H., Whitfield, S. L., & Ford, J. M. (2003). Anatomy of an error: ERP and fMRI. *Biological Psychology*, 64(1), 119–141. [http://doi.org/10.1016/S0301-0511\(03\)00105-4](http://doi.org/10.1016/S0301-0511(03)00105-4)
- Matsuzaka, Y., & Tanji, J. (1996). Changing directions of forthcoming arm movements: neuronal activity in the presupplementary and supplementary motor area of monkey cerebral cortex. *Journal of Neurophysiology*, 76(4), 2327–2342. Retrieved from <http://jn.physiology.org/content/76/4/2327.abstract>
- Meckler, C. (2010). *Supervision proactive et reactive de l'action dans les activités sensorimotrices chez l'homme: études électrophysiologiques et comportementales*. Aix-Marseille University.
- Meckler, C., Allain, S., Carbonnell, L., Hasbroucq, T., Burle, B., & Vidal, F. (2011). Executive control and response expectancy : A Laplacian ERP study. *Psychophysiology*, 48(3), 303–311. <http://doi.org/10.1111/j.1469-8986.2010.01077.x>
- Meckler, C., Carbonnell, L., Hasbroucq, T., Burle, B., & Vidal, F. (2013). To err or to guess: An ERP study on the source of errors. *Psychophysiology*, 50(5), 415–421. <http://doi.org/10.1111/psyp.12020>

- Medalla, M., & Barbas, H. (2010). Anterior cingulate synapses in prefrontal areas 10 and 46 suggest differential influence in cognitive control. *The Journal of Neuroscience*, *30*(48), 16068–81. <http://doi.org/10.1523/JNEUROSCI.1773-10.2010>
- Michelet, T., Bioulac, B., Guehl, D., Escola, L., & Burbaud, P. (2007). Impact of Commitment on Performance Evaluation in the Rostral Cingulate Motor Area. *Journal of Neuroscience*, *27*(28), 7482–7489. <http://doi.org/10.1523/JNEUROSCI.4718-06.2007>
- Michelet, T., Bioulac, B., Guehl, D., Goillandeau, M., & Burbaud, P. (2009). Single Medial Prefrontal Neurons Cope with Error. *PLoS ONE*, *4*(7). <http://doi.org/10.1371/journal.pone.0006240>
- Miller, E. K., & Cohen, J. D. (2001). An integrative theory of prefrontal cortex function. *Annual Review of Neuroscience*, *24*, 167–202.
- Miltner, W. H. R., Braun, C., ArnoldMatthias, Witte, H., & Taub, E. (1999). Coherence of gamma-band EEG activity as a basis for associative learning. *Nature*, *397*(6718), 434–436. Retrieved from <http://dx.doi.org/10.1038/17126>
- Miltner, W. H. R., Braun, C. H., & Michael, G. H. (1997). Event-Related Brain Potentials Following n a Time-Estimation Incorrect Feedback i Task : Evidence for a “ Generic ” Neural System for Error Detection. *Journal of Cognitive Neuroscience*, *9*, 788–798.
- Mitra, P. P., & Pesaran, B. (1999). Analysis of dynamic brain imaging data. *Biophysical Journal*, *76*(2), 691–708. [http://doi.org/10.1016/S0006-3495\(99\)77236-X](http://doi.org/10.1016/S0006-3495(99)77236-X)
- Mochizuki, H., Machii, K., Terao, Y., Furubayashi, T., Hanajima, R., Enomoto, H., ... Ugawa, Y. (2003). Recovery function of and effects of hyperventilation on somatosensory evoked high-frequency oscillation in Parkinson’s disease and myoclonus epilepsy. *Neuroscience Research*, *46*(4), 485–492. [http://doi.org/10.1016/S0168-0102\(03\)00129-9](http://doi.org/10.1016/S0168-0102(03)00129-9)
- Monchi, O., Petrides, M., Petre, V., Worsley, K., & Dagher, A. (2001). Wisconsin Card Sorting Revisited: Distinct Neural Circuits Participating in Different Stages of the Task Identified by Event-Related Functional Magnetic Resonance Imaging. *The Journal of Neuroscience*, *21* (19 ), 7733–7741. Retrieved from <http://www.jneurosci.org/content/21/19/7733.abstract>
- Moser, J. S., & Simons, R. F. (2009). The neural consequences of flip-flopping: The feedback-related negativity and salience of reward prediction. *Psychophysiology*, *46*(2), 313–320. <http://doi.org/10.1111/j.1469-8986.2008.00760.x>
- Munneke, G., Nap, T. S., & Schippers, E. E. (2015). A statistical comparison of EEG time- and time – frequency domain representations of error processing. *Brain Research*, *1618*, 222–230. <http://doi.org/10.1016/j.brainres.2015.05.030>
- Murphy, T. ., Masaki, R. M., & Segalowitz, S. (2006). The effect of sleepiness on performance monitoring : I know what I am doing, but do I care? *Journal of Sleep Research*, *15*(1), 15–21.
- Nachev, P., Kennard, C., & Husain, M. (2008). Functional role of the supplementary and pre-supplementary motor areas. *Nature Reviews Neuroscience*, *9*(11), 856–869. <http://doi.org/10.1038/nrn2478>
- Nakamura, K., Roesch, M. R., Olson, C. R., Nakamura, K., Roesch, M. R., & Olson, C. R.

- (2005). Neuronal Activity in Macaque SEF and ACC During Performance of Tasks Involving Conflict. *Journal of Neurophysiology*, 93, 884–908. <http://doi.org/10.1152/jn.00305.2004>
- Nakamura, K., Sakai, K., & Hikosaka, O. (1998). Neuronal Activity in Medial Frontal Cortex During Learning of Sequential Procedures. *Journal of Neurophysiology*, 80(5), 2671–2687. Retrieved from <http://jn.physiology.org/content/80/5/2671.abstract>
- Nieuwenhuis, S., Holroyd, C. B., Mol, N., & Coles, M. G. H. (2004). Reinforcement-related brain potentials from medial frontal cortex: origins and functional significance. *Neuroscience and Biobehavioral Reviews*, 28(4), 441–448. <http://doi.org/10.1016/j.neubiorev.2004.05.003>
- Nieuwenhuis, S., Ridderinkhof, K. R., Blom, J. O. S., Band, G. P. H., & Kok, A. (2001). Error-related brain potentials are differentially related to awareness of response errors: Evidence from an antisaccade task. *Psychophysiology*, 38, 752–760.
- Nieuwenhuis, S., Ridderinkhof, K. R., Talsma, D., Coles, M. G. H., Holroyd, C. B., Kok, A., & van der Molen, M. W. (2002). A computational account of altered error processing in older age: Dopamine and the error-related negativity. *Cognitive, Affective & Behavioral Neuroscience*, 2(1), 19–36. <http://doi.org/10.3758/CABN.2.1.19>
- Nigbur, R., Cohen, M. X., Ridderinkhof, K. R., & Stürmer, B. (2012). Theta Dynamics Reveal Domain-specific Control over Stimulus and Response Conflict. *Journal of Cognitive Neuroscience*, 24(5), 1264–1274. [http://doi.org/10.1162/jocn\\_a\\_00128](http://doi.org/10.1162/jocn_a_00128)
- Notebaert, W., Houtman, F., Opstal, F. Van, Gevers, W., Fias, W., & Verguts, T. (2009). Author's personal copy Post-error slowing: An orienting account. *Cognition*, 111, 275–279. <http://doi.org/10.1016/j.cognition.2009.02.002>
- Nunez, P. L. (1981). *Electric Fields of the Brain: The Neurophysics of EEG*. New York: Oxford University Press.
- Ollmann, R. (1973). Simple reactions with random countermanding of the “go” signal. In A. Press (Ed.), *Attention and Performance IV*. New York.
- Olvet, D. M., & Hajcak, G. (2008). The error-related negativity (ERN) and psychopathology: Toward an endophenotype. *Clinical Psychology Review*, 28(8), 1343–1354. <http://doi.org/10.1016/j.cpr.2008.07.003>
- Ongür, D., & Price, J. L. (2000). The organization of networks within the orbital and medial prefrontal cortex of rats, monkeys and humans. *Cerebral Cortex (New York, N.Y. : 1991)*, 10(3), 206–219. <http://doi.org/10.1093/cercor/10.3.206>
- Onton, J., Westerfield, M., Townsend, J., & Makeig, S. (2006). Imaging human EEG dynamics using independent component analysis. *Neuroscience and Biobehavioral Reviews*, 30(6), 808–822.
- Oostenveld, R., Fries, P., Maris, E., & Schoffelen, J. M. (2011). FieldTrip: Open source software for advanced analysis of MEG, EEG, and invasive electrophysiological data. *Computational Intelligence and Neuroscience*, 2011. <http://doi.org/10.1155/2011/156869>
- Orgogozo, J. M., & Larsen, B. (1979). Activation of the supplementary motor area during

- voluntary movement in man suggests it works as a supramotor area. *Science*, 206(4420), 847–850. Retrieved from <http://science.sciencemag.org/content/206/4420/847.abstract>
- Overbeek, T. J. M., Nieuwenhuis, S., & Ridderinkhof, K. R. (2005). Dissociable Components of Error Processing On the Functional Significance of the Pe vis à vis the Ne. *Journal of Psychophysiology*, 19(4), 319–329. <http://doi.org/10.1027/0269-8803.19.4.319>
- Palomero-Gallagher, N., Vogt, B. A., Schleicher, A., Mayberg, H. S., & Zilles, K. (2009). Receptor architecture of human cingulate cortex: evaluation of the four-region neurobiological model. *Human Brain Mapping*, 30(8), 2336–55. <http://doi.org/10.1002/hbm.20667>
- Pantev, C. (1995). Evoked and induced gamma-band activity of the human cortex. *Brain Topography*, 7(4), 321–330. <http://doi.org/10.1007/BF01195258>
- Passingham, R. E. (1995). *The Frontal Lobes and Voluntary Action*. Oxford: Oxford University Press.
- Penfield, W., & Welch, K. (1951). The supplementary motor area of the cerebral cortex; a clinical and experimental study. *AMA Arch. Neurol. Psychiatry*, 66, 289–317.
- Percival, D. B., & Walden, A. T. (1993). *Spectral Analysis for Physical Applications*. (D. B. Percival & A. T. Walden, Eds.). Cambridge: Cambridge University Press.
- Perez, V. B., Woods, S. W., Roach, B. J., Ford, J. M., McGlashan, T. H., Srihari, V. H., & MATHALON, D. H. (2014). Automatic Auditory Processing Deficits in Schizophrenia and Clinical High-Risk Patients: Forecasting Psychosis Risk with Mismatch Negativity. *Biological Psychiatry*, 75(6), 459–469. <http://doi.org/10.1016/j.biopsych.2013.07.038>
- Pernier, J. (2007). *Electro et magnétoencéphalographie. Biophysique, techniques et méthodes*. (J. PERNIER, Ed.). Paris Lavoisier, 2007.: Paris Lavoisier.
- Pernier, J., Perrin, F., & Bertrand, O. (1988). Scalp current density fields: Concepts and properties. *Electroencephalography and Clinical Neurophysiology*, 69, 385–389.
- Petrides, M., & Pandya, D. N. (1999). Dorsolateral prefrontal cortex: comparative cytoarchitectonic analysis in the human and the macaque brain and corticocortical connection patterns. *The European Journal of Neuroscience*, 11(3), 1011–36. <http://doi.org/10.1046/j.1460-9568.1999.00518.x>
- Petrides, M., & Pandya, D. N. (2007). Efferent association pathways from the rostral prefrontal cortex in the macaque monkey. *The Journal of Neuroscience: The Official Journal of the Society for Neuroscience*, 27(43), 11573–86. <http://doi.org/10.1523/JNEUROSCI.2419-07.2007>
- Picard, N., & Strick, P. L. (1996). Motor areas of the medial wall: a review of their location and functional activation. *Cerebral Cortex (New York, N.Y.: 1991)*, 6(3), 342–353.
- Pitman, R. K. (1987). Pierre Janet on Obsessive-Compulsive Disorder (1903)Review and Commentary. *JAMA Psychiatry*, 44(3), 226–232.
- Posner, M. I., Petersen, S. E., Fox, P. T., & Raichle, M. E. (1988). Localization of operations in the human brain. *Science*, 240(4859), 1627–1631.

- Quilichini, P., Sirota, A., & Buzsáki, G. (2010). Intrinsic Circuit Organization and Theta–Gamma Oscillation Dynamics in the Entorhinal Cortex of the Rat. *The Journal of Neuroscience*, 30 (33), 11128–11142. <http://doi.org/10.1523/JNEUROSCI.1327-10.2010>
- Rabbitt, P. M. A. (1996). Errors and error correction in choice-response task. *Journal of Experimental Psychology*, 71, 264–272.
- Ramnani, N., & Owen, A. M. (2004). Anterior prefrontal cortex: insights into function from anatomy and neuroimaging. *Nature Reviews. Neuroscience*, 5(3), 184–194. <http://doi.org/10.1038/nrn1343>
- Ray, S., Crone, N. E., Niebur, E., Franaszczuk, P. J., & Hsiao, S. S. (2008). Neural Correlates of High-Gamma Oscillations (60–200 Hz) in Macaque Local Field Potentials and Their Potential Implications in Electrocorticography. *The Journal of Neuroscience*, 28 (45), 11526–11536. <http://doi.org/10.1523/JNEUROSCI.2848-08.2008>
- Ray, S., & Maunsell, J. H. R. (2011). Different origins of gamma rhythm and high-gamma activity in macaque visual cortex. *PLoS Biology*, 9(4), e1000610. <http://doi.org/10.1371/journal.pbio.1000610>
- Ridderinkhof, K. R. (2002). Activation and suppression in conflict tasks: empirical clarification through distributional analyses. In W. Prinz & B. Hommel (Eds.), *Common Mechanisms in Perception and Action. Attention & Performance* (pp. 494–519). Oxford: Oxford University Press.
- Ridderinkhof, K. R., Ullsperger, M., Crone, E. A., & Nieuwenhuis, S. (2004). The Role of the Medial Frontal Cortex in Cognitive Control. *Science*, 306(5695), 443–447. Retrieved from <http://science.sciencemag.org/content/306/5695/443.abstract>
- Rochet, N., Spieser, L., Casini, L., Hasbroucq, T., & Burle, B. (2014). Detecting and correcting partial errors: Evidence for efficient control without conscious access. *Cognitive, Affective & Behavioral Neuroscience*, 14(3), 970–982. <http://doi.org/10.3758/s13415-013-0232-0>
- Roelfsema, P., Engel, A., König, P., & Singer, W. (1997). Visuomotor integration is associated with zero time-lag synchronization among cortical areas. *Nature*, 385(6612), 157–161.
- Roger, C., Bénar, C. G., Vidal, F., Hasbroucq, T., & Burle, B. (2010). Rostral Cingulate Zone and correct response monitoring: ICA and source localization evidences for the unicity of correct- and error-negativities. *NeuroImage*, 51(1), 391–403. <http://doi.org/10.1016/j.neuroimage.2010.02.005>
- Ruchow, M., Grothe, J., Spitzer, M., & Kiefer, M. (2002). Human anterior cingulate cortex is activated by negative feedback: evidence from event-related potentials in a guessing task. *Neuroscience Letters*, 325(3), 203–206.
- Rushworth, M. F. S., Buckley, M. J., Behrens, T. E. J., Walton, M. E., & Bannerman, D. M. (2007). Functional organization of the medial frontal cortex. *Current Opinion in Neurobiology*, 17(2), 220–227. <http://doi.org/10.1016/j.conb.2007.03.001>
- Rushworth, M. F. S., Hadland, K. A., Paus, T., Sipila, P. K., Frank, M. J., & Badre, D. (2002). Role of the Human Medial Frontal Cortex in Task Switching: A Combined fMRI and TMS Study Role of the Human Medial Frontal Cortex in Task Switching: A Combined

- fMRI and TMS Study. *Journal of Neurophysiology*, 84(5), 2577–2592.
- Rushworth, M. F. S., Noonan, M. P., Boorman, E. D., Walton, M. E., & Behrens, T. E. (2011). Frontal Cortex and Reward-Guided Learning and Decision-Making. *Neuron*, 70(6), 1054–1069. <http://doi.org/10.1016/j.neuron.2011.05.014>
- Russell, J., & Jarrold, C. (1998). Error-correction problems in autism: Evidence for a monitoring impairment? *Journal of Autism and Developmental Disorders*, 28(3), 177–188. <http://doi.org/10.1023/A:1026009203333>
- Sahin, N. T., Pinker, S., Cash, S. S., Schomer, D., & Halgren, E. (2009). Sequential processing of lexical, grammatical and phonological information within Broca's area. *Science*, 326(5951), 445–449. <http://doi.org/10.1126/science.1174481>
- Scangos, K. W., Aronberg, R., Stuphorn, V., Scangos, K. W., Aronberg, R., & Stuphorn, V. (2013). Performance monitoring by presupplementary and supplementary motor area during an arm movement countermanding task Performance monitoring by presupplementary and supplementary motor area during an arm movement countermanding task, (January), 1928–1939. <http://doi.org/10.1152/jn.00688.2012>
- Schall, J. D., & Emeric, E. E. (2010). Conflict in Cingulate Cortex Function between Humans and Macaque Monkeys: More Apparent than Real. Commentary on Cole MW, Yeung N, Freiwald WA, Botvinick M (2009): Cingulate Cortex: Diverging Data from Humans and Monkeys. *Trends Neurosci* 32:566-574. *Brain, Behavior and Evolution*, 75(4), 237–238. <http://doi.org/10.1159/000313862>
- Scheffers, M. K., Coles, M. G. H., Bernstein, P., Gehring, W. J., & Donchin, E. (1996). Event-related brain potential and error-related processing: An analysis of incorrect response to go and no-go stimuli. *Psychophysiology*, 33, 42–53.
- Scheffer-Teixeira, R., Belchior, H., Leão, R. N., Ribeiro, S., & Tort, A. B. L. (2013). On High-Frequency Field Oscillations (>100 Hz) and the Spectral Leakage of Spiking Activity. *The Journal of Neuroscience*, 33 (4), 1535–1539. <http://doi.org/10.1523/JNEUROSCI.4217-12.2013>
- Schomburg, E. W., Anastassiou, C. A., Buzsáki, G., & Koch, C. (2012). The Spiking Component of Oscillatory Extracellular Potentials in the Rat Hippocampus. *The Journal of Neuroscience*, 32 (34), 11798–11811. <http://doi.org/10.1523/JNEUROSCI.0656-12.2012>
- Sergent, J. (1993). Mapping the musician brain. *Human Brain Mapping*, 1, 20–38.
- Sergent, J., Zuck, E., Terriah, S., & B, M. (1992). Distributed neural network underlying musical sight-reading and keyboard performance. *Science*, 257, 106–109.
- Shima, K., & Tanji, J. (1998). Role for Cingulate Motor Area Cells in Voluntary Movement Selection Based on Reward. *Science*, 282(5392), 1335–1338. Retrieved from <http://science.sciencemag.org/content/282/5392/1335.abstract>
- Simon, H. A. (1979). Information processing models of cognition. *Ann. Rev. Psychol.*, 30, 363–396.
- Simons, R. F., Birbaumer, N., Coles, M., Graham, F., & Arne, O. (2010). The way of our errors: Theme and variations. *Psychophysiology*, 47(1), 1–14.

<http://doi.org/10.1111/j.1469-8986.2009.00929.x>

- Smid, H. G. O. M., Mulder, G., & Mulder, L. J. M. (1990). Selective response activation can begin before stimulus recognition is complete : A psychophysiological and error analysis of the continuous flow. *Acta Psychologica*, *74*, 169–201.
- South, M., Larson, M. J., Krauskopf, E., & Clawson, A. (2010). Error processing in high-functioning Autism Spectrum Disorders. *Biological Psychology*, *85*(2), 242–251. <http://doi.org/10.1016/j.biopsycho.2010.07.009>
- Spieser, L., van den Wildenberg, W., Hasbroucq, T., Ridderinkhof, K. R., & Burle, B. (2015). Controlling Your Impulses: Electrical Stimulation of the Human Supplementary Motor Complex Prevents Impulsive Errors. *The Journal of Neuroscience*, *35* (7), 3010–3015. <http://doi.org/10.1523/JNEUROSCI.1642-14.2015>
- Stemmer, B., Segalowitz, S. J., Dywan, J., Panisset, M., & Melmed, C. (2007). The error negativity in nonmedicated and medicated patients with Parkinson's disease. *Clinical Neurophysiology*, *118*(6), 1223–1229. <http://doi.org/10.1016/j.clinph.2007.02.019>
- Stuphorn, V., Taylor, T. L., & Schall, J. D. (2000). Performance monitoring by the supplementary eye field. *Nature*, *408*(December), 857–860.
- Suffczynski, P., Crone, N. E., & Franaszczuk, P. J. (2014). Afferent inputs to cortical fast-spiking interneurons organize pyramidal cell network oscillations at high-gamma frequencies (60–200 Hz). *Journal of Neurophysiology*, *112*(11), 3001–3011. Retrieved from <http://jn.physiology.org/content/112/11/3001.abstract>
- Sumner, P., Nachev, P., Morris, P., Peters, A. M., Jackson, S. R., Kennard, C., & Husain, M. (2007). *Human Medial Frontal Cortex Mediates Unconscious Inhibition of Voluntary Action*. *Neuron* (Vol. 54).
- Tadel, F., Baillet, S., Mosher, J. C., Pantazis, D., & Leahy, R. M. (2011). Brainstorm: A user-friendly application for MEG/EEG analysis. *Computational Intelligence and Neuroscience*, *2011*. <http://doi.org/10.1155/2011/879716>
- Talairach, J., Bancaud, J., Geier, S., Bordas-Ferrer, M., Bonis, A., Szikla, G., & Rusu, M. (1973). The cingulate gyrus and human behaviour. *Electroencephalography and Clinical Neurophysiology*, *34*(1), 45–52. [http://doi.org/10.1016/0013-4694\(73\)90149-1](http://doi.org/10.1016/0013-4694(73)90149-1)
- Talairach, J., Bancaud Jean, Bonis, A., Szikla, G., Trottier, S., Vignal, J. P., ... Chodkiewicz, J. P. (1992). Surgical therapy for frontal epilepsies. *Advances in Neurology*, *57*, 707–732.
- Talmi, D., Fuentemilla, L., Litvak, V., Duzel, E., & Dolan, R. J. (2012). NeuroImage An MEG signature corresponding to an axiomatic model of reward prediction error. *NeuroImage*, *59*(1), 635–645. <http://doi.org/10.1016/j.neuroimage.2011.06.051>
- Tanji, J., & Kurata, K. (1982). Comparison of movement-related activity in two cortical motor areas of primates. *Journal of Neurophysiology*, *48*(3), 633–653. Retrieved from <http://jn.physiology.org/content/48/3/633.abstract>
- Thakkar, K. N., Polli, F. E., Joseph, R. M., Tuch, D. S., Hadjikhani, N., Barton, J. J. S., & Manoach, D. S. (2008). Response monitoring, repetitive behaviour and anterior cingulate abnormalities in autism spectrum disorders (ASD). *Brain*, *131*(9), 2464–2478. Retrieved from <http://brain.oxfordjournals.org/content/131/9/2464.abstract>

- Trujillo, L. T., & Allen, J. J. B. (2007). Theta EEG dynamics of the error-related negativity. *Clinical Neurophysiology*, *118*(3), 645–668. <http://doi.org/10.1016/j.clinph.2006.11.009>
- Ullsperger, M., & Cramon, D. Y. Von. (2001a). Subprocesses of Performance Monitoring : A Dissociation of Error Processing and Response Competition Revealed by Event-Related fMRI and ERPs. *NeuroImage*, *14*(6), 1387–1401. <http://doi.org/10.1006/nimg.2001.0935>
- Ullsperger, M., & Cramon, D. Y. Von. (2001b). Subprocesses of Performance Monitoring : A Dissociation of Error Processing and Response Competition Revealed by Event-Related fMRI and ERPs, *1401*, 1387–1401. <http://doi.org/10.1006/nimg.2001.0935>
- Ullsperger, M., & von Cramon, D. (2004). Neuroimaging of performance monitoring: error detection and beyond. *Cortex*, *40*, 593–604.
- Ullsperger, M., & von Cramon, D. Y. (2003). Error monitoring using external feedback: specific roles of the habenular complex, the reward system, and the cingulate motor area revealed by functional magnetic resonance imaging. *The Journal of Neuroscience*, *23*(10), 4308–4314. <http://doi.org/23/10/4308> [pii]
- Ursu, S., Stenger, V. A., Shear, M. K., Jones, M. R., Carter, C. S., Katherine Shear, M., ... Carter, C. S. (2003). OBSESSIVE-COMPULSIVE DISORDER : Evidence From Functional Magnetic Resonance Imaging. *Psychological Science*, *14*(4), 347–353. <http://doi.org/10.1111/1467-9280.24411>
- Van Boxtel, G. J., Geraats, L. H., Van den Berg-Lenssen, M. M., & Brunia, C. H. (1993). Detection of EMG onset in ERP research. *Psychophysiology*, *30*, 405–412.
- van den Wildenberg, W. P. M., van Boxtel, G. J. M., & van der Molen, M. W. (2003). The duration of response inhibition in the stop-signal paradigm varies with response force. *Acta Psychologica*, *114*(2), 115–129. [http://doi.org/10.1016/S0001-6918\(03\)00062-3](http://doi.org/10.1016/S0001-6918(03)00062-3)
- van den Wildenberg, W. P. M., van Boxtel, G. J. M., van der Molen, M. W., Bosch, D. A., Speelman, J. D., & Brunia, C. H. M. (2006). Stimulation of the Subthalamic Region Facilitates the Selection and Inhibition of Motor Responses in Parkinson's Disease. *Journal of Cognitive Neuroscience*, *18*(4), 626–636. <http://doi.org/10.1162/jocn.2006.18.4.626>
- van den Wildenberg, W. P. M., van der Molen, M. W., & Logan, G. D. (2002). Reduced response readiness delays stop signal inhibition. *Acta Psychologica*, *111*(2), 155–169.
- van Duijvenvoorde, A. C. K., Zanolie, K., Rombouts, S. A. R. B., Raijmakers, M. E. J., & Crone, E. A. (2008). Evaluating the Negative or Valuing the Positive? Neural Mechanisms Supporting Feedback-Based Learning across Development. *Journal of Neuroscience*, *28*(38), 9495–9503. <http://doi.org/10.1523/JNEUROSCI.1485-08.2008>
- Van Veen, V., & Carter, C. (2002). The anterior cingulate as a conflict monitor: fMRI and ERP studies. *Physiology & Behavior*, *77*, 477–482.
- Vidal, F., Burle, B., Bonnet, M., Grapperon, J., & Hasbroucq, T. (2003). Error negativity on correct trials: a reexamination of available data. *Biological Psychology*, *64*(3), 265–282. [http://doi.org/10.1016/S0301-0511\(03\)00097-8](http://doi.org/10.1016/S0301-0511(03)00097-8)
- Vidal, F., Burle, B., Spieser, L., Carbonnell, L., Meckler, C., Casini, L., & Hasbroucq, T. (2015). Linking EEG signals, brain functions and mental operations: Advantages of the

- Laplacian transformation. *International Journal of Psychophysiology*, 97(3), 221–232. <http://doi.org/10.1016/j.ijpsycho.2015.04.022>
- Vidal, F., Grapperon, J., & Bonnet, M. (2003). The nature of unilateral motor commands in between- hand choice tasks as revealed by surface Laplacian estimation. *Psychophysiology*, 40(5), 796–805.
- Vidal, F., Hasbroucq, T., Grapperon, J., & Bonnet, M. (2000). Is the “ error negativity ” specific to errors ? *Biological Psychology*, 51(2-3), 109–128.
- Vincent, S. B. (1912). *The function of the vibrissae in the behavior of the white rat. Behavioral monography* (Vol. 1). Cambridge.
- Vlamings, P. H. J. M., Jonkman, L. M., Hoeksma, M. R., Van Engeland, H., & Kemner, C. (2008). Reduced error monitoring in children with autism spectrum disorder: An ERP study. *European Journal of Neuroscience*, 28(2), 399–406. <http://doi.org/10.1111/j.1460-9568.2008.06336.x>
- Vocat, R., Pourtois, G., & Vuilleumier, P. (2008). Unavoidable errors : A spatio-temporal analysis of time-course and neural sources of evoked potentials associated with error processing in a speeded task. *Neuropsychologia*, 46, 2545–2555. <http://doi.org/10.1016/j.neuropsychologia.2008.04.006>
- Vogt, A. (2009). Architecture, Neurocytology and Comparative Organization of Monkey and Human Cingulate Cortices. In A. B. Vogt (Ed.), *Cingulate neurobiology and disease* (pp. 66–91). Oxford: Oxford University Press.
- Vogt, B. A., Nimchinsky, E. A., Vogt, L. J., & Hof, P. R. (1995). Human cingulate cortex: Surface features, flat maps, and cytoarchitecture. *Journal of Comparative Neurology*, 359(3), 490–506. <http://doi.org/10.1002/cne.903590310>
- Vogt, B. A., Rosene, D. L., & Pandya, D. N. (1979). Thalamic and cortical afferents differentiate anterior from posterior cingulate cortex in the monkey. *Science*, 204(4389), 205–207. Retrieved from <http://science.sciencemag.org/content/204/4389/205.abstract>
- Vogt, C., & Vogt, O. (1919). Ergebnisse unserer hirnforschung. 1.-4. Mitteilung. *J. Psychol. Neurol*, 25, 279–461.
- Wagner, A. D., Maril, A., Bjork, R. A., & Schacter, D. L. (2001). Prefrontal Contributions to Executive Control : fMRI Evidence for Functional Distinctions within Lateral Prefrontal Cortex. *NeuroImage*, 14(6), 1337–1347. <http://doi.org/10.1006/nimg.2001.0936>
- Waldert, S., Lemon, R. N., & Kraskov, A. (2013). Influence of spiking activity on cortical local field potentials. *The Journal of Physiology*, 591(21), 5291–303. <http://doi.org/10.1113/jphysiol.2013.258228>
- Whittingstall, K., & Logothetis, N. K. (2009). Frequency-Band Coupling in Surface EEG Reflects Spiking Activity in Monkey Visual Cortex. *Neuron*, 64(2), 281–289. <http://doi.org/10.1016/j.neuron.2009.08.016>
- Willemsen, R., Müller, T., Schwarz, M., Hohsbein, J., & Falkenstein, M. (2008). Error processing in patients with Parkinson’s disease: The influence of medication state. *Journal of Neural Transmission*, 115(3), 461–468. <http://doi.org/10.1007/s00702-007-0842-1>

- Yeung, N., Bogacz, R., Olroyd, C. B., & Cohen, J. D. (2004). Detection of synchronized oscillations in the electroencephalogram: An evaluation of methods. *Psychophysiology*, *41*(6), 822–832.
- Yeung, N., Botvinick, M. M., & Cohen, J. D. (2004). The Neural Basis of Error Detection : Conflict Monitoring and the Error-Related Negativity. *Psychological Review*, *111*(4), 931–959. <http://doi.org/10.1037/0033-295X.111.4.931>
- Zilles, K., Schlaug, G., Matelli, M., Luppino, G., Schleicher, A., Qü, M., ... Roland, P. E. (1995). Mapping of human and macaque sensorimotor areas by integrating architectonic, transmitter receptor, MRI and PET data. *Journal of Anatomy*, *187*(December), 515–537.

## Table of Figures

Figure I.1 :	An example of a two-choice choice RT task. ....	11
Figure I.2 :	Post-error slowing.....	13
Figure I.3 :	Simon task. ....	14
Figure I.4 :	Electromyographic activity during a partial error trial.....	17
Figure I.5 :	Dipole and neuronal disposition .....	23
Figure I.6 :	Equivalent dipole .....	24
Figure I.7 :	Excitatory and inhibitory synapses.....	26
Figure I.8 :	Radial and tangential dipole measurement on the scalp.....	27
Figure I.9 :	Magnetic field of the brain.....	28
Figure I.10 :	The Error Negativity .....	34
Figure I.11 :	The Ne and the Ne-like .....	36
Figure I.12 :	The feedback-related negativity.....	37
Figure I.13 :	Premotor areas.....	39
Figure I.14 :	Connectivity of the Supplementary Motor Areas .....	41
Figure I.15 :	Subregions of the medial frontal wall. ....	42
Figure I.16 :	Human cingulate cortex.....	44
Figure I.17 :	Orbito-medial cortex .....	45
Figure I.18 :	Medial frontal cortex in action monitoring .....	50
Figure II.1 :	Experimental procedure.....	54
Figure II.2 :	EMG recording of the flexor pollicis brevis.....	55
Figure II.3 :	Behavioral pattern. ....	61
Figure II.4 :	EMG-locked LFPs in the SMA and all recording sites.....	64
Figure II.5 :	Localization of action monitoring activity in the SMA.....	65
Figure II.6 :	Spatial sampling of the caudal part of medial frontal lobe. ....	66
Figure II.7 :	Medial prefrontal LFPs evoked by erroneous activations.....	67
Figure II.8 :	Caudo-rostral latency of activation in the medial frontal wall .....	68
Figure II.9 :	Single trial LFPs time-locked to EMG onset in error trials.....	69
Figure II.10 :	medial prefrontal cortices (MPFC) and SMA activities .....	70
Figure II.11 :	Example of a partial error trial and corresponding SMA LFP.....	71
Figure II.12 :	Correlation between LFPs and EMG latencies in partial error. ....	72
Figure II.13 :	Behavioural pattern.....	85
Figure II.14 :	Supplementary motor area (SMA) cluster.....	87

<b>Figure II.15 :</b>	<b>Pre-Supplementary motor area (preSMA) cluster.....</b>	<b>88</b>
<b>Figure II.16 :</b>	<b>Mid-cingulate cortex (MCC) cluster.....</b>	<b>89</b>
<b>Figure II.17 :</b>	<b>Rostral anterior cingulate cortex (rACC) cluster.....</b>	<b>90</b>
<b>Figure II.18 :</b>	<b>Dorso-lateral pre-frontal cortex (DLPFC) cluster. ....</b>	<b>91</b>
<b>Figure II.19 :</b>	<b>Ventro-lateral prefrontal cortex (VLPFC) cluster. ....</b>	<b>93</b>
<b>Figure II.20 :</b>	<b>Orbito-frontal cortex (OFC) cluster.....</b>	<b>94</b>
<b>Figure II.21 :</b>	<b>Frontal operculum cluster.....</b>	<b>95</b>
<b>Figure II.22 :</b>	<b>Anterior Insula cluster.....</b>	<b>96</b>
<b>Figure II.23 :</b>	<b>Performance-monitoring and feedback evaluation paradigm.....</b>	<b>108</b>
<b>Figure II.24 :</b>	<b>The Ne on EEG data in the Simon phase.....</b>	<b>113</b>
<b>Figure II.25 :</b>	<b>Response-related MEG data in the Simon phase.....</b>	<b>114</b>
<b>Figure II.26 :</b>	<b>Source localization of response-related MEG data.....</b>	<b>115</b>
<b>Figure II.27 :</b>	<b>Time-courses and topography of feedback related EEG data.....</b>	<b>116</b>
<b>Figure II.28 :</b>	<b>Time-courses and topography of feedback related MEG data.....</b>	<b>117</b>
<b>Figure II.29 :</b>	<b>Source localization of feedback-related MEG activity.....</b>	<b>118</b>

S1 to S4), even though they showed equivalent activities regarding phosphorylation of VEGFR-2 (fig. S3A). This effect was shown not to depend on binding to the co-receptor neuropilin-1 (figs. S2C, S3A, and S12). The engineering of VEGF-A to tightly bind the ECM appears to decouple angiogenesis from hyperpermeability, potentially solving a major problem with VEGF-A's clinical translation.

In the context of bone repair, we tested whether PIGF-2<sub>123-144</sub>-fused BMP-2 and PDGF-BB could drive bone regeneration at low doses. Again, taking advantage of a hypothetic combinatorial effect between GFs (2, 3), we reasoned that PDGF-BB could induce progenitor cell recruitment, whereas the differentiation to bone tissue would be driven by BMP-2 (15). As a relevant model to illustrate translational potential, we used the critical-size calvarial defect in the rat (24). Because delivering micrograms of wild-type BMP-2 is usually barely sufficient to repair such calvarial defects (25), we tested a combination of BMP-2/PIGF-2<sub>123-144</sub>\* and PDGF-BB/PIGF-2<sub>123-144</sub> (200 ng of each) delivered in a fibrin matrix or delivered topically to the dura before surgical skin closure at a somewhat higher dose (1 µg of each, combined). After 4 weeks, bone healing—characterized by bone tissue deposition and coverage of the defects—was analyzed with microcomputed tomography (µCT). Delivery of wild-type GFs alone or within fibrin slightly increased bone healing when compared to the healing of defects without treatment or treated with fibrin only (Fig. 3, A to D, F, and I). In contrast, treatment with PIGF-2<sub>123-144</sub>-fused GFs led to a marked increase of bone tissue deposition as to wild-type GF (Fig. 3, A to D, G, and J), yielding coverage at 96% when delivered in fibrin and at 74% when simply administered on the dura. The

improved tissue regeneration with PIGF-2<sub>123-144</sub>-fused GFs most likely involves elevated recruitment of progenitor cells, because we could detect more mesenchymal stem cells/pericytes in the defects treated with PIGF-2<sub>123-144</sub>-fused GFs than in those treated with wild-type GFs (fig. S13).

In conclusion, we found that PIGF-2, through PIGF-2<sub>123-144</sub>, displays extraordinarily strong and promiscuous binding to the ECM. When this domain was conferred to other GFs, we could dramatically improve their efficacy and reduce their dosing in preclinical models of skin and bone repair. We further show that a critical limitation of VEGF-A, its induction of vascular hyperpermeability, may be ameliorated through this protein engineering concept. Because localized GF delivery and dose reduction are critical for optimal efficacy and clinical safety, this simple and broadly applicable approach to engineering second-generation ECM super-affinity GFs may be useful in a number of applications in regenerative medicine.

#### References and Notes

- S. P. Herbert, D. Y. Stainier, *Nat. Rev. Mol. Cell Biol.* **12**, 551–564 (2011).
- K. W. Lo, B. D. Ulery, K. M. Ashe, C. T. Laurencin, *Adv. Drug Deliv. Rev.* **64**, 1277–1291 (2012).
- A. L. Ponte *et al.*, *Stem Cells* **25**, 1737–1745 (2007).
- J. J. Rice *et al.*, *Adv. Healthc. Mater.* **2**, 57–71 (2013).
- M. Simons, J. A. Ware, *Nat. Rev. Drug Discov.* **2**, 863–871 (2003).
- E. J. Woo, *Spine J.* **12**, 894–899 (2012).
- L. A. Solchaga, C. K. Hee, S. Roach, L. B. Snel, *J. Tissue Eng.* **3**, 2041731412442668 (2012).
- "Panel Executive Summary for P050036 Medtronic's AMPLIFY™ rhBMP-2 Matrix" (U. S. Food and Drug Administration, Silver Spring, MD, 2010).
- "Safety warning on becaplermin in Regranex®" (U. S. Food and Drug Administration, Silver Spring, MD, 2008).
- L. Macri, D. Silverstein, R. A. Clark, *Adv. Drug Deliv. Rev.* **59**, 1366–1381 (2007).

- G. S. Schultz, J. M. Davidson, R. S. Kirsner, P. Bornstein, I. M. Herman, *Wound Repair Regen.* **19**, 134–148 (2011).
- M. M. Martino, J. A. Hubbell, *FASEB J.* **24**, 4711–4721 (2010).
- M. M. Martino, P. S. Briquez, A. Ranga, M. P. Lutolf, J. A. Hubbell, *Proc. Natl. Acad. Sci. U.S.A.* **110**, 4563–4568 (2013).
- L. De Laporte, J. J. Rice, F. Tortelli, J. A. Hubbell, *PLOS ONE* **8**, e62076 (2013).
- M. M. Martino *et al.*, *Sci. Transl. Med.* **3**, 100ra89 (2011).
- S. De Falco, *Exp. Mol. Med.* **44**, 1–9 (2012).
- S. R. Sullivan *et al.*, *Plast. Reconstr. Surg.* **113**, 953–960 (2004).
- T. P. Richardson, M. C. Peters, A. B. Ennett, D. J. Mooney, *Nat. Biotechnol.* **19**, 1029–1034 (2001).
- R. K. Chan *et al.*, *J. Burn Care Res.* **27**, 202–205 (2006).
- R. D. Galiano *et al.*, *Am. J. Pathol.* **164**, 1935–1947 (2004).
- G. C. Gurtner, S. Werner, Y. Barrandon, M. T. Longaker, *Nature* **453**, 314–321 (2008).
- N. Ferrara, *Mol. Biol. Cell* **21**, 687–690 (2010).
- W. W. Kilarski *et al.*, *PLOS ONE* **8**, e57135 (2013).
- P. P. Spicer *et al.*, *Nat. Protoc.* **7**, 1918–1929 (2012).
- H. G. Schmoekel *et al.*, *Biotechnol. Bioeng.* **89**, 253–262 (2005).

**Acknowledgments:** The Protein Expression, Proteomics, and Histology Core Facilities of the Ecole Polytechnique Fédérale de Lausanne and M. Pasquier, X. Quaglia, and C. Dessibourg provided technical assistance. Funding was from the European Community's Seventh Framework Programme in the project Angioscaff, the Swiss National Science Foundation, and the Fondation Bertarelli. J.A.H., M.M.M., and P.S.B. are named as inventors on a patent application filed by the Ecole Polytechnique Fédérale de Lausanne that covers the technology described in this paper.

#### Supplementary Materials

www.sciencemag.org/content/343/6173/885/suppl/DC1  
Materials and Methods

Figs. S1 to S13

Table S1

References (26–35)

Movies S1 to S4

25 October 2013; accepted 28 January 2014

10.1126/science.1247663

## Action Monitoring and Medial Frontal Cortex: Leading Role of Supplementary Motor Area

Francesca Bonini,<sup>1,2,3,4\*</sup> Boris Burle,<sup>1,3</sup> Catherine Liégeois-Chauvel,<sup>1,2</sup> Jean Régis,<sup>1,2,4</sup> Patrick Chauvel,<sup>1,2,4</sup> Franck Vidal<sup>1,3</sup>

The capacity to evaluate the outcomes of our actions is fundamental for adapting and optimizing behavior and depends on an action-monitoring system that assesses ongoing actions and detects errors. The neuronal network underlying this executive function, classically attributed to the rostral cingulate zone, is poorly characterized in humans, owing to the limited number of direct neurophysiological data. Using intracerebral recordings, we show that the leading role is played by the supplementary motor area (SMA), which rapidly evaluates successful and erroneous actions. The rostral part of medial prefrontal cortex, driven by the SMA, was activated later and exclusively in the case of errors. This suggests a hierarchical organization of the different frontal regions involved in implementation of action monitoring and error processing.

Imagine a tennis player when serving. If the ball lands out, the subsequent serve is more likely to succeed. The required behavioral adjustments are subordinated to an error-identification

process. Even during a successful first serve, the player may have tossed the ball too high, requiring a prompt adjustment of serving action. Such remedial actions rely on the existence of an

action-monitoring system in charge of evaluating ongoing activities to adjust them and improve subsequent actions.

Studies in monkeys and humans have demonstrated the critical role of the medial frontal cortex (MFC) in such an evaluative process (1–3). A particular subregion within the MFC, the rostral cingulate zone (RCZ) (4), is often considered the crucial node in this control network (1).

We investigated the anatomical substrate of action monitoring in humans in more detail using intracerebral electroencephalography (iEEG). Five subjects (5), undergoing presurgical evaluation of their epilepsy with iEEG, performed a Simon task (6). In this conflict task, different classes of behaviorally relevant responses can be distinguished by means of electromyography (EMG):

<sup>1</sup>Aix-Marseille Université, 13385, Marseille, France. <sup>2</sup>INSERM, Institut de Neurosciences des Systèmes UMR 1106, 13385, Marseille, France. <sup>3</sup>CNRS, Laboratoire de Neurosciences Cognitives, UMR 7291, 13331, Marseille, France. <sup>4</sup>APHM (Assistance Publique–Hôpitaux de Marseille), Pôle de Neurosciences Cliniques, Timone Hospital, 13005, Marseille, France.

\*Corresponding author. E-mail: francesca.bonini@univ-amu.fr

correct responses, overt errors, and covert errors (7) (Fig. 1 and supplementary materials). If we consider our initial analogy of the tennis player, overt errors represent a missed serve, whereas covert errors [often termed partial errors (8)] represent the ongoing serve's successful adjustment.

Local field potentials (LFPs) were recorded from 562 contacts on 42 electrodes positioned predominantly in the frontal cortex (Fig. 2 and table S1). LFPs were averaged time-locked to subjects' responses (as recorded by the EMG of the

responding muscle; see Fig. 1B), so as to evaluate action-monitoring activity (behavioral results are presented in the supplementary materials and fig. S1).

Error-evoked LFPs were observed exclusively in the medial part of the frontal lobe. One set of electrodes clustered caudally, whereas other electrodes were more dispersed rostrally (Fig. 2, colored dots, and table S2).

In the caudal cluster, all subjects presented a sharp LFP, peaking between 100 and 190 ms af-

ter EMG activation. The largest LFPs occurred after overt errors; smaller LFPs appeared after covert errors; and even smaller, but clearly still present, LFPs occurred after correct responses (Fig. 2 and table S3). This pattern replicates previous scalp EEG data (9–11). Inspection of individual electrode placement showed that none of these active electrodes were positioned within the RCZ, but all were clearly located within the SMA—namely, above the calloso-marginal fissure and immediately posterior to the vertical commissure anterior (VCA) boundary (Fig. 2).

Although intracerebral electrodes are sensitive to current within only a small volume of cerebral tissue, it is possible that the recorded activity may have been volume-conducted from a remote generator outside the SMA. However, supplementary results (note S2 and figs. S2 and S3) exclude this possibility.

Other electrodes disclosing performance-sensitive activity were located more rostrally, in the medial prefrontal region—namely, in pregenual anterior cingulate cortex (pACC; i.e., in the anterior division of the RCZ) in patient 3 and in orbito-medial prefrontal cortex (OMPFC) in patients 3 and 5 (Fig. 3, B and D, and table S2). The activation profile of those more rostral electrodes differed from that of the caudal cluster in three ways (Fig. 3, A and C, fig. S8, and table S3): (i) The prefrontal activity was delayed and had a longer duration, with a caudo-rostral latency gradient; (ii) it was specific to errors (overt and covert); and (iii) it was more widespread than the activity within the SMA, as demonstrated by recordings from electrodes' lateral contacts.

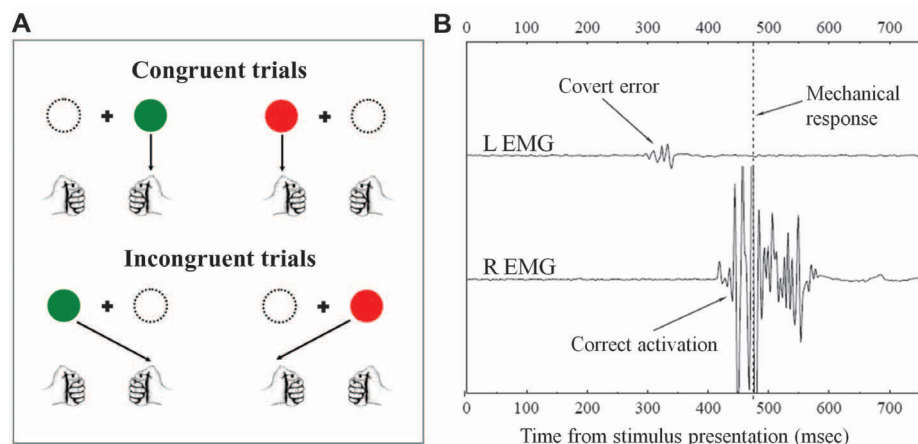
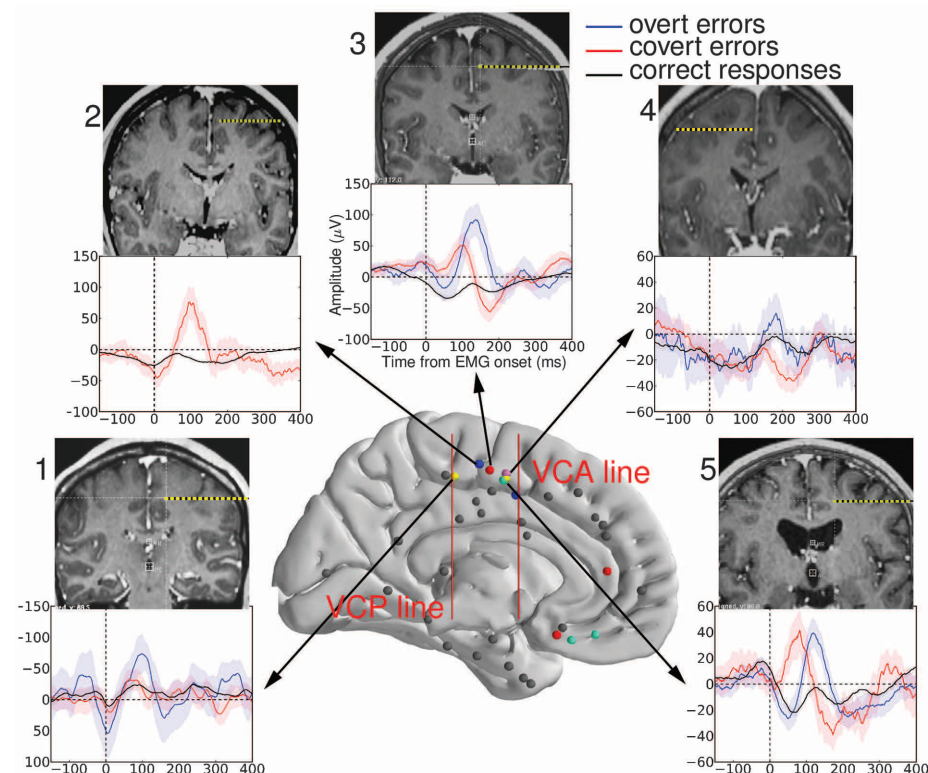


**Fig. 1. Experimental procedure.** (A) The Simon task is a between-hand choice reaction time task that induces errors: Subjects had to respond with a left or right thumb key-press as a function of the color of a target stimulus. The target could be presented on the same side as the response to be given (congruent trials), or on the opposite side (incongruent trials). (B) Covert errors (often called partial errors) are characterized by a small subthreshold EMG burst on the incorrect side preceding the correct response.

**Fig. 2. Overview of EMG-locked LFPs and of all recording sites in the medial wall.** A total of 562 contacts from 42 electrodes were included in the analysis, 34 of which were implanted up against the medial wall. The anatomical location of these 34 electrodes' internal contacts, converted into normalized MNI (Montreal Neurological Institute) brain space to allow comparison across subjects, is shown on a three-dimensional MNI standard brain in its medial aspect. The two red vertical bars represent the VCA (vertical commissure anterior) line and the VCP (vertical commissure posterior) line. A cluster of performance-sensitive electrodes (colored dots) is located in the SMA (caudal cluster, behind the VCA line), while other electrodes are more widespread in the rostral part of the medial prefrontal cortex (electrodes anterior to VCA). For each participant, averaged EMG-locked LFPs recorded from the SMA are displayed: The largest LFP occurs after overt errors (blue); a smaller LFP appears after covert errors (red); and an even smaller LFP occurs after correct responses (black). Colored bands represent between-trials confidence intervals set to 0.05. For each subject, an individual MRI and computed tomography (CT) fusion is provided, showing, in coronal view, the trajectory of the performance-sensitive electrode. All these electrodes were clearly located above the calloso-marginal fissure and behind the VCA line (that is, in the SMA).



We further investigated the relation between rostral and caudal activity using trial-by-trial analysis (fig. S4 and note S3). Single-trial LFPs recorded in the SMA and in the medial prefrontal regions were significantly and positively correlated both in terms of latencies [ $\rho = 0.8$ ,  $P < 0.01$  between SMA and pACC on patient 3, and  $\rho = 0.35$ ,  $P < 0.05$  between SMA and OMPFC on patient 5 (12)] and, less strongly, amplitudes ( $\rho = 0.63$ ,  $P < 0.01$  and  $\rho = 0.28$ ,  $P < 0.1$ , for patient 3 and 5 respectively; fig. S5). Medial prefrontal activity appeared to be contingent upon activity in the SMA because it was always preceded by SMA activity, and importantly, it was never present when SMA activity was absent. By contrast, SMA activity can and occasionally did occur without the subsequent prefrontal activity. This suggests a strong connection and potential hierarchy between these two regions in error processing. Such a connection is not necessarily direct and might be mediated by a third structure.

To further describe the functional importance of the SMA activity, we focused on covert errors. These trials are a prototypical case of efficient ongoing action control because the incorrect activation is interrupted and corrected (by the opposite “corrective” response). We therefore searched for a functional link between SMA activity and error correction (fig. S6 and note S4).

We correlated the latencies of LFPs and EMG activity in three patients for whom covert-error LFPs were detectable in the SMA on a trial-by-trial basis. The offset of EMG bursts linked to incorrect responses, representing response interruption, strongly correlated with the peak of the SMA LFP ( $\rho = 0.63$ ,  $P < 0.01$ ), whereas the onset of EMG bursts linked to corrective responses strongly correlated with the end of the SMA LFP ( $\rho = 0.7$ ,  $P < 0.01$ ) (fig. S7 and note S4).

In covert errors, SMA activity began with the first incorrect muscular activation, culminated when this incorrect action was inhibited, decreased, and finally extinguished when the subsequent corrective response was issued. This correlation, consistent with previous scalp EEG data (13), suggests that the SMA intervenes in action monitoring by emitting a performance-modulated “default” signal that possibly acts as an alert or a warning signal. Each time a behaviorally relevant response is produced, this default signal is emitted. For correct responses, it is rapidly subdued, giving rise to a small LFP. For covert errors, the warning signal keeps rising but begins to decrease once the incorrect action is inhibited and terminates with the activation of the corrective response. A slightly later suppression and correction would result in a prolonged alarm; that is, a longer and larger LFP. For overt errors, this alarm reaches its highest level, corresponding to the highest LFP’s amplitude. We thus hypothesize that this alarm, when crossing a given threshold, hints at the need to enhance cognitive control.

This study shows that action monitoring is largely carried out by the SMA. This is consistent with limited data reported in humans (11, 14–18)

and in monkeys (19, 20). However, much of the current literature indicates that human primate and nonprimate RCZ is sensitive to action outcome (14, 15, 17, 18, 21–25).

Even though the precise role of the RCZ vis à vis the SMA should be further evaluated with more extensive sampling, our data allow discussion of the apparent inconsistency in the literature from a new perspective. Functional magnetic resonance imaging (fMRI) data (contrasting errors minus correct responses) mainly show RCZ activity (1). By comparison, we showed a caudo-rostral latency gradient in medial frontal areas. On this basis one may expect RCZ to be active only for erroneous action, shortly after SMA, but the extent to which RCZ activity depends on SMA remains an open question. However, our results suggest a schema of how this cognitive control function operates, and of its underlying cortical network. We propose that this network, encompassing caudal and rostral parts of the MFC, is hierarchically organized to implement action control: medial prefrontal cortex, including the anterior RCZ, is engaged in the case of

erroneous actions and thus, as usually assumed, is implicated in error processing following a caudo-rostral gradient. The role of the most rostral activities remains to be elucidated, but it could be related to the estimated (negative) value of errors (26). However, this process seems to be embedded in an action-monitoring process, which is carried out by the SMA. The SMA is therefore a core node in performance monitoring, whose function consists of continuously assessing ongoing actions and, in the case of errors only, recruiting the medial prefrontal cortex.

Action monitoring and error processing are thus two crucial stages of executive control in humans, allowing for efficient behavioral adjustment and optimization of performance. The involvement of the SMA in action monitoring appears functionally grounded, because the SMA is widely considered to be implicated in movement initiation and inhibition (27), response selection, and motor planning (28). The present study reveals a new function for SMA: the early evaluation of the outcome of actions that it has contributed to initiating.

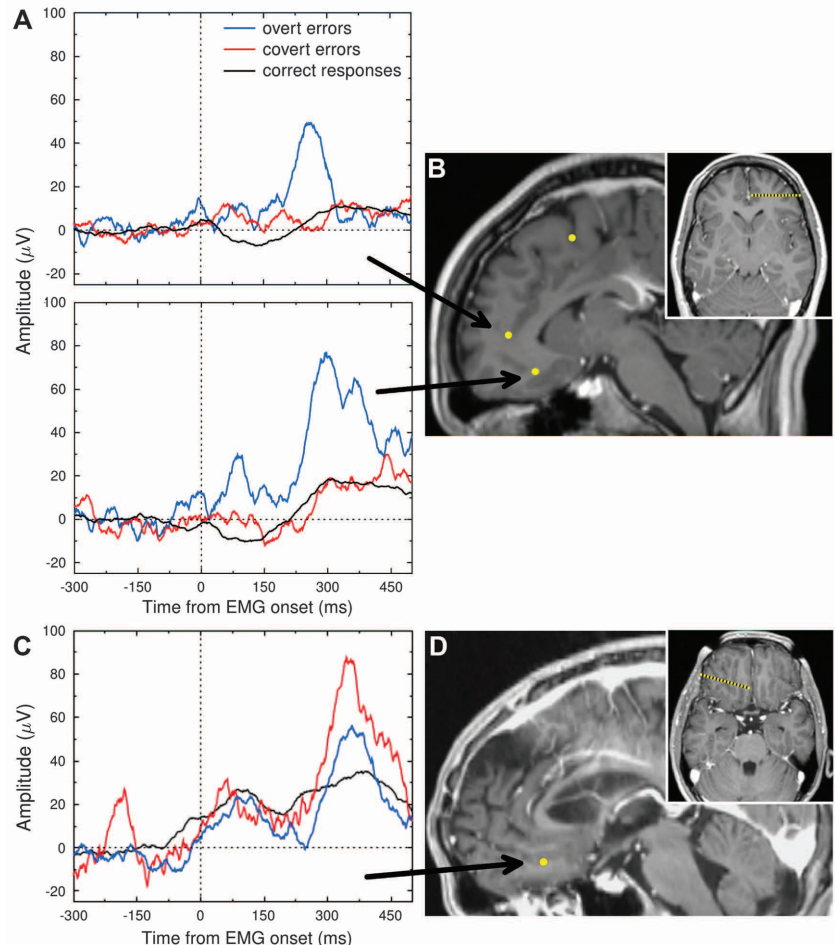


**Fig. 3. Medial prefrontal LFPs evoked by erroneous activations.** (A) Averaged LFPs evoked by overt errors peaking at 260 ms in pACC (top) and at 295 ms in OMPFC (bottom) in subject 3. (B) Individual reconstruction of subject 3’s prefrontal electrodes based on an MRI-CT fusion scan in axial and sagittal view (note also the overlying electrode placed in the SMA). (C) Averaged LFPs peaking at 355 ms evoked by covert and overt errors in subject 5. (D) Individual reconstruction of subject 5’s prefrontal electrode based on an MRI-CT fusion scan in axial and sagittal view.

## References and Notes

- K. R. Ridderinkhof, M. Ullsperger, E. A. Crone, S. Nieuwenhuis, *Science* **306**, 443–447 (2004).
- V. van Veen, C. S. Carter, *J. Cogn. Neurosci.* **14**, 593–602 (2002).
- M. M. Botvinick, J. D. Cohen, C. S. Carter, *Trends Cogn. Sci.* **8**, 539–546 (2004).
- N. Picard, P. L. Strick, *Cereb. Cortex* **6**, 342–353 (1996).
- A sixth subject was not included (see note S1).
- J. R. Simon, in *Stimulus-Response Compatibility: An Integrated Perspective* (R. W. Proctor, T. G. Reeve, Eds. (North-Holland, Amsterdam, 1990), pp. 31–86.
- H. G. Smid, G. Mulder, L. J. Mulder, *Acta Psychol. (Amst.)* **74**, 169–201 (1990).
- M. G. Coles, M. K. Scheffers, L. Fournier, *Acta Psychol. (Amst.)* **90**, 129–144 (1995).
- F. Vidal, T. Hasbroucq, J. Grapperon, M. Bonnet, *Biol. Psychol.* **51**, 109–128 (2000).
- M. Falkenstein, J. Hoormann, S. Christ, J. Hohnsbein, *Biol. Psychol.* **51**, 87–107 (2000).
- C. Roger, C. G. Bénar, F. Vidal, T. Hasbroucq, B. Burle, *Neuroimage* **51**, 391–403 (2010).
- Although the averaged activity in OMPFC in patient 3 was larger than activity in pACC, its signal/noise ratio was too low to reliably detect single-trial activity on a sufficient number of trials for analysis.
- B. Burle, C. Roger, S. Allain, F. Vidal, T. Hasbroucq, *J. Cogn. Neurosci.* **20**, 1637–1655 (2008).
- H. Garavan, T. J. Ross, K. Murphy, R. A. P. Roche, E. A. Stein, *Neuroimage* **17**, 1820–1829 (2002).
- P. Luu, D. M. Tucker, D. Derryberry, M. Reed, C. Poulsen, *Psychol. Sci.* **14**, 47–53 (2003).
- M. J. Herrmann, J. Römmeler, A. C. Ehlis, A. Heidrich, A. J. Fallgatter, *Brain Res. Cogn. Brain Res.* **20**, 294–299 (2004).
- K. D. Fitzgerald *et al.*, *Biol. Psychiatry* **57**, 287–294 (2005).
- E. R. A. de Bruijn, F. P. de Lange, D. Y. von Cramon, M. Ullsperger, *J. Neurosci.* **29**, 12183–12186 (2009).
- V. Stuphorn, T. L. Taylor, J. D. Schall, *Nature* **408**, 857–860 (2000).
- K. W. Scangos, R. Aronberg, V. Stuphorn, *J. Neurophysiol.* **109**, 1928–1939 (2013).
- K. A. Kiehl, P. F. Liddle, J. B. Hopfinger, *Psychophysiology* **37**, 216–223 (2000).
- S. Debener *et al.*, *J. Neurosci.* **25**, 11730–11737 (2005).
- E. E. Emeric *et al.*, *J. Neurophysiol.* **99**, 759–772 (2008).
- S. Hoffmann, M. Falkenstein, *Hum. Brain Mapp.* **31**, 1305–1315 (2010).
- T. E. Ham *et al.*, *Cereb. Cortex* **23**, 703–713 (2013).
- N. Kolling, T. E. J. Behrens, R. B. Mars, M. F. S. Rushworth, *Science* **336**, 95–98 (2012).
- P. Y. Chauvel, M. Rey, P. Buser, J. Bancaud, *Adv. Neurol.* **70**, 199–209 (1996).
- B. Nachev, C. Kennard, M. Husain, *Nat. Rev. Neurosci.* **9**, 856–869 (2008).

**Acknowledgments:** We thank P. Marquis for technical help in acquiring intracerebral recordings; D. Schön for critical discussion and reading the manuscript; and R. Hewett, M. Woodman, and J. Coull for English revision. B.B. was supported by the European Research Council under the European Community's Seventh Framework Program (FP7/2007–2013 Grant Agreement no. 241077). F.B. was supported by the Ecole Doctorale Science de la Vie et de la Santé, Aix-Marseille Université. F.V. and B.B. designed the study. F.B. administered the Simon task and obtained intracerebral recordings. J.R. performed the surgical procedure and provided coordinates of intracerebral electrodes. F.B. analyzed data. B.B. and F.B. performed statistical analysis. F.V., B.B., F.B., P.C., and C.L.-C. interpreted data and discussed results. F.B. and F.V. wrote the manuscript. All authors commented on and edited the manuscript. The authors declare no conflict of interest.

## Supplementary Materials

www.sciencemag.org/content/343/6173/888/suppl/DC1  
Materials and Methods  
Supplementary Text  
Figs. S1 to S8  
Tables S1 to S3  
References (29–36)

21 October 2013; accepted 24 January 2014  
10.1126/science.1247412

# Grid-Layout and Theta-Modulation of Layer 2 Pyramidal Neurons in Medial Entorhinal Cortex

Saikat Ray,\* Robert Naumann,\* Andrea Burgalossi,\*† Qiusong Tang,\* Helene Schmidt,\* Michael Brecht‡

Little is known about how microcircuits are organized in layer 2 of the medial entorhinal cortex. We visualized principal cell microcircuits and determined cellular theta-rhythmicity in freely moving rats. Non-dentate-projecting, calbindin-positive pyramidal cells bundled dendrites together and formed patches arranged in a hexagonal grid aligned to layer 1 axons, parasubiculum, and cholinergic inputs. Calbindin-negative, dentate-gyrus-projecting stellate cells were distributed across layer 2 but avoided centers of calbindin-positive patches. Cholinergic drive sustained theta-rhythmicity, which was twofold stronger in pyramidal than in stellate neurons. Theta-rhythmicity was cell-type-specific but not distributed as expected from cell-intrinsic properties. Layer 2 divides into a weakly theta-locked stellate cell lattice and spatiotemporally highly organized pyramidal grid. It needs to be assessed how these two distinct principal cell networks contribute to grid cell activity.

**T**emporal (1–3) and spatial (4) discharge patterns in layer 2 of the medial entorhinal cortex (MEC) are related through phase precession (5) and the correlation of gridness (hexagonal regularity) and theta-rhythmicity (2). Layer 2 principal neurons divide into pyramidal and stellate cells, the latter of which have been

suggested to shape entorhinal theta (6, 7) and grid activity (8) by their intrinsic properties. Progress in understanding entorhinal microcircuits has been limited because most though not all data (9–11) stem from extracellular recordings of unidentified cells. Such recordings have characterized diverse functional cell types (12–14) in layer 2. Clustering of grid cells (15) points to spatial organization. It is not clear, however, how functionally defined cell types correspond to stellate and pyramidal cells (7, 16), which differ in conductances, immunoreactivity, projections, and inhibitory inputs (6, 17–20). We combined juxtacellular labeling with principal cell identification (20) to visualize microcircuits in the MEC (Fig. 1A).

Calbindin immunoreactivity (20) identifies a relatively homogeneous pyramidal neuron population in MEC layer 2. Parasagittal sections stained for calbindin (Fig. 1B) showed that calbindin-positive (calbindin<sup>+</sup>) pyramidal cells were arranged in patches (21). Apical dendrites of calbindin<sup>+</sup> pyramidal cells bundled together in layer 1 to form tent-like structures over the patches (Fig. 1B). The patchy structure is well defined at the layer 1/2 border, whereas a “salt-and-pepper” appearance of calbindin<sup>+</sup> and calbindin<sup>-</sup> cells is observed deeper in layer 2 (fig. S1). Patches contained  $187 \pm 70$  cells ( $111 \pm 42$ , ~60% calbindin<sup>+</sup>;  $76 \pm 28$ , ~40% calbindin<sup>-</sup> cells; counts of 19 patches from four brains). We double-stained tangential sections for calbindin (green) and the neuronal marker NeuN (red) to visualize patches in the cortical plane. Calbindin<sup>+</sup> (green/yellow) patches covered the MEC except for a 400- to 500- $\mu$ m-wide patch-free medial stripe adjacent to the parasubiculum (Fig. 1C). Clustering was not observed in calbindin<sup>-</sup> neurons (red) (Fig. 1C). We noted a striking hexagonal organization of calbindin<sup>+</sup> patches (Fig. 1, C and D) and characterized this organization by means of three techniques. (i) We used two-dimensional spatial autocorrelation analysis (4), which captures spatially recurring features and revealed a hexagonal regularity (Fig. 1E). (ii) We modified grid scores (12) to quantify hexagonality also in elliptically distorted hexagons (22), distortions that result from tissue curvature and anisotropic shrinkage. Grid scores range from -2 to +2, with values >0 indicating hexagonality. The example in Fig. 1D had a grid score of 1.18, suggesting a high degree of hexagonality. (iii) We assessed the probability of hexagonal patch arrangements given preserved local structure (14) by means of a shuffling procedure. We found that the strongest Fourier component of the sample

Bernstein Center for Computational Neuroscience, Humboldt University of Berlin, Philippstrasse 13 Haus 6, 10115 Berlin, Germany.

\*These authors contributed equally to this work.

†Present address: Werner Reichardt Centre for Integrative Neuroscience, Otfried-Müller-strasse 25, 72076 Tübingen, Germany.

‡Corresponding author. E-mail: michael.brecht@bccn-berlin.de

Ma se il suo errore non avesse fatto altro che cancellare un errore precedente?  
Se la sua distrazione fosse stata apportatrice non di disordine ma di ordine?  
“ Forse il mercante sapeva bene quel che faceva, – pensa il signor Palomar – dandomi quella pantofola spaiata ha messo riparo a una disparità che da secoli si nascondeva in quel mucchio di pantofole, tramandato da generazioni in quel bazar”

*Palomar, Italo Calvino*



## Abstract

The capacity to evaluate the outcome of our actions is fundamental for adapting and optimizing behaviour. Indeed in flexible goal-directed behaviour, performance is continuously adjusted in order to avoid negative consequences and improve subsequent actions. This capability depends on an action monitoring system in charge of assessing ongoing actions, detecting errors, and evaluating outcomes.

Sensitivity to errors is considered to be the main manifestation of action monitoring, and electrical brain activity evoked by negative outcomes is thought to originate within the medial part of the frontal cortex. Likewise, functional neuroimaging studies suggest that this region has a decisive role in action monitoring. Nonetheless, the underlying neuronal network is incompletely characterised in humans.

In the two first studies, we investigated the anatomical substrates of action monitoring in humans using intracerebral local field potential (LFP) recordings of cerebral cortex from epileptic patients. Response evoked LFPs sensitive to outcome were recorded from the Supplementary Motor Area proper (SMA), with the largest LFPs occurring after errors and the smallest after correct responses. LFPs evoked exclusively by errors were recorded later and more rostrally in the medial prefrontal cortex. We then assessed gamma-frequency activity (60-180 Hz) - whose increase is considered a marker of neural recruitment during cognitive processing - induced by behaviourally relevant responses. Gamma power was modulated as a function of action outcome in a vast frontal and extra-frontal network.

In a third study we investigated the electro-magnetic activity evoked by internally versus externally delivered feedback using simultaneous recording of electroencephalography (EEG) and magnetoencephalography (MEG). While error related activity was detected by EEG (but not by MEG), feedback-related activity was detected by MEG, indicating that the sources of these two forms of outcome-modulated brain activity are different.

Our results show that the SMA is much more involved in action monitoring than previously thought. SMA rapidly and continuously assesses ongoing actions and likely engages more rostral prefrontal structures in the case of error. Processing of action errors and of negative externally delivered feedback therefore appears to be supported by distinct cortical networks.

## Résumé

La capacité à évaluer les résultats nos actions est fondamentale pour adapter et optimiser notre comportement. En effet dans les comportements dirigés vers un but, l'être humain est capable d'ajuster et modifier ses actions pour éviter les conséquences négatives et améliorer son niveau de performance au fil du temps. Cette habilité dépend de l'existence d'un système superviseur chargé d'évaluer l'action en cours, de détecter les erreurs, de déclencher souvent des corrections, et d'évaluer les conséquences de l'action.

La sensibilité aux erreurs est considérée comme l'une des principales manifestations de l'action du système superviseur et on considère que certaines activités électriques cérébrales évoquées par les erreurs sont générées par la partie médiane du cortex frontal. Ainsi, des études de neuroimagerie fonctionnelle suggèrent que cette région joue un rôle décisif dans la supervision de l'action. Néanmoins le réseau neuronal sous-jacent n'a pas été complètement caractérisé chez l'homme.

Dans les deux premières études nous avons étudié les bases anatomiques de la supervision de l'action chez l'homme au moyen des potentiels de champs locaux (LFP pour « *local field potentials* ») enregistrés dans le cortex cérébral de patients épileptiques.

Nous avons enregistré dans l'Aire Motrice Supplémentaire proprement dite (AMSp) des LFP évoqués par les réponses et modulés par la performance; les LFP plus amples survenaient après une erreur et les moins amples après une réponse correcte. Des LFP évoqués exclusivement par les erreurs ont été enregistrés plus tardivement et plus rostralement dans le cortex préfrontal médian.

Dans la deuxième étude, nous avons analysé les activités de hautes-fréquences de la bande gamma (60-180 Hz) induites par les réponses des sujets. Nous avons observé que ces activités gamma, dont l'augmentation est considérée un marqueur du recrutement neuronal, sont, elles aussi, modulées par la performance des sujets, mais dans un vaste réseau frontal et extra-frontal.

Dans une troisième étude, nous avons comparé les activités électromagnétiques évoquées par un feedback interne, à celles évoquées par un feedback externe, en utilisant des enregistrements simultanés électroencéphalographiques (EEG) et magnétoencéphalographiques (MEG). Une activité évoquée par les erreurs était visible sur les enregistrements EEG (mais pas sur les enregistrements MEG), alors qu'une activité évoquée par le feedback externe était bien visible sur les enregistrements MEG, indiquant que les générateurs de ces deux formes d'activité cérébrale, modulées par la performance, sont différents.

Nos résultats montrent une implication de l'AMSp dans la supervision de l'action chez l'homme, bien plus importante que ce que l'on soupçonnait auparavant. Cette structure évalue précocement, et de façon continue, l'action en cours et elle engage vraisemblablement des structures préfrontales plus rostrales en cas d'erreur seulement. Le traitement de l'erreur d'action, selon qu'il se fonde sur des informations internes ou externes est certainement sous-tendu par des réseaux corticaux différents.